KfK 3027
August 1980

Review and Tables of Pion-Nucleon Forward Amplitudes

G. Höhler, F. Kaiser
Institut für Kernphysik

Kernforschungszentrum Karlsruhe

KERNFORSCHUNGSZENTRUM KARLSRUHE

Institut für Kernphysik

KfK 3027

Review and tables of pion-nucleon forward amplitudes

G. Höhler[+] and F. Kaiser[+]

Kernforschungszentrum Karlsruhe GmbH, Karlsruhe

[+] Institut für Theoretische Kernphysik der Universität Karlsruhe

Bericht über Pion-Nukleon-Vorwärtsstreuung und Tabellen der Vorwärtsamplituden

Zusammenfassung: Ausgehend von einer Interpolation der totalen $\pi^{\pm}p$ Wirkungsquerschnitte werden aus Dispersionsrelationen Voraussagen für die Realteile nach einer Methode berechnet, bei der man mit geringem Aufwand verschiedene Hochenergieannahmen einsetzen kann. Die Ergebnisse werden mit neuen experimentellen Resultaten verglichen, die aus Phasenanalysen, Coulomb-Interferenzdaten und Vorwärtsquerschnitten bei der Ladungsaustauschreaktion folgen. Die allgemeine Übereinstimmung ist zufriedenstellend, sodaß die den Dispersionsrelationen zugrunde liegende Kausalitätsbedingung bis zu Pion-Laborimpulsen von 200 GeV/c bestätigt ist.

Es wird auf eine Reihe von kleineren Diskrepanzen hingewiesen und zahlreiche andere Methoden für die Analyse der Vorwärtsamplituden werden kritisch diskutiert. Im letzten Teil werden ausgewählte theoretische Probleme behandelt, bei denen die experimentell bestimmten Vorwärtsamplituden eine Rolle spielen.

Review and Tables of Pion-Nucleon Forward Amplitudes

Abstract: Starting from an interpolation of the $\pi^{\pm}p$ total cross section data predictions for real parts of pion-nucleon forward amplitudes have been calculated from dispersion relations in such a way that one can easily use different parametrizations for the high energy behaviour. The results are compared with new experimental values for real parts from phase shift analyses and Coulomb interference experiments and with charge-exchange forward cross sections. It turns out that the general agreement is satisfactory, i.e. there is no reason to doubt the validity of the causality condition up to 200 GeV/c lab. momentum in πN scattering.

It is pointed out that there exist several small discrepancies. Numerous other methods for the analysis of forward amplitudes are critically reviewed. In the last part several theoretical topics are treated in which the experimental forward amplitudes play an important role.

Table of Contents

1. Introduction

The present report is an updated and extended version of our "Table of Pion-Nucleon Forward Amplitudes", of which several earlier editions have been published or distributed since 1964 (Refs. 1, 2). We restrict ourselves to the no-flip amplitudes as derived from total cross sections and dispersion relations. The other forward amplitudes and amplitudes at fixed c.m. angle and fixed t can be determined only from the result of phase shift analyses. Tables and figures based on the "Karlsruhe-Helsinki 1978" analysis can be found in our "Handbook of Pion-Nucleon Scattering" (Ref. 3). In a forthcoming "Supplement" similar tables and figures will be shown for the new CMU-LBL phase shift solution (Ref. 4).

The main changes in comparison with the earlier edition are the following:

i) Our fit to the total cross sections has been adjusted to the new data of Carroll et al.[5].

ii) In our main table the fit to the total cross section difference has been chosen such that the prediction for the charge-exchange forward cross section is compatible with the new data of Apel et al.[6] and the earlier data of Barnes et al.[7], if an estimation for the radiative corrections is taken into account. It turns out that $\alpha_\rho = 0.500$ is an acceptable value for the intercept of the ρ-trajectory. We have also included a second table of forward amplitudes which is based on the best fit to the total cross section data without an adjustment to the charge-exchange data ($\alpha_\rho = 0.53$). A comparison of the real parts given in these two tables shows the sensitivity to the high energy assumption.

iii) In the case of the isospin even amplitude we present results for 5 fits to the total cross section data above 10 GeV/c, which have a different high energy behaviour. The predictions for the real parts are compared with the existing data.

iv) The predictions for the real parts of the elastic $\pi^{\pm}p$ forward amplitudes are compared with the results of new Coulomb interference experiments[8-11]. The discrepancy which was noticed in Ref. 2 in the case of $\pi^- p$ scattering is not present any more, if one considers the new accurate data[8,9] and our discussion of a problem with the analysis of the Brookhaven Coulomb interference experiment[12] (see Ref. 13).

v) Results from recent phase shift analyses[3,4] have been used in order to reconstruct the forward amplitudes, which are then compared with the values

listed in our table. The comparison is of interest for several reasons:

(a) for a redetermination of the s-wave scattering lengths,

(b) for an estimation of the errors of the real parts in our main table. As discussed in Ref. 2 it is very difficult to estimate the errors from those of the total cross sections, because the most important errors arise from discrepancies between different experiments.

(c) Since tables of forward amplitudes are used in phase shift analysis as part of the input, discrepancies between these tables and the reconstructed values give indications for systematic errors in the differential or total cross sections.

In sect. 2 we shall discuss the input for the evaluation of the dispersion relations, our method for the treatment of the principal value integrals and a simple "do-it-yourself-method" for modifications of the high energy assumption. Other recent determinations of the real part will be discussed in sect. 3. Next we compare the prediction for the real parts with experimental data obtained in Coulomb interference experiments (sect. 4) and with real parts reconstructed from phase shifts (sect.5). Sect.6 is devoted to extrapolations to the unphysical region and sect. 7 to zeros of the forward amplitude. Sect.8 deals with different aspects of charge-exchange forward scattering and sect. 9 gives a summary of theoretical results, including bounds, Pomeranchuk theorems, relations between phase and modulus, other types of dispersion relations,sum rules and acausal models.

2. Tables of pion-nucleon forward amplitudes and total cross sections

Our tables have been calculated from dispersion relations for the isospin even and odd forward amplitudes $C^{\pm}$, starting from interpolations of the accurate total cross section data for $\sigma(\pi^{\pm}p) \equiv \sigma_{\pm}$ which give

$$\text{Im } C^{\pm} = k\sigma^{\pm} , \qquad \sigma^{\pm} = (\sigma_{-} \pm \sigma_{+})/2 , \tag{2.1}$$

according to the optical theorem. k denotes the pion laboratory momentum. For the asymptotic behaviour we use a number of different parametrizations which fit the data above 10 GeV/c. In addition σ^{-} is constrained by the data for charge-exchange forward scattering. The pion-nucleon coupling constant f^2 and the subtraction constant $C^{+}(0)$ follow from results of phase shift analysis for the real parts.

2.1 Input for the total cross sections

The input for the total cross sections in Table 80/1 differs from that of Table 77/1 (Ref. 2) only by small changes of the parametrization at high energies. In the range 0.4 - 0.9 GeV/c it follows the Rutherford data (Ref. 14) and ignores the Arizona data (Ref. 15), as was done in Tables 77/1, 77/2 and 77/4 of Ref. 2. We have no reason to believe that the discrepancy between these two data sets is mainly due to an error of the Arizona data, but it would not make sense to take an average. In order to enable the user of our tables to see the corresponding uncertainty of the real parts and of the forward cross sections, we have presented in Table 77/3 of Ref. 2 an evaluation which is based on the Arizona data.

In the threshold region our fit to the total cross sections is consistent with the results for the s-wave scattering lengths $a^{\pm}$ (Refs. 3, 16)

$$\sigma^{+}/4\pi = (a^{+})^2 + 2(a^{-})^2 + O(q^2),$$
$$\sigma^{-}/4\pi = (a^{-})^2 + 2a^{+}a^{-} + O(q^2). \qquad (2.2)$$

Around the first resonance we still use our earlier fit which follows the result of Carter et al. (Ref. 17), because the charge-dependent effects due to a mass difference between the 1233 MeV isobar states Δ^{++} and Δ^{o} are not yet well understood.

Fig. 1 shows the difference between our fit and the data of Pedroni et al.[18] and also the values reconstructed from the recent phase shift analysis of Koch and Pietarinen (Ref. 3). It is also of interest to compare our fit for the isospin one half combination $\sigma^{1/2}$ of the total cross sections with the same quantity derived from these phase shifts and from the total cross section data of Pedroni et al.[18]. Due to the threshold factor and the smallness of the p-waves the s-wave contribution dominates strongly below a laboratory momentum of 300 MeV/c. Fig. 2 shows that there are problems and that a further investigation is necessary.

In the high energy region our parametrization for σ^{+} (Ref. 19) has been adjusted to the new total cross section data of Carroll et al.[5]. Our fit reads

$$\sigma^{+}(k) = \sigma_o + \sigma_1 \left[\ln(k/k_1)\right]^2 + b\, k^{\alpha-1}; \quad k \geq 10 \text{ GeV/c}, \qquad (2.3a)$$

$$\sigma_o = 22.26 \text{ mb}, \quad \sigma_1 = 0.418261 \text{ mb}, \quad k_1 = 37.8338 \text{ GeV/c}, \tag{2.3b}$$

$$b = 8.2287 \text{ mb GeV}^{1-\alpha}, \quad \alpha = 0.53395.$$

Of course, the large number of decimals is not significant, but it is necessary if one wants to reproduce the values for Re C^+ given in our table (which, in order to have a simple format, frequently gives too many digits). Fig. 3 shows the data, the fit (2.3) and other fits which will be discussed in sect. 2.3. The ansatz (2.3) has no theoretical foundation except that it is compatible with the asymptotic behaviour demanded by the Froissart bound. In particular there is no reason to associate the last term with f-meson exchange, since the leading terms are just one choice among many possible ones. Presumably, f-meson exchange is connected with the "peripheral peak" in the impact parameter transform Im $F^o_{++}(s,b)$ of the imaginary part of the isospin even s-channel helicity no-flip amplitude (Ref. 20) and can be studied there in a less ambigous way. - It is remarkable that the decrease of $\sigma^+(k)$ can be described in the large range 2.5 - 70 GeV/c by the simple law $\sigma^+ = \sigma_o + b/k$ (Fig. 4).

Carroll et al.[5] have fitted their data for σ^- to the usual power law, which agrees with the expression for the contribution of reggeized ρ-exchange. They find $\alpha_\rho = 0.54 \pm 0.03$. Our fit is slightly different because it starts already at 10 GeV/c and includes some additional data[22] (see Fig. 5)

$$\sigma^-(k) = c\, k^{\alpha_\rho - 1}; \quad k \geq 10 \text{ GeV/c}, \tag{2.4}$$

$$c = 2.931 \text{ mb GeV}^{1-\alpha_\rho}; \quad \alpha_\rho = 0.5337.$$

The approximate agreement of α in (2.3) and α_ρ in (2.4) is accidental.

Since we assume the validity of charge-independence, there is a second possibility to determine α_ρ. The charge-exchange differential cross sections at high energies are well described by the formula

$$\frac{d\sigma_o(s,t)}{dt} = T(t)(k/k_o)^{2\alpha_\rho(t)-2}, \tag{2.5}$$

which has been derived from the Regge model for ρ-exchange, according to which we have at $t = 0$ ($\alpha_\rho = \alpha_\rho(0)$)

$$\text{Re } C^-(s,0) = c \tan(\alpha_\rho \pi/2)\, k^{\alpha_\rho}, \quad \text{Im } C^-(s,0) = k\sigma^- = c\, k^{\alpha_\rho} \tag{2.6}$$

and

$$\frac{d\sigma_o(s,o)}{dt} = \frac{1}{8\pi k^2}\left| C^-(s,o)\right|^2 = \frac{c^2\, k^{2\alpha_\rho - 2}}{8\pi \cos^2(\alpha_\rho \pi/2)} \,. \qquad (2.7)$$

There are two recent results for charge-exchange differential cross sections:

i) the Fermilab experiment of Barnes et al.[7] in the range 20 - 200 GeV/c. The fit of the authors led to the parameters

$$\alpha_\rho = 0.481 \pm .004, \quad c = (5.58 \pm .10)\ \sqrt{mb}\ GeV^{-\alpha_\rho} = (3.48 \pm .06)\ mb\ GeV^{1-\alpha_\rho} \qquad (2.8a)$$

ii) the new Serpuchov experiment of Apel et al.[6] which is more accurate than the earlier Serpuchov experiment of Bolotov et al.[23]. The authors fitted their data together with those of Barnes et al.[7] and Stirling et al.[24] in the range 10 - 200 GeV/c. Taking into account the systematic errors they found

$$\alpha_\rho = 0.48 \pm .01, \; c = (5.75 \pm .13)\ \sqrt{mb}\ GeV^{-\alpha_\rho} = (3.59 \pm .08)\ mb\ GeV^{1-\alpha_\rho} \qquad (2.8b)$$

Another estimate of the uncertainty of the data follows from a comparison of the results at 40 GeV/c. Since Barnes et al.[7] have measured at 40.8 GeV/c we compare the values of $k d\sigma_o/dt$, which is practically energy independent:

$$k\, d\sigma_o/dt = 2031\ \mu b\ GeV^{-1} \quad \text{Barnes et al.}^{7}$$
$$= 2196 \pm 60\ \mu b\ GeV^{-1} \quad \text{Apel et al.}^{6}$$

The difference amounts to 8 % which is in agreement with an error of about 4 % for the overall fit.

Up to now radiative corrections to the charge-exchange cross sections have been ignored. According to an investigation by Ginzburg et al.[25] this is not justified. An accurate evaluation of their formulas can be made only by the authors of the experiments, since one needs a detailed information on the energy resolution of the detectors. Therefore we can use only the crude estimation given by Ginzburg et al.[25] in their table 1 according to which the strong interaction forward cross section $d\sigma_o/dt$ at $t = 0$ is larger by a factor of 1.10, 1.05 and 1.03 than the experimental cross sections at 200, 20, and 10 GeV/c respectively.

E. Borie[26] has made another evaluation, assuming that the energy resolution amounts to half a pion mass. She finds a correction which is about twice as large in the range 20 - 200 GeV/c.
It is remarkable that the sign and the order of magnitude of the correction is such that the discrepancy between the α_ρ-values following from σ^--data and from $d\sigma_o/dt$-data becomes smaller and that α_ρ approaches 0.50.
In order to demonstrate that a reggeized ρ-exchange model with $\alpha_\rho = 0.500$ can describe both σ^- and $d\sigma_o/dt$, we have plotted $(4\pi k d\sigma_o/dt)^{1/2}$ (Fig. 6) in addition to $\sqrt{k}\,\sigma^-$. In our special case $\alpha_\rho = 0.50$ eqs. (2.6) and (2.7) read

$$\text{Re } C^- = \text{Im } C^- = c\sqrt{k},\ \sigma^- = c/\sqrt{k},\ \frac{d\sigma_o}{dt} = \frac{c^2}{4\pi k}\ . \tag{2.9}$$

Therefore the question is whether a horizontal straight line can fit both types of data in our figure. A best fit is not of interest because of the unknown systematic errors. Figs.5 and 6 show that the following choice is acceptable

$$\alpha_\rho = 0.50, \qquad c = 3.30 \text{ mb GeV}^{-0.5} \tag{2.10}$$

2.2 Evaluation of the dispersion relations

The real parts have been calculated from the dispersion relations (see Ref. 3)

$$\begin{aligned} \text{Re } C^+(\omega) &= C^+(\mu) + C_N^+(\omega) - C_N^+(\mu) + k^2 \frac{2}{\pi} \int_o^\infty \frac{\sigma^+(k')dk'}{k'^2-k^2}\ , \\ \text{Re } C^-(\omega) &= C_N^-(\omega) + \omega \frac{2}{\pi} \int_o^\infty \frac{\sigma^-(k')}{k'^2-k^2} \frac{k'^2\,dk'}{\omega'}\ , \end{aligned} \tag{2.11}$$

where the nucleon pole terms and $C^+(\mu)$ are given by (see also (9.83))

$$C_N^+(\omega) - C_N^+(\mu) = \frac{4\pi f^2 k^2 \mu^2}{m(\mu^2-\omega_B^2)(\omega^2-\omega_B^2)}\ ,\ C_N^-(\omega) = \frac{8\pi f^2 \omega}{\omega^2-\omega_B^2}\ ,\ C^+(\mu) = 4\pi a^+(1+\mu/m). \tag{2.12}$$

The notation is the same as in Ref. 3: k and $\omega = \sqrt{\mu^2+k^2}$ denote the laboratory momentum and energy of the pion. $\mu = 0.13957$ GeV and $m = 0.93828$ GeV are the masses of $\pi^\pm$ and of the proton, which have been used in all kinematical calculations, $\omega_B = -\mu^2/2m$, $f^2 = 0.079$, $g^2/4\pi = (2m/\mu)^2 f^2 = 14.28$. The value $f^2 = 0.079$ is compatible with the Karlsruhe-Helsinki phase shift analysis (Ref. 3) and our choice $C^+(\mu) = -0.99\ \text{GeV}^{-1}$ corresponds to the s-wave scattering length $3a^+ = -0.0288\ \mu^{-1}$ (see sect. 5).

The $\pi^{\pm}p \to \pi^{\pm}p$ and $\pi^{-}p \to \pi^{o}n$ forward amplitudes are denoted by $C_{\pm}$ and C_{o} respectively. The normalization of $C \equiv A'$ is given by the expression for the optical theorem

$$\text{Im } C = k\sigma \ . \tag{2.13}$$

The forward cross sections follow from

$$\frac{d\sigma}{dt} = \frac{1}{16\pi k^2} |C|^2 = \frac{\pi}{q^2} \frac{d\sigma}{d\Omega_{c.m.}} , \tag{2.14}$$

where q is the center of mass momentum. The validity of charge-independence has been assumed throughout. Isospin notation:

$$C^{\pm} = \frac{1}{2}(C_{-} \pm C_{+}), \quad C_{o} = -\sqrt{2}\, C^{-}. \tag{2.15}$$

The evaluation of the dispersion relation has been performed by numerical integration up to 10 GeV/c for C^{+} and up to 20 GeV/c (Table 80/1) or 10 GeV/c (Table 80/2) for C^{-}. Parametrizations of $\sigma^{\pm}$ have been assumed for higher momenta up to infinity.

Contrary to some statements in the literature, the evaluation of the principal value integrals is not a "formidable task" (Ref. 28). Some details of our computer program are given in the Appendix. The program has been tested[29] by inserting a Breit-Wigner function for which the integral can be calculated exactly. For a width of 50 MeV the errors of the real parts are of the order of 1 % or less. The CPU-time for the evaluation of one dispersion integral amounts to 0.1 sec on our UNIVAC 1108.

The technique for calculating the real parts at high energies is described in sect. 2.3. The real parts are given as a sum of Re C_{par} and a correction which becomes negligible at very high energies. Re C_{par} is obtained by constructing an analytic function whose imaginary part is given by the parametrizations for the total cross sections, eqs. (2.3), (2.4), (2.10a)

$$\text{Re } C^{+}_{par} = \pi\sigma_1 \, k \, \ln(k/k_1) - b \cot(\alpha\pi/2) k^{\alpha} \tag{2.16}$$

$$\text{Re } C^{-}_{par} = c \tan(\pi \, \alpha_\rho/2) \, k^{\alpha_\rho}. \tag{2.17}$$

If one wants to use the numerical values of the parameters, eq. (2.3), (2.4), (2.10), one should notice that the real parts are usually listed in GeV^{-1} units (1 mb = 2.568 GeV^{-2}).

At momenta somewhat above 10 GeV/c in the first and third case and 30 GeV/c in the second case the real parts of our Tables 80/1 and 80/2 can be calculated from the approximations (k in GeV/c, Re C in GeV^{-1})

$$\begin{aligned}
&\text{Re } C^+ = \text{Re } C^+_{par} + 3.28 - 0.42(\tfrac{10}{k})^2 + \ldots && \text{Tables 80/1 and 80/2} \\
&\text{Re } C^- = \text{Re } C^-_{par} + \tfrac{1}{k}(14.0 + 2.0(20/k)^2 + \ldots) && \text{Table 80/1 } \alpha_\rho = 0.50 \quad (2.18) \\
&\text{Re } C^- = \text{Re } C^-_{par} + \tfrac{1}{k}(5.43 + 0.45(10/k)^2 + \ldots) && \text{Table 80/2 } \alpha_\rho = 0.5337.
\end{aligned}$$

It is remarkable that in eq. (2.18) the real part of C^+ at high momenta becomes relatively large, because the logarithmic term is increasing ~ k ln k and $\text{Re } C^+/\text{Im } C^+$ goes to zero asymptotically only as 1/ln k. At 1 000 GeV/c our table predicts $\text{Re } C^+/\text{Im } C^+ = 0.148$ and this quantity has not yet its asymptotic behaviour, because the ratio is still increasing (Fig. 7).

An Argand diagram for C^- at high energies is shown in Fig. 14. It will be discussed in sect. 7.

2.3 The "do it yourself method"

Our choice for the parametrization of the total cross sections, eq. (2.3), (2.4), (2.10) is rather arbitrary and therefore it is of interest to consider other parametrizations which fit the data equally well, but have a different high energy behaviour. If one wants to calculate the prediction for the real part following from another ansatz, it is not necessary to repeat the evaluation of the dispersion relation at all energies. As pointed out in Ref. 19, it is sufficient to perform a small calculation (on a pocket computer) which proceeds as follows. One starts with an ansatz for $\sigma^+_{par}(k)$ at high energies, which is suitable for a fit to the data. Then a crossing symmetric analytic function $C^+_{par}(\omega)$ is determined such that $\text{Im } C^+_{par} = k\sigma^+_{par}$; ($\omega/k = \sqrt{1+\mu^2/k^2} \sim 1$ above 10 GeV/c).

A simple possibility is to choose a function $\sigma^+(k)$ for which a table of integrals gives an expression for

$$\text{Re } C^+_{par}(\omega) = k^2 \frac{2}{\pi} \int_0^\infty \frac{\sigma^+_{par}(k')}{k'^2 - k^2}\, dk' \qquad (2.19)$$

in terms of known functions. In the following it is not essential that the cut starts at k = 0.
Most of the parametrizations discussed in the literature belong to special values of α and β in the ansatz

$$C^+_{par} = (-ik)^\alpha \{\ln(k/k_1) - i\pi/2\}^\beta , \tag{2.20}$$

for instance Regge poles (β = 0), Regge dipoles (β = 1) or special Regge cuts (β < -1) (Ref. 30).

The next step is now to combine eqs. (2.11) and (2.19) and to expand the denominator for $k \gg k_h$, k_h being the momentum above which the data have been fitted to σ^+_{par} (i.e. $\sigma^+ - \sigma^+_{par} \equiv 0$ for $k > k_h$)

$$\begin{aligned} \mathrm{Re}\, C^+ &= \mathrm{Re}\, C^+_{par} + C^+_N(\omega) - C_N(\mu) + C^+(\mu) + k^2 \frac{2}{\pi} \int_o^{k_h} \frac{\sigma^+ - \sigma^+_{par}}{k'^2 - k^2}\, dk' \\ &= \mathrm{Re}\, C^+_{par} + C^+(\mu) + 4\pi f^2/m + (c_o^{par} - c_o) + (c_2^{par} - c_2)(k_h/k)^2 + \ldots \end{aligned} \tag{2.21}$$

Small terms in the expansion of C^+_N have been neglected.

The coefficients

$$c_{2n} = \frac{2}{\pi} \int_o^{k_h} \left(\frac{k}{k_h}\right)^{2n} \sigma^+(k)\, dk \tag{2.22}$$

are calculated only once from the fit to the total cross sections below $k = k_h$. Our evaluation gives for k_h = 10 GeV/c

$$\bar{c}_o = c_o - C^+(\mu) - 4\pi f^2/m = 490.72\ \mathrm{GeV}^{-1},\ c_2 = 146.43\ \mathrm{GeV}^{-1}. \tag{2.23}$$

The coefficients c^{par}_{2n} follow from the integral (2.22) by inserting σ^+_{par} instead of σ^+.
It is remarkable that σ^+_{par} is now used in a range where it deviates strongly from the data. The correction $c_o^{par} - \bar{c}_o$ is small, if σ^+_{par} fits the average of the resonance structures.

We summarize the description of the "do it yourself method":

i) First one has to choose a parametrization $\sigma^+_{par}(k)$ and a value for k_h and to calculate a fit to the data above $k = k_h$.

ii) Then one has to determine Re C^+_{par} such that together with Im $C^+_{par} = k\,\sigma^+_{par}$ a crossing symmetric analytic function is obtained. Usually one takes a combination of special cases of eq. (2.20).

iii) Finally one has to calculate the integral

$$c_o^{par} = \frac{2}{\pi} \int_o^{k_h} \sigma^+_{par}(k)\, dk. \tag{2.24}$$

The real part at momenta above $k = k_h$ then follows from the value of $\bar{c}_o$, eq. (2.23) and

$$\text{Re } C^+(k) = \text{Re } C^+_{par} + (c_o^{par} - \bar{c}_o) + O(k^{-2}). \tag{2.25}$$

In most applications the last term is negligible. However, if σ^+ goes asymptotically to a constant, it can happen that Re $C^+(\infty)$ is finite. Then the correction $c^{par} - \bar{c}_o$ remains important even in the asymptotic region (see Ref. 31).

As an example we consider the parametrizations

$$\text{II} \qquad \begin{aligned} \sigma^+_{par} &= b_1\, k^{\alpha_1 - 1} + b_2\, k^{\alpha_2 - 1} \\ \text{Re } C^+_{par} &= -b_1 \cot(\alpha_1 \pi/2)\, k^{\alpha_1} - b_2 \cot(\alpha_2 \pi/2)\, k^{\alpha_2} \end{aligned} \tag{2.26}$$

and

$$\text{III} \qquad \begin{aligned} \sigma^+_{par} &= \sigma_o + \sigma_1 \ln(k/k_1) + b\, k^{\alpha - 1}, \\ \text{Re } C^+_{par} &= \frac{\pi}{2} k\, \sigma_1 - b \cot(\alpha\pi/2)\, k^{\alpha}. \end{aligned} \tag{2.27}$$

The fits to the data give the following values for the parameters

$$\text{II)} \quad \begin{aligned} b_1 &= 8.2991 \text{ mb GeV}^{1-\alpha_1} & b_2 &= 27.987 \text{ mb GeV}^{1-\alpha_2} \\ \alpha_1 &= 1.1497 & \alpha_2 &= 0.70187 \end{aligned} \tag{2.26a}$$

and

$$\text{III)} \quad \begin{aligned} \sigma_o &= 26.143 \text{ mb} & \sigma_1 &= 3.3021 \text{ mb} & b &= 38.848 \text{ mb GeV}^{1-\alpha} \\ & & k_1 &= 4516.1 \text{ GeV/c} & \alpha &= 0.70771 \end{aligned} \tag{2.27a}$$

c_o^{par} follows from eq. (2.24):

II) $$c_o^{par} = \frac{2}{\pi}\{\frac{b_1}{\alpha_1} k_h^{\alpha_1} + \frac{b_2}{\alpha_2} k_h^{\alpha_2}\} = 494.71 \qquad (2.26b)$$

III) $$c_o^{par} = \frac{2}{\pi}\{\sigma_o k_h + \sigma_1 k_h(\ln \frac{k_h}{k_1} - 1) + \frac{b}{\alpha} k_h^{\alpha}\} = 501.24 \qquad (2.27b)$$

and the expressions (2.25) for the real parts read

II) $$\mathrm{Re}\, C^+ = \mathrm{Re}\, C^+_{par} + 3.99 + O(k^{-2}) \quad \mathrm{GeV}^{-1}, \qquad (2.26c)$$

III) $$\mathrm{Re}\, C^+ = \mathrm{Re}\, C^+_{par} + 10.52 + O(k^{-2}) \quad \mathrm{GeV}^{-1}, \qquad (2.27c)$$

where $\mathrm{Re}\, C^+_{par}$ follows from eqs. (2.26), (2.27), (2.26a), (2.27a).

Since Fajardo et al.[11] mentioned a difference between our prediction for the real/imaginary part ratio $\rho_\pm$ and that of Lipkin[32], we shall also discuss the ansatz for his two-component Pomeron model. Lipkin was not interested in the best fit to the pion-nucleon data alone but rather to an overall fit to the total πp, Kp and pp cross sections, in which the coefficients are related by quark counting rules. His ansatz for the total isospin even and odd πN cross sections reads

IV) $$\sigma^+ = 2c_1(\frac{k}{20})^{0.13} + 4c_2(\frac{k}{20})^{-0.20} + \frac{3}{2} c_R (\frac{k}{20})^{-0.5}, \qquad (2.28)$$

$$\sigma^- = \frac{1}{2} c_R (\frac{k}{20})^{-0.50}. \qquad (2.29)$$

The total $\pi^\pm p$ cross sections $\sigma_\pm$ follow from eq. (2.1). His results for the parameters are[+)] (σ in mb, k in GeV/c)

$$c_1 = 6.5, \qquad c_2 = 2.2, \qquad c_R = 1.75. \qquad (2.30)$$

There are several deviations from our fit and from total cross section data:

i) The expression for σ^- agrees with our parametrization as far as the value of α_ρ is concerned, but our coefficient corresponds to $c_R = 1.48$ which is considerably lower than Lipkin's value. Figs. 5 and 6 show that Lipkin's fit is at variance with the data, in particular in the lower part of his momentum range ($k \gtrsim 2$ GeV/c).

+) Eqs. (2.28) and (2.30) differ from formulas and statements in Lipkin's papers because of printing errors. The above version is in agreement with his tables.

ii) Fig. 3 shows that Lipkin's fit to σ^+ is systematically lower than the Fermilab data[5] for the total cross sections above 200 GeV/c, which were not yet available when he wrote his paper.

We have used our method in order to produce a fit denoted by "IV", which uses Lipkin's parametrization eq. (2.28) from 10 GeV/c to infinity. The correction from the low energy part of the dispersion integral has been calculated from eq. (2.25)

$$\text{Re } C^+ = \text{Re } C^+_{par} + 9.1 \text{ GeV}^{-1} + O(k^{-2}) \qquad k > 10 \text{ GeV/c}$$

$$\text{Re } C^+_{par} = 2c_1 \tan(0.13\,\pi/2)\left(\frac{k}{20}\right)^{1.13} - 4c_2 \tan(0.2\pi/2)\left(\frac{k}{20}\right)^{0.8} - \frac{3}{2} c_R \left(\frac{k}{20}\right)^{0.5}. \tag{2.31}$$

The correction is negligible above 100 GeV/c, but at 20 GeV/c it is clearly visible in plots of ρ^+ (see below, Fig. 11).

Finally one can ask for the information which can be obtained if the experimental real part data deviate systematically from the prediction. We denote by k_H the momentum up to which total cross section data are available and assume that real part data have been measured only up to a momentum which is appreciably smaller, as it is usually the case. Then we consider the dispersion relation for the difference $\Delta\sigma^+ = \sigma^+ - \sigma^+_{Table}$ for $k<k_H$

$$\Delta\text{Re } C^+ = \text{Re } C^+_{exp} - \text{Re } C^+_{Table} = k^2 \frac{2}{\pi} \int_{k_H}^{\infty} \frac{\Delta\sigma^+}{k'^2 - k^2}\, dk = k^2 \frac{2}{\pi} \int_{k_H}^{\infty} \frac{\Delta\sigma^+}{k^2}\, dk + \ldots \tag{2.32}$$

We conclude that one can expect an increase of the discrepancy which is linear in k^2. If this can be established (at present the real part data are not accurate enough) one has one constraint for a modification of the high energy ansatz for σ^+. Because of the weight factor $1/k^2$ one cannot learn anything about the behaviour of the total cross sections at momenta far above k_H.

Since the behaviour of σ^+ at very high momenta is of great interest, one could think that the constraint derived from the real part data could be improved, for instance by introducing a weight factor in the dispersion relation or by considering sum rules which have very slowly convergent integrals. However, if one looks at the details, it is always seen that one cannot derive more information as long as one does not introduce an additional theoretical input (see sect. 9).

Eq. (2.32) can also be used if one wants to see the sensitivity of the prediction for Re C^+ to the input at much higher energies. As an example we show in Fig. 11 the case that the logarithmic term in eq. (2.3a) is cancelled above 1000 GeV/c.

$$\Delta\sigma^+ = -\sigma_1 \ln(\frac{k}{k_1})^2 \text{ for } k > k_H \tag{2.33}$$

$$\begin{aligned}\Delta \mathrm{Re}\ C^+ &= -\sigma_1 k^2 \frac{2}{\pi} \int_{k_H}^{\infty} k^{-2} \ln(\frac{k}{k_H})^2 dk + \ldots \\ &= -\frac{4}{\pi}\frac{\sigma_1}{k_H}\left[1 + \ln(\frac{k}{k_H}) + \frac{1}{2}\ln^2(\frac{k}{k_H})\right] k^2 + \ldots\end{aligned} \tag{2.34}$$

The application of the do-it-yourself method to the isospin odd case will be treated in sect. 8 and its relation to superconvergent sum rules in sect.9.6.

3. Other recent determinations of the real parts

3.1 Evaluations of the dispersion relation

The method of Hendrick et al. (Ref. 33) has some problems which have been discussed in Ref. 2. In the mean time, the authors performed an improved calculation (Ref. 34) which led to a good agreement with our table except in the high energy region, where the authors used another assumption for the asymptotic behaviour. Their estimate for the errors of the real part at high energies is rather arbitrary and should not be taken seriously.
Another evaluation has been made by Carter et al. (Ref. 35). Their table differs strongly from ours in the high energy region, because they use a subtracted version of the dispersion relation for C^- which is not compatible with the Goldberger-Miyazawa-Oehme sum rule (Ref. 36). We shall come back to this problem in section 8.4(see also Ref. 2).

3.2 Application of Pietarinen's expansion method

Instead of evaluating the principal value integrals, one can use an expansion method which was proposed by Pietarinen in 1972 (Ref. 37). The idea is to represent the invariant amplitudes by expansions in which each term has the correct cut structure. The ansatz reads

$$C^+(\omega) = C_N^+(\omega) + \hat{C}^+/(1+Z) \sum_{n=0}^{N} c_n^+ Z^n,$$
$$C^-(\omega) = C_N^-(\omega) + \omega(1+Z)^{1-\alpha_\rho} \sum_{n=o}^{N} c_n^- Z^n, \tag{3.1}$$

where the c_n are real and the variable Z is related to ω by a conformal mapping

$$Z = \frac{a - \sqrt{\mu^2 - \omega^2}}{a + \sqrt{\mu^2 - \omega^2}} = \frac{a+ik}{a-ik} . \tag{3.2}$$

$Z = 1$ corresponds to the threshold and the physical range $0 < k < \infty$ is mapped onto the upper half of the unit circle. The center of the most interesting range can be mapped onto $Z = i$ by a suitable choice of a. The region outside the unit circle belongs to the 2nd sheet of the ω-plane. For high momenta we have

$$1 + Z = \frac{2a}{a-ik} = \frac{2a}{k} i + \frac{2a^2}{k^2} + \ldots = \frac{2a}{-i\omega} + \ldots \tag{3.3}$$

Therefore a Regge term for C^- can be written as follows

$$C_\rho^-(\omega) = \gamma \frac{1 - e^{-i\pi\alpha_\rho}}{\sin\pi\alpha_\rho} \left(\frac{\omega}{\omega_o}\right)^{\alpha_\rho} = \frac{\gamma i}{\cos\pi\alpha_\rho/2} e^{-i\pi\alpha_\rho/2} \left(\frac{\omega}{\omega_o}\right)^{\alpha_\rho} \tag{3.4}$$
$$\sim \gamma\omega(-i\omega)^{\alpha_\rho - 1} \sim \omega(1+Z)^{1-\alpha_\rho},$$

i.e. the factor in front of the 2nd line of eq. (2.26) describes the Regge law eq. (2.6). In a similar way the function $\hat{C}^+/(1+Z)$ is adjusted to the asymptotic behaviour of σ^+, eq. (2.3a).

An advantage of this method is that the existing experimental values for Re $C^\pm$ can be fitted simultaneously with those of Im $C^\pm = k\sigma^\pm$ and that the question of subtractions does not occur.

The result of the fit does not depend on the number N as long as N is large enough ($\gtrsim 50$), since the cut-off is performed by a convergence test function method, adding a term

$$\chi_1^2 = \lambda \sum_{n=o}^{N} c_n^2 n^3 \tag{3.5}$$

to the χ^2 of the data and minimizing the sum.

Using an analytic function of the Breit-Wigner type, corresponding to

$$\sigma(k) = \frac{ak}{(k-b)^2 + c^2} , \tag{3.6}$$

the real part can be easily calculated analytically. We have compared the exact result with the approximate one, based on the expansion or on the evaluation of the principal value integral of the dispersion relation with our method. In both cases the agreement was satisfactory, the errors of Re $C^{\pm}$ being much smaller than the experimental uncertainties (Ref. 29).

For practical applications we prefer the dispersion method, because it is easier to insert different high energy assumptions. However, at $t \neq 0$ the expansion method is much superior to all others. More general and flexible expansions have been proposed and applied by R.Cutkosky (Ref.4,165).

3.3 Analytic parametrization methods

Several authors restricted themselves to the high energy region and fitted parametrizations with the correct analyticity and crossing properties to the total cross section data and sometimes also to the real part data (see for instance Refs. 30 and 38). The ansatz is usually based on combinations of the expression in eq. (2.20).
This method is a simplified version of the expansion method. It can easily happen that the result is at variance with the forward dispersion relation, where the real part receives contributions from low and intermediate energies, which are expressed mainly by the constant $c_o^{par} - c_o$ in eq. (2.21).
The analytic parametrization methods are of interest only at very high energies where this constant is negligible, or in reactions where the methods of sect. 2.2 to 2.42 are not applicable because the data are not available (see the reviews Refs. 39, 40 for further discussions).

3.4 The "derivative analyticity relation"

Several authors claimed that the analyticity properties, which are embodied in dispersion relations, can be equally well implemented by writing "derivative dispersion relations" (Refs. 41-43). A simple version is (Ref. 43)

$$\begin{aligned} \text{Im } C^{+} &= -\tan\left(\frac{\pi}{2}\frac{d}{d\xi}\right) \text{Re } C^{+}, \\ \text{Re } C^{-} &= \tan\left(\frac{\pi}{2}\frac{d}{d\xi}\right) \text{Im } C^{-}, \end{aligned} \tag{3.7}$$

where $\xi = \ln \omega$. The operator is approximated by a finite number of terms in the expansion

$$\tan\left(\frac{\pi}{2}\frac{d}{d\xi}\right) = \frac{\pi}{2}\frac{d}{d\xi} + \frac{1}{3}\left(\frac{\pi}{2}\right)^3 \frac{d^3}{d\xi^3} + \ldots \tag{3.8}$$

The formal expression is related to the dispersion relation as follows

$$\tan\left(\frac{\pi}{2}\frac{d}{d\eta}\right) = \frac{2}{\pi} k \int_0^\infty \frac{dk'}{k'^2 - k^2} \exp\left\{(\eta - \eta')\frac{d}{d\eta}\right\}, \tag{3.9}$$

where $\eta = \ln k$ (Ref. 44).

The method gives the correct result in the case of the ansatz (2.20), which is known for a long time (see for instance Ref. 45), but serious problems arise, if one attempts to apply it in the general case. This has been shown by Eichmann et al. (Ref. 46, see also Ref. 44 and Ref. 47). The result diverges in the resonance region.

Therefore Sukhatme et al.[42] treated resonance contributions separately, using analytic Breit-Wigner parametrizations fixed by inspection. If one wants accurate and reliable results, the method becomes much more complicated than a straight forward evaluation of the dispersion relation or Pietarinen's expansion.

At momenta above the resonance region the "derivative analyticity method" and the "analytic parametrization method" are closely related to our method described in sect. 2.3 which, however, gives in addition a correction term. This term represents the effects "nonlocal in energy", which are not always negligible. They can be calculated only from data at low and intermediate energies (see Refs. 19, 39, 44).

Another attempt to avoid the evaluation of the dispersion relation has been made by Gerdt et al. (Refs. 48, 28), who started from a uniformization of the forward scattering amplitude. For practical applications this method has similar shortcomings as the derivative analyticity method to which it is related.

A rigorous mathematical investigation of derivative analyticity relations has been performed by Fischer et al. (Ref. 49). The authors were able to show that under certain assumptions, which are stronger than the general principles of axiomatic field theory, derivative analyticity relations similar to those of Refs. 41-43 exist, but they contain only first derivatives. They point out that there is no theoretical basis for applications of such relations at a fixed finite energy.

4. Comparison of the predictions with real parts derived from Coulomb interference data

The real parts of the elastic forward amplitudes can be determined from differential cross sections in the Coulomb interference region. First we compare the published values for

$$\rho_{\pm} = \mathrm{Re}\ C_{\pm}/\mathrm{Im}\ C_{\pm} \qquad (4.1)$$

with the prediction from our tables.

In ρ_- (Fig. 8) the Brookhaven data of Foley et al.[12] and the earlier Serpuchov data of Apokin et al.[10] show a systematic deviation from the prediction which would be significant, if the error bars were taken seriously.
However, our reanalysis of the Brookhaven data has shown that there is no reason to doubt the validity of the dispersion relation[13]. The data are compatible with the prediction for the real part, if one admits a small normalization error. Evidence for problems with the fit of the authors is seen for instance at 16 GeV/c in the $\pi^- p$ data (Fig. 2c in Ref. 13) where the fit is made in the interval $0 > t > -0.05$ GeV^2 and its continuation to larger $-t$ deviates considerably from the other data of the same experiment.
The Serpuchov group has remeasured the real part at 40 GeV/c and the new result is in good agreement with our prediction[9].
At higher momenta, the CERN data of Burq et al.[8] and the final version of the Fermilab data of Fajardo et al.[11] show also no significant discrepancy.

At lower momenta, the agreement with the data of Vorobyev et al.[50] in the 2-6 GeV/c region is reasonable, but these data (as well as those of Ableev et al.[9] at 40 GeV/c and of Burq et al.[8] at 30 GeV/c) are not sufficient for a simultaneous

determination of the slope and this makes the test less reliable than in other cases.
The agreement with the Coulomb interference data of Baillon et al.[51] at and below 2 GeV/c is not satisfactory. It might be that the formalism for the interference between strong and electromagnetic interactions, which was developed for high energies[52], has to be modified if there are strong contributions from resonances.

In the case of ρ_+ the experimental information is much poorer (Fig. 9). There is a reasonable agreement with the Brookhaven data[12], the Serpuchov data[10] and the Fermilab data[11], but again there are discrepancies with the data of Baillon et al.[51] in the resonance region.

As mentioned above the high energy assumption for $\sigma^{\pm}$ is to some extent arbitrary and one could expect that the data for the real parts can help to exclude certain possibilities. For this purpose it is useful to consider the combinations

$$\rho^- = \frac{\sigma^+}{2\sigma^-}(\rho_- - \rho_+) + \frac{1}{2}(\rho_- + \rho_+) \tag{4.2}$$

and

$$\rho^+ = \frac{1}{2}(\rho_- + \rho_+) + \frac{\sigma^-}{2\sigma^+}(\rho_- - \rho_+). \tag{4.3}$$

If the seconds terms are neglected, the error in (4.2) amounts to 10% at 20 GeV/c and to 3% at 50 GeV/c, whereas the error in (4.3) the error is only 1% at 10 GeV/c.

Fig. 10 shows the quantity $\sqrt{k}\,(\rho_- - \rho_+)/2$ vs k as calculated from our Tables 80/1 and 80/2. As expected it is almost energy independent, because $\sqrt{k}\,\sigma^-$, ρ^- and σ^+ have a slow energy dependence separately. In addition we have plotted the same quantity as following from the Coulomb interference experiment of Fajardo et al.[11].

The uncertainty of the prediction is probably not larger than the difference between the two curves belonging to the Tables 80/1 and 80/2, since the l.h.side of eq. (4.2) is well determined from the charge-exchange forward cross sections and the total cross section data (see Figs. 5 and 6). We conclude that the plot in Fig. 10 is a good test for Coulomb interference data, from which the difference $\rho_- - \rho_+$ follows at present only with a much lower accuracy. Three of the points of Fajardo et al.[11] agree well with the prediction whereas two others

(125 and 150 GeV/c) even have a wrong sign, i.e. the ρ_--values are too small and/or the ρ_+-values are too large. This has to be kept in mind if one judges the deviations in Figs. 8 and 9.

Our figure for $(\rho_- + \rho_+)/2 \approx \rho^+$ (Fig. 11) shows the Fermilab data[11] and data constructed from the CERN data of Burq et al.[8] combined with the prediction for $\rho^+ - \rho_-$ from Table 80/1.

$$\rho^+ - \rho_- = -\frac{1}{2}(\rho_- - \rho_+) \approx -\rho^- \frac{\sigma^-}{\sigma^+} \approx -\frac{\sigma^-}{\sigma^+} . \qquad (4.4)$$

In addition we have plotted our prediction from Table 80/1 and from other high energy assumptions (sect. 2.3).

The curves belong to various fits to the σ^+ data in the range 10 - 370 GeV/c. The fits I - IV have been explained in sect. 2.3. Fit V agrees with fit I (= Table 80/1 and 80/2) up to 1000 GeV/c and assumes a constant σ^+ at all higher momenta. The dashed line in Fig. 11 is the prediction from Lipkin's Regge pole type formula. It coincides with fit IV above 100 GeV/c.

Fits I, II and V agree well with all σ^+ data up to 370 GeV/c (Fig. 3). Correspondingly the predictions for ρ^+ remain close together up to about 50 GeV/c. Even at 200 GeV/c the spread is not larger than the experimental error. It is remarkable that this includes fit V, which differs strongly from the others above 1000 GeV/c.

Obviously, the dispersion relation is not a good "crystal ball which can view the road to asymptopia" (Ref. 53). The sensitivity to the behaviour of the total cross sections at higher momenta is somewhat better in the isospin odd case.

Fit III passes slightly below the σ^+-data above 200 GeV/c. Its ρ^+-value lies close to the others up to 50 GeV/c, but it is somewhat lower at 200 GeV/c. Lipkin's parametrization for σ^+ (fit IV) is appreciably lower than the data above 200 GeV/c and therefore its ρ^+-value separates from the others already at about 30 GeV/c and it remains lower at all higher momenta of our range.

The distance between the dashed and dot-dashed lines in Fig.11 shows the error of Lipkin's Regge pole formula for the real part. It is not of interest to show the continuation of Lipkin's prediction to 2 GeV/c as it was done in Figs. 13b and e of Ref.[11], since the error is increasing and one cannot expect to see the

correct transition to the resonance structure of ρ, which is accurately described by our Tables (see Figs. 8 and 9).

The small differences between our prediction and that of Engelmann et al.[34] are due to the fact that we assumed that all structures of σ^- in the range 5 - 45 GeV/c are due to errors of the somewhat contradictory data (see Fig. 5) and that (in Table 80/1) we fitted the charge-exchange forward cross sections simultaneously. Engelmann et al.[34] used in this range a spline fit, following the apparent structures of σ^- more closely and did not attempt to fit the charge-exchange data. This led to the discrepancy shown in their figure 3.

5. Comparison of the predictions with real parts derived from phase shift solutions

The input of phase shift analysis includes usually a table of forward amplitudes, whose real parts have been calculated from dispersion relations, using a smooth interpolation of the total cross sections in the integrand. Since a finite error is assigned to this input, it will be somewhat different form the forward amplitudes $C_{ph}(\omega)$ reconstructed from the phase shift solution.

First we consider the change of the real parts

$$\Delta \mathrm{Re}\ C \equiv \mathrm{Re}\ C_{ph} - \mathrm{Re}\ C_{Table} \tag{5.1}$$

and look for systematic deviations of ΔRe C from zero.

In calculations of the real part from the dispersion relation one has to take two numbers from the result of earlier phase shift analyses: the subtraction constant $C^+(\mu)$ and the coupling constant f^2.

In principle, one could try to determine a correction Δf^2 from Re C, but this method is less accurate than the determination of f^2 from the fixed-t dispersion relation for the amplitude B^+ at different t-values, which has been carried out in connection with phase shift analysis (see sect. 10 in Ref. 3)[+)]. Therefore we

[+)] Samaranayake has recently published a new determination of f^2 from forward dispersion relations, continuing his earlier work with Woolcock (Ref. 54). Unfortunately he used only old phase shift analyses of 1959 - 73 and the result derived from one of the new experiments, ignoring more recent phase shift analyses which include other new data. We think that new determinations of f^2 are of interest only if they include the most recent information, which can be easily found for instance in the "Compilation of Coupling Constants and Low-Energy Parameters" (Ref. 16), which is updated in regular intervals.

work with $f^2 = 0.079$ and test only the value of $C^+(\mu)$, checking simultaneoulsly the consistency of $C^-(\mu)$ with the result following from the unsubtracted dispersion relation (Goldberger-Miyazawa-Oehme sum rule, Ref. 36)

$$C^-(\mu) = \frac{8\pi f^2 \mu}{\mu^2 - \omega_B^2} + 4\pi\mu J \ , \tag{5.2}$$

$$J = \frac{1}{2\pi^2} \int_0^\infty \sigma^-(k)\, dk/\omega \ . \tag{5.3}$$

The threshold values are related as follows to the isospin 1/2 and 3/2 scattering lengths a_1 and a_3

$$C^\pm(\mu) = 4\pi a^\pm (1+\mu/m), \quad a^+ = \frac{1}{3}(a_1+2a_3), \quad a^- = \frac{1}{3}(a_1-a_3). \tag{5.4}$$

In order to search for systematic deviations of ΔRe C from zero, which indicate that corrections to the threshold values $C^\pm(\mu)$ are necessary, we ignore possible errors of the total cross sections and of f^2 and construct ΔRe C from once subtracted dispersion relations for $C^\pm$.

One obtains

$$\Delta\text{Re } C_+(\omega) = \Delta C^+(\mu) - \frac{\omega}{\mu}\Delta C^-(\mu) = \Delta\text{Re } C_-(-\omega). \tag{5.5}$$

In Fig. 12 we have plotted ΔRe C_+ on the right hand side and ΔRe C_- on the left hand side. The question is whether the best straight line through the points differs from the abscissa in a significant way.

It is difficult to estimate errors of Re C_{ph} and of Re C_{table}, because the most important errors are systematic ones which must exist because of discrepancies between different data sets. Sometimes they are much larger than the error estimates of the authors (see for instance Ref. 14 and Ref. 15). Although errors of C_{ph} could have been calculated from the error correlation matrix of the CMU-LBL group, we consider only the best fit to the points shown in Fig. 12.
The parameters of the best fit are in the case of the Karlsruhe-Helsinki 78 phase shift solution

$$\Delta C^+(\mu) = 0.11 \ \text{GeV}^{-1}, \qquad \Delta C^-(\mu) = 0.016 \ \text{GeV}^{-1} \tag{5.6}$$

These numbers have to be compared with the input for $C^+(\mu)$ the result for $C^-(\mu)$ in our Table 80/1

$$
\begin{aligned}
C^+(\mu) &= -0.99\ \text{GeV}^{-1}, \qquad \frac{C^+(\mu)}{4\pi} = -0.011\ \mu^{-1} \\
C^-(\mu) &= \ 9.53\ \text{GeV}^{-1}, \qquad \frac{C^-(\mu)}{4\pi} = \ 0.106\ \mu^{-1} \\
3a^+ &= -0.0288\ \mu^{-1}, \qquad 3a^- = 0.276\ \mu^{-1}.
\end{aligned}
\tag{5.7}
$$

In our opinion, eq. (5.6) shows that the agreement is reasonable, in particular since there are other sources of errors which have been ignored in the fit. If one uses Re C as calculated from the CMU-LBL phase shift solution, one obtains from the fit

$$
\Delta C^+(\mu) = \ 1.42\ \text{GeV}^{-1}, \qquad \Delta C^-(\mu) = 0.248\ \text{GeV}^{-1}. \tag{5.8}
$$

The value of $\Delta C^+(\mu)$ is now larger. This is related to the fact that the CMU-LBL group used their own table of forward amplitudes (Ref. 34). Unfortunately the authors of Ref. 34 have not made a precise statement on the values assumed for $C^+(\mu)$ and f^2.

An estimate from the Re C-values at the lowest momenta suggests that their $C^+(\mu)$ value is higher by about 0.8 GeV^{-1} than ours.

We have also included a table of the differences ΔRe C, eq. (5.1), because it is of interest to know at which momenta the largest values of ΔRe C occur. A possible reason is a normalization error, another one is that Re C varies rapidly and the momentum scales of the total and differential cross section experiments have an error relative to each other.
Furthermore, this table give a realistic estimate of the uncertainties of the real parts (see sect. 3 of Ref. 2 and Ref. 34 for further discussions).

Fig. 13 shows the difference between the total cross sections reconstructed from phase shifts and the smooth interpolations of the total cross section data in our table. The structures in the region of the first resonance are due to the fact that our interpolation in the tables does not take into account all charge-dependent corrections (see the paper by Koch and Pietarinen[3] for a description of phase shift analysis in this range).

6. Extrapolation into the Unphysical Region

The evaluation of the dispersion integrals gives not only the real parts in the physical region but also the (real) amplitudes between the s- and u-channel thresholds. Since the nucleon pole terms are rapidly varying in this range, we prefer to consider

$$\tilde{C}^{\pm} \equiv C^{\pm} - C_N^{\pm}, \tag{6.1}$$

where C_N is given in eq. (2.12) Table 80/5 lists $\tilde{C}^-/\omega$ and $\tilde{C}^+ - g^2/m$ in the unphysical region in units of μ^{-2} and μ^{-1} respectively. This table follows from the dispersion relations, using the same input as in table 80/1. At present it is not possible to give reliable estimates of the errors, since the result depends to some extent on total cross sections at low energies, where accurate data do not exist. Moreover, there are still problems with charge-dependent effects.

The relation between tables 80/1 and 80/5 at threshold is explained by the following equations:

$$\text{Re } C^+(\mu) = -\frac{4\pi f^2}{m(1-\mu^2/4m^2)} + \{\tilde{C}^+(\mu) - g^2/m\} \tag{6.2}$$

$$= (-0.1485 + 0.010)\ \mu^{-1} = -0.991\ \text{GeV}^{-1}.$$

$$\text{Re } C^-(\mu) = \frac{8\pi f^2/\mu}{1-\mu^2/4m^2} + \tilde{C}^-(\mu) \tag{6.3}$$

$$= (1.996 - 0.666)\mu^{-1} = 9.53\ \text{GeV}^{-1}.$$

The s-wave scattering lengths following from these amplitudes are given in eq. (5.7). For some applications it is of interest to know the value of

$$J = \frac{1}{4\pi\mu}\tilde{C}^-(\mu) = \frac{1}{2\pi^2}\int_0^\infty \frac{\sigma^-(k)}{\omega}\,dk = -0.0530\ \mu^{-2} = -1.06\ \text{mb}. \tag{6.4}$$

The amplitudes of Table 80/5 are of interest for a comparison of πN amplitudes with predictions from Current Algebra. The quantity $\tilde{C}^+ - g^2/m$ at $\omega = 0$ is needed, if one wants to determine the "sigma term" by an extrapolation along the line $\nu = 0$ (Refs. 55, 59).

$\tilde{C}^-/\omega$ is of interest for a test of the Adler-Weisberger relation (Ref. 82). If it is combined with the Goldberger-Treiman relation one obtains the prediction

$$\tilde{C}^-/\nu \Big|_{\substack{\nu=0,\\ t=0}} = (1 - g_A^2)/f_\pi^2 = -0.66\ \mu^2 \qquad (6.5)$$

which is valid for zero mass pions. $f_\pi = 0.945\mu$ is the pion decay constant and $g_A = 1.26$ the axial vector coupling constant. The prediction eq. (6.5) differs appreciably from our result in Table 80/5 ($-0.46\mu^2$) which is valid for physical pions. It is difficult to estimate the effect of the extrapolation in pion mass. There are two other kinematical points which go to the origin of the ν,t-plane in the zero pion mass limit: $\nu = 0$, $t = 4\mu^2$ and $\nu = \mu$, $t = 0$, where $\tilde{C}^-/\nu$ has the values $-0.61\ \mu^2$ and $-0.68\ \mu^2$ respectively (see sect. 10 of Ref. 3 for details).

An other application of Table 80/5 is that one can derive the value of the low energy expansion of the C-amplitudes at $\nu = t = 0$. This expansion has been used by many authors (sect. 5.6 in Ref. 16) for discussions of low-energy models, since it was introduced in 1972 (Ref. 59). - A singularity in the 2nd sheet of the ω-plane,which is related to the nucleon Born term,has been studied by Sawada[157]. Finally Table 80/5 shows the magnitude of the cusp effects in Re $C^\pm$ at threshold, which are a consequence of unitarity. These effects have been neglected in many models for πN scattering at low energies (cf. Fig. 1 in Ref. 59).

7. Zeros of forward scattering amplitudes

Complex zeros of pion-nucleon forward scattering amplitudes have been of interest in several theoretical investigations[56-62, 77]. A rigorous result of Jin and Martin[57] based on positivity has the consequence that in the range $0 \le t < 4\mu^2$ the amplitude[+)]

$$D^+(\nu,t) = A^+ + \nu B^+ \qquad (7.1)$$

has at most two zeros in the physical sheet of the ν^2-plane ($\nu = \omega + t/4m$). At $t=0$ the amplitude D^+ agrees with C^+. According to our calculation the forward ampli-

+) G. Sommer has shown that the combination D^+ of the πN amplitudes has the positivity property which is needed if one wants to extend results derived for the spinless case to spin 0 - spin 1/2 scattering (Ref. 63, 64). The usual spin no-flip amplitude can also be chosen for this purpose (Ref. 65). The amplitude D has the advantage to have simple analyticity properties.

tude C^+ has only one zero in the ω^2-plane at $\omega^2 = -0.085\ \mu^2 = -0.0018\ GeV^2$ (see Fig. 1 in Ref. 59, which differs only slightly from the new result of Table V).
The zeros at $t \neq 0$ have been discussed in Ref. 60. It turns out that there are two zeros in the physical sheet between $t = 4\mu^2$ and a small positive t-value, where the 2nd zero, which lies near threshold, enters the 2nd sheet. With the present experimental accuracy one cannot exclude the possibility that the 2nd zero lies in the first sheet at threshold (i.e. that $a^+ = 0$). Both zeros can be continued to the neighborhood of the Cheng-Dashen point $\nu = 0$, $t = 2\mu^2$ and it can be shown that they are related to the double zero of the pseudovector nucleon Born term at $t = 2\mu^2$, which is strongly distorted by the influence of the non-vanishing sigma term of current algebra (Ref. 60).

The zeros of the isospin odd forward amplitude C^- have been discussed by Sugawara and Tubis[56]. From an earlier version of our Table they concluded that the number of zeros in the first sheet of the ω-plane is either 7 or 11.
A zero at $\omega = 0$ follows from crossing antisymmetry. Then there are two zeros at $\omega = \pm 0.58i$ GeV and 4 zeros at $\omega = \pm 1.38 \pm 0.07i$ GeV. The existence of 4 further zeros is strongly suggested by the fact that the prediction for the modulus of the charge-exchange forward amplitude at 120 MeV/c is zero within the errors. Again it cannot be decided from the present experimental data whether these zeros occurs in the first or in the 2nd sheet. The continuation of these zeros to $t \neq 0$ and the relations to zeros at real s and complex t has been discussed in Ref. 60 - 62.
The location of zeros in the s-plane is important, if one wants to apply dispersion relations for the logarithm of the amplitude which connect the modulus and the phase (Refs. 66, 67, see sect. 9.52).
Further results on zeros of amplitudes are discussed in sect.3.8 of Eden's review[77].

8. Charge-exchange forward scattering

In sect. 2.1 we have already discussed a common fit to the data for charge-exchange forward scattering and to the total cross section difference σ^- at high energies, the result being that the data are compatible with the simple choice $\alpha_\rho(0) = 0.500$, if radiative corrections to the charge-exchange cross section are taken into account. In the following we add several comments to questions which have been discussed in the literature and consider also data at intermediate and low energies.

8.1 Extrapolation of the trajectory to t > 0

When the first charge-exchange data at high energies became available in 1965-66 (Refs. 68, 69) it was found that fits to the reggeized ρ-exchange model led to a trajectory which aimed approximately to $\alpha = 1$ at $t = m_\rho^2$ (Ref. 70) as expected in this model. The discovery of a spin 3 particle, the g-meson, on the same trajectory was a further confirmation. The parameters of a straight line through the points belonging to the ρ and g mesons in the α,t-plane are

$$\mathrm{Re}\ \alpha_\rho(t) = 0.46 + 0.89\ t, \tag{8.1}$$

if the masses are taken from the 1978 edition of the "Review of Particle Properties". A new determination of the g-meson mass led to a value which is higher by more than two standard deviations (Ref. 71) and we have instead of (8.1)

$$\mathrm{Re}\ \alpha_\rho(t) = 0.50 + 0.83\ t. \tag{8.2}$$

Both sets of parameters are close to the best fit reported by Barnes et al.[7] in the range 20 - 200 GeV/c for charge-exchange scattering

$$\alpha_\rho(t) = 0.481 + 0.928\ t. \tag{8.3}$$

However, one should notice that an accurate agreement between the parameters cannot be expected for the following reason. According to Regge theory (Refs. 72, 73) $\alpha_\rho(t)$ fulfills in simple cases a dispersion relation

$$\alpha_\rho(t) = \alpha_o + \alpha_1 t + \frac{1}{\pi}\int_{4\mu^2}^{\infty} \frac{\mathrm{Im}\ \alpha_\rho(t')}{t'-t}\,dt', \tag{8.4}$$

which shows that the trajectory has a branch point at $t = 4\mu^2$. α_ρ is real for $t < 4\mu^2$ and complex-valued for larger t. Other types of trajectories have been discussed for instance by Oehme (Ref. 166).
$\mathrm{Im}\ \alpha_\rho$ is known at some points $t = m_{res}^2$ from the widths Γ_{res} of the resonances (see Fig. 5.7 in Ref. 73)

$$\mathrm{Im}\ \alpha_\rho(t_{res}) = \Gamma_{res}\ \mathrm{Re}\ \alpha_\rho'(t_{res})\ m_{res}. \tag{8.5}$$

The derivative $\mathrm{Re}\ \alpha_\rho'$ is taken from eq. (8.2): $\alpha_\rho' = 0.83\ \mathrm{GeV}^{-2}$.

Since Im $\alpha_\rho > 0$ is small, a small upward curvature of $\alpha_\rho(t)$ is expected on the left of $t = 4\mu^2$. The cusp effect at the branch point is weak, since it is of the type $\alpha_\rho \sim (4\mu^2-t)^\lambda$ (Ref. 72), where $\lambda = \alpha_\rho(4\mu^2) + 0.5 = 1.06$ (from eq. (8.2)).

The Regge model is only a framework; one cannot predict the trajectory. Lovelace was able to derive a prediction by imposing Adler zeros in a Veneziano model for $\pi\pi$-scattering (Ref. 74)

$$\alpha_\rho(t) = 0.5 + 0.5(t-\mu^2)/(m_\varrho^2-\mu^2) = 0.48 + 0.86t. \qquad (8.6)$$

At that time the charge-exchange data led to $\alpha_\rho = 0.58$. It is remarkable that the data at higher momenta approach the prediction (8.6) rather closely, but one should remember that the Veneziano-Lovelace model has problems in other applications (Ref. 75).

8.2 Asymptotic behaviour of C^-

We do not intend to give a complete summary of the large number of papers devoted to charge-exchange scattering at high energies (at least in the early seventies it was larger than the number of data points). Instead we shall discuss only a few of them which have been published recently or are of interest for other reasons.

Fig. 14 shows the Argand diagram of C^- at high energies. The discrepancy between the result derived from a best fit to the total cross section data (Table 80/2) and that derived from a best fit to the charge-exchange forward scattering data of Barnes et al.[7] has led to several proposals for modifications of the ansatz for the asymptotic behaviour of C^-. Some time before, another discrepancy between the prediction for C^- derived from the Serpuchov data for the total cross section difference and for the charge-exchange forward cross section triggered a number of speculations about a possible violation of the Pomeranchuk theorem (for instance Refs. 76, 77). Nowadays it is believed that the earlier Serpuchov data for the total cross sections (Fig. 5) have a systematic error.

i) An additional term in the unsubtracted dispersion relation for C^-

If the unsubtracted dispersion relation is derived from quantum field theory, one obtains an additional real term $c\omega$ on the right hand side of eq. (2.11),

which cannot be calculated and for which a physical interpretation is not known*) (Ref. 36). It is generally assumed that this term is zero, because the evaluation of the dispersion relation (2.11) (Tables 80/1 and 80/2) gives a result for the value of $C^-(\mu)$ which is in good agreement with the direct determination from phase shift analysis at low energies (see eq. (5.7) and Ref. 3). The dispersion relation at $\omega = \mu$ is the "Goldberger-Miyazawa-Oehme sum rule" and $C^-(\mu)$ is usually expressed in term of the s-wave scattering length difference $a_1 - a_3$.

Of course a small finite value of c cannot be detected in this way. Since c is multiplied by a factor ω, there is a better chance to see it in the real part at high energies. In some earlier discussions (Ref. 78) $c = 0$ was derived from the assumption Re $C_\pm/\omega \to 0$ for $\omega \to \infty$, which was plausible at a time when it was believed that the total cross sections go to a constant in the high energy limit. However, our present ansatz eqs. (2.3a) and (2.16) violates this condition: Re $C^+/\omega \sim \ln k \to \infty$. Therefore it is of interest to search in the high energy data for possible effects of a non-vanishing c in Re C^- (Ref. 79-81, 84, 39, 19). Fig. 10 shows that charge-exchange data are more suitable for this purpose than Coulomb interference data.

In our Argand diagram of C^- at high energies (Fig. 14) the additional term $c\omega$ should cause a systematic deviation from the straight line, which belongs to the Regge model.
First we have plotted the amplitude C^- of Table 80/1, which follows from our Regge fit with $\alpha_\rho = 0.500$, and of Table 80/2, which is derived from a fit to the total cross section difference. A third curve has been constructed from the charge-exchange forward cross section data without assuming the Regge model: $|C^-|$ follows from $d\sigma_o/dt$ and Im $C^- = k\sigma^-$ is taken from the total cross section difference (curve "F").

Curve "F" behaves approximately as expected, if an additional term $c\omega$ existed in the dispersion relation. An estimation of c from {Re C^- (Table 80/2) - Re C^- (curve "F")}$/\omega$ gives (Ref. 19, 39, we have now used the final data of Ref. 7)

$$c \approx -0.27\ \text{GeV}^{-2} = -0.11\text{mb}, \quad c\mu/C^-(\mu) = -0.004.$$

The correction to $C^-(\mu)$ or $a_1 - a_3$ and to the Adler-Weisberger relation (Ref. 82) are far below the present accuracies.

---

*) except for the "Odderon"-exchange model of Leader et al.[84].

Bourrely et al. (Ref. 38) determined a value for c from a fit to their analytic parametrization. The result cannot be taken seriously, because they used only Coulomb interference data and their value is at variance with the charge-exchange data. The work of Joynson et al. (Ref. 84) will be discussed in iii).

As mentioned in sect. 2.1 we prefer another explanation for the discrepancy. The radiative corrections[25,26] to the charge-exchange forward cross sections have the correct sign and order of magnitude to resolve the discrepancy between curves "F" and 80/1 in Fig. 14.
Furthermore, it is useful to compare the discrepancy with the errors. We have plotted in Fig. 14 in addition to the result of fits an experimental point from the data for $d\sigma_o/dt$ and σ^- at 200 GeV/c, showing the statistical errors only. It is obvious that, with the present data, there is no significant evidence against the simple reggeized ρ-exchange model.

ii) The "odd Pomeron" exchange

A group of authors[83] proposed to add to the ρ-exchange term an expression

$$C^-_{OP}(s) = c_{OP}\, s \left\{ \ell n^2 \frac{s}{s_{OP}} - i\pi\, \ell n \frac{s}{s_{OP}} \right\}, \qquad (8.7)$$

which cannot be excluded from general arguments, but looks very strange from a physical point of view (the name "odd Pomeron"-exchange is misleading). The ansatz is a special case of eq. (8.16)

It is clear that for a suitable choice of the parameters ($c_{OP} < 0$) one can describe the deviation of curve "F" in Fig. 14 from curve 80/2. However, since the discrepancy is within the present uncertainties as discussed above, and since two additional parameters are introduced, we think that there is no significant evidence for this proposal, which leads to the strange conclusion that σ^- has a minimum at 5 000 GeV/c and then grows to infinity.

iii) ($\rho+\rho'$)-exchange models, "Odderon-exchange"

Since in a reggeized ρ-exchange model the no-flip and flip amplitudes have the same phase, the polarization P_o in charge-exchange scattering is predicted to be zero. However, non-zero values have been measured at small $|t|$ up to 11 GeV/c. Therefore, there must be a secondary contribution, for which one can attempt a

parametrization as an effective ρ'-Regge pole exchange term. Barger and Phillips (Refs. 85, 86) noticed that the 2nd pole is not needed in the forward direction and therefore they assumed a factor of t in both residue functions.

Other authors (we mention only two recent investigations: Refs. 84, 87) introduce a non-vanishing ρ'-contribution at $t = 0$. If one looks at the Argand diagram in Fig. 14, it is clear that fits of this type cannot be successful, since the prediction will approach the straight line belonging to ρ-exchange at high energies and this is qualitatively different from the shape of curve "F".
Another problem with Nakata's work[87] is that his value $\alpha_{\rho'}(0) = -1.8$ lies below -1. According to the dispersion relation for C^- the low energy contribution to Re C^- decreases as k^{-1}. Therefore, the application of the Regge formulas is wrong, unless one has shown that due to the validity of a sum rule the ("non-local") low energy contribution vanishes. Since the coefficient of the k^{-1}-term depends on the high energy ansatz for Im C^-, one cannot use earlier evaluations of the sum rule (see sect. 9.6).
In another paper (Ref. 88) Nakata discusses the well-known fact (see for instance Refs. 80, 84, 86, 19) that there is a problem, if one wants to fit the data for σ^- and for $d\sigma_o/dt$ with a simple Regge pole model.

Leader et al. (Ref. 84) tried to fit a $(\rho+\rho')$ model to these data and found, as expected from the above argument, that a satisfactory result cannot be obtained and that a new term is needed which has a negative increasing real part at Fermilab energies. These authors prefer two possibilities:
(a) The existence of a new odd-signatured Regge pole, whose intercept at $t = 0$ is at 1. Since it is analogous to the Pomeron they call it "Odderon":

$$C^-_{\text{odderon}}(\omega,t) = c\left[i + \tan\alpha(t)\,\frac{\pi}{2}\right]\left(\frac{\omega}{\omega_o}\right)^{\alpha(t)}\{1-\alpha(t)\}\,e^{\lambda t} \qquad (8.8)$$

where c is real and $\alpha(t) = 1 + \alpha' t$. At $t = 0$ this agrees with the case treated above in i).

(b) An amplitude which has the maximal growth possible according to quantum field theory. It agrees with the "odd Pomeron", eq. (8.7).

Leader et al.[84] stressed an important point: substantial progress in the understanding of the C^- amplitude at high energies can only be expected if the polari-

zation in the charge-exchange reaction is measured. At present[27] the experimental information is contradictory at 4 -8 GeV/c and no data exist above 11 GeV/c, whereas elastic polarizations have been measured up to 100 GeV/c. If the "Odderon"-model is correct, the polarization P_o should increase in the Fermilab energy range and then finally decrease at ultrahigh energies.
A shortcoming of this investigation is that the authors used the preliminary data of Barnes et al., which differ appreciably from the published version[7]. Since the energy dependence of the phase of the forward amplitude is important for these discussions, we show a plot of ρ^- in Fig. 15.

iv) Regge cuts

At one time it was believed that Regge cuts give a substantial contribution to the charge-exchange amplitude. However, "excellent fits" to the data are not impressive, if a model contains not only a number of adjustable parameters but includes also a prescription which is to some extent arbitrary. In our opinion, there exists no convincing evidence for important contributions of Regge cuts to pion-nucleon scattering amplitudes. Critical reviews can be found in Refs. 73, 88, whereas the review by Kane and Seidl (Ref. 89) on absorption models comes to a more optimistic conclusion.

v) Do-it-yourself method for C^-

It might be of interest to calculate the real parts for a high energy assumption on σ^- which differs from that in Tables 80/1 or 80/2. We start from eq.(2.18)

$$\text{Re } C^-(\omega) = c_\rho \tan(\alpha_\rho \pi/2)\ k^{\alpha_\rho} + 14.0/k + \ldots \tag{8.9}$$

which belongs to Table 80/2, the values of the parameters being $\alpha_\rho = 0.5337$ and $c = 7.527\ \text{GeV}^{-1-\alpha_\rho}$.

In analogy to the procedure in sect. 2.3 we choose a parametrization which fulfills the dispersion relation

$$\text{Re } C^-_{par}(\omega) = \omega \frac{2}{\pi} \int_o^\infty \frac{\sigma^-_{par}}{k'^2-k^2} \frac{k'^2\, dk'}{\omega'} = \omega \frac{2}{\pi} \int_\mu^\infty \frac{k'\, \sigma^-_{par}\, d\omega'}{\omega'^2-\omega^2}. \tag{8.10}$$

Then we subtract eq. (8.10) from the dispersion relation eq. (2.11) and obtain

$$\text{Re } C^-(\omega) = \text{Re } C^-_{par} + C^-_N + \omega \frac{2}{\pi} \int_\mu^{\omega_h} \frac{k'(\sigma^- - \sigma^-_{par})}{\omega'^2-\omega^2}\, d\omega' \tag{8.11}$$

$$= \mathrm{Re}\, C^-_{par} + \frac{1}{\omega}\{8\pi f^2 + (d_o^{par} - d_o) + \ldots\} + O(\omega^{-3}), \tag{8.11a}$$

where

$$d_o = \frac{2}{\pi}\int_o^{\omega_h} \sigma^-(\omega)\, k\, d\omega = \frac{2}{\pi}\int_o^{\omega_h} \mathrm{Im}\, C^-(\omega)\, d\omega \tag{8.12}$$

and d_o^{par} is the same integral with σ^-_{par}. Instead of eq. (2.6) we take now an ansatz for ρ-exchange which practically agrees with (2.6) at high energies since $\omega = k\sqrt{1+\mu^2/k^2} \approx k$:

$$C^-(\omega) = c_\rho\,(\tan(\alpha_\rho\,\pi/2) + i)\;\omega^{\alpha_\rho}, \tag{8.13}$$

(This version follows from Regge theory, whereas (8.9) is used as a very good high energy approximation.) Inserting (8.13) into (8.12) we find with our choice for the parameters and ω_h = 10 GeV

$$d_o^{par} = \frac{2c}{\pi}\,\frac{\omega_h^{\alpha_\rho+1}}{\alpha_\rho+1} = 106.8 \tag{8.14}$$

and with eq. (8.9) and (8.11)

$$d_o = 103.28 \tag{8.15}$$

A modified high energy assumption is usually constructed as a superposition of the analytic parametrizations

$$C^-(\omega) = i(-i\omega)^\alpha\,(\ell n\omega - i\pi/2)^\beta\,, \tag{8.16}$$

which differs from eq. (2.20) mainly by a factor i, because C^- is odd under crossing.(see Ref.77, Chapter 7.1 of the book).
The relation of the above discussion to superconvergent sum rules will be discussed in sect. 9.

8.3 Charge-exchange scattering at intermediate and low energies

Only a few experiments have been performed on charge-exchange scattering at very small $|t|$-values in the intermediate and low energy region and all of them 15 or more years ago.

i) A Saclay-Orsay collaboration has measured charge-exchange near-forward scattering at many momenta between 2.5 and 6 GeV/c. Unfortunately these data have never been published in detail. Only a small part of the results is briefly mentioned in Ref. 69. The other data have been distributed as private communications from M. Yvert and O. Guisan. They are available on the Karlsruhe data tape (Ref. 91). The extrapolation to $t = o$ has been performed by W. Grein and P. Kroll, who used the Regge pole formula for ρ-exchange and parametrized the t-dependence in a flexible way (Refs. 70, 92). Their result has been plotted in Fig. 6, a table is given in the Appendix. One should notice that the extrapolation to $t = 0$ is difficult, because the cross section has a peak at $t \approx -0.03$ GeV^2 and there are only a few points on the steep decrease towards $t = 0$.

Fig. 6 shows that, at some momenta, there are appreciable deviations from the prediction. We believe that the structures are correctly given by the prediction, because they are determined by the structures of the total cross section difference in the same momentum region and these have been measured in a reliable way by Citron et al.[21].

ii) Further data at very small $|t|$ have been measured by Borgeaud et al. (Ref. 93) in 1964. The agreement with the prediction is reasonable above 1.2 GeV/c, but there some discrepancies around 1.0 GeV/c, where the prediction comes mainly from the optical theorem.

iii) At and above 1.59 GeV/c the data of Nelson et al.[94] give a lower forward cross section than our prediction. However, the discrepancy is not larger than some discrepancies between this experiment and the more recent one by Brown et al.[95].

In earlier discussions of charge-exchange forward scattering (Ref. 96) we have compared the prediction with many other "experimental" forward cross sections, which were determined from Legendre fits to data in large angular intervals or to data, in which only the γ-distribution has been measured (Bulos et al.[97], Kistiakowski et al.[98]).

Nowadays the overall agreement of the prediction from the dispersion relations with the charge-exchange forward cross sections and with results of Coulomb interference experiments is so good that the comparison is not made any more in

order to test the dispersion relations. Instead one wants to test the compatibility between the total cross section data and the differential cross sections, a discrepancy being considered as an indication for an experimental error. Furthermore, fits to the angular distributions are improved, if the prediction at $t = 0$ is treated as an additional experimental point.
In their paper[95] Brown et al. compared their results, which have the most forward points at $\cos\theta = 0.93 \ldots 0.95$, with our predictions. They noticed that the figures suggest a good agreement in some cases and a large disagreement in others.

In Ref. 99 we have performed a careful analysis of the data and came to the following conclusion. If Legendre fits to the differential cross sections are made and the prediction at $t = 0$ is used as part of the input, there are no significant problems. In some cases the first points are not well fitted, but the deviations are not larger than those which occur between the data of Refs. 95 and 94. An accurate extrapolation of the $d\sigma_o/dt$ data to $t = 0$ is not possible with the data of Brown et al.[95], because this experiment has been designed for taking data in a large angular range ($-0.95 < \cos\theta < 0.95$). It turns out that, in some energy ranges, $d\sigma_o/dt$ has a strong near-forward structure, the variation being large even in the small interval $0.95 < \cos\theta < 1$.
It would be desirable to perform another experiment (similar to that of Borgeaud et al.[93]), in which this structure is accurately measured, because the result would be a valuable input for phase shift analysis. The information on the highest partial waves comes mainly from the structures near 0^o and 180^o.

At 2.7 GeV/c the data of Brown et al.[95] can be compared with the above mentioned data of the Saclay-Orsay group (Yvert et al.). It turns out that, at some t-values, the cross sections differ considerably from each other.
Because of these problems with the extrapolation to $t = 0$ of the most accurate experiment[95], we shall not discuss the comparison with earlier data (Refs. 97, 98 and others, see Ref. 96).
Finally we would like to point out that the prediction for the charge-exchange forward cross section on the left wing of the first resonance $\Delta(1233)$ shows a very rapid rise. Accurate data in this region would be of interest for a phase shift analysis which tries to find charge-dependent effects like a difference between the widths of Δ^{++} and Δ^o.

8.4 The subtracted dispersion relation for C^-

We start with the unsubtracted relation (2.11) and subtract only the integral

$$\mathrm{Re}\ C^-(\omega)/\omega = C_N(\omega)/\omega + 4\pi J + \frac{2k^2}{\pi} \int_0^\infty \frac{dk'}{\omega'} \frac{\sigma^-(k')}{k'^2-k^2} \tag{8.17}$$

The parameter J is given by

$$J = \frac{1}{2\pi^2} \int_0^\infty \frac{\sigma^-(k)}{\omega}\, dk \tag{8.18}$$

if the integral exists. This is not doubted nowadays, since there is no significant deviation from a decrease $\sigma^- \sim k^{\alpha_\rho - 1}$, $\alpha_\rho \approx 0.5$, in the large interval 5 - 340 GeV/c.

If one wants to admit possible deviations of σ^- from the Regge law, one can treat J in eq. (8.17) as an unknown parameter. In the momentum range of the charge-exchange experiments the integral in eq. (8.17) is rapidly converging, even if one considers drastic deviations from the Regge law. Therefore one can determine accurately the value of J from charge-exchange forward scattering data and use the result together with eq. (8.18) in order to get information on the behaviour of σ^- at very high energies, since (8.18) converges only slowly (Ref. 100, 96).

In the usual subtracted dispersion relation we have instead of $4\pi J$ the values of C^- and C_N^- at threshold

$$4\pi J = \frac{C^-(\mu)}{\mu} - \frac{8\pi f^2}{\mu^2 - \omega_B^2}. \tag{8.19}$$

Since J can be determined with a good accuracy as mentioned above, eq.(8.19), predicts a relation between f^2 and $C^-(\mu)$ or the s-wave scattering length $a_1 - a_3$, eq. (5.4) (Ref. 100).

Some authors inserted values derived from an analysis of low energy data[35] which violate eq. (8.19). As a consequence their evaluation of the subtracted dispersion relation led to forward amplitudes at high energies which disagreed strongly with the constraint from total cross section and charge-exchange forward scattering data.

The "modified Goldberger-Miyazawa-Oehme sum rule" of Pham and Truong (Ref. 101) follows from the subtracted dispersion relation by rearranging and approximating some terms. It has no advantage in comparison with the earlier methods of Refs. (96, 100) and is less reliable, because charge-exchange data were ignored.

A similar critical remark applies to the tests of forward dispersion relations by Gundzik and Sudarshan[102] who were interested in possible deviations, because they hoped to find evidence for a theory in which the forward amplitude is only piecewise analytic.

9. Summary of further theoretical results on forward amplitudes*)

9.1 Bounds for total cross sections

The Froissart-Martin bound

$$\sigma^+(s) < \frac{\pi}{\mu^2} \ln^2(s/s_o), \quad s \to \infty \tag{9.1}$$

was first established by Froissart on the basis of Mandelstam analyticity and polynomial boundedness (except for the factor in front of $\ln^2$). Later Jin and Martin gave a proof from results derived from the axioms of quantum field theory. (see Refs. 103, 104, where further references are given).

Since the bound is valid only in the high energy limit and since the scale s_o is not known, it has no direct application for possible fits to data. For instance Collins et al.[105] and Craigie and Preparata[106] considered models in which the total cross sections are rising as a power, similar to our ansatz (2.26). They argued that the increase is comparable with that of an ansatz with $\sigma^+ \sim \ln^2 s$ in a large interval above the present experimental region and that finally a unitarization procedure has to be applied which makes it compatible with the bound (9.1).
Our ansatz (2.3) has a growth $\sigma^+ \sim \ln^2 s$, but the factor in front of the logarithm is much smaller (0.42 mb) than the maximum allowed by eq. (9.1), which is 63 mb.

A bound which is based on similar ideas and which can be compared with data at finite energies has been derived by Common and Yndurain (Ref. 107). They start from a Froissart-Gribov representation for the $\pi\pi\bar{N}N$ partial wave $f_+^2(t)$ and consider the limit of $f_+^2(t)/(4\mu^2-t)$ as $t \to 4\mu^2$. Taking the numerical value of this "scattering length" from an earlier version of our determination of $\pi\pi\bar{N}\bar{N}$ amplitudes (Ref. 3, sect. 4.6) they derived a bound for a moment of the total cross sections, i.e. for integrals over all physical energies with a weight function.

---

*) The summary is far from being complete. We have restricted ourselves to papers which are related to the earlier work of our group. In the next edition we intend to include for instance the interesting work of Cheng et al.[167].

It turns out that the bound is about one order of magnitude higher than the experimental values.

Using similar methods, it has been shown[103,104] that the forward amplitude is bounded as follows

$$|C| < \text{const. } s \, \ell n^2(s/s_o) \tag{9.2}$$

where C denotes the isospin even or one of the elastic amplitudes. It follows that the dispersion relation requires at most two subtractions.

One of the subtraction constants vanishes in the case of C^+ because of crossing symmetry. The data show that the other subtraction is needed.

We do not discuss lower bounds for the total cross sections, because they are very far below the data[104].

9.2 The Pomeranchuk theorems

The original version of Pomeranchuk's theorem (1958) asserts that the total cross sections for particle - target and antiparticle - target collisions become equal in the high energy limit, i.e. $\sigma^- = (\sigma(\pi^- p) - \sigma(\pi^+ p))/2 \to 0$. The theorem cannot be proven from quantum field theory alone. One needs additional assumptions, which restrict possible oscillations of the total cross sections and require that the real parts are not too large compared with the imaginary parts.
Starting with the assumption that $\sigma(\pi^{\pm} p) \to$ const at high energies, a finite limit for σ^- would lead to a strange conclusion. According to a special case of eq.(8.16), the corresponding real part would grow like $\omega \, \ell n \, \omega$

$$C^- = -\frac{2}{\pi} \sigma^-(\infty) \omega \, (\ell n \omega - i\pi/2) \tag{9.3}$$

and the Re/Im ratio for $\pi^{\pm} p$ forward scattering would go to infinity, i.e. diffraction scattering would finally be described by a real amplitude instead of being dominated by the imaginary part, which is given by the optical theorem.

Subsequently, considerable progress has been made in generalizing the theorem and relaxing the assumptions. It is remarkable that for increasing total $\pi^{\pm}p$ cross sections a Pomeranchuk theorem can be proven from unitarity (Eden and Kinoshita, see Ref. 77). If the total cross sections are rising as fast as allowed by the Froissart-Martin bound the theorem reads

$$\left|\frac{\sigma_- - \sigma_+}{\sigma_- + \sigma_+}\right| < \frac{\text{const}}{\ell n\, k} \,. \tag{9.4}$$

The present status of Pomeranchuk-type theorems is described in a recent paper by Fischer et al. (Ref. 108), which contains a number of new results. See also Ref.168 Experimentally the total cross section difference follows a simple law $\sigma^- \sim c/\sqrt{k}$ in the range 5 - 340 GeV/c and there are no physical arguments which require a different behaviour in the asymptotic limit.

During a certain period theoretical consequences of a violation of the Pomeranchuk theorem were studied by a number of authors (in his review Roy[104] gives 16 references), because the Serpuchov data for σ^- disagreed with the expectation from the charge-exchange data and the dispersion relation. However, there was no positive evidence for a violation and the discrepancy was not worse than others which occur if experimental errors are taken too seriously (Ref. 96).

Assuming isospin invariance, Roy and Singh[109] derived an upper bound for the total cross section difference in terms of the integrated charge-exchange cross section σ_{ex}

$$\lim_{s\to\infty} |\sigma^-| \leq \frac{1}{\mu}\sqrt{\frac{\pi^3}{8}} \lim_{s\to\infty} \sqrt{\sigma_{ex}} \,. \tag{9.5}$$

It follows that σ^- goes to zero in the high energy limit if $\sigma_{ex} \to 0$. For a comparison with data at high but finite energies one should notice that the inequality (9.5) is expected to hold only, if σ_{ex} does <u>not</u> go to zero.

It is of some interest to mention that an exact relation between σ^- and σ_{ex} reads (Ref. 65)

$$|\sigma^-| = \frac{\sqrt{\sigma_{ex}}}{\sqrt{I(\omega)/8\pi}\ \sqrt{1+\rho^{-2}}} \,, \tag{9.6}$$

where $\rho^- = \mathrm{Re}\, C^-/\mathrm{Im}\, C^-$ at $t = 0$, and

$$I(\omega) = \int_{-4q^2}^{o} \frac{d\sigma_o/dt}{(d\sigma_o/dt)_{t=0}}\, dt \,. \tag{9.7}$$

Ignoring the limit, the bound (9.5) leads to the inequality

$$\lim_{s\to\infty} \frac{\pi^2 I(\omega)}{64\,\mu^2}\,(1+\rho^{-2}) > 1. \tag{9.8}$$

Charge-exchange data up to 200 GeV/c (Ref. 7) give $\rho^- = \text{const} \approx 1$ and a decreasing behaviour of $I(\omega)$ ("shrinkage"). At 200 GeV/c the bound (9.8) is still fulfilled, but it will be violated at somewhat higher momenta, unless the charge-exchange data start to behave in a different way than observed at 5 - 200 GeV/c. **The violation is no problem, since the correct bound is (9.5) and not (9.8).**
Of course, this conclusion follows already from the behaviour of the forward cross section. We wanted to show the connection with the bound (9.5).

9.3 Relations between modulus and phase of forward amplitudes

Since the experimental data at high energies have a slow energy dependence, they can be described by combinations of special cases of parametrizations

$$\begin{aligned} C^+(\omega) &= \gamma^+(-i\omega)^\alpha\,(\log\omega - i\pi/2)^\beta\,, \\ C^-(\omega) &= \gamma^-\, i(-i\omega)^\alpha\,(\log\omega - i\pi/2)^\beta, \end{aligned} \tag{9.9}$$

which have the correct crossing and analyticity properties. $\gamma^\pm$ are real coefficients.
The crossing properties read

$$C^\pm(\omega + i0) = \pm C^\pm(-\omega - i0) = \pm C^{\pm *}(-\omega + i0), \tag{9.10}$$

or, if we restrict ourselves to the upper half plane and use the notation $C^+(x) = C^+(x+i0)$

$$C^\pm(\omega) = \pm C^{\pm *}(\omega\,\exp(i\pi)). \tag{9.11}$$

In the case of power laws ($\beta = 0$ in eq. (9.9)) the modulus is $\gamma\omega^\alpha$ and the phase can be expressed by the familiarformula from Regge theory

$$C^+/|C^+| \sim -\frac{1+e^{-\alpha\pi i}}{\sin\pi\alpha} = \frac{-e^{-\frac{i\pi\alpha}{2}}}{\sin\pi\alpha/2} = -\cot\frac{\alpha\pi}{2}+i\,,$$
$$C^-/|C^-| \sim \frac{1-e^{-\alpha\pi i}}{\sin\pi\alpha} = \frac{e^{\frac{i\pi}{2}(1-\alpha)}}{\cos\alpha\pi/2} = \tan\frac{\alpha\pi}{2}+i\,. \qquad (9.12)$$

For general considerations it is sometimes useful to determine the phase from a corollary to a special case of the Phragmén-Lindelöf theorem (Ref. 77):

Let $f(z)$ be bounded by a polynomial in $\mathrm{Im}\, z > 0$ and tend to limits L_1 and L_2 along the rays $z = x + i0$ as $x \to +\infty$ and $-\infty$ then we must have $L_1 = L_2$.

As an example we consider a forward amplitude $C^+(\omega)$ which has the following behavior for $\omega \to \infty$

$$\frac{C^+(\omega)}{\omega^\alpha} \to M\, e^{i\theta} \qquad (9.13)$$

where α, θ and M are real constants.

We use the above corollary and insert the crossing relation, eq. (9.11),

$$\frac{C^+(-\omega)}{\omega^\alpha \exp i\pi\alpha} = \frac{C^{+*}(\omega)}{\omega^\alpha \exp i\pi\alpha} \to M\, e^{i\theta}, \qquad (9.14)$$

From (9.13) and (9.14) it follows that

$$\theta = -\frac{\pi\alpha}{2} + n\pi\,, \quad n = 0, 1, 2, \ldots \qquad (9.15)$$

$$C^+(\omega) = \pm M\,\omega^\alpha \exp(-i\pi\alpha/2) = \pm M(-i\omega)^\alpha \qquad (9.16)$$

The sign follows from positivity for $\mathrm{Im}\, C^+$. This is a special case of eq. (9.9).

In general a function of $(-i\omega)$, which is real analytic ($f(z^*) = f^*(z)$), fulfills crossing symmetry. In the crossing odd case the function has to be multiplied by a factor i as in eq. (8.16).

The first applications of the Phragmén-Lindelöf theorem in this context are due to Meiman, Logunov and van Hove (1962 - 64) (see Ref. 77).

Further results on relations between modulus and phase are due to authors who studied phase representations (Sugawara and Tubis[56], Jin and McDowell[110]) and to others who derived general theorems using univalent functions (Khuri and Kinoshita[111]).

A continuation of these investigations, which includes interesting new results, can be found in the paper by Fischer et al.[112].

These mathematical investigations are important for an understanding of the theoretical formalism and in cases where the comparison with experimental data seems to lead to serious difficulties with well-established principles.

At present this does not occur and we have only the practical problem to determine the class of forward amplitudes which are compatible with the data, without attempting to include exotic possibilities for the high energy behaviour. For this purpose combinations of the simple expressions (9.9) are sufficient.

As an example for the fact that more sophisticated methods are not helpful we mention the work of Pham and Truong[113], in which "averaged forward dispersion relations" were used together with real part data, following the work of Khuri and Kinoshita[111]. The authors concluded that any appreciable increase of σ^+ between 60 and 500 GeV/c is ruled out, a prediction which turned out to be wrong (Fig. 3). Fig. 5 in Ref. 114 shows that a better judgment on the sensitivity of the real parts to an increase of σ^+ follows from a simple study of the usual dispersion relation.

9.4 Asymptotic behaviour of dispersion integrals

In this section we shall discuss another aspect of the relation between modulus and phase at high energies. We start with an ansatz for the asymptotic behaviour of the total cross sections and ask for the asymptotic behaviour of the dispersion integral. First we list some formulas which have been given by Lehmann[31] and by Hamilton and Woolcock[78].

We consider a pair of Hilbert transforms

$$h(y) = \frac{1}{\pi} \int_{-\infty}^{+\infty} \frac{f(x)}{x-y}\, dx. \qquad (9.17)$$

(a) The simplest case is that f(x) decreases so rapidly that

$$\int_{0}^{\infty} |f(x)|\, dx \qquad \text{and} \qquad \int_{-\infty}^{0} |f(x)|\, dx \qquad \text{exist.} \tag{9.18}$$

With the additional assumption that for a given ε there exists a V such that

$$\frac{xf(x) - x_o f(x_o)}{x - x_o} < \frac{\varepsilon}{x_o} \qquad \text{for all } x \geq x_o > V \tag{9.19}$$

one can neglect x in the denominator in eq. (9.17) and

$$h(y) \to -\frac{1}{\pi y} \int_{-\infty}^{+\infty} f(x)\, dx, \qquad \text{as } y \to \infty. \tag{9.20}$$

(b) More interesting for our applications is a slower decrease of f(x) such that $\int_{0}^{\infty} f(x)dx$ does not exist

$$f(x) \to A\, x^{-1+\alpha} + F(x), \qquad \text{as } x \to \infty, \tag{9.21}$$

where A is a constant, $0 \leq \alpha < 1$ and $xF(x) \to 0$ as $x \to \infty$.

Furthermore we require a Hölder-type condition

$$|xF(x) - x_o F(x_o)| < K\left|\frac{1}{x} - \frac{1}{x_o}\right|^{\varepsilon} \tag{9.22}$$

for any large x and x_o and positive constants K and ε. Then as $y \to \infty$

$$\begin{aligned} h(y) &\to A y^{-1+\alpha} \cot\pi\alpha + B(y)/y, && \text{if } 0 < \alpha < 1, \\ h(y) &\to \frac{-A}{\pi}\frac{\ln y}{y} + \frac{B(y)}{y}, && \text{if } \alpha = 0. \end{aligned} \tag{9.23}$$

B(y) is a bounded function.

Eq. (9.23) leads to a generalization of (9.12). In the language of derivative dispersion relations (sect. 3.4) the 2nd term B(y)/y represents "non-local" effects (for instance tails of low energy resonances).

(c) Next we consider

$$h(y) = \oint_{1}^{\infty} \frac{f(x)}{\sqrt{x}\,(x-y)}\, dx \tag{9.24}$$

and suppose that

$$\int_1^\infty \frac{f(x)}{x}\,dx \quad \text{exists,} \quad f(x)\,\ell nx \to 0 \text{ as } x \to \infty, \quad \text{and } |f'(x)| \leq M \tag{9.25}$$

where M is a constant. Then

$$\sqrt{y}\,h(y) \to 0 \text{ as } y \to \infty. \tag{9.26}$$

(d) Finally let

$$h(y) = \int_1^\infty \frac{f(x)}{x-y}\,dx \tag{9.27}$$

and suppose that the conditions (9.25) are valid. Then

$$h(y) \to 0 \text{ as } y \to \infty, \tag{9.28}$$

The above results are of interest, if one wants to discuss a high energy behaviour which is more complicated than suggested by the present data. Applications and proofs can be found in the review by Hamilton and Woolcock[78].

Now we shall mention some formulas which are needed in calculations with the usual or inverse dispersion relation[115]

$$\begin{aligned} &\frac{2}{\pi}\int_0^\infty \frac{dx}{x^2+y^2} = 0 && \text{if } y^2 < 0 \\ &\frac{2}{\pi}\int_0^\infty \frac{dx}{x^2+y^2} = \frac{1}{|y|} && \text{if } y^2 > 0 \end{aligned} \tag{9.29}$$

$$\begin{aligned} \frac{2}{\pi}\int_1^\infty \frac{x\,dx}{\sqrt{x^2-1}\,(x^2-y^2)} &= 0 \text{ for } y > 1 \\ &= \frac{1}{\sqrt{1-y^2}} \text{ for } y < 1 \end{aligned} \tag{9.30}$$

$$\lim_{y\to 1+} \frac{2}{\pi}\int_1^\infty \frac{dx}{x\sqrt{x^2-1}\,(x^2-y^2)} = -1 \tag{9.31}$$

$$\lim_{y\to 1+} \int_1^\infty \frac{dx}{\sqrt{x^2-1}\,(x^2-y^2)} = -1 \tag{9.32}$$

Finally we add formulas which are needed for the evaluation of high energy contributions to Re C in different models for Im C (sect. 2.3).

(a) The term $\sigma_1 \ln^2(k/k_1)$ in σ^+, eq. (2.3a), gives the following contribution to the dispersion integral eq. (2.11) from $k = k_H$ to ∞

$$\mathrm{Re}\, C_H^+(\omega) = \frac{2}{\pi} k^2 \int_{k_H}^\infty \frac{dk'}{k'^2-k^2}\ \sigma_1 \ln^2(k/k_1) \tag{9.33}$$

$$\mathrm{Re}\, C_H^+(\omega) = \frac{4}{\pi} k_H \sigma_1 \{\frac{\ln^2\gamma}{4} \frac{k}{k_H} \ln \frac{k_H+k}{k_H-k} + (\ln\gamma+1)(\frac{k}{k_H})^2 + (\frac{\ln\gamma}{9} + \frac{1}{27})(\frac{k}{k_H})^4 + \ldots\}$$

$$= \frac{4}{\pi}\frac{\sigma_1}{k_H}\{1 + \ln\gamma + \frac{1}{2}\ln^2\gamma\}\, k^2 + \ldots \quad \text{if } \underline{k < k_H} \tag{9.34}$$

$$\mathrm{Re}\, C_H^+(\omega) = k\pi\sigma_1 \ln\frac{k}{k_1} + \frac{4}{\pi} k_H \sigma_1 \{\frac{\ln\gamma}{4}\frac{k_H}{k} \ln\frac{k+k_H}{k-k_H} + (1-\ln\gamma)(\frac{k_H}{k})^2 + (\frac{1}{27} - \frac{\ln\gamma}{9})(\frac{k_H}{k})^4 + \ldots\} \tag{9.35}$$

$$= k\pi\sigma_1 \ln\frac{k}{k_1} + \frac{4}{\pi} k_H \sigma_1 \{\frac{1}{2}\ln^2\gamma - \ln\gamma + 1)(\frac{k_H}{k})^2 + \ldots \quad \text{if } \underline{k > k_H}$$

We have used $\gamma = k_H/k_1$. The first term in the last line is Re C^+_{par} (sect. 2.3). It follows from

$$\int_0^\infty \frac{\ln^2 x}{x^2-y^2}\, dx = \frac{\pi^2}{2y} \ln y \tag{9.36}$$

(see Gradsteyn-Ryzhik[116] Nr. 4.271, 4.261).

The other integrals can be found in Meyer zur Capellen Nr. 4.1.2.0, p. 229 (Ref. 117).

(b) We list also the formula for the term $b\, k^{\alpha-1}$ in σ^+, eq. (2.26).

$$\mathrm{Re}\, C_H^+(\omega) = \frac{2}{\pi} k^2 \int_{k_H}^\infty \frac{b\, k'^{\alpha-1}}{k'^2-k^2}\, dk' \tag{9.37}$$

$$= \frac{2}{\pi} b\, k_H^\alpha (\frac{k}{k_H})^2 \{\frac{1}{2-\alpha} + \frac{(k/k_H)^2}{4-\alpha} + \ldots\}, \quad \text{if } \underline{k < k_H} \tag{9.38}$$

$$\text{Re } C_H^+(\omega) = - b\, k^\alpha \cot(\pi\alpha/2) + \frac{2}{\pi} b\, k_H^\alpha \{\frac{1}{\alpha} + \frac{(k_H/k)^2}{\alpha+2} + \ldots\} \text{ , if } \underline{k > k_H} \qquad (9.39)$$

The first term in the last line is Re C_{par}^+. It follows from the integral *)

$$\frac{2}{\pi} \int_0^\infty \frac{x^\nu}{x^2-y^2}\, dx = y^{\nu-1} \tan\frac{\pi\nu}{2} \text{ , } \quad -1 < \text{Re}\nu < 1 \qquad (9.40)$$

where y is real (see Erdelyi[118], Vol. 2, p. 216). **Further formulas for principal value integrals can be found in the paper by Frye and Warnock(Appendix of Ref.133).**

9.5 Other types of dispersion relations

9.51 Weighted dispersion relations

Up to now we have considered only the usual form of the forward dispersion relations (2.11), in which the real parts follow from principal value integrals over the imaginary parts, i.e. over the total cross sections. A number of authors (Refs. 115, 119 - 127) proposed modified dispersion relations which are written for the product $g(\omega)C(\omega)$, where $g(\omega)$ is a function whose analytic properties are analogous to those of the forward amplitude $C(\omega)$: $g(\omega)$ is a real analytic function bounded at infinity and having at most the same cuts as $C(\omega)$.

$g(\omega)$ can be chosen to act as a "weight function", emphasizing a certain energy interval where accurate data are available and suppressing others where data are missing. However, $g(\omega)$ is in general complex-valued, whereas the usual weight functions are real and positive.

Another motivation is to obtain a dispersion relation in which the input for the integral consists of real parts in one energy region and imaginary parts in others.

The earliest modification was that of Gilbert[115] who used

$$g(\omega) = \frac{1}{i\sqrt{\omega^2-\mu^2}} = \frac{1}{ik} \text{ .} \qquad (9.41)$$

This factor leads to the "inverse" dispersion relations, in which the imaginary parts are expressed in terms of principal value integrals over real parts. These dispersion relations read ($\omega_B = -\mu^2/2m$)

$$\sigma^+(\omega) = \sigma^+(\mu) + \frac{8\pi f^2 \omega_B}{(\mu^2-\omega_B^2)^{3/2}} \frac{k^2}{\omega^2-\omega_B^2} - \frac{2k^2}{\pi} \int_0^\infty \frac{dk'}{k'^2} \frac{\text{Re } C^+(\omega) - \text{Re } C^+(\mu)}{k'^2-k^2} \text{ ,} \qquad (9.42)$$

*) Eq.(9.39) is valid also for negative values of α in the ranges $0>\alpha>-2, -2>\alpha>-4, \ldots$ where eq.(9.40) cannot be used.

$$\sigma^-(\omega) = -\frac{8\pi f^2}{\sqrt{\mu^2-\omega_B^2}} \frac{\omega}{\omega^2-\omega_B^2} - \omega \frac{2}{\pi} \int_0^\infty \frac{dk'}{k'^2-k^2} \frac{\mathrm{Re}\, C^-(\omega')}{\omega'} \,. \tag{9.43}$$

They have been used only in a few cases, because the experimental information on the real parts is much poorer than that on the imaginary parts.

Kanazawa and Sugawara[128] proposed to determine the forward amplitude by iterating the usual and the inverse dispersion relations, starting with the known part of Im C and a guess for the unknown part. Then, in the inverse relation, the result is corrected inserting the known part of Re C, etc. We think that Pietarinen's method[37], which was not yet known to the authors, is clearly preferable.

Adler[119] proposed a "broad area subtraction method" which is based on

$$g(\omega) = \frac{1}{\left[(\omega-\mu)(\omega+\mu)(\omega-\omega_m)(\omega+\omega_m)\right]^{1/2}} \tag{9.44}$$

where $\omega_m > \mu$. The square root is chosen to have its cut from μ to ω_m and the dispersion integral goes over real parts in the range $\mu < \omega < \omega_m$ and over imaginary parts at larger ω. Since the information on the subtraction constant comes from real parts derived from phase shifts at many energies, Adler wanted to use these real parts directly instead of the usual two-step procedure in which $C^+(\mu)$ is determined in the first step and eq. (2.11) is used in the second step.

This method would work, if the data had statistical errors only. However, when it was used by Cheng and Dashen[129] in their determination of the πN sigma term,*) it led to a much higher value that our determination with the conventional method (Ref. 55, 59), in which one checks simultaneously the consistency of the real and imaginary parts with the dispersion relation and smoothens the remaining structures. Subsequent authors confirmed our result and Liu et al.[130] showed that it could also be obtained, if a variety of "broad areas" is considered in Adler's method. However, the conventional method is much simpler.

Khalfin's proposal[120] is a further generalization of Adler's ansatz. It has not been applied in practice.

Liu and Okubo[121] used a more flexible generalization of Gilbert's ansatz

$$g(\omega) = e^{i\pi\beta}(\omega^2-\mu^2)^{-\beta}/\omega = (-ik)^{-2\beta}/\omega \tag{9.45}$$

*) These authors used a generalized version with the denominator $(\omega_1^2-\omega^2)(\omega_2^2-\omega^2)^{1-\beta}$.

$(\omega^2-\mu^2)^\beta$ is chosen to be real positive, if the cut $\mu<\omega<\infty$ is approached from above. Then $\mathrm{Im}\{g(\omega)C^+(\omega)\}$ is zero for $|\omega|<\mu$ except for the pole terms. For $\mu<\omega<\infty$ it reads

$$\mathrm{Im}\{g(\omega)C^+(\omega)\} = \frac{k^{-\beta}}{\omega}\{\cos\pi\beta\ \mathrm{Im}\ C^+ + \sin\pi\beta\mathrm{Re}\ C^+\}. \tag{9.46}$$

The main application of the weighted dispersion relations is the construction of sum rules. Originally it was thought that they have an advantage over the ordinary dispersion relations, eqs.(2.11), for a test of the analytic properties and for the determination of low and high energy parameters. However, there is a serious disadvantage: Re C is needed for the evaluation of all modified dispersion integrals. Experimentally, the information on Re C is much poorer than that on Im C, which follows from the accurate total cross section data. Therefore, it is difficult to see the usefulness of the weighted dispersion relations for the forward amplitudes for the above mentioned applications.

9.52. Dispersion relations for functions or derivatives of the amplitudes

i) The logarithm of the amplitude

$$\ln C(\omega) = \ln|C(\omega)| + i\delta(\omega) \tag{9.47}$$

has the same cut structure as $C(\omega)$, but there are additional singularities from the zeros of the amplitude.

A dispersion relation for ln C leads to an expression for the amplitude in terms of an integral over its phase along the cut. In the simplest case, if there are no poles and zeros and the phase goes to a finite limit at infinite energies, the solution is given by the "Omnes function" (Ref.131)

$$\mathfrak{D}(\omega) = \exp\{\frac{\omega}{\pi}\int_{cut} d\omega' \frac{\delta(\omega')}{\omega'(\omega'-\omega)}\}. \tag{9.48}$$

The asymptotic behaviour is

$$\mathfrak{D}(\omega) \sim \omega^{\delta(\infty)/\pi}. \tag{9.49}$$

Sugawara and Tubis [56] derived a phase representation for the pion-nucleon forward amplitude, starting from the usual analytic properties and making additional assumptions(a finite limit for $\delta(\omega)$ at high energies and a finite number of zeros of C^+ in the ω-plane)

$$C^+(\omega) = \frac{P_n(\omega^2)}{\omega^2-\omega_B^2} \exp\{ \frac{2\omega^2}{\pi}\int_{\mu}^{\infty} \frac{\delta(\omega')d\omega'}{\omega'(\omega'^2-\omega^2)} \} . \tag{9.50}$$

P_n is a real polynomial of an order which is given by the number of zeros. Aside from logarithmic terms the asymptotic behaviour is given by

$$C^+(\omega) \sim \omega^{2n-2-2\delta(\infty)/\pi} \, e^{i\delta(\infty)} . \tag{9.51}$$

The phase $\delta(\omega)$ is defined by

$$\begin{aligned} C^+(\omega) &= |C^+(\omega)| \, e^{i\delta(\omega)} \quad , \text{ if } C^+(\mu) \geq 0, \\ &= -|C^+(\omega)| \, e^{i\delta(\omega)} \quad , \text{ if } C^+(\mu) < 0 , \end{aligned} \tag{9.52}$$

and $\delta(\omega) \equiv 0$ for $\omega^2 \leq \mu^2$.

Assuming the Froissart bound and the limit $|\delta(\infty)| = \pi/2$, there remain two possibilities:

$$\begin{aligned} &C^+(\mu) \geq 0, \ \delta(\infty) = \pi/2, && C^+(\omega) \text{ has 4 zeros}, \\ &C^+(\mu) < 0, \ \delta(\infty) = -\pi/2, && C^+(\omega) \text{ has 2 zeros}. \end{aligned} \tag{9.53}$$

The parameters are restricted by the condition that the residues at the nucleon poles are given by the coupling constant

$$f^2 = - \frac{P_n(\omega_B^2)}{2\omega_B} \exp\{\frac{2\omega_B^2}{\pi}\int_{\mu}^{\infty} \frac{\delta(\omega')d\omega'}{\omega'(\omega'^2-\omega_B^2)} \} . \tag{9.53}$$

According to eq.(5,7) $C^+(\mu)$ is slightly negative. The two zeros have been discussed in sect.7. They lie at $\omega^2 = -0.85\ \mu^2$.
Sugawara and Tubis have also studied the case of the isospin odd forward amplitude, where the number of zeros is 7 or 11 (sect.7).
The phase representation has been used by Jin and McDowell in order to derive properties of the phase at very high energies under different assumptions.[110]

Since the modulus of the forward amplitude can be determined from extrapolations of charge-exchange cross sections, the inverse problem is even more important. The solution has been given by Odorico (Ref.132), but we shall not list the rather complicated formulas. Applications to fixed-t amplitudes can be found in papers by McClure and Pitts (Ref.67). In general,it is preferable to work with the usual fixed-t dispersion relation or with the expansion method (sect.3.2).

Unfortunately, the existing data for charge-exchange near-forward scattering in the intermediate energy region cover only the angular range up to $\cos\theta = 0.95$. It is surprising that a reliable extrapolation to the forward direction is not possible, even if data are available up to $\cos\theta = -0.95$. The reason is that the cross sections have a tendency for large structures even in the small range $0.95 < \cos\theta < 1$ (Ref.99).

ii) A second possibility is to consider the inverse of the amplitude: $1/C$. Again, the cut structure is the same and one has the disadvantage that the location of the poles of $1/C$ (i.e. of the zeros of C) is not known, whereas in the ordinary dispersion relations the only poles come from the nucleon intermediate state. This method has been used by Zovko (Ref.145 , see also Ref.136). Martin and Wit (Ref.134) noticed that the problem with the zeros can be avoided, if one considers the inverse of the amplitude C^+ minus its nucleon pole term, because this combination has no zeros due to the positivity of Im C^+.

iii) A third case has been discussed by Ferrari and Violini (Ref.135), who derived dispersion relations for the square of the amplitude. They also considered the amplitude minus its nucleon pole term (notation: $\tilde{C}$) because the square of the pole term would cause a complication. The subtracted version

$$\mathrm{Re}\,\tilde{C}(\omega)\;\mathrm{Im}\,\tilde{C}(\omega) = \frac{\omega}{\pi}(\omega^2-\omega_o^2)\int_o^\infty \frac{(\mathrm{Im}\,\tilde{C})^2-(\mathrm{Re}\,\tilde{C})^2}{(\omega'^2-\omega^2)(\omega'^2-\omega_o^2)}\,d\omega' \qquad (9.54)$$

has the property that the integral converges rapidly in the case of C^-. If one inserts our fit of Table 80/1 which has $|\mathrm{Re}\,C^-| = |\mathrm{Im}\,C^-|$ in the asymptotic region, one can even take the unsubtracted version

$$\mathrm{Re}\,\tilde{C}^-(\omega)\;\mathrm{Im}\,\tilde{C}^-(\omega) = \frac{\omega}{\pi}\int_o^\infty \frac{(\mathrm{Im}\,\tilde{C}^-)^2-(\mathrm{Re}\,\tilde{C}^-)^2}{\omega'^2-\omega^2}\,d\omega' \,. \qquad (9.55)$$

The integral on the r.h.s. has the property to vanish identically for $\omega^2<\mu^2$ where $\mathrm{Im}\,C^- \equiv 0$. We have not seen applications which show any advantage in comparison with the ordinary dispersion relation.

iv) Finally one can use the fact that the derivative $dC/d\omega$ has the same cut structure as the amplitude. For the calculation of the derivative of the dispersion relation one can use the relation

$$\frac{d}{d\omega}\oint_{\omega_1}^{\omega_2}\frac{g(\omega')}{\omega'-\omega}\,d\omega' = \frac{g(\omega_1)}{\omega_1-\omega} - \frac{g(\omega_2)}{\omega_2-\omega} + \oint_{\omega_1}^{\omega_2}\frac{g'(\omega')d\omega'}{\omega'-\omega} \tag{9.56}$$

Queen et al.(Ref.137) have applied this method in KN scattering for the determination of coupling constants.

9.53 Finite contour dispersion relations

We start with a subtracted dispersion relation for C^+

$$\mathrm{Re}\ C^+(\omega) = C^+(0) + C_N^+(\omega) + \frac{2\omega^2}{\pi}\oint_{\mu}^{\infty}\frac{d\omega'}{\omega'}\frac{\mathrm{Im}\ C^+(\omega')}{\omega'^2-\omega^2}\ , \tag{9.57}$$

which can be derived from a Cauchy integral over $C^+(\omega)/\omega$. One starts with the contour shown in the figure and considers the limit where the radii of the semicircles go to infinity.

Since one always works with an analytic parametrization in the range $\Omega<\omega<\infty$, one can as well evaluate the integral over the contour with semicircles of finite radius. This leads to the following dispersion relation

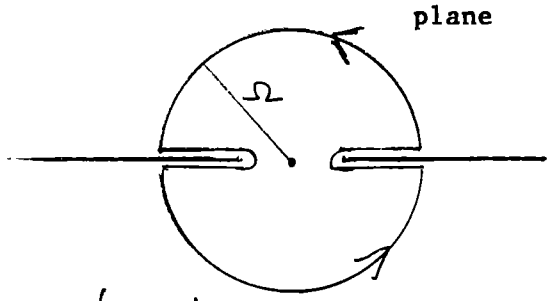

$$\mathrm{Re}\ C^+(\omega) = C^+(0) + C_N^+(\omega) + \frac{2\omega^2}{\pi}\int_{\mu}^{\Omega}\frac{d\omega'}{\omega'}\frac{\mathrm{Im}\ C^+(\omega')}{\omega'^2-\omega^2} + \frac{\omega}{2\pi i}\oint\frac{d\omega'}{\omega'}\frac{C^+(\omega')}{\omega'-\omega}\ . \tag{9.58}$$

Using crossing symmetry, one can transform the second integral into another one which goes only over the upper semicircle

$$\frac{\omega^2}{\pi\ i}\int_{\curvearrowleft}\frac{d\omega'}{\omega'}\frac{C^+(\omega')}{\omega'^2-\omega^2}\ , \tag{9.59}$$

As an example we consider a Regge term C_R^+ in the high energy expansion of C^+

$$C_R^+(\omega) = -\gamma \frac{1+e^{-i\pi\alpha}}{\sin\pi\alpha} \left(\frac{\omega}{\omega_o}\right)^\alpha, \qquad \text{Im } C_R^+ = \gamma \left(\frac{\omega}{\omega_o}\right)^\alpha . \tag{9.60}$$

The high energy part of the ordinary dispersion relation eq.(2.11) can easily be calculated by expanding the denominator in a geometrical series. One obtains

$$\frac{2\omega^2}{\pi} \int_\Omega^\infty \frac{d\omega'}{\omega'} \frac{\text{Im } C_R^+(\omega')}{\omega'^2 - \omega^2} = \frac{2}{\pi} \gamma \sum_{n=o}^{\infty} \left(\frac{\omega}{\Omega}\right)^{2n+2} \left(\frac{\Omega}{\omega_o}\right)^\alpha \frac{1}{2+2n-\alpha}, \quad \omega<\Omega . \tag{9.61}$$

Of course one obtains the same result, if one evaluates the integral over the semicircles. In this case, however, one needs not only Im C^+ but also Re C^+. At energies where the imaginary part is well approximated by the Regge formula, it can happen that the real part has appreciable corrections from the low energy part of the dispersion integral (see sect.2.3). Nevertheless the result is the same.

Now, we insert the identity

$$\frac{\omega^2}{\omega'(\omega'^2 - \omega^2)} \equiv \frac{\omega'}{\omega'^2 - \omega^2} - \frac{1}{\omega'} \tag{9.62}$$

into eq.(9.58),(9.59) and obtain

$$\begin{aligned} \text{Re } C^+(\omega) = C_N^+(\omega) + \frac{2}{\pi} \int_\mu^\Omega \frac{\omega' \text{Im } C^+(\omega')}{\omega'^2 - \omega^2} d\omega' + \frac{1}{\pi i} \int_{\curvearrowleft} \frac{\omega' C^+(\omega')}{\omega'^2 - \omega^2} d\omega' \\ + C^+(0) - \frac{2}{\pi} \int_\mu^\Omega \text{Im } C^+(\omega) \frac{d\omega}{\omega} - \frac{1}{\pi i} \int_{\curvearrowleft} C^+(\omega) \frac{d\omega}{\omega} . \end{aligned} \tag{9.63}$$

Next we compare this result, which follows from the subtracted relation, with the Cauchy integral over $C^+(\omega)$, using the same contour

$$\text{Re } C^+(\omega) = \frac{g^2}{m} \frac{\omega_B^2}{\omega_B^2 - \omega^2} + \frac{2}{\pi} \int_\mu^\Omega \frac{\omega' \text{Im } C^+(\omega')}{\omega'^2 - \omega^2} d\omega' + \frac{1}{\pi i} \int_{\curvearrowleft} \frac{\omega' C^+(\omega')}{\omega'^2 - \omega^2} d\omega' . \tag{9.64}$$

In particular, we find for $\omega=0$

$$C^+(0) = \frac{g^2}{m} + \frac{2}{\pi} \int_\mu^\Omega \text{Im } C^+(\omega) \frac{d\omega}{\omega} + \frac{1}{\pi i} \int_{\curvearrowleft} C^+(\omega) \frac{d\omega}{\omega} . \tag{9.65}$$

$C^+(0) - g^2/m$ is small because of the smallness of the sigma term(see sect.10 of Ref.3). Therefore the 2nd and 3rd term in eq.(9.65), which go to infinity as Ω increases, almost cancel each other.

If dispersion relations are derived from quantum field theory, one can always add a real polynomial, which is restricted in the present case to a constant because

of Froissart's bound and crossing symmetry. This constant can be determined from real parts as following from phase shifts or from Coulomb interference measurements. Aside from the effects of a continuation in pion mass the values of $C^+(0)$ and of $C^-(\omega)/\omega$ at $\omega=0$ are determined by the low energy theorems of current algebra (Refs. 82, 119).

Finally, the subtraction constant $C^+(0)$ is fixed if one assumes that the scattering amplitude can be continued in angular momentum (Refs.73,144).

A test of eq.(9.65) is difficult, because the r.h.s. is the difference between two large terms. It is practical to choose a parametrization C^+_{par} which has the same cut structure as C^+ and to replace C^+ along the semicircle by C^+_{par}. The discussion will be continued in sect. 9.62.

We want to add some remarks on $C^+(0)$. Its numerical value is near to

$$g^2/m = 26.7\ \mu^{-1} \triangleq 191 \quad \text{GeV}^{-1} \tag{9.66}$$

(assuming $f^2 = 0.079$), which is the value of the pseudovector nucleon Born term contribution to $A^+(0) = C^+(0)$. Our Table 80/1 gives

$$C^+(0) = g^2/m - 10.5\ \text{GeV}^{-1} = 180.8\ \text{GeV}^{-1}. \tag{9.66}$$

The smallness of the correction is a consequence of the fact that, according to Adler's consistency condition(Ref.119), A^+ has the value g^2/m at a nearby unphysical point and that the sigma term is small(see sect.10 of Ref.3).

If an unsubtracted dispersion relation is valid for the A^+ amplitude, which is not yet excluded by the experimental data for the polarizations and the spin-rotation parameters at high energies, we have another sum rule for $C^+(0)$

$$C^+(0) = A^+(0) = \frac{2}{\pi}\int_{\mu}^{\infty} \text{Im}\, A^+(\omega)\, d\omega/\omega, \tag{9.67}$$

It is remarkable that the integral over the $\Delta(1232)$ peak gives about 80% of the experimental value of $C^+(0)$. The existence of the dispersion integral in eq.(9.67) has asymptotic helicity conservation as a consequence.

Since it is sometimes stated that the subtraction function $C^+(\nu=0,t)$ has no simple physical interpretation, it might be of interest to mention that it can be replaced by the $J=0$ $\pi\pi N\bar{N}$ amplitude minus its nucleon Born term: $\tilde{f}^0_+(t)$ (Ref.114)

$$\frac{4\pi}{m^2-t/4}\mathrm{Re}\,\tilde{f}_+^{o}(t) = C^+(0,t) + \frac{2}{\pi}\int \mathrm{Im}\,C^+(\nu',t)Q_1(z')d\nu'/\nu', \qquad (9.68)$$

$\nu' = \omega' + t/4m$, $z' = m\nu'/(\sqrt{m^2-t/4}\,\sqrt{\mu^2-t/4})$, $\nu_1 = \mu + t/4m$.

Finite contour dispersion relations have been proposed by Barger and Phillips[138] and applied to πN scattering by H.Nielsen[139] and by Baacke and Engels[140], who noticed that an important point was already discussed in the earlier work of Igi[141]. Brandt and Preparata[142] attempted to estimate the magnitude of the nucleon sigma term by using an equivalent method, but their result was much too large. A direct extrapolation to the unphysical region gives a more accurate value (see sect.10 in Ref.3).

Since an evaluation of the ordinary fixed-t dispersion relation is available[3] and the new data for the total cross sections do not suggest a violation of Pomeranchuk's theorem, the only remaining interesting point is the sum rule (9.65).

The subtraction function $C^+(\nu=0,t)$ is determined by the condition that the scattering amplitude can be continued in angular momentum (see p.60 in Ref.144). Therefore it is of interest to check,whether the parametrization of the high energy amplitude is consistent with the value (9.66). This point has been discussed by Igi[141] (using $C^+(\mu)$) and by Ellis and Weiss[143], but the results were based on the assumption of a constant asymptotic total cross section.

9.6 Sum rules

There exists a very large number of papers on sum rules for scattering amplitudes (the review by Ferro Fontan et al.[146] lists more than 600 in 1972) and most of them are applicable to pion-nucleon scattering. The dispersion sum rules follow from the same analyticity properties from which the forward dispersion relations are derived and from additional assumptions on the high energy behaviour, which is usually chosen as a superposition of the parametrizations (2.2) and (8.16).

It is the aim to find relations between the parameters of the high energy expansion and integrals over the forward amplitudes at low and intermediate energies, where it is known from phase shift analysis.

9.61 A sum rule for the isospin odd amplitude

We start with the Igi-Matsuda sum rule (Ref.147) which gives information on the secondary term of the charge-exchange forward amplitude. According to Refs.6,7 the cross section data for the charge-exchange reaction are well fitted by a simple reggeized ρ-exchange formula which is therefore assumed to represent the leading term of the asymptotic expansion. Our plots for the total cross section difference (Fig.5) and for the charge-exchange forward cross section (Fig.6) show that the second term, which describes the transition to the asymptotic behaviour, is not well defined by the data.

Igi and Matsuda[147] considered the difference between $C^-(\omega)$ and the reggeized ρ-exchange amplitude

$$\hat{C}(\omega) \equiv C^-(\omega) - C_\rho(\omega), \qquad C_\rho(\omega) = 2\pi\beta\{P_\alpha(\omega/\mu) - P_\alpha(-\omega/\mu)\}/\sin\pi\alpha \tag{9.69}$$

and assumed the validity of the unsubtracted dispersion relation (2.11). Since C_ρ has the same cut structure and crossing symmetry

$$\{P_\alpha(\omega/\mu) - P_\alpha(-\omega/\mu)\}/\sin\pi\alpha = \frac{2\omega}{\pi}\int_\mu^\infty d\omega' \frac{P_\alpha(\omega'/\mu)}{\omega'^2 - \omega^2}, \tag{9.70}$$

$\hat{C}(\omega)$ fulfills the dispersion relation

$$\mathrm{Re}\ \hat{C}(\omega) = C_N^-(\omega) + \frac{2\omega}{\pi}\int_\mu^\infty \frac{\mathrm{Im}\ \hat{C}(\omega')}{\omega'^2 - \omega^2} d\omega, \tag{9.71}$$

where

$$\mathrm{Im}\ \hat{C}(\omega) = k\sigma^- - 2\pi\beta\ P_\alpha(\omega/\mu). \tag{9.72}$$

If one wants to know the numerical value of β, one needs the relation between eq.(9.69) and the usual high energy approximation of the Regge formulas

$$P_\alpha(\omega/\mu) \to \frac{2^\alpha}{\sqrt{\pi}}\frac{\Gamma(\alpha+1/2)}{\Gamma(\alpha+1)}\left(\frac{\omega}{\mu}\right)^\alpha, \qquad \alpha > -0.5 \tag{9.73}$$

$$P_\alpha(-\omega/\mu) \to P_\alpha(\omega/\mu)\ e^{-i\pi\alpha}$$

$$\frac{1 - e^{-i\pi\alpha}}{\sin\pi\alpha} = \tan(\pi\alpha/2) + i = e^{i\pi(1-\alpha)/2} / \cos(\pi\alpha/2). \tag{9.74}$$

In order to perform a test whether the second term of the asymptotic expansion vanishes faster than ω^{-1}, Igi and Matsuda imposed the condition

$$\omega\,|\hat{C}(\omega)|\to 0 \text{ for } \omega\to\infty\,, \tag{9.75}$$

An integral over $\hat{C}(\omega)$ with the contour shown on page 51 leads in the limit to the "Igi-Matsuda sum rule"

$$\int_{\mu}^{\infty} \mathrm{Im}\,\hat{C}(\omega)d\omega = \int_{\mu}^{\infty}\{k\sigma^{-} - 2\pi\beta\, P_{\alpha}(\omega)\}\,d\omega = 4\pi^2 f^2, \tag{9.76}$$

Since the Regge pole formula has been derived as the leading term of an asymptotic expansion, it looks strange that it is used at low energies in eq.(9.76).However, the sum rule can as well be written with another expression $\bar{C}_{\rho}$ for the ρ-exchange contribution which asymptotically agrees with eq.(9.69) such that $\omega|C_{\rho}-\bar{C}_{\rho}|\to 0$ for $\omega\to\infty$.

As an example we consider

$$\bar{C}_{\rho}(\omega) = c_{\rho}\omega k^{\alpha-1}\left(\tan\frac{\pi\alpha}{2} + i\right) = c_{\rho}\omega(-ik)^{\alpha-1}/\cos\frac{\pi\alpha}{2} \tag{9.77}$$

which fulfills the same dispersion relation. c follows from β and eq.(9.73).

Now we assume that the second term can also be described by a Regge pole

$$\mathrm{Im}\,\bar{C}^{-}(\omega) = c_{\rho}\omega\, k^{\alpha_{\rho}-1} + c_{\rho'}\omega\, k^{\alpha_{\rho'}-1} \tag{9.78}$$

and that higher terms are negligible at $\omega>\Omega$.

If $\alpha_{\rho'} < -1$, the sum rule reads

$$4\pi^2 f^2 = \int_{\mu}^{\Omega}(\mathrm{Im}\,C^{-} - c_{\rho}\omega k^{\alpha_{\rho}-1})d\omega + \int_{\Omega}^{\infty} c_{\rho'}\omega\, k^{\alpha_{\rho'}-1}\,d\omega \tag{9.79}$$

$$= \int_{\mu}^{\Omega} k\sigma^{-}d\omega - c_{\rho}\frac{\Omega^{\alpha_{\rho}+1}}{\alpha_{\rho}+1} - c_{\rho'}\frac{\Omega^{\alpha_{\rho'}+1}}{\alpha_{\rho'}+1} \tag{9.80}$$

where we have used the approximation $\sqrt{\Omega^2-\mu^2}\approx\Omega$.

If the second term is small in eq.(9.78) it can nevertheless be appreciable in eq.(9.79) if the denominator $\alpha_{\rho'}+1$ is small.

In the case $\alpha_{\rho'} > -1$, we have to write the sum rule for $C^{-}-\bar{C}_{\rho}-C_{\rho'}$ and it turns out that one obtains again eq.(9.80).

Eq.(9.80) is called a "Finite Energy Sum Rule". It was derived by Logunov et al.[148] and studied in detail by Dolen et al.[149]

It would be surprising if the sum rule (9.76) were valid as it stands, because one expects contributions from a Pomeron-ρ cut and from ρ'(1250) exchange. The cut contribution is predicted to be small according to Arbabanel and Sugar (Ref.150), who derived from Reggeon field theory in first order that the pole term is modified by a factor $(\ln \omega)^{1/12}$ and that the trajectory is only weakly perturbed near t=0. However, in some earlier models large effects of the cut are predicted or obtained in fits (Refs. 73,88,90,144).

A ρ'(1250) resonance is needed in the dispersion theory of the electromagnetic form factor of the nucleon in order to explain the approximate dipole structure of the isovector spectral function (Ref.151). The experimental evidence for this resonance is listed in Ref.152 and 153.

Another interesting question is whether Re C^- has at high energies a non-vanishing contribution which decreases $\sim \omega^{-1}$ and comes from the dispersion integral at low and intermediate energies. The answer follows from eq.(8.11a)

$$\text{Re } C^- = \text{Re } C^-_{par} + \frac{2}{\pi\omega}\left[4\pi^2 f^2 - \int_0^\Omega (\sigma^- - \sigma^-_{par})k\,dk\right] + O(\omega^{-3}). \qquad (9.81)$$

It is seen that the vanishing of the bracket is equivalent to the validity of the superconvergent sum rule. σ^-_{par} includes all contributions with $\alpha \gtrsim -1$.

As discussed in sect. 8, our fits give a small non-vanishing value for the bracket, but we have included only the leading term in σ^-_{par}. I.Sabba-Stefanescu has attempted to fulfill the sum rule by taking into account a small secondary term with $\alpha < -1$. Because of the uncertainties of the data, this is possible if one takes $\alpha_\rho(0) = 0.53$ (Table 80/2), but there are difficulties for the choice $\alpha_\rho(0) = 0.500$ (Table 80/1).

9.62 A sum rule for the isopin even amplitude

We continue our discussion of the sum rule (9.65) for the C^+-amplitude. In order to test this relation, it is necessary to assume an analytic parametrization for the high energy behaviour. $C^+_{par}(\omega)$ is assumed to agree with $C^+(\omega)$ in a good approximation for all $|\omega| > \Omega$. Instead of inserting C^+_{par} along the semicircle in the 2nd integral of eq.(9.65) we prefer to write an unsubtracted dispersion relation for $C^+(\omega) - C^+_{par}(\omega)$, following Igi's method (Ref. 141)

$$\text{Re } C^+(\omega) = \text{Re } C^+_{par}(\omega) + \frac{g^2}{m}\frac{\omega_B^2}{\omega_B^2 - \omega^2} + \frac{2}{\pi}\int_\mu^\Omega \frac{\text{Im}\,(C^+ - C^+_{par})}{\omega'^2 - \omega^2}\,\omega'\,d\omega', \qquad (9.82)$$

C^+_{par} is chosen in such a way that the upper limit of the integral can be replaced by Ω.

The nucleon pole term of the unsubtracted relation, eq.(9.82), and of the subtracted relation, C_N^+, are related by

$$C_N^+(\omega) = -\frac{g^2}{m}\frac{\omega^2}{\omega^2-\omega_B^2} = C^+_{N,uns.}(\omega) - g^2/m. \tag{9.83}$$

The leading terms in the high energy expansion of eq.(9.82) are

$$\text{Re } C^+(\omega) = \text{Re } C^+_{par}(\omega) - \omega^{-2}\left[\frac{g2}{m}\omega_B^2 + \frac{2}{\pi}\int_{\mu}^{\Omega} \text{Im } (C^+-C^+_{par})\omega' d\omega'\right] \tag{9.84}$$

i.e. a constant term does not occur, unless it is included in C^+_{par}, but this is not allowed in Regge theory.

Our fits do not automatically satisfy the sum rule (9.65) or the unsubtracted relation (9.82), since they were derived from total cross section data alone. In sect.2.3 we have already discussed the magnitude of the constant terms in the high energy expansion. Eq.(2.21) can be written

$$\text{Re } C^+(\omega) = \text{Re } C^+_{par}(\omega) + C_N^+(\infty) - C_N^+(\mu) + C^+(\mu) - \frac{2}{\pi}\int_0^{\Omega}(\sigma^+ - \sigma^+_{par})dk + O(k^{-2}). \tag{9.85}$$

We insert $C^+(\mu)$ as following from the unsubtracted dispersion relation (9.82) using eq.(9.83), $C_N^+(\infty) = -g^2/m$ and $C^+_{par}(\mu) = 0$ from eq.(2.19)

$$C^+(\mu) = C_N^+(\mu) + \frac{g2}{m} + \frac{2}{\pi}\int_0^{\Omega}(\sigma^+ - \sigma^+_{par})dk. \tag{9.86}$$

It is seen that the constant contribution comes out to be zero as expected.

The small non-zero values obtained in our fits

fit I, eq.(2.8)	3.3 GeV^{-1}
fit II, eq.(2.26c)	4.0 GeV^{-1}
fit III, eq.(2.27c)	10.5 GeV^{-1}

show the magnitude of the discrepancies with the unsubtracted dispersion relation and with the sum rule (9.65). If one wants to find a parametrization C^+_{par}, which does not only fit the σ^+ data but satisfies also the sum rule, one can demand that eq.(9.86) is valid as a constraint. It turns out that this leads to an equally good fit to the data. Instead of eqs.(2.3b),(2.26a) one obtains the following values for the parameters

fit

σ_o = 21.89 mb, σ_1 = 0.4257 mb, k_1 = 35.43 GeV/c, b = 8.372 mb GeV$^{1-\alpha}$, α = 0.5889 I

b_1 = 6.837 mb GeV$^{1-\alpha_1}$, b_2 = 28.927 mb GeV$^{1-\alpha_2}$, α_1 = 1.173, α_2 = 0.733. II

9.7 Models for a violation of microcausality

The dispersion relations haven been proven from the axioms of quantum field theory (see the reviews by Oehme[154] and Sommer[64]), the crucial assumption being the principle of microcausality, according to which the fields commute at spacelike separations.

Up to now, all indications for violations of the dispersion relations were not confirmed in subsequent measurements. At present, the dispersion relations are compatible with the data up to 200 GeV/c in pion-nucleon scattering and up to about 2 000 GeV/c in pp-scattering. One can ask for the corresponding bound for the value of the "fundamental length", which usually occurs in acausal models.

Oehme has studied a class of acausal models (Re. 154), which have singularities in the s-plane in addition to those following from unitarity. He has also shown how modified dispersion relations can be derived.

One of his models, in which an acausal region exists for spacelike points at a distance smaller than a fundamental length ℓ and the amplitude has an essential singularity at infinity, has been used by Lindenbaum[155] in order to determine a bound for ℓ from the data of his group.

However, Creutz and Jaffe[156] pointed out that Lindenbaum's result is not tenable, because the modified dispersion relation does not give a unique prediction for Re C^+ if Im C^+ is given. As long as the usual dispersion relation is compatible with the data, the relations derived from acausal models add no further information.

The only argument for a bound on a possible fundamental length is a dimensional one: since the dispersion relation is valid up to at least 200 GeV/c in pion-nucleon scattering, it is unlikely that the fundamental length is larger than $\hbar c/200$ GeV/c $\hat{=}$ 10^{-16} cm. The pp-scattering data lead to a value which is smaller by an order of magnitude.

Another model in which the usual dispersion relations are violated has been proposed by Gundzik and Sudarshan[102]. Their scattering amplitude is piecewise analytic due to the presence of a negative metric threshold in the s-channel.

10. Summary and Conclusions

(1) Our tables are based on interpolations of the total cross section data, assuming high energy parametrizations, whose parameters have been determined from fits to the data in large momentum intervals (10 or 30 GeV/c to 340 GeV/c).

The two parameters of the dispersion relations: the coupling constant f^2 and the subtraction constant $C^+(\mu)$, have been determined from amplitudes reconstructed from our phase shifts. f^2 follows from the fixed-t dispersion relation[3] for the amplitude B(s,t) at $t \neq 0$ and $C^+(\mu)$ from the forward dispersion relations (sect.5). The Tables are based on $f^2 = 0.079$ and $C^+(\mu) = -0.99\ \text{GeV}^{-1}$. Our fit (Fig.12) to eq.(5.5) suggests a correction to $C^+(\mu)$ of $+0.11\ \text{GeV}^{-1}$. A realistic error can be estimated from Fig. 5. Because of the uncertainties of the low energy data and of the Coulomb corrections, a value of $C^+(\mu) = 0$ is probably not yet excluded.

(2) Assuming an once subtracted dispersion relation for C^+ and an unsubtracted dispersion relation for C^- one can test their validity by comparing the prediction for Re $C_\pm$ with amplitudes reconstructed from phase shifts or determined from Coulomb interference experiments.

It turns out that there are small discrepancies at some places, but they do not show a systematic trend. The overall agreement is so good that there is at present no doubt that the forward amplitudes fulfill the dispersion relations.

The most interesting indication for a discrepancy occurs in the charge-exchange amplitude (Fig. 14). It is pointed out that the sign and the order of magnitude agree with that of a radiative correction, which has not been applied to the experimental data. The simple law $\sigma^- \sim 1/\sqrt{k}$ for the decrease of the total cross section difference in the asymptotic region, i.e. $\alpha_\rho = 0.500$, is compatible with the present data.

(3) The assumption of Regge theory, that the amplitudes can be continued in angular momentum, leads to sum rules which restrict the parameters of the high energy expansion. Although our parametrizations for C^+ are empirical ones, it is of interest to note that they can easily be adjusted such that the sum rule is fulfilled. As a consequence, the coefficient of the constant term in the high energy expansion of Re C^+ - Re C^+_{par} vanishes and $C^+ - C^+_{par}$ fulfills the unsubtracted dispersion relation.

In the case of C^- the 2nd term of the high energy expansion can be chosen such that the Igi-Matsuda sum rule is fulfilled and the term $\sim \omega^{-1}$ in the expansion of Re C^- - Re C^-_{par} vanishes. However, the second term is very uncertain, because the total cross section difference data and the charge-exchange data in the 5-25 GeV/c region are still rather poor and to some extent contradictory (Figs.5 and 6).

(4) The extrapolation of our amplitudes to the unphysical region below threshold gives results for the amplitudes C^+ and C^-/ω at $\omega=0$, which agree with the expectations from the Adler consistency condition and the Adler-Weisberger relation within the uncertainties following from the extrapolation in the pion masses (see also sect.10 of Ref.3).

(5) Zeros of $C^{\pm}(\omega)$ are of interest for several applications. Our solution for $C^+(\omega^2$ has one zero at $\omega = -0.085\mu^2$ in the first sheet and a second zero very near threshold in the 2nd sheet, the error being comparable to the distance to the threshold. In $C^-(\omega)$ we have at least 7 zeros in the first sheet.One follows from crossing antisymmetry, two lie at $\omega=\pm 0.58i$ and 4 at $\omega = \pm 1.38\pm 0.07$ GeV. It cannot be decided at present, whether 4 additional zeros near the cut lie in the first or second sheet.

(6) There exist many papers in which the authors proposed modified dispersion relations or other methods which exploit the analyticity properties of the amplitudes. In our opinion, none of them has an advantage over the straightforward evaluation of the ordinary dispersion relations in the case of pion-nucleon forward scattering (sect.2), but many of them have a serious disadvantage.

For instance modified dispersion relations have usually the real parts under the dispersion integral which is bad, because the experimental information on Re C is very much poorer than that on Im C. Some other methods are equivalent to the neglection of the correction to our Re C_{par}. This is justified at very high energies, but at 10 or 20 GeV/c one has to check whether the corrections are small and this can be done only by using the data at low and intermediate energies(sect.2.3 and sect.9.6).

(7) The study of ordinary dispersion relations shows clearly that the prediction for the real parts depends only very weakly on the behaviour assumed for the total cross sections at very high energies. Some authors have claimed that the sensitivity to the input for σ^{tot} at energies far above that of the real part data can be strongly enhanced by considering certain sum rules and that this method can be used in order to reject models which are acceptable otherwise.

In our opinion, a correct application of modified dispersion relations or sum rules cannot lead to results different from those obtained with the ordinary dispersion relations, unless one has introduced additional assumptions.

(8) Accurate results for pion-nucleon forward amplitudes are of great interest for many applications, for instance

i) as a basic input for phase shift analysis. Improved phase shift solutions are needed if one wants to test quark models for the excited states of the nucleon,

ii) for extrapolations to the unphysical region below threshold, where some properties of the pion-nucleon system can be treated in terms of current algebra and PCAC,

iii) for determinations of scattering amplitudes at high energies where, aside from the reggeized ρ-exchange model for the charge exchange amplitude, a generally accepted model does not exist. One can hope that applications of QCD methods will lead to an improved understanding in the near future.

Therefore, it is desirable to close the gaps in the experimental data and to resolve discrepancies between different data sets.

Total cross section data: Figs.1,3b and 5(and also Figs. 1 and 3c of Ref.2) show the main discrepancies. Of course, total cross section data,which have small errors for the $\pi^{\pm}p$ difference, would be of great interest in connection with charge-exchange data in the range above the last Fermilab experiments.New data would also be of interest at energies below these of the data of Pedroni et al.[18], because there are some uncertainties in the Coulomb corrections and it is difficult to determine the accurate normalization of the differential cross section data.

Charge-exchange scattering: Measurements of the charge-exchange cross sections at very small t have not been performed in the range below 15 GeV/c for more than 15 years. The shape of the cross section at very small t in the resonance region cannot be determined from data in the range $-0.95 < \cos\theta < 0.95$, because there is a tendency for a large variation in the range $0.95 < \cos\theta < 1$(Ref. 99).. Fig.6 shows the present situation.

Coulomb interference scattering: One could argue that new Coulomb interference experiments are of interest only at the highest accessible momenta, because possible violations of the dispersion relation are expected to be larger there than at lower momenta. However, one should note that these data are also important for other applications. The analysis gives values for the slope of the diffraction peak, which shows an unexpected variation in the range $0 > t > -0.1$ GeV^2 above and at 50 GeV/c (Refs.8,11,13,164). At present, it is not known whether this effect exists also at lower momenta. Aside from the theoretical interest, which follows from a possible relation to a contribution from the cut at $t > 4\mu^2$, the change of the slope has also consequences for the normalization of data, which is frequently carried out by a simple extrapolation to the prediction at $t=0$ (Refs.13,164). Further more, data at very small t in the resonance region would support phase shift analysis

Acknowledgments: We wish to thank E.Borie for a discussion on electromagnetic corrections and I.Sabba-Stefanescu for his interesting comments on many points, in particular in sect. 9.

Appendix

Method for Evaluation of Dispersion Integrals

In the evaluation of the dispersion relation it is necessary to calculate integrals of the type

$$\int_0^\infty \frac{f(k')}{k'^2-k^2}\,dk' \tag{A1}$$

where $f(k') = \sigma^+(k')$ or $f(k') = \sigma^-(k')\,\frac{k'^2}{\omega'^2}$.

First of all, because the computer cannot handle infinite numbers, the integral has to be broken up into two parts

$$\int_0^{k_o} \frac{f(k')}{k'^2-k^2}\,dk' + \int_{k_o}^\infty \frac{f(k')}{k'^2-k^2}\,dk' \tag{A2}$$

In the second integral one uses a parametrization $f(k') = f_{par}(k')$.

The integral from k_o to infinity

For $k < k_o$ the integral can be transformed into a sum

$$\int_{k_o}^\infty \frac{f(k')}{k'^2-k^2}\,dk' = \frac{1}{k^2}\sum_{n=1}^\infty a_n\left[\frac{k}{k_o}\right]^{2n} \qquad (k < k_o) \tag{A3}$$

with
$$a_n = \int_{k_o}^\infty f_{par}(k')\left[\frac{k_o}{k'}\right]^{2n} dk'. \tag{A4}$$

There exists an analytic expression for each a_n and the sum converges rapidly if k is not very close to k_o. If $k > k_o$ a similar transformation is possible but now we have to introduce the function

$$g_{par}(k) = \int_0^\infty \frac{f_{par}(k')}{k'^2-k^2}\,dk' \tag{A5}$$

which can be found in a table of integrals. The integral is then given by

$$\int_{k_o}^\infty \frac{f(k')}{k'^2-k^2}\,dk' = g_{par}(k) + \frac{1}{k^2}\sum_{n=0}^\infty b_n\left[\frac{k_o}{k}\right]^{2n}$$

with
$$b_n = \int_0^{k_o} f_{par}(k')\left[\frac{k'}{k_o}\right]^{2n} dk'. \tag{A6}$$

The integral from 0 to k_o

We represent the function f(k') by a cubic spline function, e.g. the function f(k') is approximated by cubic parabolas in intervals $[k_i, k_{i+1}]$ (i=1,...,N). The parabolas join continuously and with continuous first and second derivatives at the points k_i (i = 2,...,N):

$$f(k') = a_i + b_i(k'-k_i) + c_i(k'-k_i)^2 + d_i(k'-k_i)^3 \; ; \quad k' \in [k_i, k_{i+1}] \; . \tag{A7}$$

Each integral

$$I_i = \int_{k_i}^{k_{i+1}} \frac{f(k')}{k'^2-k^2} \, dk' \tag{A8}$$

can now be calculated analytically from the parameters a_i, b_i, c_i, d_i. The result diverges logarithmically at $k = k_i$ and $k = k_{i+1}$. If one uses the above mentioned continuity condition and f(0) = 0, it is possible to show that all divergent terms in the sum

$$\sum_{i=1}^{N} N_i = \int_0^{k_o} \frac{f(k')}{k'^2-k^2} \, dk' \tag{A9}$$

cancel except that at $k = k_{N+1} = k_o$. There remain terms $(k-k_i)^3$ n $k-k_i$ which can be handled easily.

If $k > k_o$ it is numerically safer to represent the integral in (A9) by a series

$$\int_o^{k_o} \frac{f(k')}{k'^2-k^2} \, dk' = -\frac{1}{k^2} \sum_{n=0}^{\infty} c_n \left[\frac{k_o}{k}\right]^{2n} \tag{A10}$$

with

$$\begin{aligned} c_n &= \int_o^{k_o} f(k') \left[\frac{k'}{k_o}\right]^{2n} dk' \quad \text{and} \\ c_n &= \sum_{i=1}^{N} J_i^{(n)} \; ; \quad J_i^{(n)} = \int_{k_i}^{k_{i+1}} f(k') \left[\frac{k'}{k_o}\right]^{2n} dk' . \end{aligned} \tag{A11}$$

To avoid difficulties with k-values around k_o we take k_o = 12 GeV/c and calculate the integrals for k-values up to 10 GeV/c. Then we set k_o = 8 GeV/c and calculate the remaining part for $k \geq$ 10 GeV/c.

References

1. G. Höhler, G. Ebel and J. Giesecke: Zeitschrift f. Physik 180 (1964) 430
2. G. Höhler, H.P. Jakob and F. Kaiser: KFK 2457 (April 1977) Kernforschungszentrum Karlsruhe, TKP 75-13 (1975) and earlier editions
3. G. Höhler, F. Kaiser, R. Koch and E. Pietarinen: Handbook of Pion-Nucleon Scattering, Physics Data 12-1 (1979)
   R. Koch and E. Pietarinen: Nucl. Phys. A336 (1980) 331
4. R.E. Cutkosky et al.: Phys. Rev. 20 (1979) 2782, 2804, 2839
5. A.S. Carroll et al.: Phys. Lett. 80B (1979) 423
6. W.D. Apel et al.: Nucl. Phys. B154 (1979) 189
7. A.V. Barnes et al.: Phys. Rev. Lett. 37 (1976) 76
8. J.P. Burq et al.: Phys. Lett. 77B (1978) 438
9. V.G. Ableev et al.: Yad. Fiz. 28 (1979) 1529
10. V.D. Apokin et al.: Soviet J. Nucl. Phys. 25 (1977) 51, Nucl. Phys. B106 (1976) 413 , Phys.Lett. 56B(1975)391
11. L.A. Fajardo et al.: FERMILAB-PUB-80/27 EXP, submitted to Phys. Rev.
12. K.J. Foley et al.: Phys. Rev. 181 (1969) 1775
13. G. Höhler, F. Kaiser and H.M. Staudenmaier, Karlsruhe preprint TKP 79-4 to be published
14. A.A. Carter et al.: Phys. Rev. 168 (1968) 1457
15. D. Davidson et al.: Phys. Rev. D6 (1972) 1199
16. Compilation of Coupling Constants and Low-Energy Parameters, Physics Data 4-2, 1979
17. J.R. Carter et al.: Nucl. Phys. B58 (1973) 378, A.A. Carter et al., Rutherford report RL-73-024 (May 1973)
18. E. Pedroni et al.: Nucl. Phys. A300 (1978) 321
19. G. Höhler, H.P. Jakob and F. Kaiser: Phys. Lett. 58B (1975) 348
20. G. Höhler and R. Koch: Karlsruhe preprint TKP 80-2 (Febr. 1980)
21. A. Citron et al.: Phys. Rev. 144 (1966) 1101 and G. Giacomelli: Progr. Nucl. Phys. 12 (1970) Part 2

22. K.J. Foley et al.: Phys. Rev. Lett. 19 (1967) 330

23. V.N. Bolotov et al.: Nucl. Phys. B37 (1974) 365

24. A.V. Stirling et al.: Phys. Rev. Lett. 14 (1965) 763

25. I.N. Ginzburg et al.: Phys. Lett. 80B (1978) 101

26. E. Borie: Z. Naturforschung 33a (1978) 1436 and private communication

27. G. Höhler: List of Pion-Nucleon Elastic and Charge-exchange Scattering Experiments, Karlsruhe preprint TKP 79-10 (Sept. 1979). This list will be kept up to date.

28. V.A. Matveev: Proceedings of the XVIIIth International Conference on High Energy Physics (Tbilisi, 1976) p. A5-35

29. F. Flocke: Diplomarbeit, Karlsruhe 1977

30. V. Barger and R.J.N. Phillips: Nucl. Phys. B40 (1972) 205

31. H. Lehmann: Nucl. Phys. 29 (1962) 300

32. H.J. Lipkin: Phys. Rev. D11 (1975) 1827 and D17 (1978) 366

33. R.E. Hendrick and B. Lautrup: Phys. Rev. D11 (1975) 529

34. T.R. Engelmann and R.E. Hendrick: Phys. Rev. 16 (1977) 2891

35. A.A. Carter et al.: Rutherford report RL-73-024 (May 1973)

36. M.L. Goldberger, H. Miyazawa and R. Oehme: Phys. Rev. 99 (1955) 986

37. E. Pietarinen: Nuovo Cim. 12A (1972) 522 and Nucl. Phys. B49 (1972) 315, B107 (1976) 21

38. C. Bourrely, J. Fischer and Z. Sekera: Nucl. Phys. B67 (1973) 452

39. G. Höhler: Czechoslovak Journal of Physics B26 (1976) 55

40. G. Höhler in "Hadron Structure", ed. M. Martinis and N. Zovko. Proceedings of the 2nd Adriatic Meeting on Particle Physics, 1976

41. J.B. Bronzan et al.: Phys. Lett. 49B (1974) 272
D.P. Sidhu et al.: Phys. Rev. D11 (1975) 1351

42. U. Sukhatme et al.: Phys. Rev. D12 (1975) 3431

43. J.D. Jackson in "Phenomenology of Particles at High Energies". Proceedings of the XIVth Scottish Summer School. Ed. R.L. Crawford and R. Jennings, 1974

44. G. Höhler in "Hadron Interactions at Low Energies". Proceedings of the Triangle Meeting. Vol. 1, page 11, edited by D. Krupa and J. Pisut. VEDA, Bratislava, 1975

45. L. van Hove in Springer Tracts in Modern Physics 39 (1965) 1

46. G. Eichmann and J. Dronkers: Phys. Lett. 52B (1974) 428

47. A. Bujak and O. Dumbrajs: J. Phys. G: Nucl. Phys. 2, No. 9 (1976)

48. V.P. Gerdt, V.I. Inozemtsev and V.A. Meshcheryakov: Dubna preprint (1976), paper submitted to the Tbilisi Conference 1976

49. J. Fischer and P. Kolar: Phys. Rev. 17D (1978) 2168

50. G.G. Vorobyev et al.: Sov. J. Nucl.Phys. 19 (1974) 433

51. P. Baillon et al.: Phys. Lett. 50B (1974) 387

52. M.P. Locher: Nucl. Phys. B2 (1967) 525
G.B. West and D.R. Yennie: Phys. Rev. 172 (1968) 1413

53. S.J. Lindenbaum in "Pion-Nucleon Scattering", ed. G.L. Shaw and D.Y. Wong Wiley, 1969

54. V.K. Samaranayake: J. Phys. G: Nucl. Phys. 5 (1979) 657
V.K. Samaranayake and W.S. Woolcock: Nucl. Phys. B48 (1972) 225
W.S. Woolcock: Nucl. Phys. B75 (1974) 455

55. G. Höhler, H.P. Jakob and R. Strauss: Phys. Lett. 35B (1971) 445

56. M. Sugawara and A. Tubis: Phys. Rev. 130 (1963) 2127

57. Y.S. Yin and A. Martin: Phys. Rev. 135B (1964) 1369

58. H. Burkhardt and A. Martin: Nuovo Cim. 29A (1975) 141

59. G. Höhler, H.P. Jakob and R. Strauss: Nucl. Phys. B39 (1972) 237

60. E. Borie, W. Gampp, G. Höhler, R. Koch and I. Sabba Stefanescu: Karlsruhe preprint TKP 78-18, to be published. Part of this preprint has been published in Z.Physik C,Particles and Fields 4(1980)333

61. A. Shafee: Nucl. Phys. B35 (1971) 556
Jorna and J.A. McClure: Nucl. Phys. B13 (1969) 68

62. H. Boll: Diplomarbeit, University of Karlsruhe, 1974

63. G. Sommer: Nuovo Cim. 52A (1967) 373

64. G. Sommer: Fortschritte der Physik 18 (1970) 577

65. G. Höhler and H.P. Jakob: Comparison of πN Data with Unitarity Bounds, University of Karlsruhe preprint (March 1971)

66. R. Odorico: Nuovo Cim. 54A (1968) 96

67. J.A. McClure and L.E. Pitts: Phys. Rev. D5 (1972) 109
J.A. McClure: Nuovo Cim. 67A (1970) 667

68. I. Mannelli et al.: Phys. Rev. Lett. 14 (1965) 408

69. A.V. Stirling et al.: Phys. Rev. Lett. 14 (1965) 763
P. Sonderegger et al.: Phys. Lett. 20 (1966) 75

70. G. Höhler et al.: Phys. Lett. 20 (1966) 79 and 22(1966)203

71. M.J. Corden et al.: Nucl. Phys. B157 (1979) 250

72. R. Oehme in "Strong Interactions and High Energy Physics", ed. R. Moorhouse, Oliver and Boyd, London, 1964, p. 149

73. P.D.B. Collins: Regge theory and high energy physics, Cambridge University Press, 1977

74. C. Lovelace: Nucl. Phys. B12 (1969) 253

75. B.R. Martin, D. Morgan and G. Shaw: Pion-Pion Interactions in Particle Physics, Academic Press, 1976

76. R.J. Eden and G.D. Kaiser: Nucl. Phys. B28 (1971) 253

77. R.J. Eden: Rev. Mod. Phys. 43 (1971) 15
R.J. Eden: High Energy Collisions of Elementary Particles, Cambridge University Press, 1967

78. H. Hamilton and W.S. Woolcock: Rev. Mod. Phys. 35 (1963) 737

79. L.D. Soloviev and A. Shchelkachev: JETP Lett. 17 (1973) 154

80. H.P. Jakob and P. Kroll: Nucl. Phys. B92 (1975) 171

81. S. D'Angelo, E. Ferrari, G. Violini, Y. Srivastava: unpublished results (March 1974). E.Ferrari et al.: Lett.al Nuovo Cim. 10(1974)762

82. S. Adler: Phys. Rev. 140 (1965) B736

83. G. Bialkowski, K. Kang and B. Nicolescu: Lett. Nuovo Cim. 13 (1975) 401

84. D. Joynson, E. Leader and B. Nicolescu: Nuovo Cim. 30A (1975) 345

85. V. Barger and R.J.N. Phillips: Phys. Rev. 187 (1969) 2210

86. V. Barger and R.J.N. Phillips: Phys. Lett. 53B (1974) 195

87. H. Nakata: Phys. Rev. D16 (1977) 1354 and D18 (1978) 2392

88. B. and F. Schrempp: Springer Tracts in Modern Physics 61(1972)68

89. G.L. Kane and A. Seidl: Rev. Mod. Phys. 48 (1976) 309

90. P.D.P Collins: Springer Tracts in Modern Physics 60(1971)204

91. K.H. Augenstein, G. Höhler, E. Pietarinen and H.M. Staudenmaier: Physics Data 1-2 1977. The data tape is available on request from Dr. G. Ebel, Fachinformationszentrum Karlsruhe, 7514 Eggenstein-Leopoldshafen 2.

92. J. Dronkers and P. Kroll: Nucl. Phys. B47 (1972) 291

93. P. Borgeaud et al.: Phys. Lett. 10 (1964) 134

94. J.E. Nelson et al.: Phys. Lett. 47B (1973) 281

95. R.M. Brown et al.: Nucl. Phys. B117 (1976) 12 and B137 (1978) 542 Erratum

96. G. Höhler et al.: Z. Physik 240 (1970) 377 and 261 (1973) 401

97. F. Bulos et al.: Phys. Rev. 187 (1969) 1827

98. V. Kistiakowski et al.: preprint submitted to the International Conference at Tbilisi (1976). An earlier version was submitted to the Batavia Conference (Yamamoto et al., 1972)

99. G. Höhler, H.P. Jakob, F. Kaiser, G. Brandenburger: KfK 2735 (Feb. 1979), Kernforschungszentrum Karlsruhe

100. G. Höhler, J. Baacke and R. Strauss: Phys. Lett. 21 (1966) 223

101. T.N. Pham and T.N. Truong: Phys. Rev. Lett. 30 (1973) 406

102. M.G. Gundzik and E.C.G. Sudarshan: Phys. Rev. D6 (1972) 798

103. A. Martin: Scattering Theory: Unitarity Analyticity and Crossing, Lecture Notes in Physics 3. Springer-Verlag Heidelberg 1969
A. Martin and F. Cheung: Analyticity properties and bounds of the scattering amplitudes. Gordon and Breach, New York, 1970

104. S.M. Roy: Physics Reports 5 (1972) 125

105. P.D.P. Collins, F.D. Gault and A. Martin: Nucl. Phys. B80 (1974) 136 and B83 (1974) 241

106. N.S. Craigee and G. Preparata: Phys. Lett. 52B (1974) 84

107. A.K. Common and F.J. Yndurain: Nucl. Phys. B26 (1971) 167 and B34 (1971) 509

108. J. Fischer, R.S. Saly and I. Vrkoe: Phys. Rev. D18 (1978) 4271

109. S.M. Roy and V. Singh: Phys. Lett. 32B (1970) 50

110. Y.S. Jin and S.W. McDowell: Phys. Rev. 138B (1965) 1279

111. N.N. Khuri and T. Kinoshita: Phys. Rev. 137B (1965) 720 and 140B (1965) 706

112. J. Fischer, P. Kolav and I. Vrkoe: Phys. Rev. D13 (1976) 133

113. T.N. Pham and T.N. Truong: Phys. Rev. Lett. 31 (1973) 330

114. G. Höhler and H.P. Jakob: Z. Physik 268 (1974) 75

115. W. Gilbert: Phys. Rev. 108 (1957) 1078

116. I.S. Gradshteyn and I.M. Ryzhik: Tables of Integrals, Series and Products. Academic Press, 1965

117. W. Meyer zur Capellen: Integraltafeln. Springer-Verlag, Berlin 1950

118. A. Erdelyi et al.: Tables of Integral Transforms. McGraw Hill, New York, 1954

119. S. Adler: Phys. Rev. 137 (1965) B 1022

120. L.A. Khalfin: Soviet Physics JETP Lett.6(1967)107

121. Y. Liu and S. Okubo: Phys. Rev. 168 (1968) 1712

122. J. Fischer, J. Pisut, P. Presnajder and J. Sebesta: Czech. J. Phys. B19 (1969) 1486

123. J. Pisut, P. Presnajder, J. Fischer: Nucl. Phys. B12 (1969) 586

124. P. Presnajder and J. Pisut: Nucl. Phys. B22 (1970) 365

125. S. Ciulli and G. Nenciu: Comm. Math. Phys. 26 (1972) 237

126. J. Fischer: Commun. Math. Phys. 30 (1973) 249

127. Y. M. Lomsadze et al.: Nucl. Phys. B73 (1974) 536

128. A. Kanazawa and M. Sugawara: Phys. Rev. 40B (1972) 265

129. T.P. Cheng and R. Dashen: Phys. Rev. Lett. 26 (1971) 594

130. Yu-Chien Liu and J.A.M.Vermaseren: Phys.Rev. D8(1973)1602

131. R.Omnes: Nuovo Cim. 8 (1958)316

N.I.Muskhelishvili, Singular Integral Equations,P.Noordhoff Ltd,Groningen 1953

132. R.Odorico: Nuovo Cim.54 (1968)96

133. G.Frye and R.L.Warnock: Phys.Rev.130(1963)478

134. A.D.Martin and R.Wit: Nucl.Phys. B25(1971)85

135. E.Ferrari and G.Violini: Lett.al Nuovo Cim.5(1972)1027

136. N.Zovko: Phys.Lett.23(1966)143

137. N.M.Queen, S.Leeman and F.E.Yeomans: Nucl.Phys. B11(1969)115

138. V.Barger and R.J.N.Phillips: Phys.Lett. 31B(1970)643

R.J.N.Phillips: Acta Phys.Austr. Suppl.VII(1970)214,Schladming Lecture

139. H.Nielsen: Nucl.Phys. B30(1971)317, B33(1971)152

140. J.Baacke and J.Engels: Nucl.Phys. B51(1973)434

141. K.Igi: Phys.Rev.130(1963)820

142. R.Brandt and G.Preparata: Phys.Rev. D7(1973)218

143. J.Ellis and P.Weiss: CERN TH 1296 (Feb. 1971)

144. P.D.B.Collins and E.J.Squires: Springer Tracts in Modern Physics 45(1968)

145. N.Zovko: Nucl.Phys.B11(1969)231

146. C.Ferro Fontan,N.M.Queen and G.Violini: Rivista del Nuovo Cim. 2(1972)357

147. K.Igi and S.Matsuda: Phys.Lett.18 (1967) 625

148. A.A.Logunov,L.D.Soloviev and A.N.Tavkhelidze: Phys.Lett. 24B(1967) 181

149. R.Dolen, D.Horn and C.Schmid: Phys.Rev. 166(1968) 1768

150. H.D.I.Abarbanel and R.L.Sugar: Phys.Rev.D10(1974) 721

151. G.Höhler in Lecture Notes in Physics 56(1976)159, Springer Verlag

152. Review of Particle Properties, Particle Data Group (June 1978)

153. Bonn-CERN-Ecole Polytechnique-Glasgow-Lancaster-Manchester-Orsay-Paris VI-Paris VII-Rutherford-Sheffield Collaboration, CERN-EP/80-04 (Jan.1980) submitted to Phys.Lett.B

154. R.Oehme: Phys.Rev.100 (1955)1503 and Festschrift in honor of Gregor Wentzel, University of Chicago Press, 1969

155. S.J.Lindenbaum in Pion-Nucleon Scattering. ed.G.L.Shaw and D.Y.Wong, Wiley, 1969, p.81

156. M.Creutz and R.Jaffe: Phys.Rev.D2(1970)2359

157. T.Sawada: Phys.Rev. 158(1967)1421 and earlier papers with A.O.Barut

158. B.Tromborg, S.Waldenstrøm and I.Øverbø: Phys.Rev.D15(1977)725

159. A.S.Carroll et al.:Phys.Lett. 61B(1976)303

160. S.P.Denisov et al.: Nucl.Phys. B65(1973)1

161. G.Höhler:Proceedings of the International Conference on High Energy Physics (Geneva 1979), Vol 2, p.594

R.Koch: Talk given at the workshop on low and intermediate energy kaon nucleon physics,Rome (1980), to be published in the Proceedings

162. V.D.Apokin et al.: Sov.J.Nucl.Phys. 25(1977)51 and 24(1976)49, Nucl.Phys. B106(1976)413

163. Yu.P.Bushnin et al.: Sov.J.Nucl.Phys. 16(1973)674

164. G.Höhler, M.Hutt and R.Koch: Analysis of near-forward πN scattering at high energies, Karlsruhe preprint TKP 80-10 (June 1980)

165. R.E.Cutkosky: J.Math.Phys. 14(1973)1231

166. R.Oehme: Springer Tracts in Modern Physics 61(1972)109

167. H.Cheng, J.K.Walker and T.T.Wu: Phys.Lett. 44B(1973)283,

H.Cheng and T.T.Wu: Phys.Rev.Lett.24(1970) 1456

168. J.Fischer and R.Saly:Fortschritte der Physik 28(1980)237

Figure Captions

Fig. 1 Difference between $\pi^{\pm}p$ total cross section data and our interpolation (data minus table 80/1). Only statistical errors are shown.
o Carter et al. (Rutherford data)[14], × Davidson et al. (Arizona data)[15]
□ Pedroni et al. (Table 1 of Ref. 18). These cross sections have not yet been corrected for Coulomb distortion. The systematic errors are 0.6 % for $\pi^{+}p$ and 0.8 % for $\pi^{-}p$.
△ Data of Pedroni et al. + Coulomb distortion correction according to Koch and Pietarinen[3]. Only some of the points are shown in the range where the correction is large.
● Total cross sections reconstructed from the phase shifts of Koch and Pietarinen[3], who assumed charge-independence. The remaining deviation can be due to a charge-dependence of mass and width of Δ(1233). A similar plot in Fig. 1 of Ref. 2 shows the comparison with some earlier data and with predictions from old phase shifts.

Fig. 2 Isospin 1/2 total cross section
$\sigma^{1/2}$ was calculated by R. Koch from the formula

$$\sigma^{1/2} = \{3\sigma(\pi^{-}p) - \sigma(\pi^{+}p)\}/2$$

using the data of Pedroni et al.[18] after having removed the Coulomb distortion correction, according to the formalism of Tromborg et al.[158]
(ϕ: 20 cm target, ϕ̄: 10 cm target).
Thick solid line: $\sigma^{1/2}$ as reconstructed from phase shifts (Ref. 3).
The other curves give the contributions of the lowest partial waves.

$$\sigma^{1/2} = (4\pi/q^2)(\sin^2\delta(S11) + \sin^2\delta(P11) + 2\sin^2\delta(P13) + \ldots).$$

At 200 - 270 MeV/c the remaining charge-dependent effects are comparable with the S11 contribution.

Fig. 3a Data for σ^{+} and different high energy assumptions.
⋇ Citron et al.[21], ϕ̄ Foley et al.[22], △ Apokin et al.[10]
o Carroll et al.[159], ● Carroll et al.[5].

Fit I: $\sigma^{+} = \sigma_o + \sigma_1 \ln^2(k/k_1) + b\, k^{\alpha-1}$,

Fit II: $\sigma^{+} = b_1\, k^{\alpha_1-1} + b_2\, k^{\alpha_2-1}$,

Fit III: $\sigma^{+} = \sigma_o + \sigma_1 \ln(k/k_1) + b\, k^{\alpha-1}$.

Fit L: Lipkin's fit, eq. (2.28). The parameters of fits I - III are given in eqs. (2.3b), (2.26a) and (2.27a).

Fig.3b Data and fits for σ^+, σ_+, and σ_-

This figure shows the $\pi^{\pm}p$ data in addition to the isospin even combination for the same data as in Fig.3a. The curves belong to Table 80/2. Symbols: see Fig. 3a.

Fig. 4 The decrease of σ^+ at 2 - 100 GeV/c.
We have plotted σ^+ vs 1/k in order to demonstrate that the decrease is almost linear in a large momentum range and that the resonances are small structures on a large background. The data and the symbols are the same as in Fig.3a.

Fig. 5 The total cross section difference.

The plot shows $\sqrt{k}\,\sigma^-$ vs k in a logarithmic scale. The solid lines "80/1" and "80/2" show our interpolations of the data. They agree up to 4.5 GeV/c. At higher momenta the fit of Table 80/1 approaches a law $\sqrt{k}\,\sigma^- = c$ which is reached at 30 GeV/c. The constant c = 3.3 mb $\sqrt{\text{GeV/c}}$ was chosen such that a power law for C^- with the same parameters is compatible with the charge-exchange data (see Fig. 6). Table 80/2 is based on a fit $\sigma^- \sim k^{\alpha_\rho - 1}$ ($\alpha_\rho = 0.534$), which starts with a compromise between the data of Citron et al.[21] and of Foley et al.[22] and then follows the data of Carroll et al.[5,159] up to 340 GeV/c. It would not be reasonable to include the Serpuchov data [160,162], because in the 20 - 50 GeV/c range they show a trend which is in contradiction with the Fermilab data at higher momenta. The dashed line "L" belongs to Lipkin's fit[32], eq. (2.29), which includes other reactions in addition to $\pi^{\pm}p$. This fit should not be used in quantitative discussions of πN data, and our figure shows also that the simple power law is not yet useful in the lower part of Lipkin's momentum range ($k \leq 2$ GeV/c). Data points are shown above 3 GeV/c only. × Citron et al.[21], ✱ Foley et al.[22], ✦ Carroll et al.[5], ✦ Carroll et al.[159], ✦ Denisov et al.[160], ✦ Apokin et al.[162], ✦ Bushnin et al.[163]

Resonance structures are seen in σ^- more clearly than in σ^+ (Fig. 4) or σ_+, σ_-. Phase shift analysis at high energies[20,161] indicates that the peak at about 3.0 GeV/c belongs to the states I1,11 N(2577) and K1,13 N(2612). The dip near 4.0 GeV/c belongs to I3,13 Δ(2794) and K3,15 Δ(2990). Further small structures at higher momenta are expected, because there is evidence for resonance-like structures in Argand diagrams of some L, M and N waves.

Dot-dashed lines: fits constrained by the superconvergent sum rule.
"1" $\alpha_\rho < -1$; "2" secondary term in σ^-: $-0.97\ k^{-1.5}$.

Fig. 6 Charge-exchange forward cross sections.

We have plotted $(4\pi k d\sigma_o/dt)^{1/2}$ vs k in a logarithmic scale. The ordinate has been chosen such that the experimental points in Figs. 5 and 6 would lie on the same curve, if both sets of data could be described by a reggeized ρ-exchange law. The solid lines belong to the fits of our Tables 80/1 and 80/2. Fit 80/1 has a high energy ansatz which is a compromise between the total cross section and charge-exchange data ($\alpha_\rho = 0.50$), if the validity of the ρ-exchange model is assumed. Fit 80/2 is based on a power law fit to the total cross section data above 10 GeV/c ($\alpha = 0.534$).
⊕ Barnes et al.[7], ◇ Apel et al.[6], ✕ Saclay (Ref. 69 and priv. comm., extrapolation by W. Grein and P. Kroll), △ Nelson et al.[94]
Above 10 GeV/c the symbols have been plotted twice, the upper ones include the radiative corrections of Ginzburg et al.[25] Dot-dashed lines: see Fig.5.

Fig. 7 Argand diagram for C^+/k.

Solid line: Tables 80/1 and 80/2. Dotted and dashed lines: C^+_{par} according to the parametrizations eqs.(2.3),(2.27) . The numbers give the lab. momenta in GeV/c.

Fig. 8 Re C/Im C ratio for $\pi^- p$ elastic scattering.

Solid line: prediction from Table 80/1.
◇ Baillon et al.[51], △ Vorobyev et al.[50], ✕ Foley et al.[12], ◆ Burq et al.[8], ◇ Apokin et al.[10] (1976), + Apokin et al.[10] (1975), ⊕ Fajardo et al.[11], ⊕ Ableev et al.[9] .

The discrepancy in the 10 - 40 GeV/c range is discussed in sect. 4. See Fig. 11 for predictions based on different high energy parametrizations.

Fig. 9 Re C/Im C ratio for $\pi^+ p$ elastic scattering.

Solid line: prediction from Table 80/1.
◇ Baillon et al.[51], ✕ Foley et al.[12], + Apokin et al.[10] (1977), ⊕ Fajardo et al.[11].

Fig. 10 $\sqrt{k}\,(\rho_- - \rho_+)/2$ vs k.

We have plotted the difference of the Re/Im ratios for $\pi^{\pm}p$ elastic scattering, because this quality agrees approximately with $\rho^- \sigma^-/\sigma^+$, eq. (4.2), which is fairly well determined from charge-exchange forward scattering and total cross section data. In order to have a quantity which variies slowly in energy, we have added a factor $\sqrt{k}$. The solid curves are our fits 80/1 and 80/2. The uncertainty of the determination from charge-exchange data (ϕ) is shown at 100 GeV/c, where the errors have been calculated from those of the $d\sigma_o/dt$ and $\sigma^{\pm}$ data. We conclude that the points of Fajardo et al. at 125 and 150 GeV/c are too low by 2 - 3 standard deviations.

Fig. 11 Re/Im ratio ρ^+ for different high energy assumptions.

The figure shows predictions for ρ^+ for various assumptions on the asymptotic behaviour of σ^+.

I $\sigma^+ = \sigma_o + \sigma_1 \ln^2(k/k_1) + b\, k^{\alpha-1}$ (Table 80/1, 80/2)

II $\sigma^+ = b_1\, k^{\alpha_1-1} + b_2\, k^{\alpha_2-1}$

III $\sigma^+ = \sigma_o + \sigma_1 \ln(k/k_1) + b\, k^{\alpha-1}$

IV $\sigma^+ = 2\, c_1 (k/20)^{0,13} + 4\, c_2 (k/20)^{-0,20} + 1{,}5\, c_R (k/20)^{-0,5}$
Lipkin's ansatz, eq. (2.28), for the imaginary part. The real part is calculated from the dispersion relation (2.11).

V The same as I up to 1000 GeV/c. Then σ^+ = const

Dashed line: σ^+ as in IV, but Re C^+ is taken from the Lipkin's Regge pole type formula [Re C^+_{par} in eq. (2.31)]. The result agrees with IV above 100 GeV/c, but this approximation shows an increasing error at lower momenta. **Dot-dashed line: fit IV.**
$\dot{\Box}$ from data of Fajardo et al.[11], $\dot{\times}$ from π^-p data of Burq et al.[8] and our fit to ρ^- which is based on charge-exchange forward cross sections ($\rho^+ \approx \rho_- - \sigma^-\rho^-/\sigma^+$).

Fig. 12 Corrections to $C^{\pm}(\mu)$ from phase shifts.

We have plotted the difference ΔRe C = Re C (from phase shifts) - Re C (Table 80/1) vs. ω for π^+p amplitudes and the same quantity vs $(-\omega)$ for π^-p amplitudes (see eq. (5.5)). **Range of the fits: $k \leq 1$ GeV/c.**
The intercept of a best straight line at $\omega = 0$ gives a correction to $C^+(\mu) \sim a_1 + 2a_3$ and its slope suggests a correction to $C^-(\mu) \sim a_1 - a_3$.
o **Karlsruhe-Helsinki 1978 solution,** × **CMU-LBL 1979 solution.**

Fig. 13 Discrepancies of total cross sections.

We have plotted $\Delta\sigma = \sigma$ (from phase shifts) $- \sigma$ (Table 80/1) in order to show that, although the total cross section data are part of the input in phase shift analysis, the total cross sections reconstructed from phase shifts are at some momenta not well compatible with this input. In the $\Delta(1233)$ region this is due to charge-dependent effects.
○ Karlsruhe-Helsinki 1978, × CMU-LBL 1979.

Fig. 14 Argand diagram of C^- at high energies

The solid lines belong to our fits 80/1 and 80/2. The line "F" has been constructed from the fit of Barnes et al.[7] to $d\sigma_o/dt$ and from our fit 80/2 to the total cross section difference. In order to show the uncertainty, we have constructed the point at 200 GeV/c from the $d\sigma_o/dt$ and total cross section data. If the radiative correction of Ginzburg et al.[25] is taken into account, $|C^-|$ becomes 5 % larger (arrow) and the Regge law with $\alpha_\rho = 0.50$ lies well within the errors.

Fig. 15 For the discussion of the high energy behaviour of C^- it is also of interest to plot ρ^- vs k, because ρ-exchange Regge models predict $\rho^- \to \tan(\alpha_\rho \pi/2)$, whereas an additive term $c\omega$ in the dispersion relation should lead to $\rho^- \to \pm\infty$ in the high energy limit. We have plotted ρ^- for our fits and data points constructed from $d\sigma_o/dt$ and σ^--data.
⊕ Barnes et al.[7] , ⊖ Barnes et al.[7] plus radiative correction. One should remember that the values of the correction is a crude estimate. It could easily be larger by a factor of 2. × Apel et al.[6] , + Apel et al.[6] plus corrections. The error bars have been calculated from the statistical errors of σ^-. We conclude that at present there is no significant evidence against $\rho^- \to 1$.

Fig.16 a-f Plots of the forward amplitudes C_+, C_-, C^+, C^-, $C^{1/2}$ (Table 80/1)

Table Captions

Table 80/1: The table gives the forward amplitudes, total cross sections and differential forward cross sections. Pi+ and Pi- refer to the elastic $\pi^{\pm}p$ amplitudes and differential cross sections and to the total $\pi^{\pm}p$ cross sections, (+) and (-) to the isospin even and odd combinations of the amplitudes and total cross sections. CEX denotes the charge-exchange forward cross sections.
The first two columns give the values of kinematical quantities: k=pion lab. momentum, $\omega = \sqrt{k^2+\mu^2}$, $T_\pi = \omega - \mu$, $s=W^2$, q=c.m. momentum. All quantities are given in GeV-units except the first two entries in the second column: s/μ^2 , ω/μ .
This table is based on the high energy assumption of eqs.(2.3a) and (2.10).

Table 80/2: The only difference is the high energy assumption eq.(2.4) instead of eq.(2.10) for the total cross section difference.

Table 80/3:This table shows the discrepancies between table 80/1 and real parts and total cross sections derived from the result of the "Karlsruhe-Helsinki 1978" phase shift analysis (values from phase shifts minus values of table 80/1).We have also listed the relative discrepancies in %.

Table 80/4: the same as in Table 80/3, but for the phase shift analysis of the CMU-LBL group. One should note that these authors used a table which is based on a slightly different interpolation of the total cross section data.

Table 80/5: Continuation of Table 80/1 to the unphysical region. The connection of this table with table 80/1 is given in eqs.(6.2),(6.3).

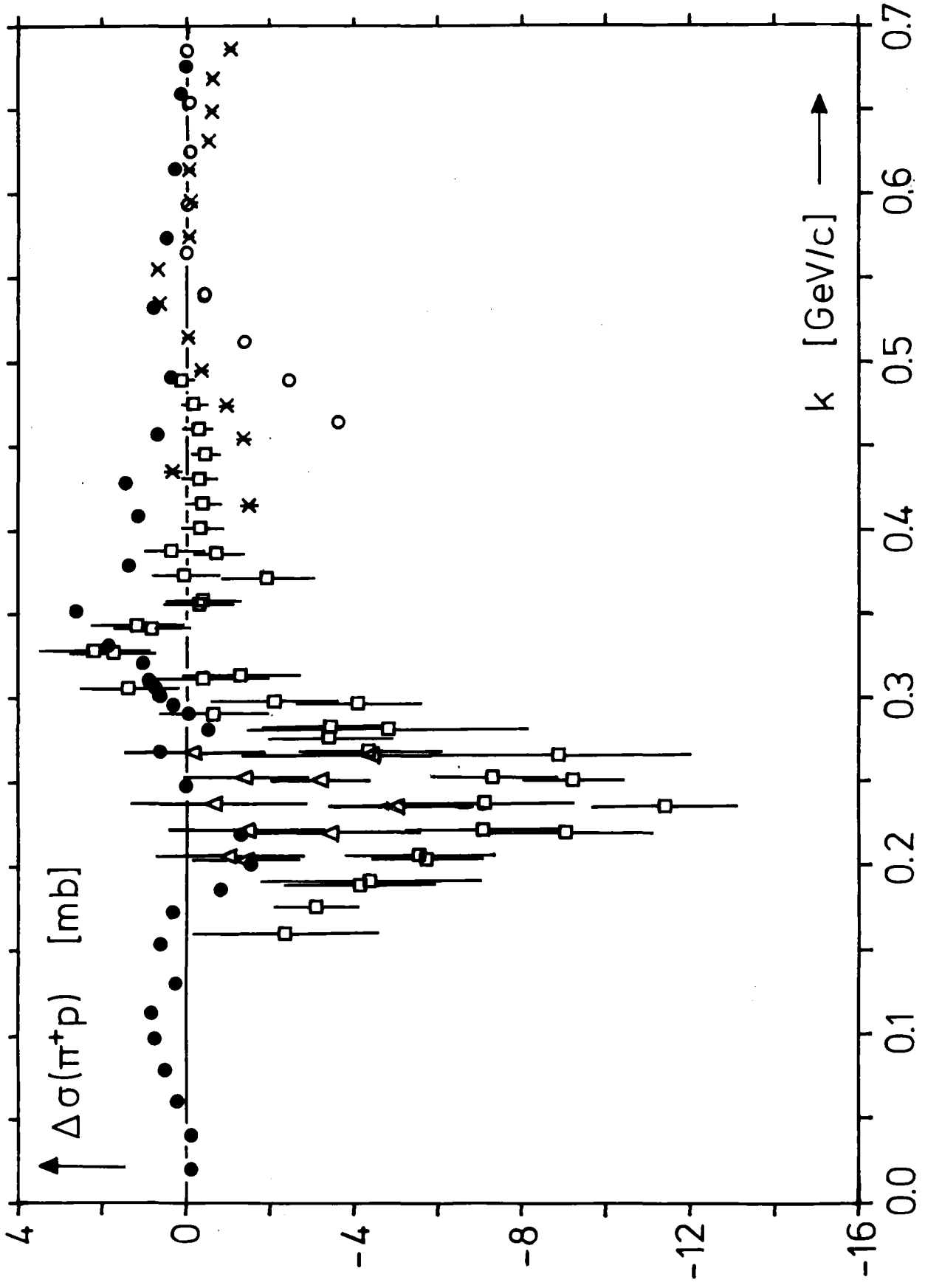

Fig. 1a

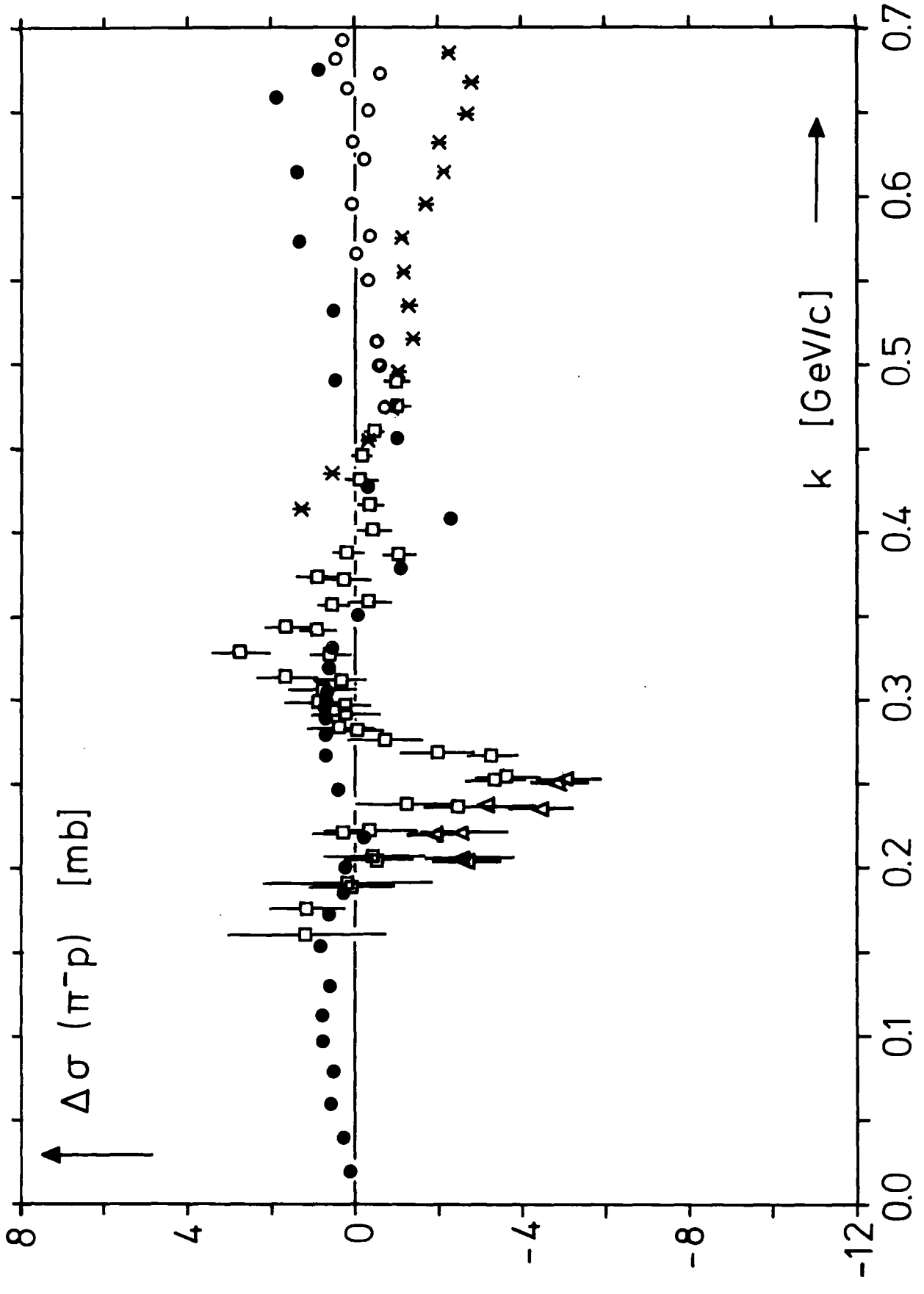

Fig. 1b

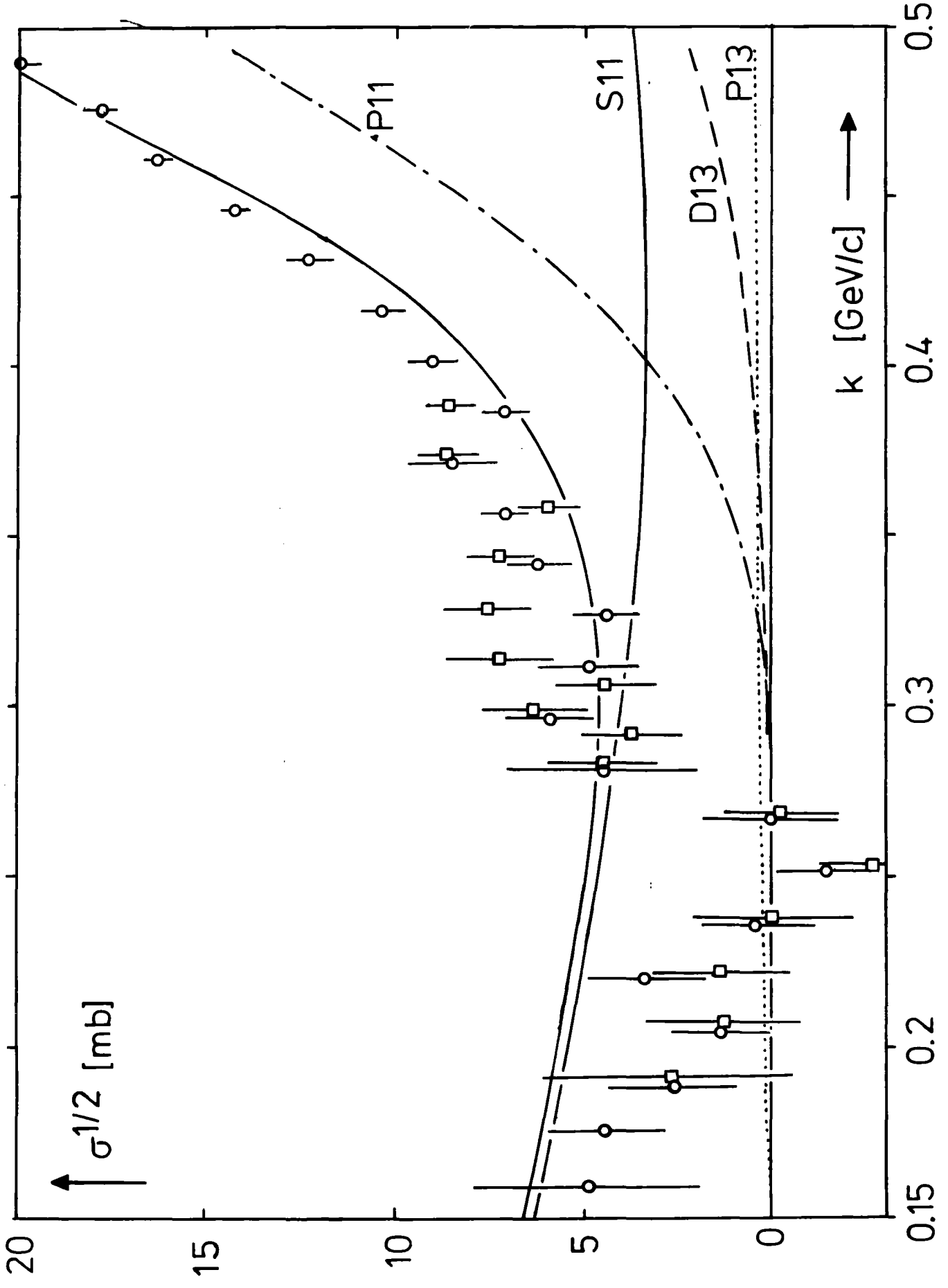

Fig. 2

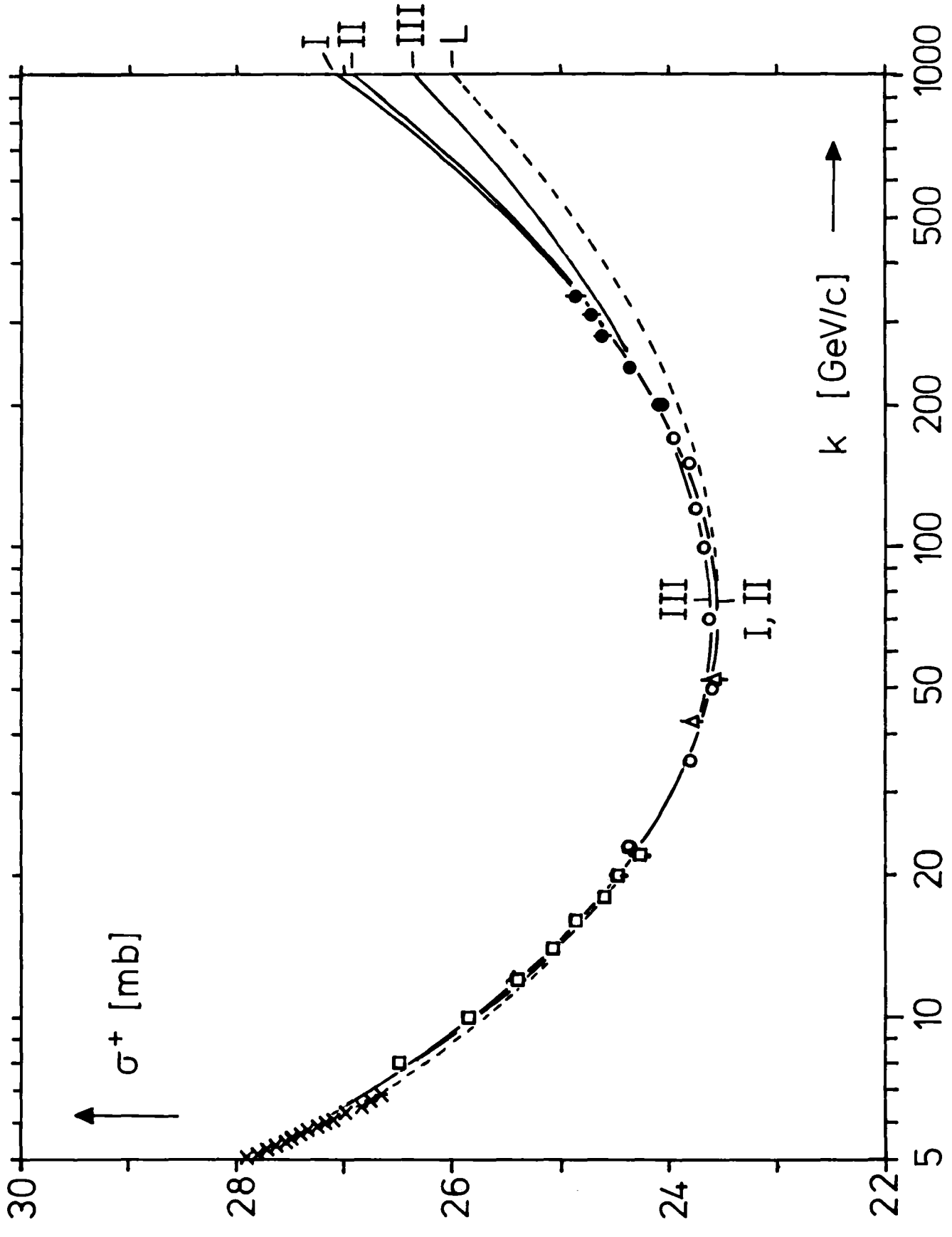
I
II
III
L
σ+ [mb]
k [GeV/c]
III
I, II
30
28
26
24
22
5
10
20
50
100
200
500
1000

Fig. 3a

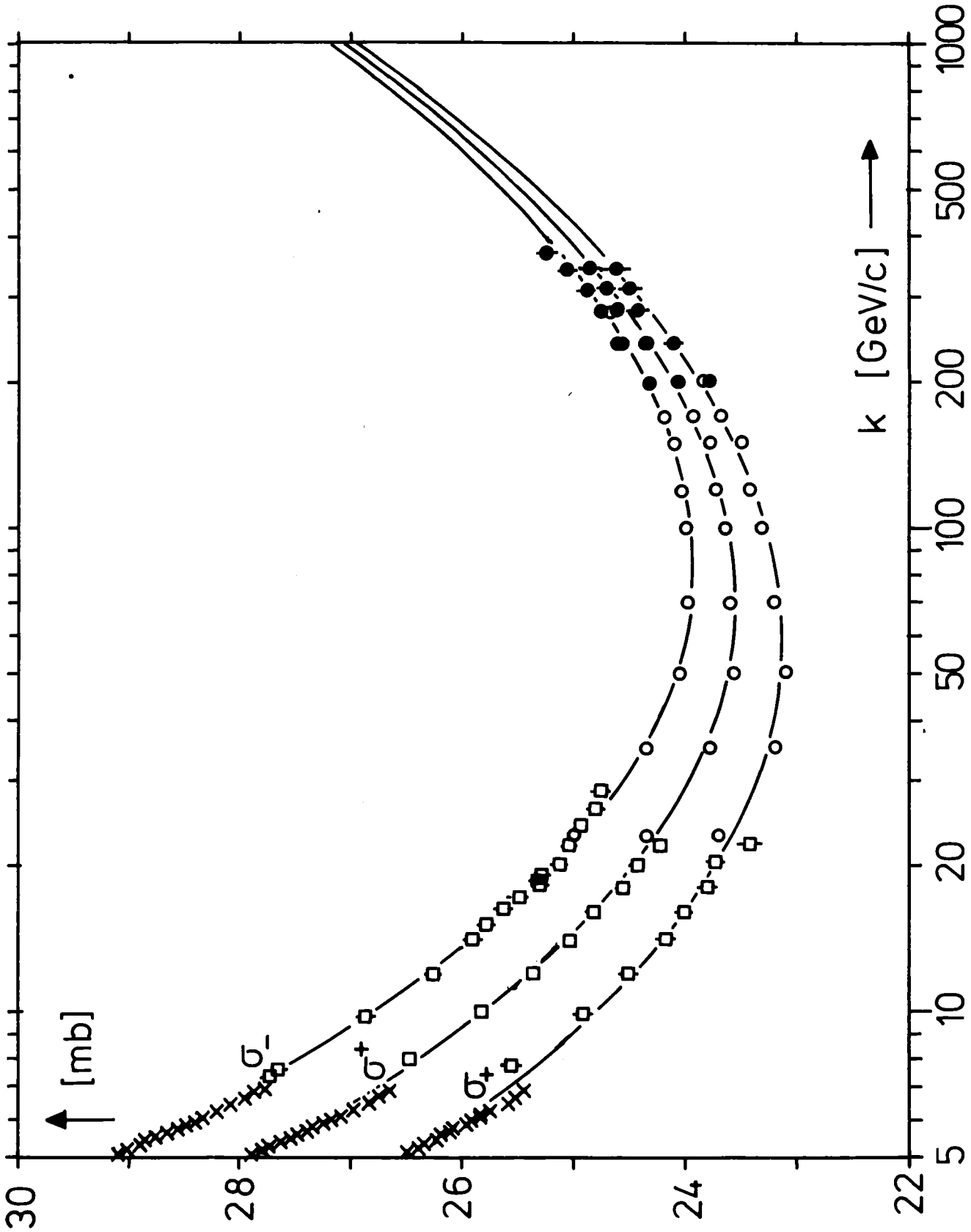

Fig. 3b

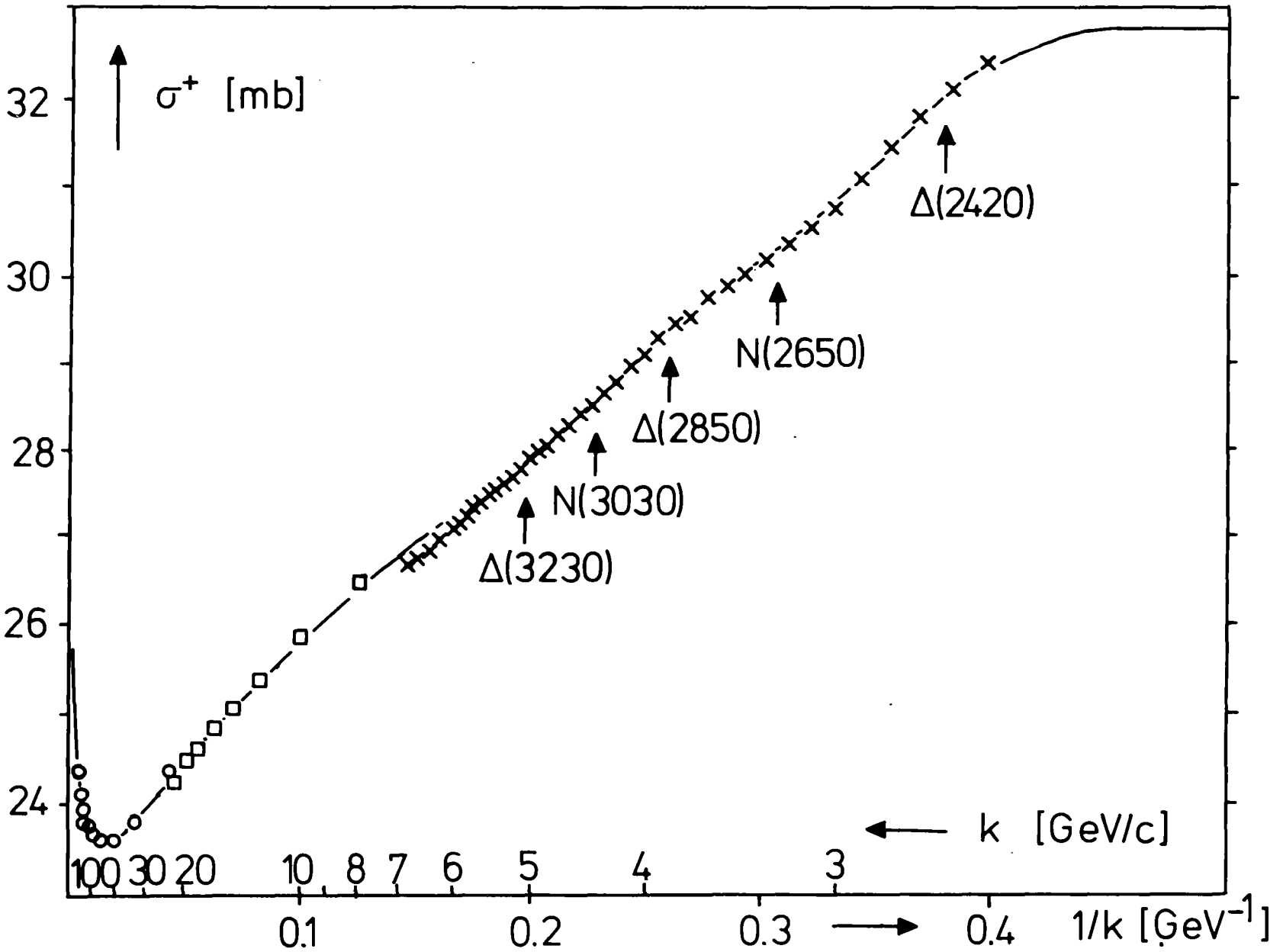
σ+ [mb]
32
30
28
26
24
Δ(2420)
N(2650)
Δ(2850)
N(3030)
Δ(3230)
k [GeV/c]
100 30 20 10 8 7 6 5 4 3
0.1 0.2 0.3 0.4 1/k [GeV-1]

Fig. 4

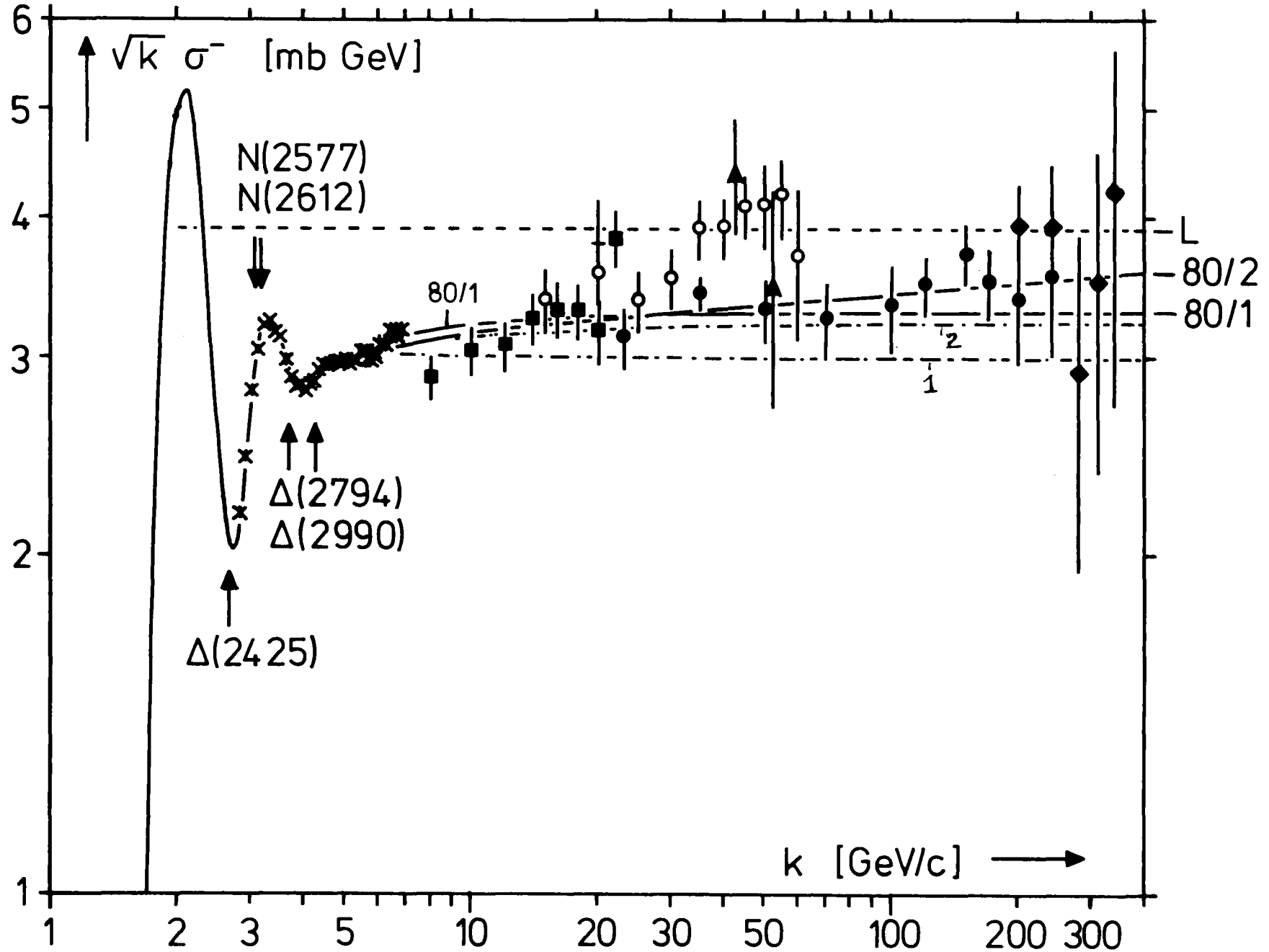
√k σ⁻ [mb GeV]
N(2577)
N(2612)
80/1
Δ(2794)
Δ(2990)
Δ(2425)
L
80/2
80/1
k [GeV/c]
6
5
4
3
2
1
1
2
3
5
10
20
30
50
100
200
300

Fig. 5

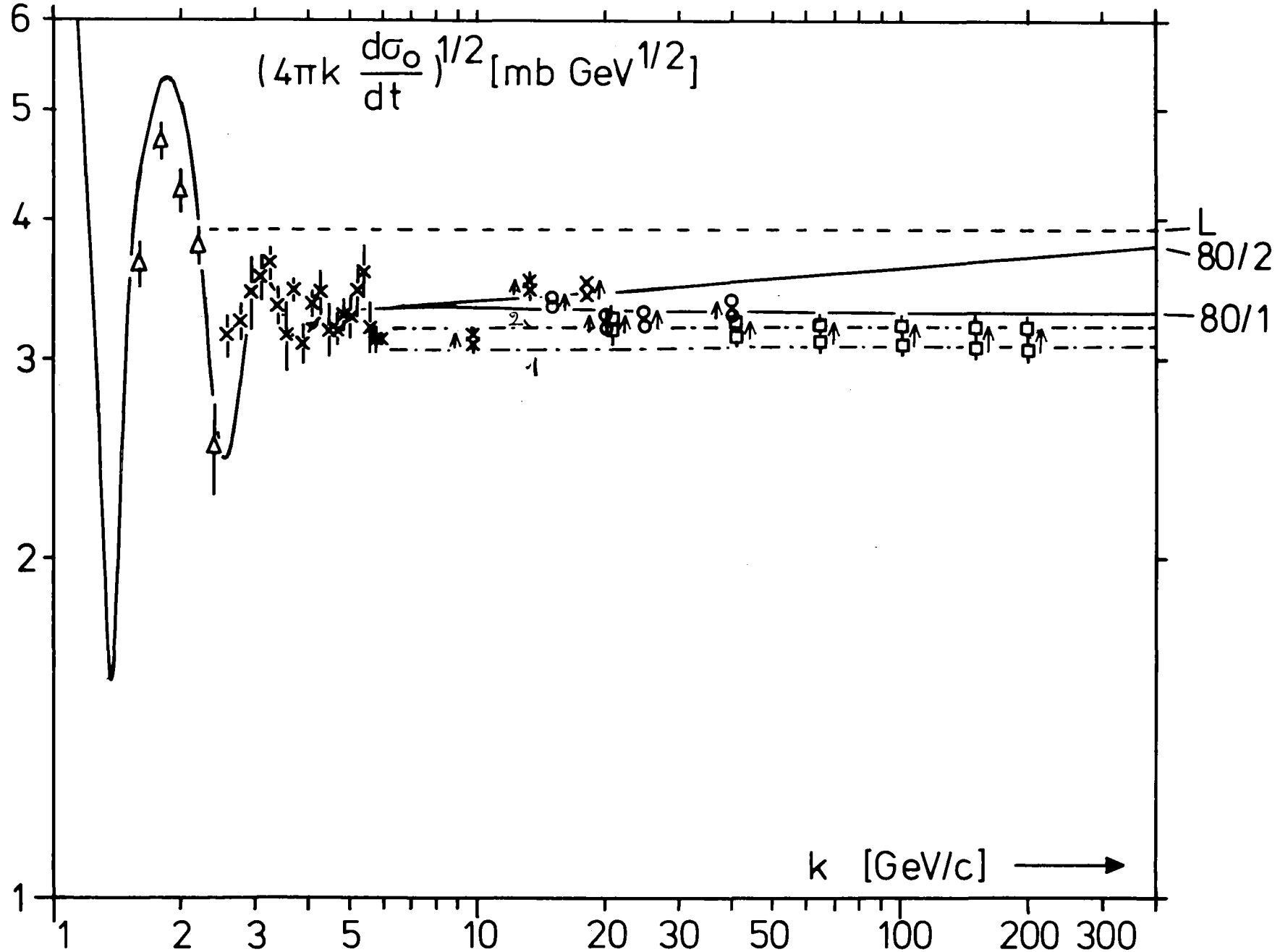
$(4\pi k \frac{d\sigma_o}{dt})^{1/2}$ [mb GeV$^{1/2}$]
L
80/2
80/1
k [GeV/c]
6
5
4
3
2
1
1
2
3
5
10
20
30
50
100
200
300

Fig. 6

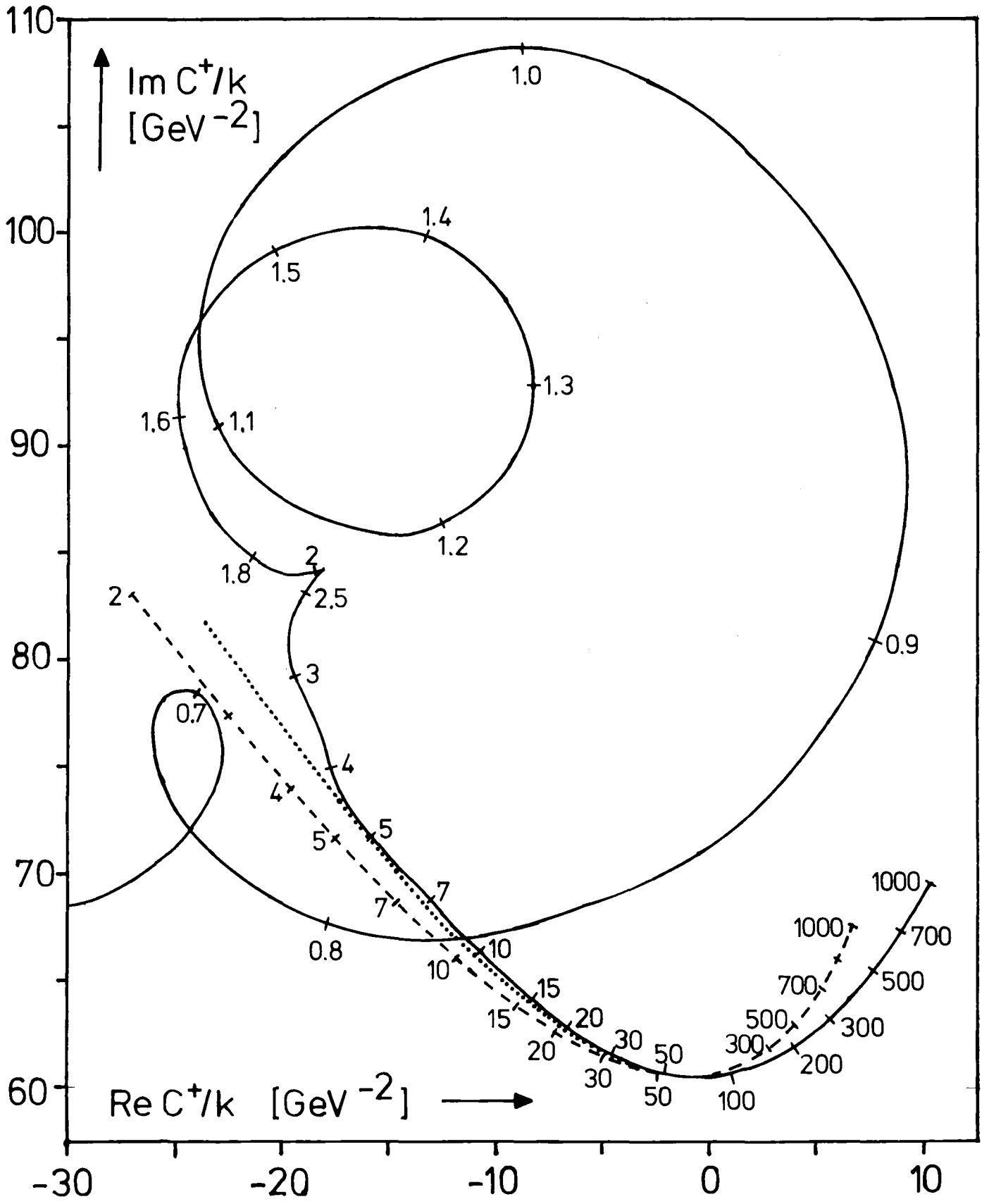
Im C+/k
[GeV -2]
Re C+/k [GeV -2]
110
100
90
80
70
60
-30
-20
-10
0
10
1.0
1.4
1.5
1.3
1.6
1.1
1.2
1.8
2
2.5
3
0.9
0.7
4
5
7
0.8
10
15
20
30
50
100
1000
700
500
300
200

Fig. 7

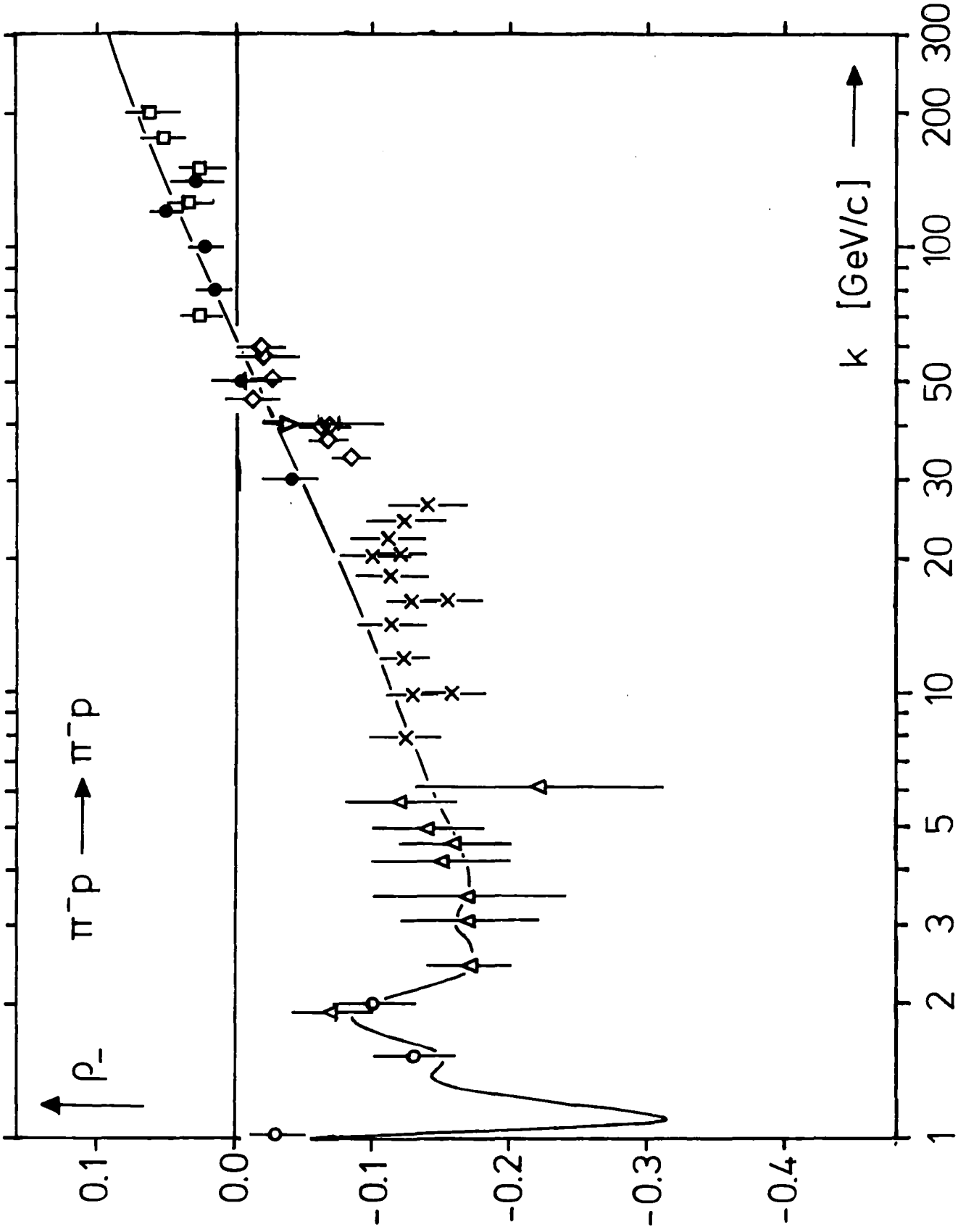
ρ_-
$\pi^-p \longrightarrow \pi^-p$
k [GeV/c]
0.1
0.0
-0.1
-0.2
-0.3
-0.4
1
2
3
5
10
20
30
50
100
200
300

Fig. 8

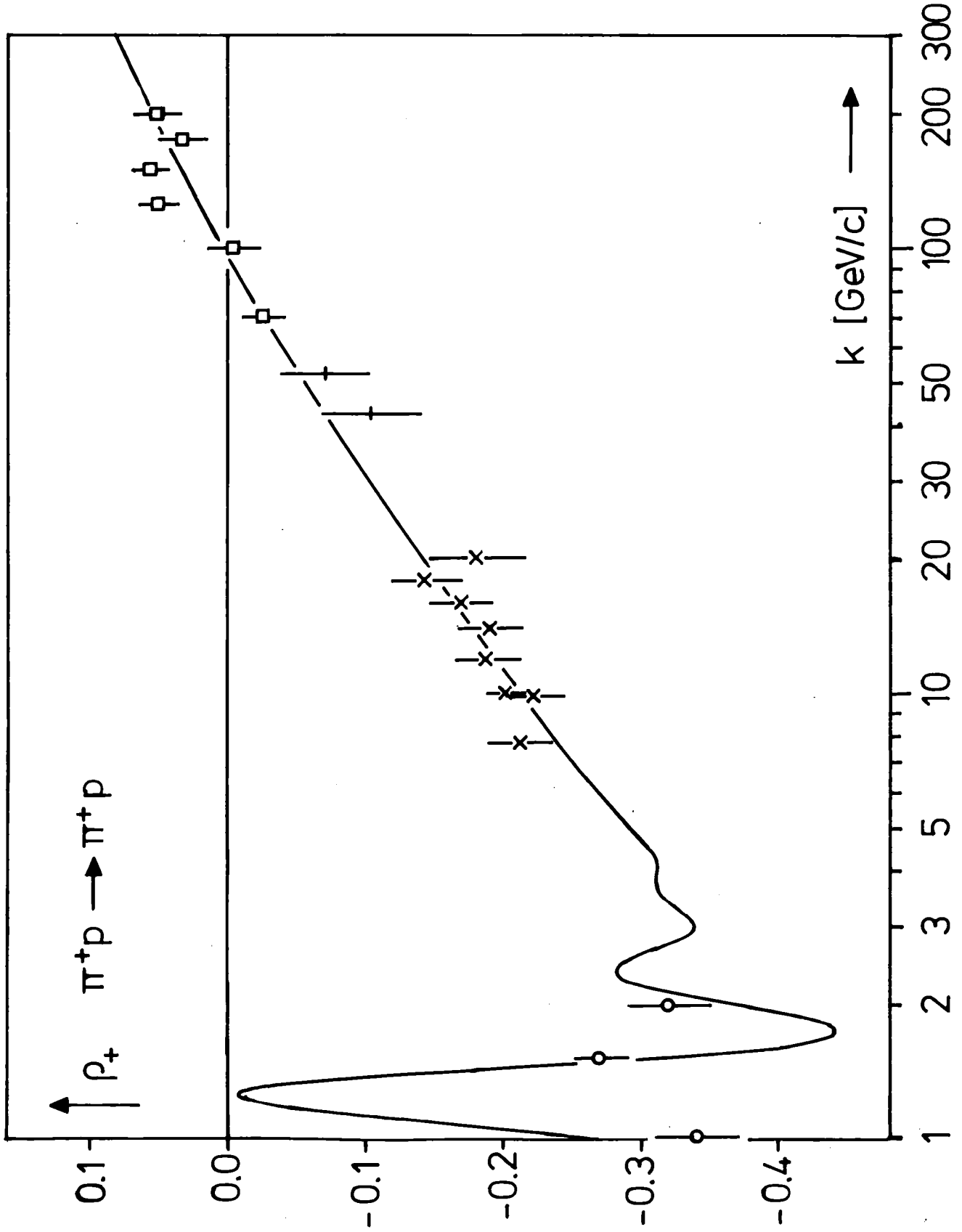

Fig. 9

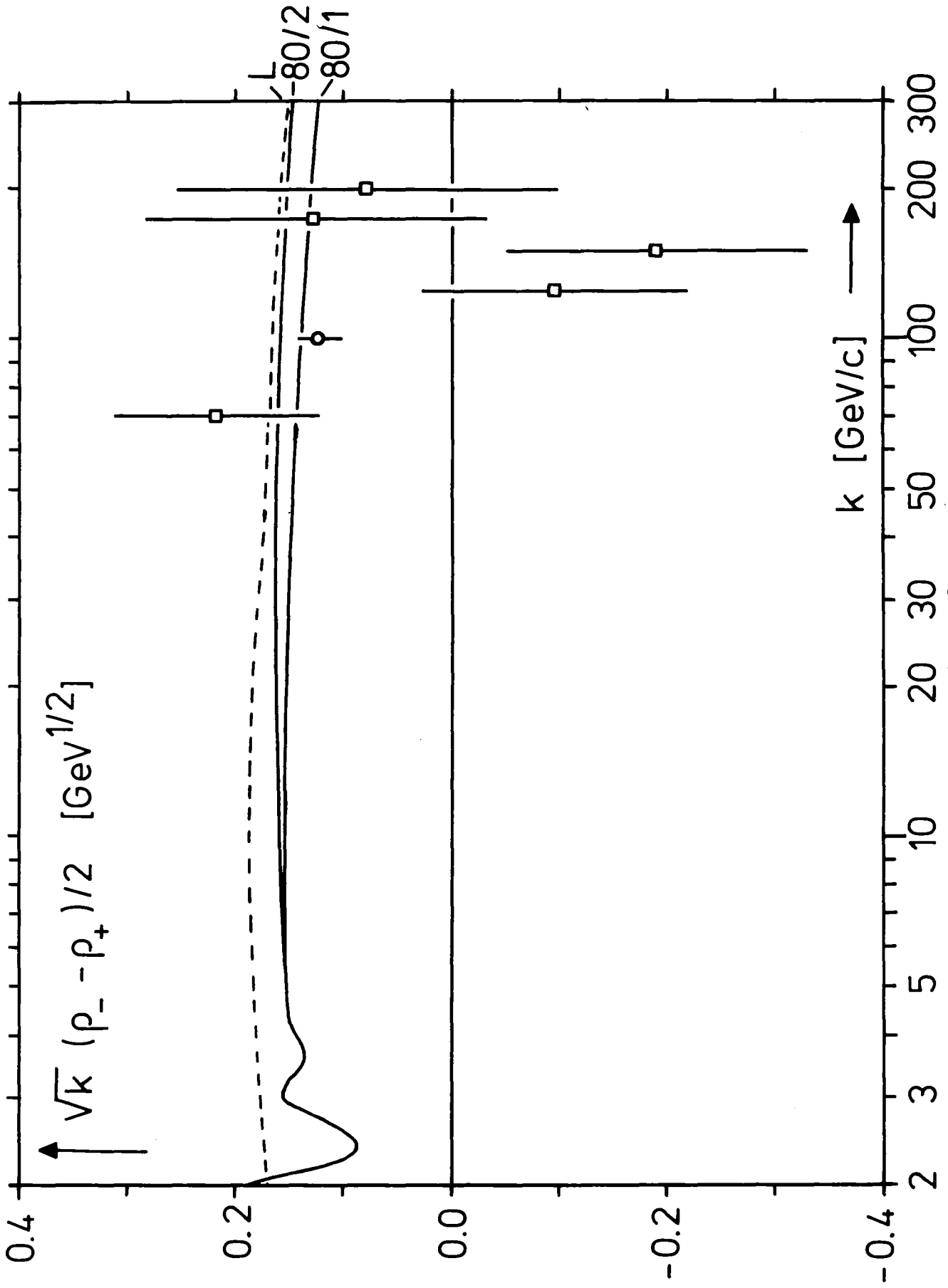
L
80/2
80/1
0.4
0.2
0.0
-0.2
-0.4
$\sqrt{k}\ (\rho_- - \rho_+)/2$ [GeV$^{1/2}$]
2
3
5
10
20
30
50
100
200
300
k [GeV/c]

Fig. 10

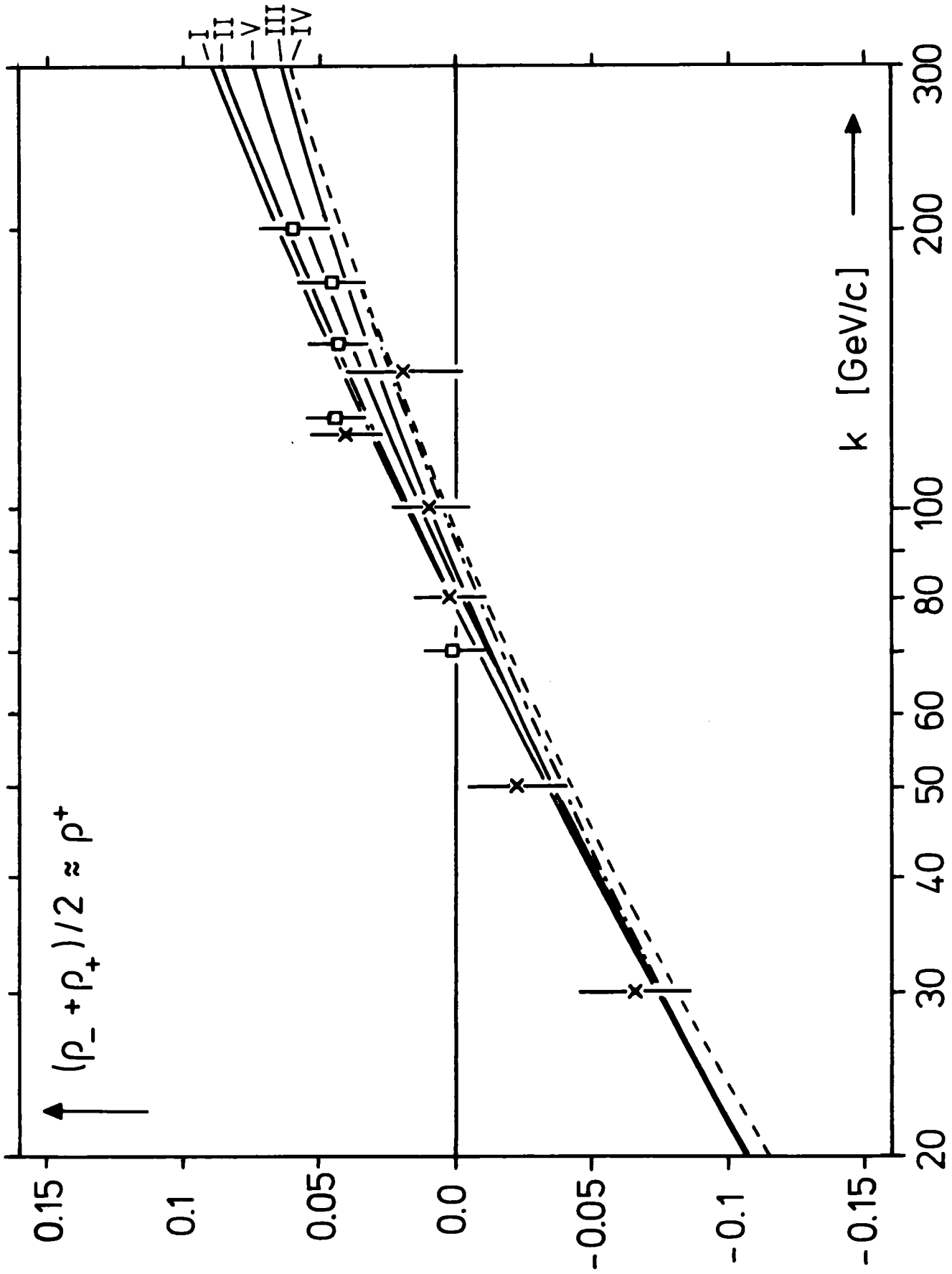
I
II
V
III
IV
$(\rho_- + \rho_+)/2 \approx \rho^+$
k [GeV/c]
0.15
0.1
0.05
0.0
-0.05
-0.1
-0.15
20
30
40
50
60
80
100
200
300

Fig. 11

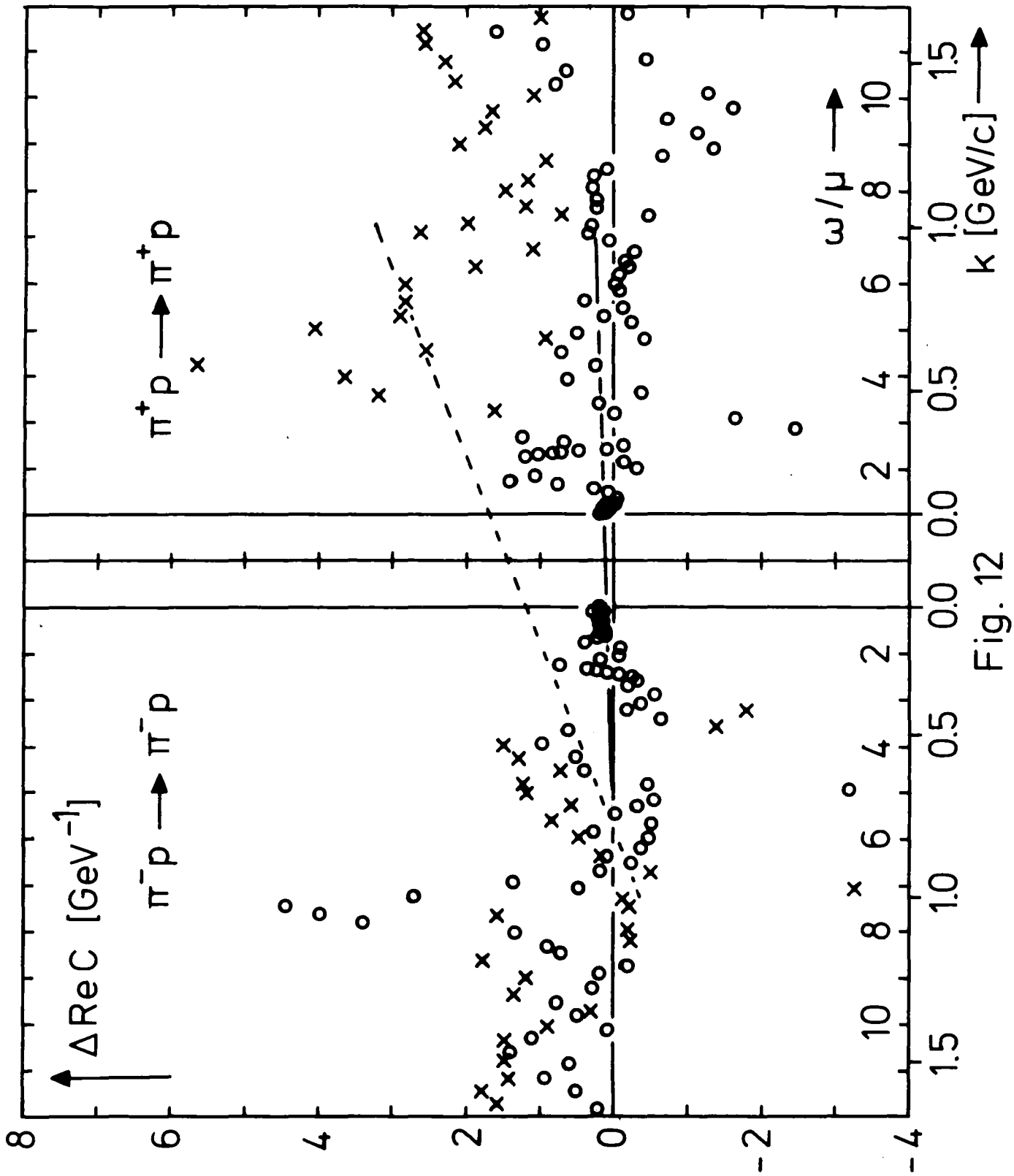

Fig. 12

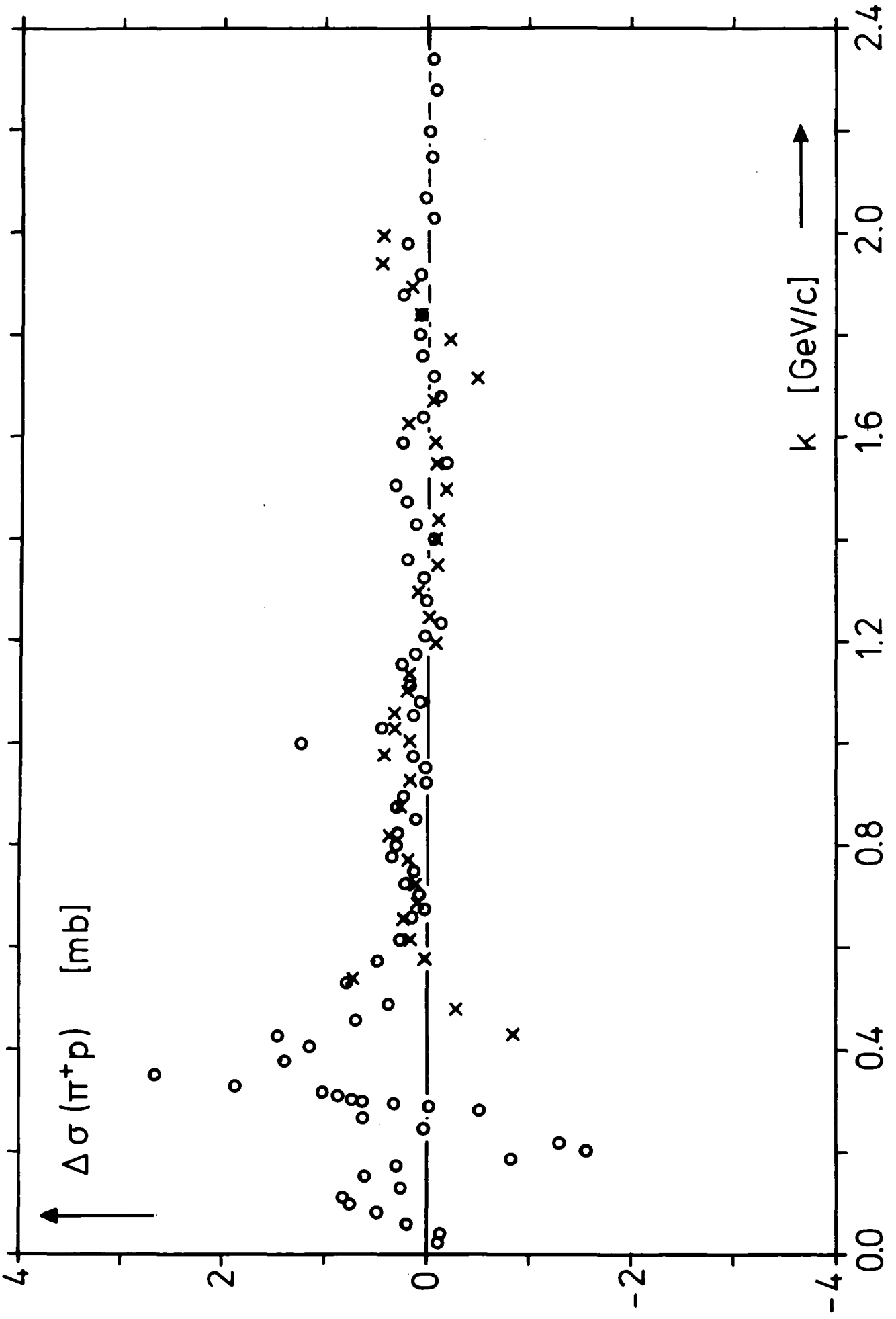

Fig. 13a

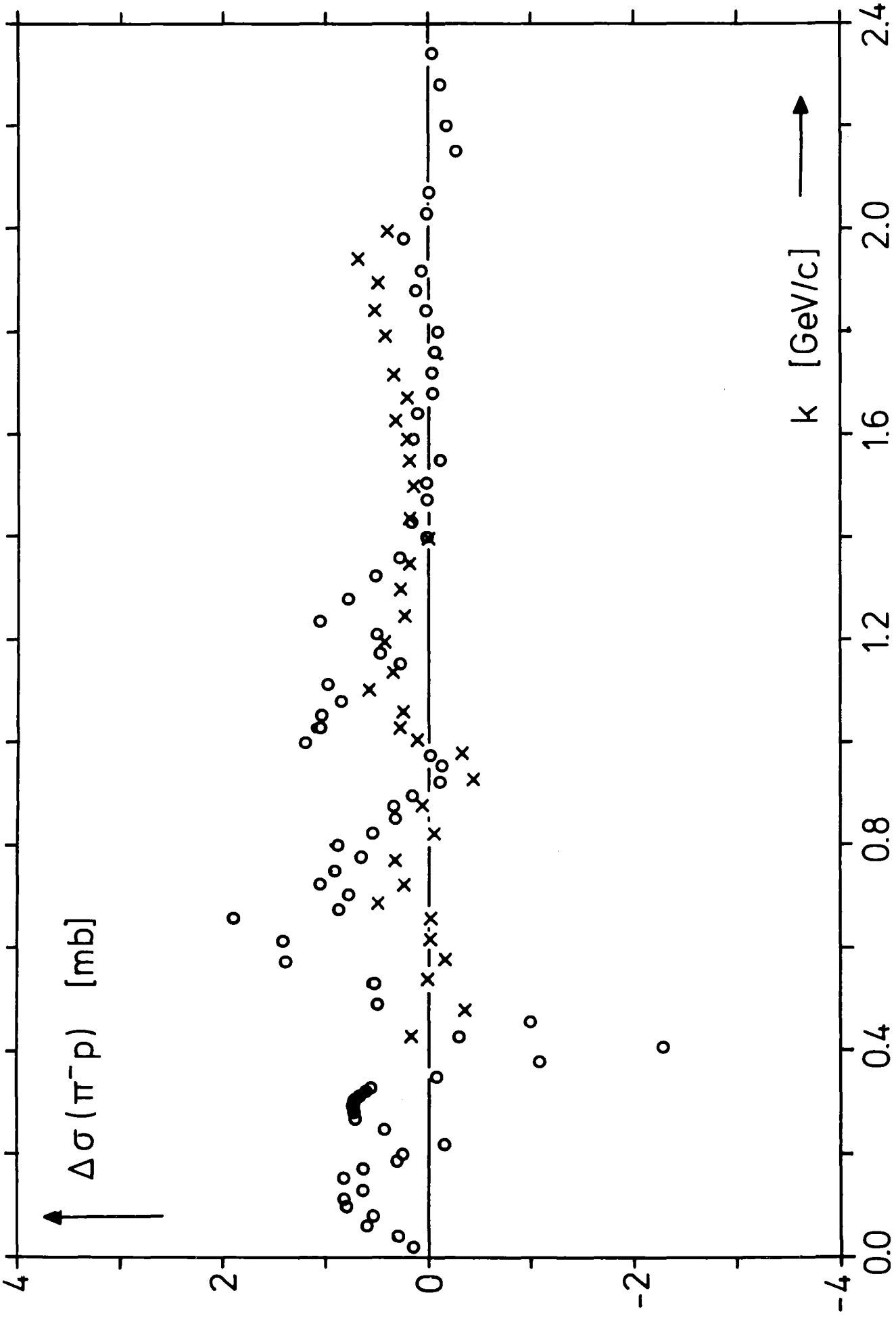

Fig. 13b

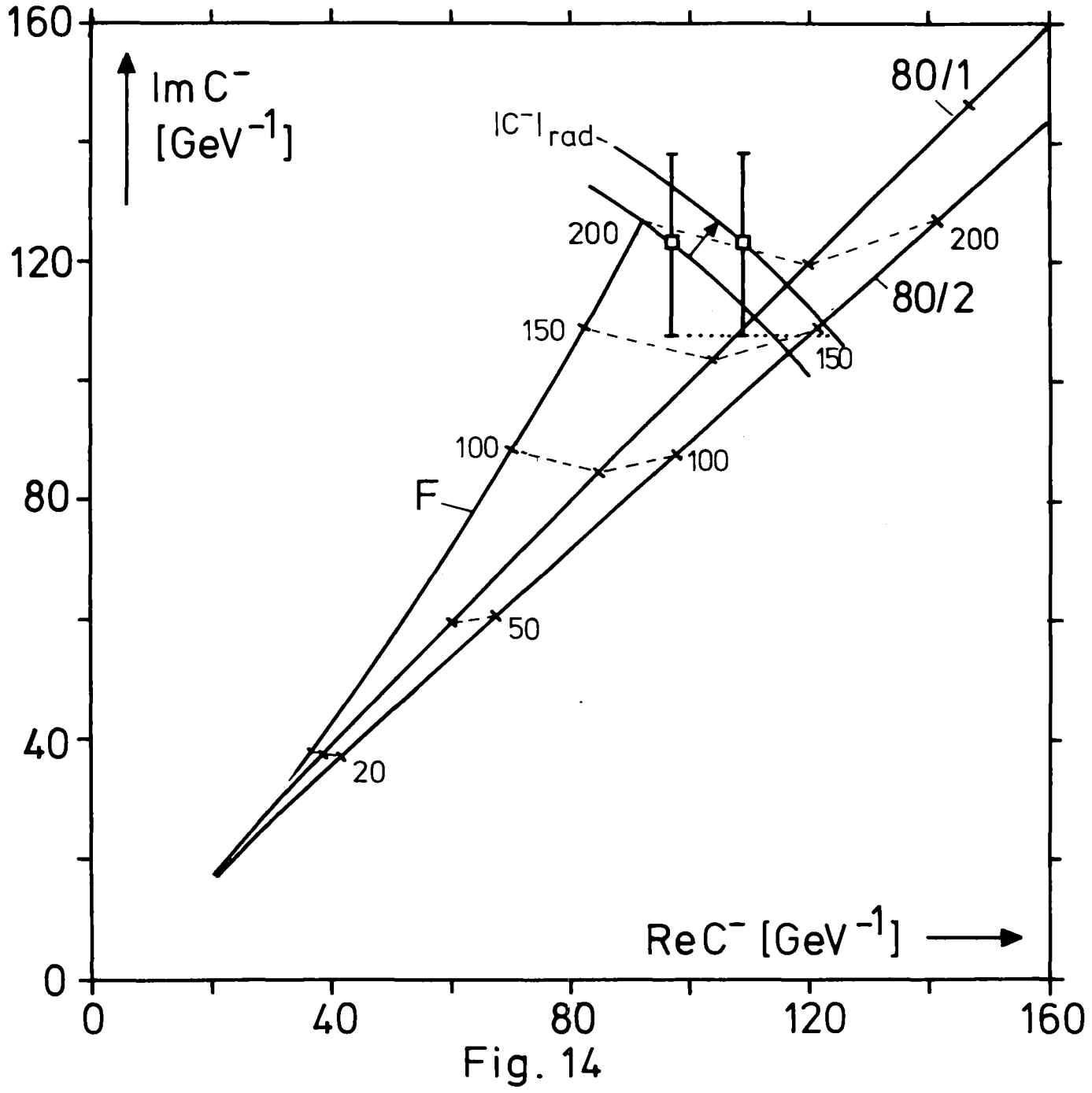
160
120
80
40
0
0
40
80
120
160
Im C⁻ [GeV⁻¹]
Re C⁻ [GeV⁻¹]
|C⁻|rad
80/1
80/2
F
200
150
100
50
20

Fig. 14

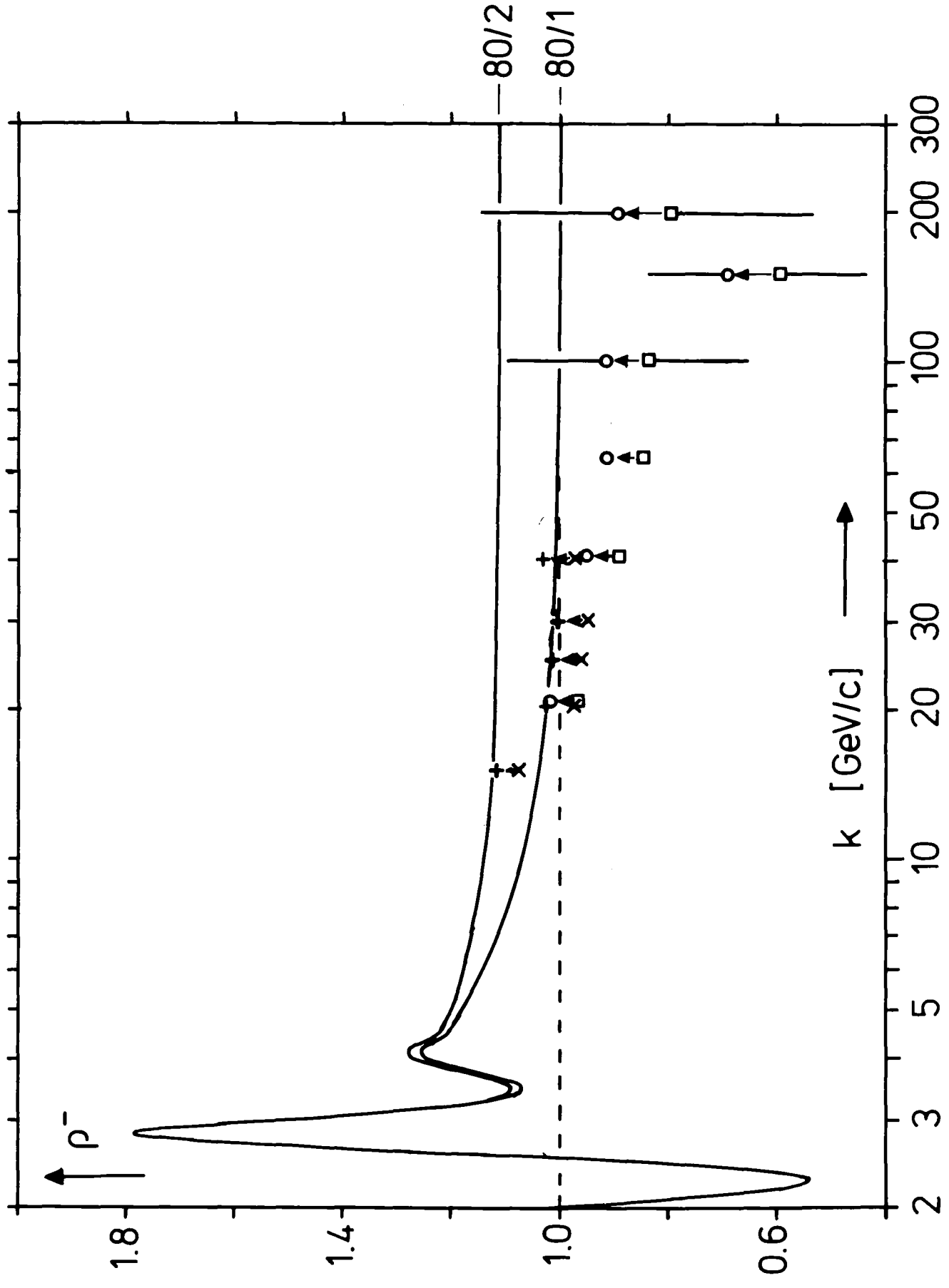

Fig. 15

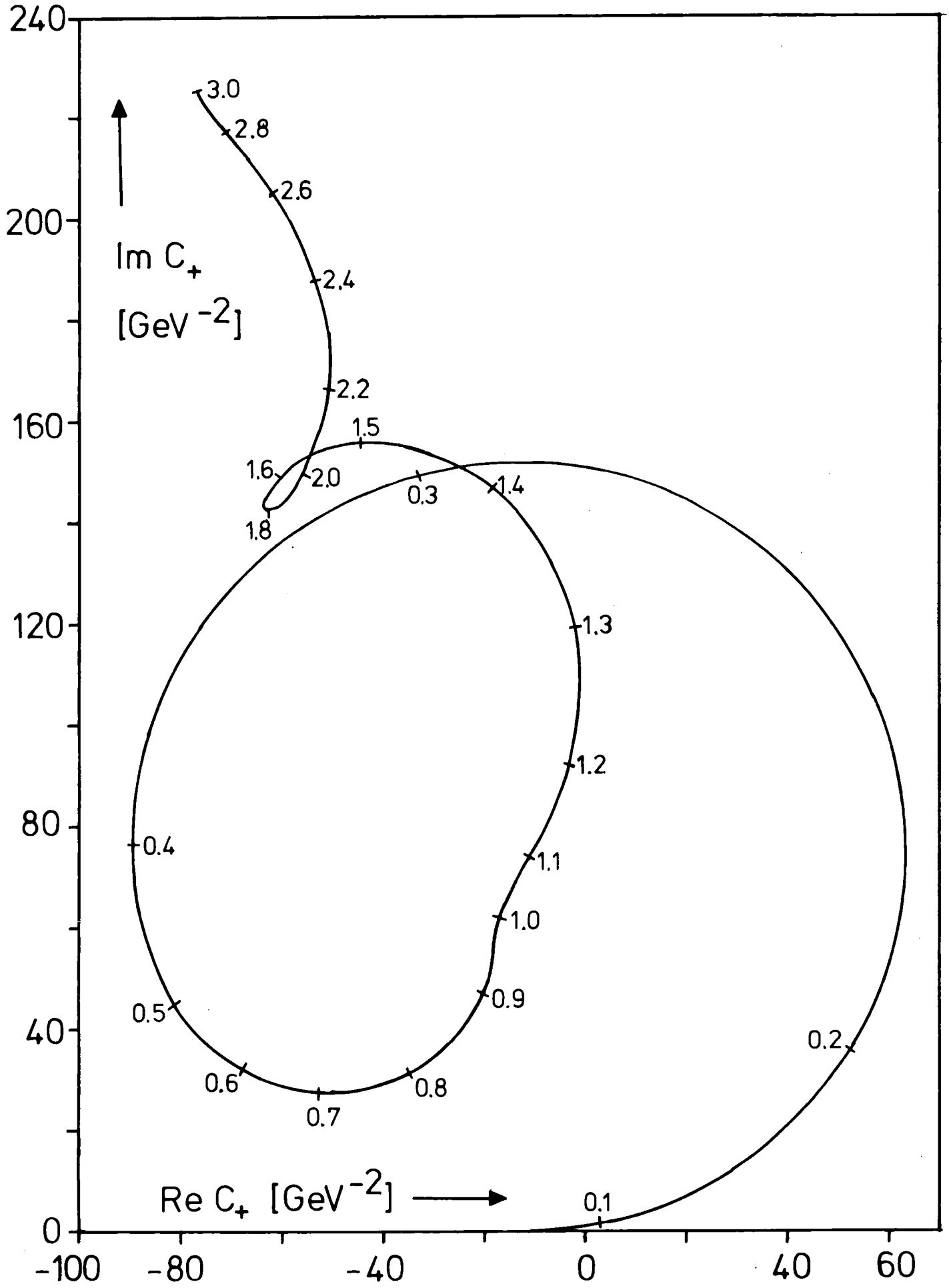
240
200
160
120
80
40
0
-100
-80
-40
0
40
60
Im C+
[GeV -2]
Re C+ [GeV -2]
3.0
2.8
2.6
2.4
2.2
1.5
1.6
2.0
1.8
0.3
1.4
1.3
1.2
1.1
1.0
0.9
0.8
0.7
0.6
0.5
0.4
0.2
0.1

Fig. 16 a

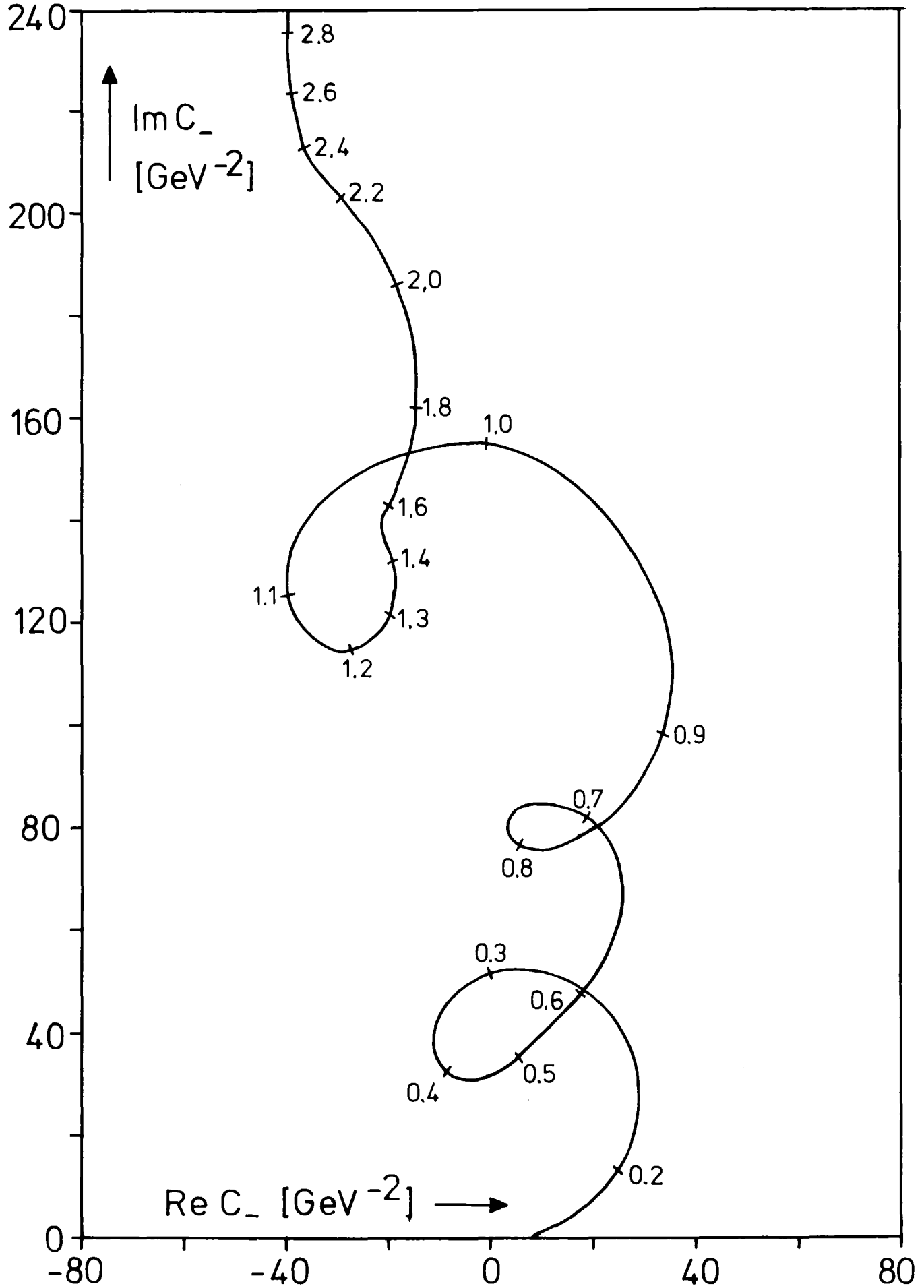
240
200
160
120
80
40
0
-80
-40
0
40
80
Im C_
[GeV -2]
Re C_ [GeV -2]
2.8
2.6
2.4
2.2
2,0
1.8
1.0
1.6
1.4
1.1
1.3
1.2
0.9
0.7
0.8
0.3
0.6
0.5
0.4
0.2

Fig. 16b

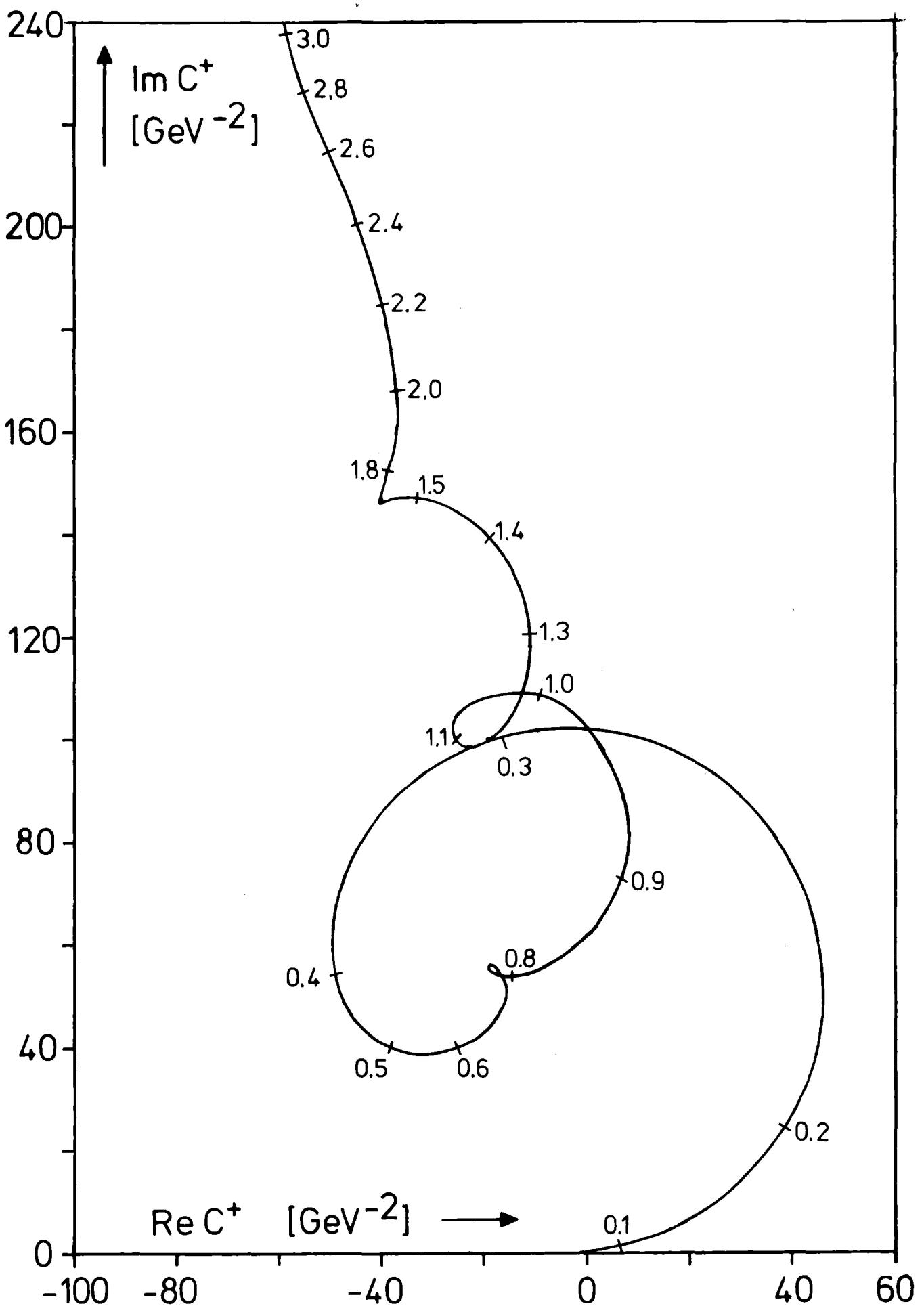
Im C+
[GeV -2]
Re C+ [GeV-2]
240
200
160
120
80
40
0
-100
-80
-40
0
40
60
3.0
2.8
2.6
2.4
2.2
2.0
1.8
1.5
1.4
1.3
1.0
1.1
0.3
0.9
0.8
0.4
0.5
0.6
0.2
0.1

Fig. 16c

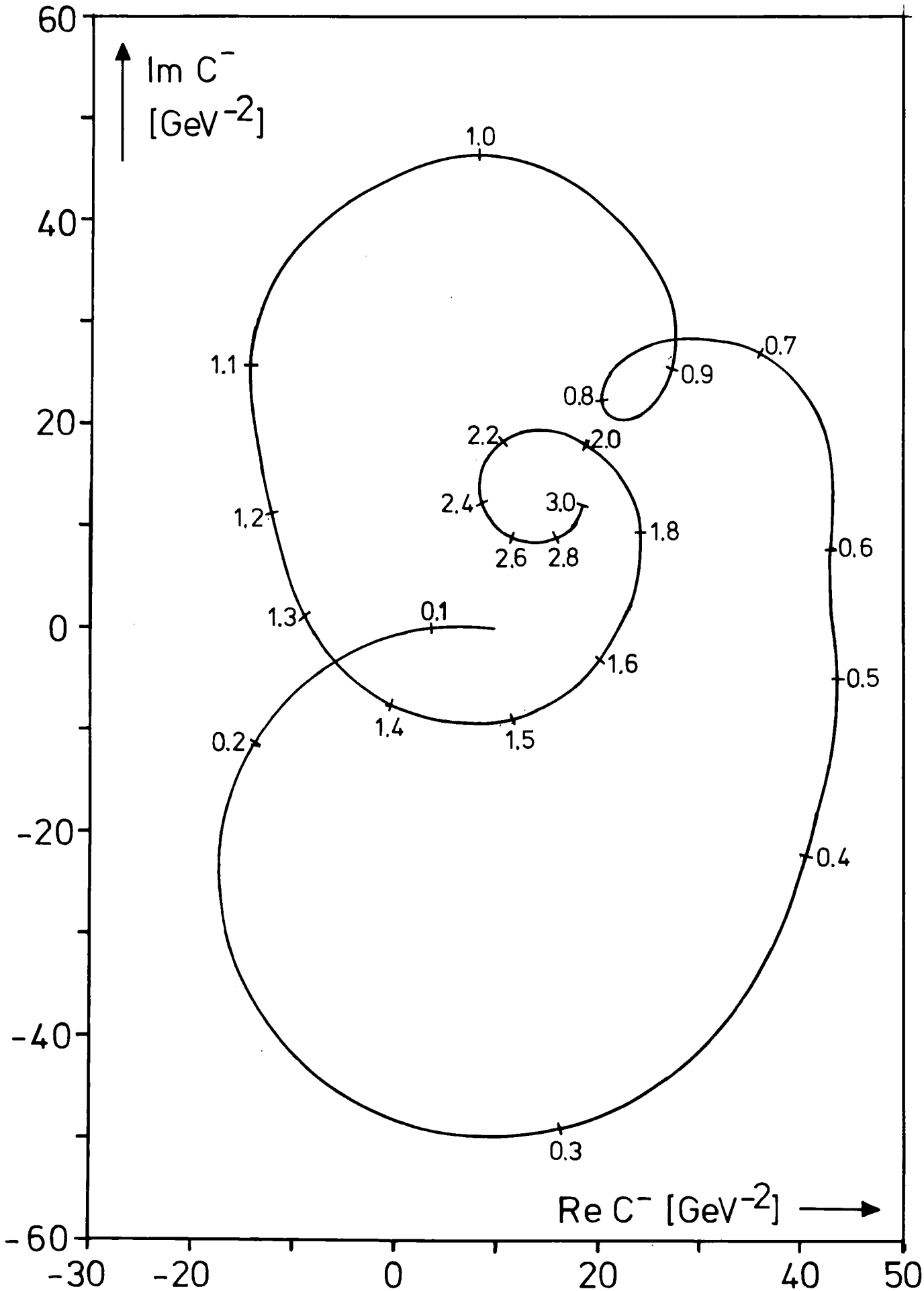
Im C⁻
[GeV⁻²]
Re C⁻ [GeV⁻²]
60
40
20
0
-20
-40
-60
-30
-20
0
20
40
50
1.0
0.7
0.9
0.8
1.1
2.2
2.0
2.4
3.0
1.2
1.8
0.6
2.6
2.8
1.3
0.1
1.6
0.5
1.4
1.5
0.2
0.4
0.3

Fig. 16 d

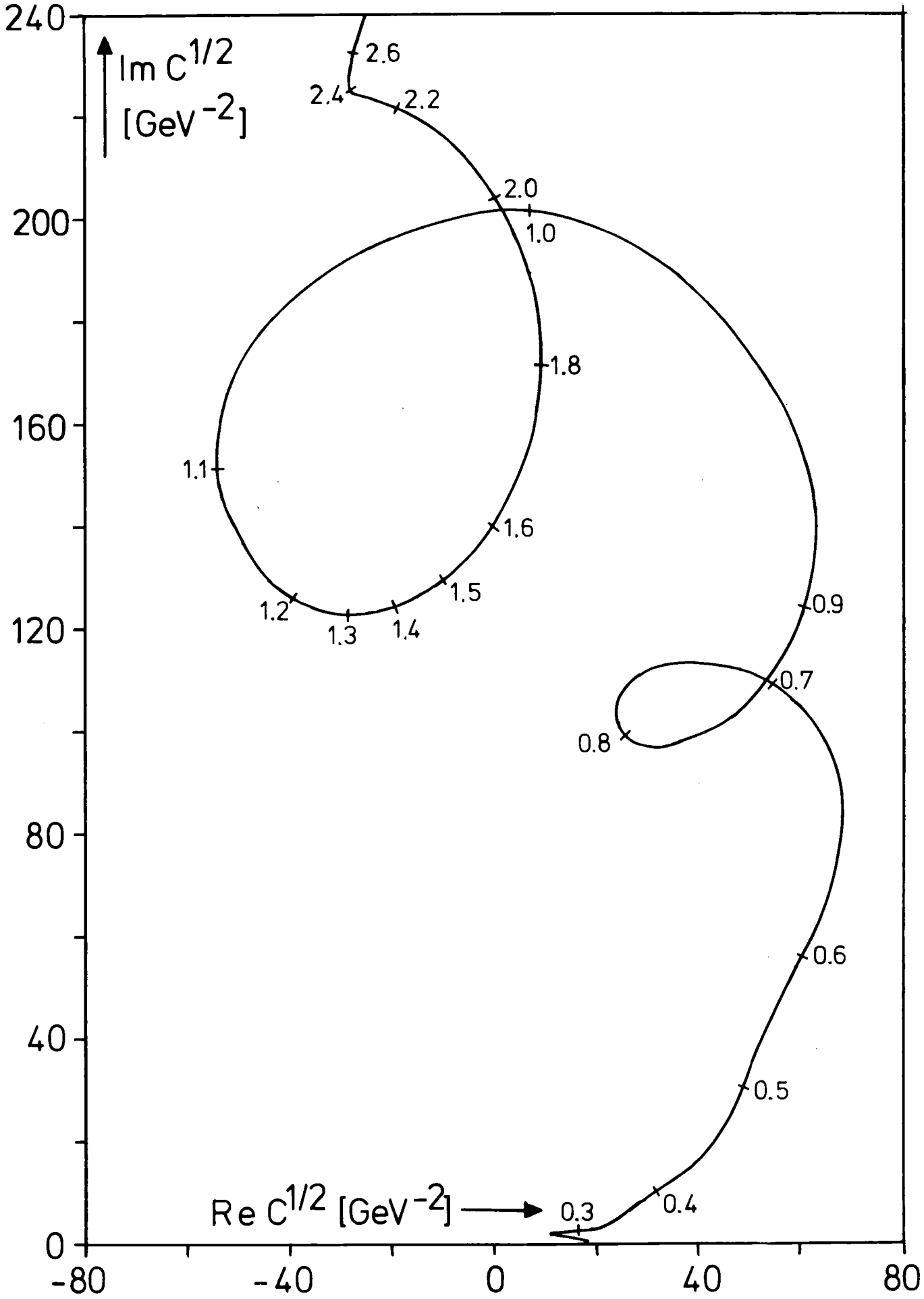
240
200
160
120
80
40
0
-80
-40
0
40
80
Im C^1/2 [GeV^-2]
Re C^1/2 [GeV^-2]
2.6
2.4
2.2
2.0
1.0
1.8
1.1
1.6
1.2
1.3
1.4
1.5
0.9
0.7
0.8
0.6
0.5
0.4
0.3

Fig. 16e

K-TPI-W-S GEV	S-OMEGA Q-2*Q**2		RE C 1/GEV	IM C 1/GEV	S TOT MB		DS/DO MB/SR	DS/DT MB/GEV**2
0.001	59.63	PI+	-10.53	0.01	2.60		0.21	******
0.000	1.00	PI-	8.55	0.02	5.90		0.14	******
1.078	0.001	(+)	-0.99	0.01	4.25		0.00	7598.4
1.162	0.000	(-)	9.54	0.00	1.650	CEX	0.34	*******
0.002	59.63	PI+	-10.53	0.01	2.62		0.21	******
0.000	1.00	PI-	8.55	0.03	5.91		0.14	******
1.078	0.002	(+)	-0.99	0.02	4.27		0.00	1892.5
1.162	0.000	(-)	9.54	0.01	1.647	CEX	0.34	*******
0.005	59.64	PI+	-10.50	0.03	2.63		0.21	34155.
0.000	1.00	PI-	8.55	0.08	5.92		0.14	22651.
1.078	0.004	(+)	-0.97	0.05	4.28		0.00	295.2
1.162	0.000	(-)	9.52	0.02	1.647	CEX	0.34	56216.6
0.010	59.67	PI+	-10.40	0.07	2.65		0.20	8379.4
0.000	1.00	PI-	8.55	0.15	5.94		0.14	5663.9
1.078	0.009	(+)	-0.93	0.11	4.29		0.00	67.3
1.162	0.000	(-)	9.47	0.04	1.643	CEX	0.34	13908.7
0.020	59.77	PI+	-10.01	0.14	2.70		0.19	1939.9
0.001	1.01	PI-	8.55	0.30	5.90		0.14	1417.1
1.079	0.017	(+)	-0.73	0.22	4.30		0.00	11.2
1.164	0.001	(-)	9.28	0.08	1.600	CEX	0.32	3334.54
0.040	60.17	PI+	-8.44	0.30	2.90		0.13	345.7
0.006	1.04	PI-	8.58	0.60	5.80		0.14	358.1
1.083	0.035	(+)	0.07	0.45	4.35		0.00	1.0
1.172	0.002	(-)	8.51	0.15	1.450	CEX	0.27	701.88
0.060	60.82	PI+	-5.81	0.49	3.20		0.06	73.1
0.012	1.09	PI-	8.75	0.86	5.60		0.14	166.5
1.089	0.052	(+)	1.47	0.68	4.40		0.00	5.7
1.185	0.005	(-)	7.28	0.18	1.200	CEX	0.19	228.25
0.080	61.68	PI+	-2.04	0.87	4.25		0.01	6.0
0.021	1.15	PI-	9.21	1.16	5.65		0.16	104.3
1.096	0.068	(+)	3.58	1.02	4.95		0.03	16.8
1.202	0.009	(-)	5.63	0.14	0.700	CEX	0.11	76.71
0.100	62.73	PI+	3.03	1.52	5.90		0.02	8.9
0.032	1.23	PI-	10.11	1.52	5.90		0.19	81.0
1.105	0.085	(+)	6.57	1.52	5.90		0.08	35.2
1.222	0.014	(-)	3.54	0.00	0.000	CEX	0.04	19.47
0.120	63.92	PI+	9.77	2.97	9.64		0.18	56.1
0.044	1.32	PI-	11.67	2.12	6.88		0.25	75.7
1.116	0.101	(+)	10.72	2.55	8.26		0.21	65.3
1.245	0.020	(-)	0.95	-0.43	-1.380	CEX	0.00	1.17
0.140	65.23	PI+	18.17	6.03	16.78		0.63	144.9
0.058	1.42	PI-	13.92	3.23	8.99		0.35	80.7
1.127	0.117	(+)	16.05	4.63	12.89		0.48	110.3
1.271	0.027	(-)	-2.12	-1.40	-3.893	CEX	0.02	5.12
0.160	66.64	PI+	28.23	11.43	27.83		1.55	280.8
0.073	1.52	PI-	16.92	5.13	12.48		0.52	94.5
1.139	0.132	(+)	22.57	8.28	20.15		0.97	175.0
1.298	0.035	(-)	-5.66	-3.15	-7.676	CEX	0.14	25.40

Table 80/1

K-TPI-W-S GEV	S-OMEGA Q-2*Q**2		RE C 1/GEV	IM C 1/GEV	S TOT MB		DS/DO MB/SR	DS/DT MB/GEV**2
0.180	68.13	PI+	39.93	20.6	44.60		3.30	482.9
0.088	1.63	PI-	20.64	8.3	17.90		0.81	118.2
1.152	0.147	(+)	30.29	14.4	31.25		1.84	269.2
1.327	0.043	(-)	-9.65	-6.17	-13.350	CEX	0.429	62.728
0.200	69.68	PI+	52.33	35.9	69.94		6.44	780.3
0.104	1.75	PI-	24.80	13.4	26.18		1.27	154.1
1.165	0.161	(+)	38.57	24.7	48.06		3.35	406.0
1.357	0.052	(-)	-13.77	-11.24	-21.880	CEX	1.010	122.340
0.220	71.28	PI+	61.98	60.2	106.61		11.67	1195.4
0.121	1.87	PI-	28.25	21.6	38.27		1.98	202.6
1.178	0.175	(+)	45.11	40.9	72.44		5.80	593.8
1.389	0.061	(-)	-16.86	-19.30	-34.169	CEX	2.054	210.329
0.240	72.93	PI+	61.32	93.8	152.21		19.19	1689.2
0.138	1.99	PI-	28.51	32.9	53.34		2.89	254.6
1.192	0.189	(+)	44.91	63.3	102.77		9.21	810.9
1.421	0.071	(-)	-16.40	-30.47	-49.436	CEX	3.659	322.088
0.260	74.61	PI+	42.06	128.8	192.95		27.43	2104.7
0.156	2.11	PI-	22.81	44.6	66.85		3.75	288.0
1.206	0.202	(+)	32.44	86.7	129.90		12.81	982.6
1.454	0.082	(-)	-9.62	-42.10	-63.050	CEX	5.570	427.398
0.280	76.32	PI+	5.70	150.1	208.72		32.93	2228.7
0.173	2.24	PI-	11.70	51.8	72.04		4.12	278.6
1.219	0.215	(+)	8.70	100.9	140.38		14.99	1014.2
1.487	0.093	(-)	3.00	-49.14	-68.339	CEX	7.077	478.959
0.300	78.06	PI+	-32.60	149.6	194.24		33.48	2019.0
0.191	2.37	PI-	0.17	51.8	67.21		3.83	230.8
1.233	0.228	(+)	-16.21	100.7	130.73		14.85	895.7
1.521	0.104	(-)	16.38	-48.93	-63.514	CEX	7.602	458.389
0.320	79.82	PI+	-60.55	135.9	165.32		30.88	1673.6
0.210	2.50	PI-	-7.24	47.3	57.57		3.20	173.3
1.247	0.241	(+)	-33.89	91.6	111.45		13.31	721.4
1.555	0.116	(-)	26.65	-44.27	-53.873	CEX	7.456	404.031
0.340	81.59	PI+	-76.93	117.9	135.07		27.08	1328.7
0.228	2.63	PI-	-10.50	42.3	48.45		2.59	127.3
1.261	0.253	(+)	-43.71	80.1	91.76		11.38	558.2
1.589	0.128	(-)	33.21	-37.82	-43.312	CEX	6.919	339.522
0.360	83.38	PI+	-85.05	101.6	109.85		23.45	1048.8
0.247	2.77	PI-	-11.21	38.0	41.14		2.10	94.0
1.275	0.265	(+)	-48.13	69.8	75.49		9.61	429.6
1.624	0.140	(-)	36.92	-31.76	-34.356	CEX	6.339	283.545
0.380	85.18	PI+	-88.52	87.8	89.95		20.33	833.7
0.265	2.90	PI-	-10.32	34.8	35.64		1.72	70.6
1.288	0.277	(+)	-49.42	61.3	62.80		8.11	332.5
1.659	0.153	(-)	39.10	-26.50	-27.153	CEX	5.836	239.345
0.400	87.00	PI+	-89.30	76.7	74.67		17.75	670.9
0.284	3.04	PI-	-8.45	32.5	31.68		1.45	54.7
1.302	0.288	(+)	-48.87	54.6	53.18		6.88	260.1
1.695	0.166	(-)	40.42	-22.08	-21.494	CEX	5.435	205.434

K-TPI-W-S GEV	S-OMEGA Q-2*Q**2		RE C 1/GEV	IM C 1/GEV	S TOT MB		DS/DO MB/SR	DS/DT MB/GEV**2
0.420	88.82	PI+	-88.73	67.8	62.85		15.64	547.6
0.303	3.17	PI-	-5.84	31.2	28.92		1.26	44.2
1.315	0.300	(+)	-47.28	49.5	45.89		5.88	205.8
1.730	0.179	(-)	41.45	-18.30	-16.968	CEX	5.150	180.293
0.440	90.65	PI+	-87.40	60.5	53.54		13.89	452.1
0.322	3.31	PI-	-2.62	30.9	27.37		1.18	38.6
1.329	0.311	(+)	-45.01	45.7	40.46		5.06	164.7
1.766	0.193	(-)	42.39	-14.78	-13.084	CEX	4.955	161.299
0.460	92.49	PI+	-85.60	54.5	46.11		12.40	376.8
0.341	3.44	PI-	0.51	31.9	27.03		1.23	37.3
1.342	0.322	(+)	-42.54	43.2	36.57		4.43	134.6
1.802	0.207	(-)	43.05	-11.27	-9.538	CEX	4.772	145.028
0.480	94.34	PI+	-83.53	49.4	40.10		11.13	316.7
0.360	3.58	PI-	3.24	33.5	27.19		1.34	38.1
1.356	0.332	(+)	-40.14	41.5	33.64		3.93	112.0
1.838	0.221	(-)	43.38	-7.96	-6.456	CEX	4.596	130.819
0.500	96.19	PI+	-81.28	45.1	35.13		10.01	267.8
0.380	3.72	PI-	5.66	35.5	27.68		1.50	40.1
1.369	0.343	(+)	-37.81	40.3	31.40		3.54	94.7
1.874	0.235	(-)	43.47	-4.78	-3.726	CEX	4.432	118.544
0.520	98.05	PI+	-78.78	41.3	30.95		8.99	226.7
0.399	3.86	PI-	7.71	37.7	28.21		1.68	42.4
1.382	0.353	(+)	-35.54	39.5	29.58		3.21	80.9
1.910	0.249	(-)	43.25	-1.83	-1.368	CEX	4.258	107.354
0.540	99.91	PI+	-75.93	38.2	27.53		8.06	191.9
0.418	4.00	PI-	9.89	39.6	28.58		1.86	44.3
1.395	0.363	(+)	-33.02	38.9	28.05		2.90	69.2
1.946	0.264	(-)	42.91	0.73	0.528	CEX	4.109	97.869
0.560	101.78	PI+	-72.97	35.8	24.92		7.24	163.3
0.438	4.13	PI-	12.48	42.0	29.21		2.10	47.4
1.408	0.373	(+)	-30.25	38.9	27.06		2.66	60.0
1.983	0.278	(-)	42.72	3.08	2.145	CEX	4.018	90.654
0.580	103.65	PI+	-70.31	34.0	22.85		6.56	140.5
0.457	4.27	PI-	15.05	44.9	30.16		2.41	51.7
1.421	0.383	(+)	-27.63	39.5	26.50		2.50	53.5
2.019	0.293	(-)	42.68	5.44	3.654	CEX	3.981	85.270
0.600	105.53	PI+	-67.68	32.2	20.92		5.93	120.9
0.476	4.41	PI-	17.83	48.1	31.22		2.78	56.6
1.434	0.393	(+)	-24.93	40.2	26.07		2.36	48.1
2.056	0.308	(-)	42.76	7.94	5.151	CEX	3.994	81.390
0.620	107.40	PI+	-64.77	30.8	19.34		5.34	103.6
0.496	4.55	PI-	21.02	52.3	32.85		3.30	64.0
1.447	0.402	(+)	-21.88	41.5	26.09		2.29	44.4
2.092	0.323	(-)	42.89	10.75	6.754	CEX	4.057	78.813
0.640	109.28	PI+	-62.00	29.7	18.08		4.82	89.4
0.515	4.69	PI-	23.91	58.0	35.29		4.01	74.4
1.459	0.412	(+)	-19.04	43.9	26.68		2.33	43.2
2.129	0.339	(-)	42.96	14.15	8.608	CEX	4.171	77.369

K-TPI-W-S GEV	S-OMEGA Q-2*Q**2		RE C 1/GEV	IM C 1/GEV	S TOT MB		DS/DO MB/SR	DS/DT MB/GEV**2
0.660	111.17	PI+	-58.84	28.5	16.84		4.29	76.1
0.535	4.83	PI-	25.83	65.4	38.59		4.96	88.0
1.472	0.421	(+)	-16.51	47.0	27.72		2.48	44.1
2.166	0.354	(-)	42.33	18.44	10.877	CEX	4.274	75.832
0.680	113.05	PI+	-55.65	28.3	16.19		3.84	65.3
0.555	4.97	PI-	24.72	74.6	42.73		6.09	103.5
1.484	0.430	(+)	-15.46	51.4	29.46		2.84	48.3
2.202	0.370	(-)	40.19	23.17	13.271	CEX	4.242	72.108
0.700	114.94	PI+	-52.60	27.7	15.43		3.43	55.9
0.574	5.11	PI-	18.98	82.1	45.68		6.89	112.3
1.496	0.439	(+)	-16.81	54.9	30.55		3.20	52.2
2.239	0.385	(-)	35.79	27.19	15.128	CEX	3.917	63.879
0.720	116.83	PI+	-49.05	27.6	14.95		3.02	47.4
0.594	5.25	PI-	12.22	84.6	45.76		6.97	109.2
1.509	0.448	(+)	-18.42	56.1	30.36		3.33	52.1
2.276	0.401	(-)	30.63	28.49	15.407	CEX	3.338	52.300
0.740	118.72	PI+	-45.52	28.0	14.73		2.68	40.4
0.613	5.40	PI-	7.12	84.6	44.50		6.76	101.9
1.521	0.457	(+)	-19.20	56.3	29.62		3.32	50.0
2.313	0.417	(-)	26.32	28.29	14.885	CEX	2.802	42.241
0.760	120.62	PI+	-41.82	28.6	14.67		2.37	34.4
0.633	5.54	PI-	3.86	82.4	42.23		6.29	91.3
1.533	0.465	(+)	-18.98	55.5	28.45		3.18	46.2
2.350	0.433	(-)	22.84	26.89	13.780	CEX	2.300	33.395
0.780	122.51	PI+	-38.02	29.9	14.92		2.13	29.8
0.653	5.68	PI-	3.41	79.4	39.62		5.74	80.3
1.545	0.474	(+)	-17.30	54.6	27.27		2.99	41.8
2.387	0.449	(-)	20.71	24.74	12.349	CEX	1.893	26.508
0.800	124.41	PI+	-34.37	31.6	15.38		1.95	26.4
0.673	5.82	PI-	5.83	76.7	37.34		5.30	71.6
1.557	0.482	(+)	-14.27	54.2	26.36		2.81	38.0
2.424	0.465	(-)	20.10	22.56	10.979	CEX	1.635	22.098
0.820	126.31	PI+	-30.71	33.8	16.03		1.84	24.0
0.692	5.96	PI-	10.81	75.9	36.04		5.19	67.7
1.569	0.490	(+)	-9.95	54.8	26.04		2.74	35.8
2.461	0.481	(-)	20.76	21.07	10.006	CEX	1.544	20.163
0.840	128.21	PI+	-27.38	36.6	16.99		1.82	23.0
0.712	6.10	PI-	16.47	77.9	36.13		5.51	69.7
1.580	0.499	(+)	-5.45	57.3	26.56		2.88	36.4
2.498	0.497	(-)	21.93	20.65	9.571	CEX	1.577	19.918
0.860	130.11	PI+	-24.45	39.8	18.00		1.87	22.8
0.732	6.24	PI-	22.70	81.5	36.90		6.13	75.0
1.592	0.507	(+)	-0.88	60.6	27.45		3.15	38.5
2.535	0.514	(-)	23.57	20.87	9.450	CEX	1.698	20.767
0.880	132.01	PI+	-21.94	43.4	19.20		2.00	23.6
0.751	6.38	PI-	29.08	88.5	39.18		7.33	86.9
1.604	0.515	(+)	3.57	66.0	29.19		3.68	43.7
2.572	0.530	(-)	25.51	22.58	9.990	CEX	1.959	23.215

K-TPI-W-S GEV	S-OMEGA Q-2*Q**2		RE C 1/GEV	IM C 1/GEV	S TOT MB		DS/DO MB/SR	DS/DT MB/GEV**2
0.900	133.92	PI+	-20.05	47.1	20.40		2.18	25.1
0.771	6.53	PI-	33.99	98.5	42.60		9.03	103.8
1.615	0.523	(+)	6.97	72.8	31.50		4.45	51.2
2.609	0.547	(-)	27.02	25.65	11.100	CEX	2.311	26.557
0.920	135.82	PI+	-18.80	51.0	21.60		2.43	27.1
0.791	6.67	PI-	35.86	111.7	47.28		11.29	126.0
1.627	0.531	(+)	8.53	81.4	34.44		5.49	61.3
2.646	0.563	(-)	27.33	30.34	12.840	CEX	2.736	30.519
0.940	137.72	PI+	-18.26	54.6	22.60		2.68	29.0
0.811	6.81	PI-	32.49	125.7	52.08		13.64	147.8
1.638	0.538	(+)	7.12	90.1	37.34		6.61	71.7
2.683	0.580	(-)	25.38	35.58	14.740	CEX	3.091	33.491
0.960	139.63	PI+	-17.96	57.4	23.30		2.89	30.4
0.831	6.95	PI-	25.36	137.8	55.90		15.67	165.0
1.649	0.546	(+)	3.70	97.6	39.60		7.62	80.2
2.720	0.597	(-)	21.66	40.18	16.300	CEX	3.326	35.034
0.980	141.54	PI+	-17.51	59.9	23.80		3.07	31.4
0.850	7.09	PI-	14.84	148.7	59.08		17.58	180.1
1.661	0.554	(+)	-1.33	104.3	41.44		8.56	87.7
2.757	0.613	(-)	16.18	44.39	17.640	CEX	3.515	36.015
1.000	143.44	PI+	-16.79	62.1	24.20		3.22	32.1
0.870	7.23	PI-	-0.68	155.3	60.48		18.74	186.9
1.672	0.561	(+)	-8.73	108.7	42.34		9.24	92.2
2.795	0.630	(-)	8.05	46.58	18.140	CEX	3.472	34.626
1.020	145.35	PI+	-15.86	64.4	24.60		3.38	32.8
0.890	7.38	PI-	-15.59	153.5	58.60		18.25	177.2
1.683	0.569	(+)	-15.72	109.0	41.60		9.29	90.3
2.832	0.647	(-)	0.14	44.53	17.000	CEX	3.040	29.529
1.040	147.26	PI+	-14.82	66.8	25.00		3.54	33.5
0.910	7.52	PI-	-26.43	148.9	55.76		17.31	163.8
1.694	0.576	(+)	-20.63	107.8	40.38		9.12	86.3
2.869	0.664	(-)	-5.81	41.08	15.380	CEX	2.604	24.652
1.060	149.17	PI+	-13.67	69.1	25.40		3.71	34.2
0.930	7.66	PI-	-34.73	141.9	52.14		15.95	147.2
1.705	0.583	(+)	-24.20	105.5	38.77		8.76	80.8
2.906	0.681	(-)	-10.53	36.39	13.370	CEX	2.145	19.794
1.080	151.08	PI+	-12.42	71.6	25.81		3.89	35.1
0.949	7.80	PI-	-39.12	133.5	48.15		14.28	128.6
1.716	0.591	(+)	-25.77	102.6	36.98		8.25	74.3
2.943	0.698	(-)	-13.35	30.98	11.170	CEX	1.679	15.115
1.100	152.99	PI+	-10.88	74.1	26.22		4.08	35.9
0.969	7.94	PI-	-39.64	125.8	44.54		12.67	111.4
1.726	0.598	(+)	-25.26	99.9	35.38		7.74	68.0
2.981	0.715	(-)	-14.38	25.88	9.160	CEX	1.276	11.220
1.120	154.90	PI+	-9.12	77.0	26.78		4.33	37.2
0.989	8.09	PI-	-37.41	120.3	41.82		11.41	98.0
1.737	0.605	(+)	-23.26	98.7	34.30		7.39	63.4
3.018	0.732	(-)	-14.15	21.63	7.520	CEX	0.961	8.250

K-TPI-W-S GEV	S-OMEGA Q-2*Q**2		RE C 1/GEV	IM C 1/GEV	S TOT MB		DS/DO MB/SR	DS/DT MB/GEV**2
1.140	156.82	PI+	-7.46	80.4	27.45		4.63	38.8
1.009	8.23	PI-	-34.61	117.5	40.15		10.67	89.5
1.748	0.612	(+)	-21.03	99.0	33.80		7.27	61.0
3.055	0.749	(-)	-13.57	18.59	6.350	CEX	0.753	6.316
1.160	158.73	PI+	-5.88	83.9	28.18		4.97	40.8
1.029	8.37	PI-	-32.41	115.9	38.90		10.16	83.4
1.758	0.619	(+)	-19.14	99.9	33.54		7.26	59.6
3.092	0.766	(-)	-13.27	15.97	5.360	CEX	0.605	4.962
1.180	160.64	PI+	-4.31	87.9	29.00		5.37	43.1
1.049	8.51	PI-	-29.74	114.7	37.84		9.73	78.1
1.769	0.626	(+)	-17.03	101.3	33.42		7.31	58.7
3.130	0.783	(-)	-12.72	13.39	4.420	CEX	0.473	3.796
1.200	162.55	PI+	-2.86	92.3	29.94		5.84	45.8
1.069	8.66	PI-	-27.11	115.0	37.33		9.58	75.1
1.780	0.633	(+)	-14.98	103.6	33.63		7.52	59.0
3.167	0.801	(-)	-12.12	11.39	3.695	CEX	0.379	2.976
1.220	164.47	PI+	-1.77	97.1	31.00		6.39	49.1
1.088	8.80	PI-	-25.27	115.8	36.96		9.52	73.1
1.790	0.639	(+)	-13.52	106.5	33.98		7.80	59.9
3.204	0.818	(-)	-11.75	9.34	2.980	CEX	0.305	2.344
1.240	166.38	PI+	-1.12	102.2	32.10		7.00	52.6
1.108	8.94	PI-	-23.49	116.7	36.66		9.50	71.4
1.800	0.646	(+)	-12.30	109.5	34.38		8.13	61.1
3.241	0.835	(-)	-11.19	7.26	2.280	CEX	0.238	1.792
1.260	168.30	PI+	-0.72	107.6	33.24		7.66	56.4
1.128	9.08	PI-	-21.93	118.2	36.53		9.57	70.5
1.811	0.653	(+)	-11.32	112.9	34.88		8.52	62.8
3.279	0.853	(-)	-10.60	5.32	1.645	CEX	0.186	1.373
1.280	170.21	PI+	-0.80	113.4	34.50		8.42	60.8
1.148	9.22	PI-	-20.63	119.8	36.46		9.68	69.9
1.821	0.660	(+)	-10.71	116.6	35.48		8.98	64.9
3.316	0.870	(-)	-9.92	3.22	0.980	CEX	0.142	1.028
1.300	172.13	PI+	-1.70	119.5	35.80		9.25	65.5
1.168	9.37	PI-	-19.62	121.9	36.50		9.86	69.8
1.831	0.666	(+)	-10.66	120.7	36.15		9.50	67.3
3.353	0.887	(-)	-8.96	1.17	0.350	CEX	0.106	0.749
1.320	174.04	PI+	-3.36	125.6	37.05		10.11	70.2
1.188	9.51	PI-	-19.00	123.9	36.55		10.06	69.9
1.841	0.673	(+)	-11.18	124.7	36.80		10.04	69.7
3.391	0.905	(-)	-7.82	-0.85	-0.250	CEX	0.079	0.550
1.340	175.96	PI+	-5.85	131.6	38.25		10.99	74.9
1.208	9.65	PI-	-18.61	126.0	36.61		10.27	70.0
1.851	0.679	(+)	-12.23	128.8	37.43		10.60	72.2
3.428	0.922	(-)	-6.38	-2.82	-0.820	CEX	0.062	0.420
1.360	177.88	PI+	-9.17	137.3	39.30		11.85	79.3
1.228	9.79	PI-	-18.49	128.0	36.66		10.48	70.1
1.862	0.685	(+)	-13.83	132.6	37.98		11.14	74.5
3.465	0.940	(-)	-4.66	-4.61	-1.320	CEX	0.054	0.360

K-TPI-W-S GEV	S-OMEGA Q-2*Q**2		RE C 1/GEV	IM C 1/GEV	S TOT MB		DS/DO MB/SR	DS/DT MB/GEV**2
1.380	179.79	PI+	-13.08	142.5	40.20		12.68	83.3
1.247	9.94	PI-	-18.43	130.1	36.70		10.69	70.2
1.872	0.692	(+)	-15.75	136.3	38.45		11.66	76.5
3.503	0.957	(-)	-2.68	-6.20	-1.750	CEX	0.057	0.371
1.400	181.71	PI+	-17.97	147.3	40.96		13.50	87.0
1.267	10.08	PI-	-18.92	132.3	36.80		10.95	70.6
1.881	0.698	(+)	-18.44	139.8	38.88		12.19	78.6
3.540	0.975	(-)	-0.48	-7.48	-2.080	CEX	0.069	0.444
1.420	183.63	PI+	-23.44	150.6	41.31		14.10	89.3
1.287	10.22	PI-	-19.66	133.7	36.67		11.09	70.2
1.891	0.704	(+)	-21.55	142.2	38.99		12.55	79.4
3.577	0.992	(-)	1.89	-8.46	-2.320	CEX	0.091	0.577
1.440	185.54	PI+	-28.75	153.1	41.41		14.58	90.7
1.307	10.37	PI-	-20.04	135.1	36.53		11.20	69.7
1.901	0.711	(+)	-24.40	144.1	38.97		12.83	79.8
3.615	1.010	(-)	4.36	-9.02	-2.440	CEX	0.121	0.750
1.460	187.46	PI+	-34.01	154.9	41.31		14.95	91.4
1.327	10.51	PI-	-20.52	136.4	36.37		11.30	69.1
1.911	0.717	(+)	-27.27	145.6	38.84		13.05	79.8
3.652	1.028	(-)	6.74	-9.26	-2.470	CEX	0.156	0.954
1.480	189.38	PI+	-39.25	155.9	41.03		15.21	91.5
1.347	10.65	PI-	-20.87	137.4	36.15		11.36	68.3
1.921	0.723	(+)	-30.06	146.7	38.59		13.19	79.3
3.689	1.045	(-)	9.19	-9.27	-2.440	CEX	0.201	1.206
1.500	191.30	PI+	-44.29	156.0	40.51		15.33	90.6
1.367	10.79	PI-	-21.12	138.4	35.93		11.42	67.5
1.930	0.729	(+)	-32.71	147.2	38.22		13.25	78.3
3.727	1.063	(-)	11.58	-8.82	-2.290	CEX	0.247	1.460
1.520	193.22	PI+	-48.75	155.4	39.81		15.30	88.9
1.387	10.94	PI-	-21.08	139.2	35.67		11.44	66.5
1.940	0.735	(+)	-34.92	147.3	37.74		13.22	76.9
3.764	1.081	(-)	13.84	-8.08	-2.070	CEX	0.296	1.722
1.540	195.13	PI+	-52.61	154.2	39.00		15.16	86.7
1.407	11.08	PI-	-21.09	140.4	35.50		11.51	65.8
1.950	0.741	(+)	-36.85	147.3	37.25		13.17	75.3
3.801	1.098	(-)	15.76	-6.92	-1.750	CEX	0.338	1.935
1.560	197.05	PI+	-55.72	152.6	38.10		14.93	84.0
1.427	11.22	PI-	-20.96	141.0	35.20		11.49	64.7
1.959	0.747	(+)	-38.34	146.8	36.65		13.02	73.3
3.839	1.116	(-)	17.38	-5.81	-1.450	CEX	0.380	2.138
1.580	198.97	PI+	-58.15	150.9	37.20		14.65	81.2
1.447	11.36	PI-	-20.35	142.0	35.00		11.53	63.9
1.969	0.753	(+)	-39.25	146.5	36.10		12.88	71.4
3.876	1.134	(-)	18.90	-4.46	-1.100	CEX	0.423	2.341
1.600	200.89	PI+	-59.74	149.1	36.28		14.31	78.0
1.467	11.51	PI-	-19.73	143.2	34.84		11.58	63.2
1.978	0.759	(+)	-39.74	146.1	35.56		12.72	69.4
3.914	1.152	(-)	20.00	-2.96	-0.720	CEX	0.454	2.475

K-TPI-W-S GEV	S-OMEGA Q-2*Q**2		RE C 1/GEV	IM C 1/GEV	S TOT MB		DS/DO MB/SR	DS/DT MB/GEV**2
1.650	205.69	PI+	-61.83	146.6	34.60		13.71	72.0
1.516	11.86	PI-	-18.00	146.9	34.66		11.86	62.3
2.002	0.773	(+)	-39.91	146.7	34.63		12.53	65.8
4.007	1.196	(-)	21.92	0.13	0.030	CEX	0.520	2.733
1.700	210.49	PI+	-63.22	144.5	33.11		13.18	66.7
1.566	12.22	PI-	-16.48	151.3	34.65		12.26	62.1
2.025	0.788	(+)	-39.85	147.9	33.88		12.42	62.9
4.101	1.241	(-)	23.37	3.36	0.770	CEX	0.590	2.989
1.750	215.29	PI+	-63.12	143.4	31.90		12.70	62.1
1.616	12.58	PI-	-15.11	156.4	34.80		12.78	62.4
2.048	0.802	(+)	-39.11	149.9	33.35		12.42	60.7
4.194	1.286	(-)	24.01	6.52	1.450	CEX	0.640	3.130
1.800	220.09	PI+	-62.47	143.1	30.95		12.34	58.3
1.666	12.93	PI-	-14.38	162.2	35.09		13.42	63.4
2.071	0.816	(+)	-38.42	152.6	33.02		12.54	59.2
4.288	1.330	(-)	24.04	9.57	2.070	CEX	0.678	3.203
1.850	224.89	PI+	-61.04	143.2	30.15		12.01	54.9
1.716	13.29	PI-	-14.24	168.1	35.39		14.11	64.4
2.093	0.829	(+)	-37.64	155.7	32.77		12.71	58.1
4.381	1.375	(-)	23.40	12.45	2.620	CEX	0.696	3.180
1.900	229.69	PI+	-58.94	144.7	29.65		11.84	52.4
1.766	13.65	PI-	-14.75	174.4	35.75		14.87	65.8
2.115	0.843	(+)	-36.84	159.5	32.70		13.01	57.5
4.475	1.420	(-)	22.10	14.88	3.050	CEX	0.689	3.046
1.950	234.50	PI+	-57.10	147.2	29.40		11.85	50.8
1.815	14.01	PI-	-16.14	180.6	36.06		15.62	67.0
2.137	0.856	(+)	-36.62	163.9	32.73		13.40	57.5
4.568	1.465	(-)	20.48	16.68	3.330	CEX	0.663	2.843
2.000	239.30	PI+	-55.62	150.2	29.24		11.94	49.7
1.865	14.36	PI-	-18.16	186.3	36.28		16.32	67.9
2.159	0.869	(+)	-36.89	168.3	32.76		13.82	57.5
4.662	1.511	(-)	18.73	18.08	3.520	CEX	0.631	2.625
2.050	244.11	PI+	-54.17	153.5	29.15		12.09	48.8
1.915	14.72	PI-	-20.64	191.6	36.39		16.95	68.4
2.181	0.882	(+)	-37.40	172.5	32.77		14.22	57.4
4.756	1.556	(-)	16.76	19.06	3.620	CEX	0.588	2.375
2.100	248.91	PI+	-52.69	157.2	29.15		12.31	48.3
1.965	15.08	PI-	-23.44	196.2	36.39		17.49	68.6
2.202	0.895	(+)	-38.07	176.7	32.77		14.63	57.4
4.849	1.601	(-)	14.63	19.52	3.620	CEX	0.533	2.091
2.150	253.72	PI+	-51.27	161.6	29.26		12.62	48.1
2.015	15.44	PI-	-26.43	200.2	36.26		17.91	68.3
2.223	0.907	(+)	-38.85	180.9	32.76		15.03	57.4
4.943	1.647	(-)	12.42	19.32	3.500	CEX	0.463	1.769
2.200	258.52	PI+	-50.25	166.7	29.50		13.06	48.5
2.065	15.79	PI-	-29.15	203.4	36.00		18.20	67.6
2.244	0.920	(+)	-39.70	185.0	32.75		15.43	57.3
5.036	1.692	(-)	10.55	18.36	3.250	CEX	0.387	1.435

K-TPI-W-S GEV	S-OMEGA Q-2*Q**2		RE C 1/GEV	IM C 1/GEV	S TOT MB		RHO	DS/DT MB/GEV**2
2.250	263.33	PI+	-50.0	172.2	29.80		-0.290	49.2
2.115	16.15	PI-	-31.5	206.3	35.70		-0.153	66.6
2.265	0.932	(+)	-40.8	189.2	32.75		-0.215	57.3
5.130	1.737	(-)	9.22	17.05	2.950	CEX	0.541	1.150
2.300	268.14	PI+	-50.5	177.8	30.10		-0.284	50.0
2.165	16.51	PI-	-33.6	208.7	35.34		-0.161	65.5
2.286	0.944	(+)	-42.1	193.3	32.72		-0.218	57.3
5.224	1.783	(-)	8.42	15.47	2.620	CEX	0.544	0.909
2.350	272.95	PI+	-51.6	183.2	30.35		-0.282	50.8
2.215	16.87	PI-	-35.2	210.9	34.95		-0.167	64.1
2.306	0.956	(+)	-43.4	197.0	32.65		-0.220	57.1
5.317	1.829	(-)	8.19	13.88	2.300	CEX	0.590	0.729
2.400	277.75	PI+	-53.1	188.2	30.54		-0.282	51.4
2.264	17.22	PI-	-36.3	213.1	34.58		-0.170	62.9
2.326	0.968	(+)	-44.7	200.7	32.56		-0.223	56.8
5.411	1.874	(-)	8.41	12.45	2.020	CEX	0.676	0.607
2.450	282.56	PI+	-54.9	193.0	30.68		-0.284	52.0
2.314	17.58	PI-	-37.0	215.6	34.26		-0.171	61.7
2.346	0.980	(+)	-45.9	204.3	32.47		-0.225	56.6
5.505	1.920	(-)	8.96	11.26	1.790	CEX	0.796	0.535
2.500	287.37	PI+	-56.9	197.6	30.78		-0.288	52.4
2.364	17.94	PI-	-37.6	218.3	34.00		-0.172	60.8
2.366	0.991	(+)	-47.2	207.9	32.39		-0.227	56.4
5.598	1.966	(-)	9.67	10.34	1.610	CEX	0.936	0.497
2.550	292.18	PI+	-59.2	201.9	30.83		-0.293	52.7
2.414	18.30	PI-	-38.2	221.0	33.75		-0.173	59.9
2.386	1.003	(+)	-48.7	211.4	32.29		-0.230	56.1
5.692	2.011	(-)	10.51	9.56	1.460	CEX	1.100	0.481
2.600	296.99	PI+	-61.7	205.7	30.81		-0.300	52.9
2.464	18.65	PI-	-38.7	223.7	33.51		-0.173	59.1
2.405	1.014	(+)	-50.2	214.7	32.16		-0.234	55.7
5.786	2.057	(-)	11.48	9.01	1.350	CEX	1.274	0.488
2.650	301.80	PI+	-64.1	209.2	30.74		-0.307	52.8
2.514	19.01	PI-	-39.1	226.5	33.28		-0.172	58.3
2.425	1.025	(+)	-51.6	217.8	32.01		-0.237	55.3
5.879	2.103	(-)	12.54	8.64	1.270	CEX	1.450	0.512
2.700	306.61	PI+	-66.6	212.3	30.62		-0.314	52.6
2.564	19.37	PI-	-39.2	229.4	33.08		-0.171	57.5
2.444	1.037	(+)	-52.9	220.8	31.85		-0.240	54.8
5.973	2.149	(-)	13.67	8.53	1.230	CEX	1.603	0.552
2.750	311.42	PI+	-68.9	215.0	30.45		-0.320	52.2
2.614	19.73	PI-	-39.3	232.4	32.91		-0.169	56.9
2.463	1.048	(+)	-54.1	223.7	31.68		-0.242	54.3
6.067	2.195	(-)	14.79	8.69	1.230	CEX	1.702	0.603
2.800	316.23	PI+	-71.0	217.4	30.24		-0.326	51.7
2.664	20.09	PI-	-39.6	235.6	32.76		-0.168	56.4
2.482	1.058	(+)	-55.3	226.5	31.50		-0.244	53.7
6.161	2.241	(-)	15.70	9.06	1.260	CEX	1.733	0.650

K- -W-S GEV	S-OMEGA Q-2*Q**2		RE C 1/GEV	IM C 1/GEV	S TOT MB		RHO	DS/DT MB/GEV**2
2.850	321.04	PI+	-72.8	219.7	30.02		-0.332	51.1
	20.44	PI-	-39.3	238.5	32.59		-0.165	55.7
2.501	1.069	(+)	-56.1	229.1	31.31		-0.245	53.1
6.254	2.287	(-)	16.8	9.4	1.285	CEX	1.783	0.705
2.900	325.85	PI+	-74.4	221.7	29.77		-0.336	50.4
	20.80	PI-	-39.2	242.6	32.57		-0.162	55.6
2.520	1.080	(+)	-56.8	232.1	31.17		-0.245	52.6
6.348	2.333	(-)	17.6	10.4	1.400	CEX	1.691	0.773
2.950	330.66	PI+	-75.6	223.6	29.52		-0.338	49.6
	21.16	PI-	-39.6	246.2	32.50		-0.161	55.4
2.538	1.091	(+)	-57.6	234.9	31.01		-0.245	52.1
6.442	2.379	(-)	18.0	11.3	1.490	CEX	1.594	0.803
3.000	335.47	PI+	-76.5	225.6	29.28		-0.339	48.8
	21.52	PI-	-40.0	249.9	32.44		-0.160	55.1
2.556	1.101	(+)	-58.2	237.7	30.86		-0.245	51.6
6.535	2.425	(-)	18.3	12.2	1.580	CEX	1.500	0.829
3.100	345.09	PI+	-77.4	230.1	28.91		-0.336	47.5
	22.23	PI-	-41.2	257.5	32.35		-0.160	54.8
2.593	1.122	(+)	-59.3	243.8	30.63		-0.243	50.8
6.723	2.517	(-)	18.1	13.7	1.720	CEX	1.325	0.833
3.200	354.71	PI+	-78.1	235.3	28.63		-0.332	46.5
	22.95	PI-	-42.9	264.7	32.21		-0.162	54.4
2.629	1.142	(+)	-60.5	250.0	30.42		-0.242	50.0
6.910	2.609	(-)	17.6	14.7	1.790	CEX	1.196	0.796
3.300	364.34	PI+	-78.5	241.0	28.44		-0.326	45.7
	23.66	PI-	-44.6	271.4	32.02		-0.164	53.8
2.664	1.162	(+)	-61.6	256.2	30.23		-0.240	49.4
7.098	2.701	(-)	17.0	15.2	1.790	CEX	1.118	0.737
3.400	373.96	PI+	-79.1	247.4	28.33		-0.320	45.2
	24.38	PI-	-46.2	277.9	31.83		-0.166	53.2
2.699	1.182	(+)	-62.6	262.6	30.08		-0.239	48.9
7.285	2.794	(-)	16.5	15.3	1.750	CEX	1.077	0.676
3.500	383.59	PI+	-80.1	254.0	28.26		-0.315	44.9
	25.10	PI-	-47.9	284.2	31.62		-0.169	52.5
2.734	1.201	(+)	-64.0	269.1	29.94		-0.238	48.4
7.473	2.886	(-)	16.1	15.1	1.680	CEX	1.066	0.616
3.600	393.21	PI+	-81.5	260.6	28.19		-0.313	44.6
	25.81	PI-	-49.3	290.0	31.37		-0.170	51.7
2.768	1.220	(+)	-65.4	275.3	29.78		-0.238	47.9
7.660	2.979	(-)	16.1	14.7	1.590	CEX	1.095	0.568
3.700	402.84	PI+	-83.1	267.2	28.12		-0.311	44.3
	26.53	PI-	-50.3	296.1	31.16		-0.170	51.0
2.801	1.239	(+)	-66.7	281.6	29.64		-0.237	47.4
7.848	3.071	(-)	16.4	14.4	1.520	CEX	1.135	0.540
3.800	412.46	PI+	-85.0	273.5	28.03		-0.311	44.0
	27.24	PI-	-51.3	302.0	30.95		-0.170	50.4
2.835	1.258	(+)	-68.2	287.8	29.49		-0.237	46.9
8.035	3.164	(-)	16.8	14.2	1.460	CEX	1.181	0.522

K- -W-S GEV	S-OMEGA Q-2*Q**2		RE C 1/GEV	IM C 1/GEV	S TOT MB		RHO	DS/DT MB/GEV**2
3.900	422.09	PI+	-87.0	279.6	27.92		-0.311	43.7
	27.96	PI-	-52.2	308.1	30.76		-0.169	49.7
2.868	1.276	(+)	-69.6	293.8	29.34		-0.237	46.4
8.223	3.257	(-)	17.4	14.2	1.420	CEX	1.225	0.515
4.000	431.71	PI+	-88.9	285.3	27.78		-0.312	43.2
	28.68	PI-	-52.9	314.1	30.58		-0.168	49.1
2.900	1.294	(+)	-70.9	299.7	29.18		-0.237	45.9
8.410	3.349	(-)	18.0	14.4	1.403	CEX	1.249	0.515
4.100	441.34	PI+	-90.7	290.8	27.62		-0.312	42.8
	29.39	PI-	-53.6	320.3	30.42		-0.168	48.6
2.932	1.312	(+)	-72.2	305.5	29.02		-0.236	45.4
8.598	3.442	(-)	18.5	14.7	1.397	CEX	1.259	0.516
4.200	450.97	PI+	-92.2	296.1	27.46		-0.311	42.2
	30.11	PI-	-54.3	326.4	30.26		-0.166	48.1
2.964	1.329	(+)	-73.3	311.3	28.86		-0.235	44.9
8.786	3.535	(-)	19.0	15.1	1.403	CEX	1.253	0.517
4.300	460.60	PI+	-93.4	301.4	27.30		-0.310	41.7
	30.82	PI-	-55.0	332.6	30.12		-0.165	47.6
2.996	1.347	(+)	-74.2	317.0	28.71		-0.234	44.4
8.973	3.628	(-)	19.2	15.6	1.411	CEX	1.233	0.513
4.400	470.22	PI+	-94.4	306.9	27.16		-0.308	41.3
	31.54	PI-	-55.7	338.7	29.98		-0.164	47.2
3.027	1.364	(+)	-75.0	322.8	28.57		-0.232	44.0
9.161	3.721	(-)	19.4	15.9	1.409	CEX	1.216	0.503
4.500	479.85	PI+	-95.3	312.5	27.04		-0.305	40.8
	32.26	PI-	-56.3	344.8	29.84		-0.163	46.7
3.057	1.381	(+)	-75.8	328.7	28.44		-0.231	43.5
9.348	3.814	(-)	19.5	16.2	1.401	CEX	1.207	0.493
4.600	489.48	PI+	-96.2	318.1	26.93		-0.302	40.4
	32.97	PI-	-56.8	351.0	29.71		-0.162	46.3
3.088	1.398	(+)	-76.5	334.5	28.32		-0.229	43.1
9.536	3.907	(-)	19.7	16.4	1.391	CEX	1.200	0.483
4.700	499.11	PI+	-97.1	323.8	26.83		-0.300	40.1
	33.69	PI-	-57.2	357.2	29.59		-0.160	45.9
3.118	1.414	(+)	-77.1	340.5	28.21		-0.227	42.7
9.723	4.000	(-)	19.9	16.7	1.382	CEX	1.195	0.473
4.800	508.73	PI+	-97.9	329.6	26.74		-0.297	39.7
	34.40	PI-	-57.6	363.4	29.48		-0.159	45.5
3.148	1.431	(+)	-77.7	346.5	28.11		-0.224	42.4
9.911	4.093	(-)	20.1	16.9	1.372	CEX	1.189	0.465
4.900	518.36	PI+	-98.7	335.4	26.66		-0.294	39.4
	35.12	PI-	-58.1	369.7	29.38		-0.157	45.2
3.178	1.447	(+)	-78.4	352.6	28.02		-0.222	42.1
10.098	4.186	(-)	20.3	17.1	1.363	CEX	1.184	0.456
5.000	527.99	PI+	-99.6	341.2	26.58		-0.292	39.2
	35.84	PI-	-58.6	376.0	29.28		-0.156	44.9
3.207	1.463	(+)	-79.1	358.6	27.93		-0.220	41.8
10.286	4.279	(-)	20.5	17.4	1.353	CEX	1.180	0.448

K- -W-S GEV	S-OMEGA Q-2*Q**2		RE C 1/GEV	IM C 1/GEV	S TOT MB		RHO	DS/DT MB/GEV**2
5.200	547.25	PI+	-101.2	353.0	26.43		-0.287	38.6
	37.27	PI-	-59.4	388.7	29.11		-0.153	44.3
3.265	1.494	(+)	-80.3	370.8	27.77		-0.216	41.2
10.661	4.466	(-)	20.9	17.8	1.335	CEX	1.171	0.432
5.400	566.51	PI+	-102.8	364.8	26.31		-0.282	38.2
	38.70	PI-	-60.3	401.3	28.94		-0.150	43.8
3.322	1.525	(+)	-81.5	383.1	27.62		-0.213	40.8
11.036	4.652	(-)	21.2	18.3	1.317	CEX	1.163	0.417
5.600	585.76	PI+	-104.4	376.7	26.19		-0.277	37.7
	40.13	PI-	-61.2	414.0	28.79		-0.148	43.3
3.378	1.555	(+)	-82.8	395.4	27.49		-0.209	40.3
11.412	4.838	(-)	21.6	18.7	1.299	CEX	1.155	0.403
5.800	605.02	PI+	-106.0	388.5	26.09		-0.273	37.4
	41.57	PI-	-62.1	426.7	28.65		-0.146	42.8
3.433	1.585	(+)	-84.0	407.6	27.37		-0.206	39.9
11.787	5.025	(-)	21.9	19.1	1.282	CEX	1.148	0.389
6.000	624.28	PI+	-107.5	400.5	25.99		-0.269	37.0
	43.00	PI-	-63.0	439.5	28.52		-0.143	42.4
3.487	1.614	(+)	-85.3	420.0	27.26		-0.203	39.5
12.162	5.212	(-)	22.3	19.5	1.266	CEX	1.142	0.377
6.200	643.54	PI+	-109.1	412.4	25.90		-0.265	36.7
	44.43	PI-	-64.0	452.2	28.40		-0.141	42.0
3.541	1.643	(+)	-86.5	432.3	27.15		-0.200	39.2
12.537	5.398	(-)	22.6	19.9	1.250	CEX	1.136	0.365
6.400	662.80	PI+	-110.7	424.3	25.81		-0.261	36.4
	45.86	PI-	-64.9	464.8	28.28		-0.140	41.7
3.593	1.671	(+)	-87.8	444.5	27.05		-0.198	38.8
12.912	5.585	(-)	22.9	20.3	1.234	CEX	1.130	0.354
6.600	682.06	PI+	-112.3	436.1	25.73		-0.257	36.1
	47.30	PI-	-65.8	477.5	28.17		-0.138	41.3
3.645	1.699	(+)	-89.0	456.8	26.95		-0.195	38.5
13.288	5.772	(-)	23.2	20.7	1.219	CEX	1.125	0.344
6.800	701.32	PI+	-113.8	448.0	25.66		-0.254	35.8
	48.73	PI-	-66.7	490.1	28.06		-0.136	41.0
3.696	1.726	(+)	-90.3	469.0	26.86		-0.192	38.2
13.663	5.959	(-)	23.5	21.0	1.204	CEX	1.120	0.334
7.000	720.58	PI+	-115.3	459.9	25.58		-0.251	35.5
	50.16	PI-	-67.6	502.6	27.96		-0.135	40.7
3.747	1.753	(+)	-91.5	481.2	26.77		-0.190	37.9
14.038	6.146	(-)	23.8	21.4	1.189	CEX	1.115	0.324
7.200	739.84	PI+	-116.8	471.7	25.51		-0.248	35.3
	51.59	PI-	-68.5	515.2	27.86		-0.133	40.4
3.796	1.779	(+)	-92.6	493.5	26.69		-0.188	37.7
14.413	6.333	(-)	24.1	21.7	1.176	CEX	1.111	0.315
7.400	759.11	PI+	-118.2	483.6	25.45		-0.244	35.1
	53.03	PI-	-69.3	527.7	27.77		-0.131	40.1
3.846	1.805	(+)	-93.8	505.7	26.61		-0.185	37.4
14.789	6.520	(-)	24.4	22.1	1.162	CEX	1.107	0.307

K- -W-S GEV	S-OMEGA Q-2*Q**2		RE C 1/GEV	IM C 1/GEV	S TOT MB		RHO	DS/DT MB/GEV**2
7.600	778.37	PI+	-119.6	495.4	25.38		-0.242	34.8
	54.46	PI-	-70.2	540.3	27.68		-0.130	39.8
3.894	1.831	(+)	-94.9	517.8	26.53		-0.183	37.2
15.164	6.706	(-)	24.7	22.4	1.149	CEX	1.103	0.299
7.800	797.63	PI+	-121.1	507.2	25.32		-0.239	34.6
	55.89	PI-	-71.0	552.7	27.60		-0.128	39.5
3.942	1.857	(+)	-96.0	530.0	26.46		-0.181	36.9
15.539	6.894	(-)	25.0	22.8	1.136	CEX	1.100	0.291
8.000	816.89	PI+	-122.4	519.0	25.27		-0.236	34.4
	57.33	PI-	-71.8	565.2	27.51		-0.127	39.3
3.989	1.882	(+)	-97.1	542.1	26.39		-0.179	36.7
15.914	7.081	(-)	25.3	23.1	1.124	CEX	1.096	0.284
9.000	913.20	PI+	-129.0	578.0	25.01		-0.223	33.5
	64.49	PI-	-75.6	627.3	27.14		-0.121	38.2
4.218	2.002	(+)	-102.3	602.6	26.08		-0.170	35.7
17.791	8.016	(-)	26.7	24.7	1.067	CEX	1.082	0.252
10.000	1009.51	PI+	-135.0	636.7	24.79		-0.212	32.8
	71.65	PI-	-79.1	689.0	26.83		-0.115	37.3
4.435	2.116	(+)	-107.0	662.9	25.81		-0.161	34.9
19.667	8.952	(-)	28.0	26.1	1.017	CEX	1.071	0.227
11.000	1105.83	PI+	-140.5	695.3	24.61		-0.202	32.2
	78.82	PI-	-82.1	750.3	26.56		-0.109	36.5
4.641	2.224	(+)	-111.3	722.8	25.59		-0.154	34.2
21.543	9.889	(-)	29.2	27.5	0.974	CEX	1.062	0.206
12.000	1202.14	PI+	-145.5	753.7	24.46		-0.193	31.7
	85.98	PI-	-84.7	811.3	26.33		-0.104	35.8
4.839	2.327	(+)	-115.1	782.5	25.39		-0.147	33.7
23.420	10.826	(-)	30.4	28.8	0.935	CEX	1.055	0.189
13.000	1298.46	PI+	-150.1	812.0	24.32		-0.185	31.3
	93.14	PI-	-87.0	872.2	26.13		-0.100	35.2
5.030	2.425	(+)	-118.5	842.1	25.22		-0.141	33.2
25.296	11.763	(-)	31.6	30.1	0.901	CEX	1.049	0.174
14.000	1394.78	PI+	-154.3	870.3	24.21		-0.177	30.9
	100.31	PI-	-89.0	932.8	25.95		-0.095	34.7
5.213	2.520	(+)	-121.6	901.5	25.08		-0.135	32.7
27.172	12.700	(-)	32.7	31.3	0.870	CEX	1.045	0.162
15.000	1491.10	PI+	-158.1	928.5	24.10		-0.170	30.5
	107.47	PI-	-90.7	993.3	25.79		-0.091	34.3
5.390	2.611	(+)	-124.4	960.9	24.94		-0.129	32.3
29.049	13.637	(-)	33.7	32.4	0.841	CEX	1.040	0.151
16.000	1587.42	PI+	-161.6	986.6	24.01		-0.164	30.2
	114.64	PI-	-92.1	1053.6	25.64		-0.087	33.9
5.561	2.700	(+)	-126.8	1020.1	24.83		-0.124	32.0
30.925	14.575	(-)	34.8	33.5	0.816	CEX	1.037	0.141
17.000	1683.74	PI+	-164.7	1044.7	23.93		-0.158	30.0
	121.80	PI-	-93.2	1113.9	25.51		-0.084	33.5
5.727	2.785	(+)	-129.0	1079.3	24.72		-0.119	31.7
32.802	15.512	(-)	35.8	34.6	0.792	CEX	1.034	0.133

K- -W-S GEV	S-OMEGA Q-2*Q**2		RE C 1/GEV	IM C 1/GEV	S TOT MB		RHO	DS/DT MB/GEV**2
18.000	1780.06	PI+	-167.6	1102.8	23.86		-0.152	29.7
	128.97	PI-	-94.1	1174.0	25.40		-0.080	33.2
5.889	2.868	(+)	-130.8	1138.4	24.63		-0.115	31.4
34.678	16.450	(-)	36.7	35.6	0.771	CEX	1.031	0.1253
19.000	1876.38	PI+	-170.2	1160.8	23.79		-0.147	29.5
	136.13	PI-	-94.8	1234.1	25.29		-0.077	32.9
6.046	2.949	(+)	-132.5	1197.5	24.54		-0.111	31.1
36.555	17.388	(-)	37.7	36.6	0.751	CEX	1.029	0.1186
20.000	1972.70	PI+	-172.5	1218.9	23.73		-0.142	29.3
	143.29	PI-	-95.2	1294.1	25.20		-0.074	32.6
6.199	3.027	(+)	-133.9	1256.5	24.46		-0.107	30.9
38.431	18.325	(-)	38.6	37.6	0.732	CEX	1.027	0.1126
22.000	2165.34	PI+	-176.4	1335.0	23.63		-0.132	29.0
	157.62	PI-	-95.6	1414.0	25.03		-0.068	32.1
6.495	3.178	(+)	-136.0	1374.5	24.33		-0.099	30.5
42.184	20.201	(-)	40.4	39.5	0.699	CEX	1.024	0.1023
24.000	2357.98	PI+	-179.4	1451.1	23.55		-0.124	28.8
	171.95	PI-	-95.1	1533.7	24.88		-0.062	31.8
6.778	3.322	(+)	-137.3	1492.4	24.22		-0.092	30.2
45.937	22.077	(-)	42.2	41.3	0.670	CEX	1.021	0.0936
26.000	2550.62	PI+	-181.7	1567.4	23.47		-0.116	28.5
	186.28	PI-	-94.0	1653.4	24.76		-0.057	31.4
7.049	3.461	(+)	-137.8	1610.4	24.12		-0.086	29.9
49.690	23.953	(-)	43.8	43.0	0.644	CEX	1.019	0.0864
28.000	2743.27	PI+	-183.1	1683.7	23.42		-0.109	28.3
	200.61	PI-	-92.3	1773.0	24.66		-0.052	31.1
7.310	3.594	(+)	-137.7	1728.3	24.04		-0.080	29.7
53.443	25.829	(-)	45.4	44.7	0.621	CEX	1.017	0.0801
30.000	2935.91	PI+	-183.9	1800.1	23.37		-0.102	28.2
	214.94	PI-	-90.0	1892.6	24.57		-0.048	30.9
7.563	3.722	(+)	-137.0	1846.4	23.97		-0.074	29.5
57.196	27.705	(-)	47.0	46.2	0.600	CEX	1.015	0.0748
35.000	3417.52	PI+	-183.3	2091.8	23.27		-0.088	27.9
	250.76	PI-	-82.1	2191.8	24.39		-0.037	30.4
8.160	4.025	(+)	-132.7	2141.8	23.83		-0.062	29.1
66.578	32.395	(-)	50.6	50.0	0.556	CEX	1.012	0.0640
40.000	3899.13	PI+	-179.4	2384.4	23.21		-0.075	27.7
	286.58	PI-	-71.3	2491.4	24.25		-0.029	30.1
8.716	4.306	(+)	-125.4	2437.9	23.73		-0.051	28.9
75.961	37.086	(-)	54.0	53.5	0.521	CEX	1.010	0.0559
45.000	4380.75	PI+	-172.6	2678.1	23.17		-0.064	27.6
	322.41	PI-	-58.1	2791.6	24.16		-0.021	29.8
9.238	4.570	(+)	-115.4	2734.8	23.67		-0.042	28.7
85.344	41.776	(-)	57.2	56.7	0.491	CEX	1.009	0.0497
50.000	4862.36	PI+	-163.3	2972.8	23.15		-0.055	27.5
	358.23	PI-	-42.8	3092.5	24.08		-0.014	29.6
9.733	4.820	(+)	-103.0	3032.7	23.62		-0.034	28.5
94.726	46.467	(-)	60.3	59.8	0.466	CEX	1.007	0.0447

K- -W-S GEV	S-OMEGA Q-2*Q**2		RE C 1/GEV	IM C 1/GEV	S TOT MB		RHO	DS/DT MB/GEV**2
55.000	5343.97	PI+	-151.8	3269.	23.14		-0.046	27.4
	394.05	PI-	-25.5	3394.	24.03		-0.008	29.5
10.203	5.058	(+)	-88.7	3331.	23.59		-0.027	28.4
104.109	51.158	(-)	63.2	62.8	0.444	CEX	1.006	0.0406
60.000	5825.59	PI+	-138.3	3566.	23.14		-0.039	27.4
	429.87	PI-	-6.5	3697.	23.99		-0.002	29.4
10.653	5.284	(+)	-72.4	3631.	23.57		-0.020	28.4
113.491	55.849	(-)	65.9	65.6	0.426	CEX	1.006	0.0372
65.000	6307.20	PI+	-123.0	3864.	23.15		-0.032	27.4
	465.70	PI-	14.2	4000.	23.96		0.004	29.3
11.085	5.502	(+)	-54.4	3932.	23.56		-0.014	28.4
122.874	60.540	(-)	68.6	68.3	0.409	CEX	1.005	0.0343
70.000	6788.82	PI+	-106.1	4163.	23.16		-0.025	27.4
	501.52	PI-	36.2	4305.	23.95		0.008	29.3
11.500	5.711	(+)	-34.9	4234.	23.55		-0.008	28.3
132.256	65.231	(-)	71.2	70.8	0.394	CEX	1.005	0.0319
75.000	7270.43	PI+	-87.6	4463.	23.17		-0.020	27.4
	537.34	PI-	59.7	4610.	23.93		0.013	29.3
11.901	5.913	(+)	-14.0	4536.	23.55		-0.003	28.3
141.639	69.922	(-)	73.6	73.3	0.381	CEX	1.004	0.0297
80.000	7752.05	PI+	-67.7	4764.	23.19		-0.014	27.5
	573.17	PI-	84.4	4916.	23.93		0.017	29.3
12.289	6.108	(+)	8.3	4840.	23.56		0.002	28.4
151.021	74.613	(-)	76.0	75.7	0.369	CEX	1.004	0.0279
85.000	8233.66	PI+	-46.5	5067.	23.21		-0.009	27.5
	608.99	PI-	110.2	5223.	23.93		0.021	29.3
12.665	6.297	(+)	31.9	5145.	23.57		0.006	28.4
160.404	79.305	(-)	78.4	78.1	0.358	CEX	1.004	0.0262
90.000	8715.28	PI+	-24.0	5370.	23.23		-0.004	27.6
	644.81	PI-	137.2	5531.	23.93		0.025	29.3
13.030	6.481	(+)	56.6	5450.	23.58		0.010	28.4
169.787	83.996	(-)	80.6	80.3	0.348	CEX	1.003	0.0248
95.000	9196.89	PI+	-0.4	5674.	23.26		-0.000	27.6
	680.63	PI-	165.2	5839.	23.94		0.028	29.3
13.385	6.659	(+)	82.4	5757.	23.60		0.014	28.5
179.169	88.687	(-)	82.8	82.6	0.338	CEX	1.003	0.0235
100.000	9678.50	PI+	24.3	5980.	23.28		0.004	27.7
	716.46	PI-	194.2	6149.	23.94		0.032	29.3
13.731	6.833	(+)	109.2	6064.	23.61		0.018	28.5
188.552	93.378	(-)	84.9	84.7	0.330	CEX	1.003	0.0223
105.000	10160.12	PI+	50.0	6286.	23.31		0.008	27.8
	752.28	PI-	224.1	6459.	23.96		0.035	29.4
14.069	7.002	(+)	137.0	6373.	23.63		0.022	28.5
197.934	98.069	(-)	87.0	86.8	0.322	CEX	1.003	0.0212
110.000	10641.74	PI+	76.7	6593.	23.34		0.012	27.8
	788.10	PI-	254.9	6771.	23.97		0.038	29.4
14.399	7.168	(+)	165.8	6682.	23.65		0.025	28.6
207.317	102.760	(-)	89.1	88.8	0.315	CEX	1.002	0.0203

K- -W-S GEV	S-OMEGA Q-2*Q**2		RE C 1/GEV	IM C 1/GEV	S TOT MB		RHO	DS/DT MB/GEV**2
115.000	11123.35	PI+	104.4	6901.	23.37		0.015	27.9
	823.92	PI-	286.5	7083.	23.98		0.040	29.4
14.721	7.330	(+)	195.4	6992.	23.68		0.028	28.7
216.700	107.452	(-)	91.0	90.8	0.308	CEX	1.002	0.0194
120.000	11604.96	PI+	132.9	7210.	23.40		0.018	28.0
	859.75	PI-	318.9	7396.	24.00		0.043	29.5
15.036	7.488	(+)	225.9	7303.	23.70		0.031	28.7
226.082	112.143	(-)	93.0	92.8	0.301	CEX	1.002	0.0186
125.000	12086.58	PI+	162.3	7520.	23.43		0.022	28.1
	895.57	PI-	352.1	7709.	24.02		0.046	29.5
15.345	7.643	(+)	257.2	7615.	23.72		0.034	28.8
235.465	116.834	(-)	94.9	94.7	0.295	CEX	1.002	0.0178
130.000	12568.19	PI+	192.5	7831.	23.46		0.025	28.1
	931.39	PI-	386.1	8024.	24.04		0.048	29.6
15.648	7.795	(+)	289.3	7927.	23.75		0.036	28.8
244.847	121.525	(-)	96.8	96.6	0.289	CEX	1.002	0.0171
135.000	13049.81	PI+	223.5	8142.	23.49		0.027	28.2
	967.22	PI-	420.7	8339.	24.05		0.050	29.6
15.945	7.944	(+)	322.1	8241.	23.77		0.039	28.9
254.230	126.217	(-)	98.6	98.4	0.284	CEX	1.002	0.0165
140.000	13531.43	PI+	255.3	8455.	23.52		0.030	28.3
	1003.04	PI-	456.1	8655.	24.07		0.053	29.7
16.236	8.090	(+)	355.7	8555.	23.80		0.042	29.0
263.612	130.908	(-)	100.4	100.2	0.279	CEX	1.002	0.0159
145.000	14013.04	PI+	287.7	8768.	23.55		0.033	28.4
	1038.86	PI-	492.1	8972.	24.10		0.055	29.8
16.523	8.234	(+)	389.9	8870.	23.82		0.044	29.0
272.995	135.599	(-)	102.2	102.0	0.274	CEX	1.002	0.0154
150.000	14494.66	PI+	320.8	9082.	23.58		0.035	28.4
	1074.68	PI-	528.7	9290.	24.12		0.057	29.8
16.804	8.375	(+)	424.8	9186.	23.85		0.046	29.1
282.378	140.290	(-)	103.9	103.8	0.269	CEX	1.002	0.0149
155.000	14976.27	PI+	354.6	9397.	23.61		0.038	28.5
	1110.51	PI-	565.9	9608.	24.14		0.059	29.9
17.081	8.514	(+)	460.3	9503.	23.87		0.048	29.2
291.760	144.982	(-)	105.6	105.5	0.265	CEX	1.001	0.0144
160.000	15457.89	PI+	389.1	9713.	23.64		0.040	28.6
	1146.33	PI-	603.7	9927.	24.16		0.061	29.9
17.353	8.651	(+)	496.4	9820.	23.90		0.051	29.3
301.143	149.673	(-)	107.3	107.2	0.261	CEX	1.001	0.0139
165.000	15939.50	PI+	424.2	10029.	23.67		0.042	28.7
	1182.15	PI-	642.1	10247.	24.18		0.063	30.0
17.622	8.785	(+)	533.2	10138.	23.93		0.053	29.3
310.525	154.364	(-)	109.0	108.8	0.257	CEX	1.001	0.0135
170.000	16421.12	PI+	459.9	10346.	23.70		0.044	28.8
	1217.97	PI-	681.1	10567.	24.21		0.064	30.1
17.886	8.918	(+)	570.5	10457.	23.95		0.055	29.4
319.908	159.055	(-)	110.6	110.5	0.253	CEX	1.001	0.0131

K- -W-S GEV	S-OMEGA Q-2*Q**2		RE C 1/GEV	IM C 1/GEV	S TOT MB		RHO	DS/DT MB/GEV**2
175.000	16902.73	PI+	496.1	10664.	23.73		0.047	28.8
	1253.80	PI-	720.6	10889.	24.23		0.066	30.1
18.146	9.048	(+)	608.3	10777.	23.98		0.056	29.5
329.291	163.747	(-)	112.2	112.1	0.249	CEX	1.001	0.0127
180.000	17384.35	PI+	532.9	10983.	23.76		0.049	28.9
	1289.62	PI-	760.6	11210.	24.25		0.068	30.2
18.403	9.177	(+)	646.8	11097.	24.01		0.058	29.5
338.673	168.438	(-)	113.8	113.7	0.246	CEX	1.001	0.0124
185.000	17865.96	PI+	570.3	11302.	23.79		0.050	29.0
	1325.44	PI-	801.1	11533.	24.28		0.069	30.3
18.656	9.304	(+)	685.7	11418.	24.03		0.060	29.6
348.056	173.129	(-)	115.4	115.2	0.243	CEX	1.001	0.0120
190.000	18347.58	PI+	608.2	11623.	23.82		0.052	29.1
	1361.27	PI-	842.1	11856.	24.30		0.071	30.3
18.906	9.429	(+)	725.1	11739.	24.06		0.062	29.7
357.438	177.820	(-)	116.9	116.8	0.239	CEX	1.001	0.0117
195.000	18829.19	PI+	646.7	11943.	23.85		0.054	29.1
	1397.09	PI-	883.5	12180.	24.32		0.073	30.4
19.153	9.553	(+)	765.1	12062.	24.09		0.063	29.8
366.821	182.512	(-)	118.4	118.3	0.236	CEX	1.001	0.0114
200.000	19310.81	PI+	685.6	12265.	23.88		0.056	29.2
	1432.91	PI-	925.5	12505.	24.35		0.074	30.4
19.396	9.675	(+)	805.5	12385.	24.11		0.065	29.8
376.203	187.203	(-)	120.0	119.8	0.233	CEX	1.001	0.0111
220.000	21237.27	PI+	846.1	13558.	24.00		0.062	29.5
	1576.20	PI-	1097.7	13809.	24.44		0.079	30.7
20.340	10.148	(+)	971.9	13683.	24.22		0.071	30.1
413.734	205.968	(-)	125.8	125.7	0.222	CEX	1.001	0.0101
240.000	23163.73	PI+	1013.7	14861.	24.11		0.068	29.8
	1719.49	PI-	1276.4	15123.	24.54		0.084	31.0
21.243	10.600	(+)	1145.1	14992.	24.32		0.076	30.4
451.264	224.733	(-)	131.4	131.3	0.213	CEX	1.001	0.0093
260.000	25090.19	PI+	1187.8	16173.	24.22		0.073	30.1
	1862.78	PI-	1461.2	16446.	24.63		0.089	31.2
22.109	11.034	(+)	1324.5	16310.	24.43		0.081	30.7
488.795	243.498	(-)	136.7	136.6	0.205	CEX	1.001	0.0086
280.000	27016.65	PI+	1367.8	17495.	24.33		0.078	30.4
	2006.08	PI-	1651.6	17779.	24.73		0.093	31.5
22.942	11.451	(+)	1509.7	17637.	24.53		0.086	31.0
526.325	262.263	(-)	141.9	141.8	0.197	CEX	1.001	0.0080
300.000	28943.11	PI+	1553.3	18826.	24.44		0.083	30.7
	2149.37	PI-	1847.0	19120.	24.82		0.097	31.8
23.746	11.854	(+)	1700.2	18973.	24.63		0.090	31.2
563.855	281.028	(-)	146.9	146.8	0.191	CEX	1.001	0.0074
350.000	33759.27	PI+	2038.7	22189.	24.69		0.092	31.4
	2507.59	PI-	2355.9	22506.	25.04		0.105	32.4
25.645	12.805	(+)	2197.3	22348.	24.86		0.098	31.9
657.681	327.941	(-)	158.6	158.5	0.176	CEX	1.000	0.0064

K- -W-S GEV	S-OMEGA Q-2*Q**2		RE C 1/GEV	IM C 1/GEV	S TOT MB		RHO	DS/DT MB/GEV**2
400.000	38575.42	PI+	2551.3	25601.	24.92		0.100	32.0
	2865.82	PI-	2890.4	25940.	25.25		0.111	33.0
27.414	13.690	(+)	2720.9	25770.	25.09		0.106	32.5
751.507	374.854	(-)	169.5	169.5	0.165	CEX	1.000	0.0056
450.000	43391.57	PI+	3087.6	29056.	25.14		0.106	32.7
	3224.05	PI-	3447.2	29415.	25.45		0.117	33.6
29.075	14.522	(+)	3267.4	29236.	25.30		0.112	33.1
845.333	421.767	(-)	179.8	179.8	0.156	CEX	1.000	0.0049
500.000	48207.73	PI+	3644.7	32551.	25.35		0.112	33.2
	3582.28	PI-	4023.8	32930.	25.65		0.122	34.1
30.646	15.308	(+)	3834.2	32741.	25.50		0.117	33.7
939.159	468.680	(-)	189.5	189.5	0.148	CEX	1.000	0.0045
600.000	57840.04	PI+	4813.2	39652.	25.73		0.121	34.3
	4298.73	PI-	5228.4	40067.	26.00		0.130	35.1
33.568	16.771	(+)	5020.8	39860.	25.87		0.126	34.7
1126.811	562.506	(-)	207.6	207.6	0.135	CEX	1.000	0.0037
700.000	67472.34	PI+	6043.7	46885.	26.08		0.129	35.3
	5015.19	PI-	6492.1	47334.	26.33		0.137	36.1
36.256	18.115	(+)	6267.9	47110.	26.21		0.133	35.7
1314.463	656.332	(-)	224.2	224.2	0.125	CEX	1.000	0.0032
800.000	77104.64	PI+	7326.9	54237.	26.40		0.135	36.3
	5731.64	PI-	7806.3	54716.	26.63		0.143	37.0
38.757	19.367	(+)	7566.6	54476.	26.52		0.139	36.6
1502.114	750.158	(-)	239.7	239.7	0.117	CEX	1.000	0.0028
900.000	86736.95	PI+	8655.9	61695.	26.69		0.140	37.1
	6448.10	PI-	9164.5	62203.	26.91		0.147	37.8
41.107	20.542	(+)	8910.2	61949.	26.80		0.144	37.5
1689.766	843.983	(-)	254.3	254.2	0.110	CEX	1.000	0.0025
1000.000	96369.27	PI+	10025.6	69251.	26.97		0.145	37.9
	7164.56	PI-	10561.6	69787.	27.18		0.151	38.6
43.329	21.654	(+)	10293.6	69519.	27.07		0.148	38.3
1877.418	937.809	(-)	268.0	268.0	0.104	CEX	1.000	0.0022

K-TPI-W-S GEV	S-OMEGA Q-2*Q**2		RE C 1/GEV	IM C 1/GEV	S TOT MB		DS/DO MB/SR	DS/DT MB/GEV**2
0.001	59.63	PI+	-10.54	0.01	2.60		0.21	******
0.000	1.00	PI-	8.56	0.02	5.90		0.14	******
1.078	0.001	(+)	-0.99	0.01	4.25		0.00	7598.4
1.162	0.000	(-)	9.55	0.00	1.650	CEX	0.34	*******
0.002	59.63	PI+	-10.53	0.01	2.62		0.21	******
0.000	1.00	PI-	8.56	0.03	5.91		0.14	******
1.078	0.002	(+)	-0.99	0.02	4.27		0.00	1892.5
1.162	0.000	(-)	9.54	0.01	1.647	CEX	0.34	*******
0.005	59.64	PI+	-10.51	0.03	2.63		0.21	34199.
0.000	1.00	PI-	8.56	0.08	5.92		0.14	22688.
1.078	0.004	(+)	-0.97	0.05	4.28		0.00	295.2
1.162	0.000	(-)	9.53	0.02	1.647	CEX	0.34	56297.2
0.010	59.67	PI+	-10.41	0.07	2.65		0.20	8390.4
0.000	1.00	PI-	8.56	0.15	5.94		0.14	5672.9
1.078	0.009	(+)	-0.93	0.11	4.29		0.00	67.3
1.162	0.000	(-)	9.48	0.04	1.643	CEX	0.34	13928.7
0.020	59.77	PI+	-10.01	0.14	2.70		0.19	1942.6
0.001	1.01	PI-	8.56	0.30	5.90		0.14	1419.4
1.079	0.017	(+)	-0.73	0.22	4.30		0.00	11.2
1.164	0.001	(-)	9.28	0.08	1.600	CEX	0.32	3339.48
0.040	60.17	PI+	-8.45	0.30	2.90		0.13	346.3
0.006	1.04	PI-	8.59	0.60	5.80		0.14	358.7
1.083	0.035	(+)	0.07	0.45	4.35		0.00	1.0
1.172	0.002	(-)	8.52	0.15	1.450	CEX	0.27	703.03
0.060	60.82	PI+	-5.81	0.49	3.20		0.06	73.3
0.012	1.09	PI-	8.76	0.86	5.60		0.14	166.7
1.089	0.052	(+)	1.47	0.68	4.40		0.00	5.7
1.185	0.005	(-)	7.29	0.18	1.200	CEX	0.19	228.70
0.080	61.68	PI+	-2.05	0.87	4.25		0.01	6.0
0.021	1.15	PI-	9.22	1.16	5.65		0.16	104.5
1.096	0.068	(+)	3.58	1.02	4.95		0.03	16.8
1.202	0.009	(-)	5.63	0.14	0.700	CEX	0.11	76.90
0.100	62.73	PI+	3.02	1.52	5.90		0.02	8.8
0.032	1.23	PI-	10.12	1.52	5.90		0.19	81.2
1.105	0.085	(+)	6.57	1.52	5.90		0.08	35.2
1.222	0.014	(-)	3.55	0.00	0.000	CEX	0.04	19.55
0.120	63.92	PI+	9.76	2.97	9.64		0.18	56.0
0.044	1.32	PI-	11.68	2.12	6.88		0.25	75.8
1.116	0.101	(+)	10.72	2.55	8.26		0.21	65.3
1.245	0.020	(-)	0.96	-0.43	-1.380	CEX	0.00	1.18
0.140	65.23	PI+	18.16	6.03	16.78		0.63	144.8
0.058	1.42	PI-	13.93	3.23	8.99		0.35	80.8
1.127	0.117	(+)	16.05	4.63	12.89		0.48	110.3
1.271	0.027	(-)	-2.12	-1.40	-3.893	CEX	0.02	5.09
0.160	66.64	PI+	28.23	11.43	27.83		1.55	280.6
0.073	1.52	PI-	16.92	5.13	12.48		0.52	94.6
1.139	0.132	(+)	22.57	8.28	20.15		0.97	175.0
1.298	0.035	(-)	-5.65	-3.15	-7.676	CEX	0.14	25.35

Table 80/2

K-TPI-W-S GEV	S-OMEGA Q-2*Q**2		RE C 1/GEV	IM C 1/GEV	S TOT MB		DS/DO MB/SR	DS/DT MB/GEV**2
0.180	68.13	PI+	39.93	20.6	44.60		3.30	482.8
0.088	1.63	PI-	20.64	8.3	17.90		0.81	118.3
1.152	0.147	(+)	30.29	14.4	31.25		1.84	269.2
1.327	0.043	(-)	-9.64	-6.17	-13.350	CEX	0.429	62.676
0.200	69.68	PI+	52.33	35.9	69.94		6.44	780.3
0.104	1.75	PI-	24.80	13.4	26.18		1.27	154.1
1.165	0.161	(+)	38.57	24.7	48.06		3.35	406.0
1.357	0.052	(-)	-13.77	-11.24	-21.880	CEX	1.010	122.310
0.220	71.28	PI+	61.98	60.2	106.61		11.67	1195.4
0.121	1.87	PI-	28.25	21.6	38.27		1.98	202.6
1.178	0.175	(+)	45.11	40.9	72.44		5.80	593.8
1.389	0.061	(-)	-16.86	-19.30	-34.169	CEX	2.054	210.317
0.240	72.93	PI+	61.33	93.8	152.21		19.19	1689.5
0.138	1.99	PI-	28.49	32.9	53.34		2.89	254.5
1.192	0.189	(+)	44.91	63.3	102.77		9.21	810.9
1.421	0.071	(-)	-16.42	-30.47	-49.436	CEX	3.660	322.217
0.260	74.61	PI+	42.06	128.8	192.95		27.43	2104.7
0.156	2.11	PI-	22.81	44.6	66.85		3.75	288.0
1.206	0.202	(+)	32.44	86.7	129.90		12.81	982.6
1.454	0.082	(-)	-9.62	-42.10	-63.050	CEX	5.570	427.403
0.280	76.32	PI+	5.87	150.1	208.72		32.93	2228.9
0.173	2.24	PI-	11.53	51.8	72.04		4.11	278.3
1.219	0.215	(+)	8.70	100.9	140.38		14.99	1014.2
1.487	0.093	(-)	2.83	-49.14	-68.339	CEX	7.074	478.768
0.300	78.06	PI+	-32.63	149.6	194.24		33.49	2019.2
0.191	2.37	PI-	0.21	51.8	67.21		3.83	230.8
1.233	0.228	(+)	-16.21	100.7	130.73		14.85	895.7
1.521	0.104	(-)	16.42	-48.93	-63.514	CEX	7.605	458.583
0.320	79.82	PI+	-60.78	135.9	165.32		30.92	1675.7
0.210	2.50	PI-	-7.01	47.3	57.57		3.19	173.1
1.247	0.241	(+)	-33.89	91.6	111.45		13.31	721.4
1.555	0.116	(-)	26.88	-44.27	-53.873	CEX	7.490	405.894
0.340	81.59	PI+	-76.99	117.9	135.07		27.09	1329.4
0.228	2.63	PI-	-10.43	42.3	48.45		2.59	127.2
1.261	0.253	(+)	-43.71	80.1	91.76		11.38	558.2
1.589	0.128	(-)	33.28	-37.82	-43.312	CEX	6.932	340.131
0.360	83.38	PI+	-85.13	101.6	109.85		23.47	1049.7
0.247	2.77	PI-	-11.13	38.0	41.14		2.10	93.9
1.275	0.265	(+)	-48.13	69.8	75.49		9.61	429.6
1.624	0.140	(-)	37.00	-31.76	-34.356	CEX	6.355	284.255
0.380	85.18	PI+	-88.58	87.8	89.95		20.34	834.3
0.265	2.90	PI-	-10.26	34.8	35.64		1.72	70.6
1.288	0.277	(+)	-49.42	61.3	62.80		8.11	332.5
1.659	0.153	(-)	39.16	-26.50	-27.153	CEX	5.849	239.894
0.400	87.00	PI+	-89.36	76.7	74.67		17.76	671.5
0.284	3.04	PI-	-8.39	32.5	31.68		1.45	54.7
1.302	0.288	(+)	-48.87	54.6	53.18		6.88	260.1
1.695	0.166	(-)	40.49	-22.08	-21.494	CEX	5.448	205.932

K-TPI-W-S GEV	S-OMEGA Q-2*Q**2		RE C 1/GEV	IM C 1/GEV	S TOT MB		DS/DO MB/SR	DS/DT MB/GEV**
0.420	88.82	PI+	-88.79	67.8	62.85		15.66	548.1
0.303	3.17	PI-	-5.78	31.2	28.92		1.26	44.2
1.315	0.300	(+)	-47.28	49.5	45.89		5.88	205.8
1.730	0.179	(-)	41.51	-18.30	-16.968	CEX	5.163	180.739
0.440	90.65	PI+	-87.46	60.5	53.54		13.90	452.5
0.322	3.31	PI-	-2.56	30.9	27.37		1.18	38.5
1.329	0.311	(+)	-45.01	45.7	40.46		5.06	164.7
1.766	0.193	(-)	42.45	-14.78	-13.084	CEX	4.968	161.709
0.460	92.49	PI+	-85.66	54.5	46.11		12.41	377.2
0.341	3.44	PI-	0.57	31.9	27.03		1.23	37.3
1.342	0.322	(+)	-42.54	43.2	36.57		4.43	134.6
1.802	0.207	(-)	43.12	-11.27	-9.538	CEX	4.785	145.408
0.480	94.34	PI+	-83.59	49.4	40.10		11.14	317.1
0.360	3.58	PI-	3.30	33.5	27.19		1.34	38.1
1.356	0.332	(+)	-40.14	41.5	33.64		3.93	112.0
1.838	0.221	(-)	43.44	-7.96	-6.456	CEX	4.608	131.172
0.500	96.19	PI+	-81.34	45.1	35.13		10.02	268.1
0.380	3.72	PI-	5.72	35.5	27.68		1.50	40.1
1.369	0.343	(+)	-37.81	40.3	31.40		3.54	94.7
1.874	0.235	(-)	43.53	-4.78	-3.726	CEX	4.444	118.873
0.520	98.05	PI+	-78.84	41.3	30.95		9.01	227.0
0.399	3.86	PI-	7.77	37.7	28.21		1.68	42.4
1.382	0.353	(+)	-35.54	39.5	29.58		3.21	80.9
1.910	0.249	(-)	43.31	-1.83	-1.368	CEX	4.271	107.660
0.540	99.91	PI+	-75.99	38.2	27.53		8.07	192.1
0.418	4.00	PI-	9.95	39.6	28.58		1.86	44.4
1.395	0.363	(+)	-33.02	38.9	28.05		2.90	69.2
1.946	0.264	(-)	42.97	0.73	0.528	CEX	4.121	98.155
0.560	101.78	PI+	-73.04	35.8	24.92		7.25	163.5
0.438	4.13	PI-	12.54	42.0	29.21		2.10	47.5
1.408	0.373	(+)	-30.25	38.9	27.06		2.66	60.0
1.983	0.278	(-)	42.79	3.08	2.145	CEX	4.030	90.923
0.580	103.65	PI+	-70.38	34.0	22.85		6.57	140.7
0.457	4.27	PI-	15.11	44.9	30.16		2.41	51.7
1.421	0.383	(+)	-27.63	39.5	26.50		2.50	53.5
2.019	0.293	(-)	42.75	5.44	3.654	CEX	3.993	85.525
0.600	105.53	PI+	-67.75	32.2	20.92		5.94	121.1
0.476	4.41	PI-	17.89	48.1	31.22		2.78	56.7
1.434	0.393	(+)	-24.93	40.2	26.07		2.36	48.1
2.056	0.308	(-)	42.82	7.94	5.151	CEX	4.006	81.633
0.620	107.40	PI+	-64.84	30.8	19.34		5.34	103.8
0.496	4.55	PI-	21.08	52.3	32.85		3.30	64.1
1.447	0.402	(+)	-21.88	41.5	26.09		2.29	44.4
2.092	0.323	(-)	42.96	10.75	6.754	CEX	4.069	79.046
0.640	109.28	PI+	-62.07	29.7	18.08		4.83	89.6
0.515	4.69	PI-	23.98	58.0	35.29		4.02	74.5
1.459	0.412	(+)	-19.04	43.9	26.68		2.33	43.2
2.129	0.339	(-)	43.02	14.15	8.608	CEX	4.183	77.593

K-TPI-W-S GEV	S-OMEGA Q-2*Q**2		RE C 1/GEV	IM C 1/GEV	S TOT MB		DS/DO MB/SR	DS/DT MB/GEV**2
0.660	111.17	PI+	-58.91	28.5	16.84		4.29	76.2
0.535	4.83	PI-	25.90	65.4	38.59		4.96	88.0
1.472	0.421	(+)	-16.51	47.0	27.72		2.48	44.1
2.166	0.354	(-)	42.40	18.44	10.877	CEX	4.286	76.043
0.680	113.05	PI+	-55.72	28.3	16.19		3.85	65.4
0.555	4.97	PI-	24.79	74.6	42.73		6.09	103.6
1.484	0.430	(+)	-15.46	51.4	29.46		2.84	48.3
2.202	0.370	(-)	40.26	23.17	13.271	CEX	4.254	72.301
0.700	114.94	PI+	-52.67	27.7	15.43		3.43	56.0
0.574	5.11	PI-	19.05	82.1	45.68		6.89	112.3
1.496	0.439	(+)	-16.81	54.9	30.55		3.20	52.2
2.239	0.385	(-)	35.86	27.19	15.128	CEX	3.927	64.045
0.720	116.83	PI+	-49.12	27.6	14.95		3.03	47.5
0.594	5.25	PI-	12.29	84.6	45.76		6.97	109.2
1.509	0.448	(+)	-18.42	56.1	30.36		3.33	52.1
2.276	0.401	(-)	30.71	28.49	15.407	CEX	3.347	52.437
0.740	118.72	PI+	-45.59	28.0	14.73		2.69	40.5
0.613	5.40	PI-	7.20	84.6	44.50		6.76	101.9
1.521	0.457	(+)	-19.20	56.3	29.62		3.32	50.0
2.313	0.417	(-)	26.40	28.29	14.885	CEX	2.810	42.355
0.760	120.62	PI+	-41.90	28.6	14.67		2.38	34.5
0.633	5.54	PI-	3.94	82.4	42.23		6.29	91.3
1.533	0.465	(+)	-18.98	55.5	28.45		3.18	46.2
2.350	0.433	(-)	22.92	26.89	13.780	CEX	2.307	33.490
0.780	122.51	PI+	-38.10	29.9	14.92		2.13	29.9
0.653	5.68	PI-	3.49	79.4	39.62		5.74	80.4
1.545	0.474	(+)	-17.30	54.6	27.27		2.99	41.8
2.387	0.449	(-)	20.79	24.74	12.349	CEX	1.899	26.592
0.800	124.41	PI+	-34.45	31.6	15.38		1.96	26.5
0.673	5.82	PI-	5.91	76.7	37.34		5.30	71.7
1.557	0.482	(+)	-14.27	54.2	26.36		2.81	38.0
2.424	0.465	(-)	20.18	22.56	10.979	CEX	1.641	22.177
0.820	126.31	PI+	-30.80	33.8	16.03		1.84	24.1
0.692	5.96	PI-	10.90	75.9	36.04		5.19	67.7
1.569	0.490	(+)	-9.95	54.8	26.04		2.74	35.8
2.461	0.481	(-)	20.85	21.07	10.006	CEX	1.550	20.242
0.840	128.21	PI+	-27.47	36.6	16.99		1.82	23.0
0.712	6.10	PI-	16.56	77.9	36.13		5.52	69.7
1.580	0.499	(+)	-5.45	57.3	26.56		2.88	36.4
2.498	0.497	(-)	22.01	20.65	9.571	CEX	1.583	19.999
0.860	130.11	PI+	-24.54	39.8	18.00		1.87	22.9
0.732	6.24	PI-	22.78	81.5	36.90		6.13	75.0
1.592	0.507	(+)	-0.88	60.6	27.45		3.15	38.5
2.535	0.514	(-)	23.66	20.87	9.450	CEX	1.705	20.852
0.880	132.01	PI+	-22.02	43.4	19.20		2.00	23.7
0.751	6.38	PI-	29.17	88.5	39.18		7.34	86.9
1.604	0.515	(+)	3.57	66.0	29.19		3.68	43.7
2.572	0.530	(-)	25.60	22.58	9.990	CEX	1.966	23.305

K-TPI-W-S GEV	S-OMEGA Q-2*Q**2		RE C 1/GEV	IM C 1/GEV	S TOT MB		DS/DO MB/SR	DS/DT MB/GEV**2
0.900	133.92	PI+	-20.14	47.1	20.40		2.19	25.1
0.771	6.53	PI-	34.08	98.5	42.60		9.03	103.8
1.615	0.523	(+)	6.97	72.8	31.50		4.45	51.2
2.609	0.547	(-)	27.11	25.65	11.100	CEX	2.319	26.649
0.920	135.82	PI+	-18.89	51.0	21.60		2.43	27.1
0.791	6.67	PI-	35.95	111.7	47.28		11.30	126.0
1.627	0.531	(+)	8.53	81.4	34.44		5.49	61.3
2.646	0.563	(-)	27.42	30.34	12.840	CEX	2.744	30.609
0.940	137.72	PI+	-18.35	54.6	22.60		2.68	29.0
0.811	6.81	PI-	32.59	125.7	52.08		13.65	147.9
1.638	0.538	(+)	7.12	90.1	37.34		6.61	71.7
2.683	0.580	(-)	25.47	35.58	14.740	CEX	3.098	33.574
0.960	139.63	PI+	-18.05	57.4	23.30		2.89	30.5
0.831	6.95	PI-	25.46	137.8	55.90		15.67	165.1
1.649	0.546	(+)	3.70	97.6	39.60		7.62	80.2
2.720	0.597	(-)	21.75	40.18	16.300	CEX	3.333	35.103
0.980	141.54	PI+	-17.61	59.9	23.80		3.07	31.4
0.850	7.09	PI-	14.94	148.7	59.08		17.58	180.1
1.661	0.554	(+)	-1.33	104.3	41.44		8.56	87.7
2.757	0.613	(-)	16.27	44.39	17.640	CEX	3.520	36.065
1.000	143.44	PI+	-16.88	62.1	24.20		3.22	32.1
0.870	7.23	PI-	-0.59	155.3	60.48		18.74	186.9
1.672	0.561	(+)	-8.73	108.7	42.34		9.24	92.2
2.795	0.630	(-)	8.15	46.58	18.140	CEX	3.475	34.650
1.020	145.35	PI+	-15.96	64.4	24.60		3.38	32.8
0.890	7.38	PI-	-15.49	153.5	58.60		18.25	177.2
1.683	0.569	(+)	-15.72	109.0	41.60		9.29	90.3
2.832	0.647	(-)	0.23	44.53	17.000	CEX	3.040	29.529
1.040	147.26	PI+	-14.92	66.8	25.00		3.54	33.5
0.910	7.52	PI-	-26.33	148.9	55.76		17.31	163.8
1.694	0.576	(+)	-20.63	107.8	40.38		9.12	86.3
2.869	0.664	(-)	-5.70	41.08	15.380	CEX	2.603	24.635
1.060	149.17	PI+	-13.78	69.1	25.40		3.71	34.3
0.930	7.66	PI-	-34.63	141.9	52.14		15.94	147.2
1.705	0.583	(+)	-24.20	105.5	38.77		8.76	80.8
2.906	0.681	(-)	-10.43	36.39	13.370	CEX	2.141	19.764
1.080	151.08	PI+	-12.52	71.6	25.81		3.89	35.1
0.949	7.80	PI-	-39.01	133.5	48.15		14.28	128.6
1.716	0.591	(+)	-25.77	102.6	36.98		8.25	74.3
2.943	0.698	(-)	-13.24	30.98	11.170	CEX	1.674	15.078
1.100	152.99	PI+	-10.99	74.1	26.22		4.08	35.9
0.969	7.94	PI-	-39.53	125.8	44.54		12.67	111.4
1.726	0.598	(+)	-25.26	99.9	35.38		7.74	68.0
2.981	0.715	(-)	-14.27	25.88	9.160	CEX	1.272	11.181
1.120	154.90	PI+	-9.23	77.0	26.78		4.33	37.2
0.989	8.09	PI-	-37.30	120.3	41.82		11.41	97.9
1.737	0.605	(+)	-23.26	98.7	34.30		7.39	63.4
3.018	0.732	(-)	-14.04	21.63	7.520	CEX	0.957	8.213

K-TPI-W-S GEV	S-OMEGA Q-2*Q**2		RE C 1/GEV	IM C 1/GEV	S TOT MB		DS/DO MB/SR	DS/DT MB/GEV**2
1.140	156.82	PI+	-7.57	80.4	27.45		4.63	38.8
1.009	8.23	PI-	-34.50	117.5	40.15		10.66	89.4
1.748	0.612	(+)	-21.03	99.0	33.80		7.27	61.0
3.055	0.749	(-)	-13.46	18.59	6.350	CEX	0.749	6.280
1.160	158.73	PI+	-5.99	83.9	28.18		4.97	40.8
1.029	8.37	PI-	-32.30	115.9	38.90		10.16	83.3
1.758	0.619	(+)	-19.14	99.9	33.54		7.26	59.6
3.092	0.766	(-)	-13.16	15.97	5.360	CEX	0.601	4.928
1.180	160.64	PI+	-4.42	87.9	29.00		5.37	43.1
1.049	8.51	PI-	-29.63	114.7	37.84		9.73	78.0
1.769	0.626	(+)	-17.03	101.3	33.42		7.31	58.7
3.130	0.783	(-)	-12.60	13.39	4.420	CEX	0.469	3.764
1.200	162.55	PI+	-2.98	92.3	29.94		5.84	45.8
1.069	8.66	PI-	-26.99	115.0	37.33		9.57	75.1
1.780	0.633	(+)	-14.98	103.6	33.63		7.52	59.0
3.167	0.801	(-)	-12.01	11.39	3.695	CEX	0.375	2.946
1.220	164.47	PI+	-1.89	97.1	31.00		6.39	49.1
1.088	8.80	PI-	-25.15	115.8	36.96		9.51	73.1
1.790	0.639	(+)	-13.52	106.5	33.98		7.80	59.9
3.204	0.818	(-)	-11.63	9.34	2.980	CEX	0.301	2.316
1.240	166.38	PI+	-1.24	102.2	32.10		7.00	52.6
1.108	8.94	PI-	-23.37	116.7	36.66		9.49	71.4
1.800	0.646	(+)	-12.30	109.5	34.38		8.13	61.1
3.241	0.835	(-)	-11.07	7.26	2.280	CEX	0.235	1.766
1.260	168.30	PI+	-0.84	107.6	33.24		7.66	56.5
1.128	9.08	PI-	-21.81	118.2	36.53		9.57	70.5
1.811	0.653	(+)	-11.32	112.9	34.88		8.52	62.8
3.279	0.853	(-)	-10.48	5.32	1.645	CEX	0.183	1.349
1.280	170.21	PI+	-0.92	113.4	34.50		8.42	60.8
1.148	9.22	PI-	-20.51	119.8	36.46		9.68	69.9
1.821	0.660	(+)	-10.71	116.6	35.48		8.98	64.9
3.316	0.870	(-)	-9.80	3.22	0.980	CEX	0.139	1.006
1.300	172.13	PI+	-1.82	119.5	35.80		9.25	65.5
1.168	9.37	PI-	-19.50	121.9	36.50		9.86	69.8
1.831	0.666	(+)	-10.66	120.7	36.15		9.50	67.3
3.353	0.887	(-)	-8.84	1.17	0.350	CEX	0.103	0.728
1.320	174.04	PI+	-3.49	125.6	37.05		10.11	70.2
1.188	9.51	PI-	-18.87	123.9	36.55		10.06	69.8
1.841	0.673	(+)	-11.18	124.7	36.80		10.04	69.7
3.391	0.905	(-)	-7.69	-0.85	-0.250	CEX	0.077	0.532
1.340	175.96	PI+	-5.98	131.6	38.25		10.99	74.9
1.208	9.65	PI-	-18.48	126.0	36.61		10.27	69.9
1.851	0.679	(+)	-12.23	128.8	37.43		10.60	72.2
3.428	0.922	(-)	-6.25	-2.82	-0.820	CEX	0.060	0.406
1.360	177.88	PI+	-9.30	137.3	39.30		11.86	79.3
1.228	9.79	PI-	-18.36	128.0	36.66		10.48	70.1
1.862	0.685	(+)	-13.83	132.6	37.98		11.14	74.5
3.465	0.940	(-)	-4.53	-4.61	-1.320	CEX	0.052	0.350

K-TPI-W-S GEV	S-OMEGA Q-2*Q**2		RE C 1/GEV	IM C 1/GEV	S TOT MB		DS/DO MB/SR	DS/DT MB/GEV**2
1.380	179.79	PI+	-13.21	142.5	40.20		12.69	83.3
1.247	9.94	PI-	-18.30	130.1	36.70		10.69	70.2
1.872	0.692	(+)	-15.75	136.3	38.45		11.66	76.5
3.503	0.957	(-)	-2.55	-6.20	-1.750	CEX	0.056	0.366
1.400	181.71	PI+	-18.10	147.3	40.96		13.50	87.0
1.267	10.08	PI-	-18.79	132.3	36.80		10.95	70.6
1.881	0.698	(+)	-18.44	139.8	38.88		12.19	78.6
3.540	0.975	(-)	-0.35	-7.48	-2.080	CEX	0.069	0.443
1.420	183.63	PI+	-23.57	150.6	41.31		14.11	89.3
1.287	10.22	PI-	-19.52	133.7	36.67		11.08	70.2
1.891	0.704	(+)	-21.55	142.2	38.99		12.55	79.4
3.577	0.992	(-)	2.02	-8.46	-2.320	CEX	0.092	0.581
1.440	185.54	PI+	-28.89	153.1	41.41		14.58	90.7
1.307	10.37	PI-	-19.91	135.1	36.53		11.20	69.7
1.901	0.711	(+)	-24.40	144.1	38.97		12.83	79.8
3.615	1.010	(-)	4.49	-9.02	-2.440	CEX	0.122	0.759
1.460	187.46	PI+	-34.15	154.9	41.31		14.95	91.4
1.327	10.51	PI-	-20.39	136.4	36.37		11.30	69.1
1.911	0.717	(+)	-27.27	145.6	38.84		13.05	79.8
3.652	1.028	(-)	6.88	-9.26	-2.470	CEX	0.158	0.968
1.480	189.38	PI+	-39.39	155.9	41.03		15.22	91.5
1.347	10.65	PI-	-20.73	137.4	36.15		11.36	68.3
1.921	0.723	(+)	-30.06	146.7	38.59		13.19	79.3
3.689	1.045	(-)	9.33	-9.27	-2.440	CEX	0.204	1.224
1.500	191.30	PI+	-44.43	156.0	40.51		15.33	90.6
1.367	10.79	PI-	-20.98	138.4	35.93		11.41	67.5
1.930	0.729	(+)	-32.71	147.2	38.22		13.25	78.3
3.727	1.063	(-)	11.73	-8.82	-2.290	CEX	0.251	1.483
1.520	193.22	PI+	-48.89	155.4	39.81		15.30	89.0
1.387	10.94	PI-	-20.94	139.2	35.67		11.43	66.5
1.940	0.735	(+)	-34.92	147.3	37.74		13.22	76.9
3.764	1.081	(-)	13.98	-8.08	-2.070	CEX	0.301	1.748
1.540	195.13	PI+	-52.75	154.2	39.00		15.17	86.8
1.407	11.08	PI-	-20.95	140.4	35.50		11.51	65.8
1.950	0.741	(+)	-36.85	147.3	37.25		13.17	75.3
3.801	1.098	(-)	15.90	-6.92	-1.750	CEX	0.344	1.965
1.560	197.05	PI+	-55.87	152.6	38.10		14.94	84.1
1.427	11.22	PI-	-20.81	141.0	35.20		11.49	64.7
1.959	0.747	(+)	-38.34	146.8	36.65		13.02	73.3
3.839	1.116	(-)	17.53	-5.81	-1.450	CEX	0.386	2.171
1.580	198.97	PI+	-58.30	150.9	37.20		14.66	81.2
1.447	11.36	PI-	-20.20	142.0	35.00		11.52	63.8
1.969	0.753	(+)	-39.25	146.5	36.10		12.88	71.4
3.876	1.134	(-)	19.05	-4.46	-1.100	CEX	0.429	2.376
1.600	200.89	PI+	-59.89	149.1	36.28		14.31	78.1
1.467	11.51	PI-	-19.58	143.2	34.84		11.58	63.2
1.978	0.759	(+)	-39.74	146.1	35.56		12.72	69.4
3.914	1.152	(-)	20.15	-2.96	-0.720	CEX	0.460	2.511

K-TPI-W-S GEV	S-OMEGA Q-2*Q**2		RE C 1/GEV	IM C 1/GEV	S TOT MB		DS/DO MB/SR	DS/DT MB/GEV**2
1.650	205.69	PI+	-61.98	146.6	34.60		13.73	72.1
1.516	11.86	PI-	-17.84	146.9	34.66		11.86	62.3
2.002	0.773	(+)	-39.91	146.7	34.63		12.53	65.8
4.007	1.196	(-)	22.07	0.13	0.030	CEX	0.528	2.772
1.700	210.49	PI+	-63.38	144.5	33.11		13.19	66.8
1.566	12.22	PI-	-16.32	151.3	34.65		12.25	62.1
2.025	0.788	(+)	-39.85	147.9	33.88		12.42	62.9
4.101	1.241	(-)	23.53	3.36	0.770	CEX	0.598	3.028
1.750	215.29	PI+	-63.28	143.4	31.90		12.71	62.1
1.616	12.58	PI-	-14.94	156.4	34.80		12.77	62.4
2.048	0.802	(+)	-39.11	149.9	33.35		12.42	60.7
4.194	1.286	(-)	24.17	6.52	1.450	CEX	0.649	3.170
1.800	220.09	PI+	-62.63	143.1	30.95		12.35	58.3
1.666	12.93	PI-	-14.21	162.2	35.09		13.42	63.4
2.071	0.816	(+)	-38.42	152.6	33.02		12.54	59.2
4.288	1.330	(-)	24.21	9.57	2.070	CEX	0.686	3.241
1.850	224.89	PI+	-61.21	143.2	30.15		12.02	54.9
1.716	13.29	PI-	-14.07	168.1	35.39		14.10	64.4
2.093	0.829	(+)	-37.64	155.7	32.77		12.71	58.1
4.381	1.375	(-)	23.57	12.45	2.620	CEX	0.704	3.216
1.900	229.69	PI+	-59.11	144.7	29.65		11.85	52.4
1.766	13.65	PI-	-14.57	174.4	35.75		14.86	65.7
2.115	0.843	(+)	-36.84	159.5	32.70		13.01	57.5
4.475	1.420	(-)	22.27	14.88	3.050	CEX	0.696	3.079
1.950	234.50	PI+	-57.28	147.2	29.40		11.86	50.8
1.815	14.01	PI-	-15.96	180.6	36.06		15.62	66.9
2.137	0.856	(+)	-36.62	163.9	32.73		13.40	57.5
4.568	1.465	(-)	20.66	16.68	3.330	CEX	0.670	2.872
2.000	239.30	PI+	-55.80	150.2	29.24		11.95	49.7
1.865	14.36	PI-	-17.97	186.3	36.28		16.32	67.9
2.159	0.869	(+)	-36.89	168.3	32.76		13.82	57.5
4.662	1.511	(-)	18.92	18.08	3.520	CEX	0.638	2.652
2.050	244.11	PI+	-54.35	153.5	29.15		12.10	48.9
1.915	14.72	PI-	-20.45	191.6	36.39		16.94	68.4
2.181	0.882	(+)	-37.40	172.5	32.77		14.22	57.4
4.756	1.556	(-)	16.95	19.06	3.620	CEX	0.594	2.398
2.100	248.91	PI+	-52.88	157.2	29.15		12.31	48.3
1.965	15.08	PI-	-23.25	196.2	36.39		17.48	68.6
2.202	0.895	(+)	-38.07	176.7	32.77		14.63	57.4
4.849	1.601	(-)	14.82	19.52	3.620	CEX	0.538	2.110
2.150	253.72	PI+	-51.46	161.6	29.26		12.63	48.2
2.015	15.44	PI-	-26.23	200.2	36.26		17.90	68.3
2.223	0.907	(+)	-38.85	180.9	32.76		15.03	57.4
4.943	1.647	(-)	12.61	19.32	3.500	CEX	0.468	1.785
2.200	258.52	PI+	-50.45	166.7	29.50		13.07	48.5
2.065	15.79	PI-	-28.95	203.4	36.00		18.19	67.6
2.244	0.920	(+)	-39.70	185.0	32.75		15.43	57.3
5.036	1.692	(-)	10.75	18.36	3.250	CEX	0.390	1.449

K-TPI-W-S GEV	S-OMEGA Q-2*Q**2		RE C 1/GEV	IM C 1/GEV	S TOT MB		RHO	DS/DT MB/GEV**2
2.250	263.33	PI+	-50.2	172.2	29.80		-0.291	49.2
2.115	16.15	PI-	-31.3	206.3	35.70		-0.152	66.6
2.265	0.932	(+)	-40.8	189.2	32.75		-0.215	57.3
5.130	1.737	(-)	9.43	17.05	2.950	CEX	0.553	1.161
2.300	268.14	PI+	-50.7	177.8	30.10		-0.285	50.0
2.165	16.51	PI-	-33.4	208.7	35.34		-0.160	65.4
2.286	0.944	(+)	-42.1	193.3	32.72		-0.218	57.3
5.224	1.783	(-)	8.62	15.47	2.620	CEX	0.557	0.919
2.350	272.95	PI+	-51.8	183.2	30.35		-0.283	50.8
2.215	16.87	PI-	-35.0	210.9	34.95		-0.166	64.1
2.306	0.956	(+)	-43.4	197.0	32.65		-0.220	57.1
5.317	1.829	(-)	8.40	13.88	2.300	CEX	0.605	0.738
2.400	277.75	PI+	-53.3	188.2	30.54		-0.283	51.5
2.264	17.22	PI-	-36.1	213.1	34.58		-0.169	62.8
2.326	0.968	(+)	-44.7	200.7	32.56		-0.223	56.8
5.411	1.874	(-)	8.63	12.45	2.020	CEX	0.693	0.617
2.450	282.56	PI+	-55.1	193.0	30.68		-0.285	52.0
2.314	17.58	PI-	-36.7	215.6	34.26		-0.170	61.7
2.346	0.980	(+)	-45.9	204.3	32.47		-0.225	56.6
5.505	1.920	(-)	9.18	11.26	1.790	CEX	0.815	0.545
2.500	287.37	PI+	-57.1	197.6	30.78		-0.289	52.4
2.364	17.94	PI-	-37.3	218.3	34.00		-0.171	60.8
2.366	0.991	(+)	-47.2	207.9	32.39		-0.227	56.4
5.598	1.966	(-)	9.89	10.34	1.610	CEX	0.957	0.507
2.550	292.18	PI+	-59.4	201.9	30.83		-0.294	52.8
2.414	18.30	PI-	-38.0	221.0	33.75		-0.172	59.9
2.386	1.003	(+)	-48.7	211.4	32.29		-0.230	56.1
5.692	2.011	(-)	10.74	9.56	1.460	CEX	1.124	0.493
2.600	296.99	PI+	-61.9	205.7	30.81		-0.301	52.9
2.464	18.65	PI-	-38.5	223.7	33.51		-0.172	59.1
2.405	1.014	(+)	-50.2	214.7	32.16		-0.234	55.7
5.786	2.057	(-)	11.71	9.01	1.350	CEX	1.299	0.501
2.650	301.80	PI+	-64.4	209.2	30.74		-0.308	52.8
2.514	19.01	PI-	-38.8	226.5	33.28		-0.171	58.2
2.425	1.025	(+)	-51.6	217.8	32.01		-0.237	55.3
5.879	2.103	(-)	12.77	8.64	1.270	CEX	1.478	0.525
2.700	306.61	PI+	-66.8	212.3	30.62		-0.315	52.6
2.564	19.37	PI-	-39.0	229.4	33.08		-0.170	57.5
2.444	1.037	(+)	-52.9	220.8	31.85		-0.240	54.8
5.973	2.149	(-)	13.91	8.53	1.230	CEX	1.630	0.566
2.750	311.42	PI+	-69.2	215.0	30.45		-0.322	52.3
2.614	19.73	PI-	-39.1	232.4	32.91		-0.168	56.9
2.463	1.048	(+)	-54.1	223.7	31.68		-0.242	54.3
6.067	2.195	(-)	15.03	8.69	1.230	CEX	1.730	0.617
2.800	316.23	PI+	-71.2	217.4	30.24		-0.328	51.7
2.664	20.09	PI-	-39.3	235.6	32.76		-0.167	56.4
2.482	1.058	(+)	-55.3	226.5	31.50		-0.244	53.7
6.161	2.241	(-)	15.95	9.06	1.260	CEX	1.760	0.665

K- -W-S GEV	S-OMEGA Q-2*Q**2		RE C 1/GEV	IM C 1/GEV	S TOT MB		RHO	DS/DT MB/GEV**2
2.850	321.04	PI+	-73.1	219.7	30.02		-0.333	51.1
	20.44	PI-	-39.1	238.5	32.59		-0.164	55.7
2.501	1.069	(+)	-56.1	229.1	31.31		-0.245	53.1
6.254	2.287	(-)	17.0	9.4	1.285	CEX	1.809	0.721
2.900	325.85	PI+	-74.7	221.7	29.77		-0.337	50.4
	20.80	PI-	-38.9	242.6	32.57		-0.160	55.6
2.520	1.080	(+)	-56.8	232.1	31.17		-0.245	52.6
6.348	2.333	(-)	17.9	10.4	1.400	CEX	1.715	0.789
2.950	330.66	PI+	-75.9	223.6	29.52		-0.339	49.6
	21.16	PI-	-39.4	246.2	32.50		-0.160	55.3
2.538	1.091	(+)	-57.6	234.9	31.01		-0.245	52.1
6.442	2.379	(-)	18.3	11.3	1.490	CEX	1.617	0.820
3.000	335.47	PI+	-76.7	225.6	29.28		-0.340	48.9
	21.52	PI-	-39.7	249.9	32.44		-0.159	55.1
2.556	1.101	(+)	-58.2	237.7	30.86		-0.245	51.6
6.535	2.425	(-)	18.5	12.2	1.580	CEX	1.521	0.845
3.100	345.09	PI+	-77.7	230.1	28.91		-0.338	47.6
	22.23	PI-	-40.9	257.5	32.35		-0.159	54.8
2.593	1.122	(+)	-59.3	243.8	30.63		-0.243	50.8
6.723	2.517	(-)	18.4	13.7	1.720	CEX	1.344	0.848
3.200	354.71	PI+	-78.4	235.3	28.63		-0.333	46.5
	22.95	PI-	-42.6	264.7	32.21		-0.161	54.4
2.629	1.142	(+)	-60.5	250.0	30.42		-0.242	50.0
6.910	2.609	(-)	17.9	14.7	1.790	CEX	1.214	0.810
3.300	364.34	PI+	-78.8	241.0	28.44		-0.327	45.7
	23.66	PI-	-44.3	271.4	32.02		-0.163	53.8
2.664	1.162	(+)	-61.6	256.2	30.23		-0.240	49.4
7.098	2.701	(-)	17.2	15.2	1.790	CEX	1.136	0.750
3.400	373.96	PI+	-79.4	247.4	28.33		-0.321	45.2
	24.38	PI-	-45.9	277.9	31.83		-0.165	53.2
2.699	1.182	(+)	-62.6	262.6	30.08		-0.239	48.9
7.285	2.794	(-)	16.7	15.3	1.750	CEX	1.095	0.688
3.500	383.59	PI+	-80.4	254.0	28.26		-0.317	44.9
	25.10	PI-	-47.6	284.2	31.62		-0.168	52.5
2.734	1.201	(+)	-64.0	269.1	29.94		-0.238	48.4
7.473	2.886	(-)	16.4	15.1	1.680	CEX	1.085	0.628
3.600	393.21	PI+	-81.8	260.6	28.19		-0.314	44.6
	25.81	PI-	-49.0	290.0	31.37		-0.169	51.7
2.768	1.220	(+)	-65.4	275.3	29.78		-0.238	47.9
7.660	2.979	(-)	16.4	14.7	1.590	CEX	1.116	0.580
3.700	402.84	PI+	-83.4	267.2	28.12		-0.312	44.3
	26.53	PI-	-50.0	296.1	31.16		-0.169	51.0
2.801	1.239	(+)	-66.7	281.6	29.64		-0.237	47.4
7.848	3.071	(-)	16.7	14.4	1.520	CEX	1.156	0.552
3.800	412.46	PI+	-85.3	273.5	28.03		-0.312	44.0
	27.24	PI-	-51.0	302.0	30.95		-0.169	50.3
2.835	1.258	(+)	-68.2	287.8	29.49		-0.237	46.9
8.035	3.164	(-)	17.1	14.2	1.460	CEX	1.202	0.533

K- -W-S GEV	S-OMEGA Q-2*Q**2		RE C 1/GEV	IM C 1/GEV	S TOT MB		RHO	DS/DT MB/GEV**2
3.900	422.09	PI+	-87.3	279.6	27.92		-0.312	43.7
	27.96	PI-	-51.8	308.1	30.76		-0.168	49.7
2.868	1.276	(+)	-69.6	293.8	29.34		-0.237	46.4
8.223	3.257	(-)	17.7	14.2	1.420	CEX	1.246	0.526
4.000	431.71	PI+	-89.2	285.3	27.78		-0.313	43.3
	28.68	PI-	-52.6	314.1	30.58		-0.168	49.1
2.900	1.294	(+)	-70.9	299.7	29.18		-0.237	45.9
8.410	3.349	(-)	18.3	14.4	1.403	CEX	1.271	0.526
4.100	441.34	PI+	-91.0	290.8	27.62		-0.313	42.8
	29.39	PI-	-53.3	320.3	30.42		-0.167	48.6
2.932	1.312	(+)	-72.2	305.5	29.02		-0.236	45.4
8.598	3.442	(-)	18.8	14.7	1.397	CEX	1.280	0.526
4.200	450.97	PI+	-92.5	296.1	27.46		-0.312	42.3
	30.11	PI-	-54.0	326.4	30.26		-0.165	48.1
2.964	1.329	(+)	-73.3	311.3	28.86		-0.235	44.9
8.786	3.535	(-)	19.3	15.1	1.403	CEX	1.273	0.527
4.300	460.60	PI+	-93.7	301.4	27.30		-0.311	41.8
	30.82	PI-	-54.7	332.6	30.12		-0.164	47.6
2.996	1.347	(+)	-74.2	317.0	28.71		-0.234	44.4
8.973	3.628	(-)	19.5	15.6	1.411	CEX	1.253	0.523
4.400	470.22	PI+	-94.7	306.9	27.16		-0.309	41.3
	31.54	PI-	-55.4	338.7	29.98		-0.163	47.1
3.027	1.364	(+)	-75.0	322.8	28.57		-0.232	44.0
9.161	3.721	(-)	19.7	15.9	1.409	CEX	1.236	0.513
4.500	479.85	PI+	-95.6	312.5	27.04		-0.306	40.8
	32.26	PI-	-56.0	344.8	29.84		-0.162	46.7
3.057	1.381	(+)	-75.8	328.7	28.44		-0.231	43.5
9.348	3.814	(-)	19.8	16.2	1.401	CEX	1.225	0.502
4.600	489.48	PI+	-96.5	318.1	26.93		-0.303	40.5
	32.97	PI-	-56.5	351.0	29.71		-0.161	46.3
3.088	1.398	(+)	-76.5	334.5	28.32		-0.229	43.1
9.536	3.907	(-)	20.0	16.4	1.391	CEX	1.218	0.491
4.700	499.11	PI+	-97.3	323.8	26.83		-0.301	40.1
	33.69	PI-	-56.9	357.1	29.59		-0.159	45.9
3.118	1.414	(+)	-77.1	340.5	28.21		-0.227	42.7
9.723	4.000	(-)	20.2	16.7	1.380	CEX	1.212	0.481
4.800	508.73	PI+	-98.1	329.6	26.74		-0.298	39.8
	34.40	PI-	-57.4	363.4	29.48		-0.158	45.5
3.148	1.431	(+)	-77.7	346.5	28.11		-0.224	42.4
9.911	4.093	(-)	20.4	16.9	1.369	CEX	1.208	0.471
4.900	518.36	PI+	-99.0	335.5	26.66		-0.295	39.5
	35.12	PI-	-57.8	369.7	29.38		-0.156	45.2
3.178	1.447	(+)	-78.4	352.6	28.02		-0.222	42.1
10.098	4.186	(-)	20.6	17.1	1.358	CEX	1.204	0.462
5.000	527.99	PI+	-99.8	341.3	26.58		-0.292	39.2
	35.84	PI-	-58.3	375.9	29.28		-0.155	44.8
3.207	1.463	(+)	-79.1	358.6	27.93		-0.220	41.8
10.286	4.279	(-)	20.8	17.3	1.347	CEX	1.200	0.452

K- -W-S GEV	S-OMEGA Q-2*Q**2		RE C 1/GEV	IM C 1/GEV	S TOT MB		RHO	DS/DT MB/GEV**2
5.200	547.25	PI+	-101.4	353.1	26.44		-0.287	38.7
	37.27	PI-	-59.2	388.5	29.09		-0.152	44.2
3.265	1.494	(+)	-80.3	370.8	27.77		-0.216	41.2
10.661	4.466	(-)	21.1	17.7	1.325	CEX	1.194	0.435
5.400	566.51	PI+	-103.1	365.0	26.32		-0.282	38.2
	38.70	PI-	-60.0	401.1	28.93		-0.150	43.7
3.322	1.525	(+)	-81.5	383.1	27.62		-0.213	40.8
11.036	4.652	(-)	21.5	18.1	1.303	CEX	1.191	0.419
5.600	585.76	PI+	-104.7	376.9	26.21		-0.278	37.8
	40.13	PI-	-60.9	413.8	28.77		-0.147	43.2
3.378	1.555	(+)	-82.8	395.4	27.49		-0.209	40.3
11.412	4.838	(-)	21.9	18.5	1.283	CEX	1.187	0.405
5.800	605.02	PI+	-106.3	388.8	26.11		-0.273	37.4
	41.57	PI-	-61.8	426.5	28.63		-0.145	42.8
3.433	1.585	(+)	-84.0	407.6	27.37		-0.206	39.9
11.787	5.025	(-)	22.3	18.8	1.263	CEX	1.183	0.391
6.000	624.28	PI+	-107.9	400.8	26.01		-0.269	37.1
	43.00	PI-	-62.6	439.1	28.50		-0.143	42.3
3.487	1.614	(+)	-85.3	420.0	27.26		-0.203	39.5
12.162	5.212	(-)	22.6	19.2	1.244	CEX	1.182	0.379
6.200	643.54	PI+	-109.6	412.7	25.92		-0.265	36.8
	44.43	PI-	-63.5	451.8	28.38		-0.141	41.9
3.541	1.643	(+)	-86.5	432.3	27.15		-0.200	39.2
12.537	5.398	(-)	23.0	19.5	1.226	CEX	1.180	0.367
6.400	662.80	PI+	-111.2	424.7	25.84		-0.262	36.4
	45.86	PI-	-64.4	464.4	28.26		-0.139	41.6
3.593	1.671	(+)	-87.8	444.5	27.05		-0.198	38.8
12.912	5.585	(-)	23.4	19.9	1.209	CEX	1.177	0.356
6.600	682.06	PI+	-112.8	436.6	25.76		-0.258	36.2
	47.30	PI-	-65.3	477.0	28.14		-0.137	41.2
3.645	1.699	(+)	-89.0	456.8	26.95		-0.195	38.5
13.288	5.772	(-)	23.8	20.2	1.193	CEX	1.175	0.346
6.800	701.32	PI+	-114.4	448.5	25.68		-0.255	35.9
	48.73	PI-	-66.1	489.6	28.04		-0.135	40.9
3.696	1.726	(+)	-90.3	469.0	26.86		-0.192	38.2
13.663	5.959	(-)	24.1	20.6	1.178	CEX	1.173	0.337
7.000	720.58	PI+	-115.9	460.3	25.61		-0.252	35.6
	50.16	PI-	-67.0	502.1	27.93		-0.133	40.6
3.747	1.753	(+)	-91.5	481.2	26.77		-0.190	37.9
14.038	6.146	(-)	24.5	20.9	1.163	CEX	1.171	0.328
7.200	739.84	PI+	-117.5	472.2	25.54		-0.249	35.4
	51.59	PI-	-67.8	514.7	27.84		-0.132	40.3
3.796	1.779	(+)	-92.6	493.5	26.69		-0.188	37.7
14.413	6.333	(-)	24.8	* 21.2	1.149	CEX	1.169	0.319
7.400	759.11	PI+	-119.0	484.1	25.47		-0.246	35.2
	53.03	PI-	-68.6	527.2	27.74		-0.130	40.0
3.846	1.805	(+)	-93.8	505.7	26.61		-0.185	37.4
14.789	6.520	(-)	25.2	21.6	1.136	CEX	1.167	0.311

K- -W-S GEV	S-OMEGA Q-2*Q**2		RE C 1/GEV	IM C 1/GEV	S TOT MB		RHO	DS/DT MB/GEV**2
7.600	778.37	PI+	-120.5	495.9	25.41		-0.243	34.9
	54.46	PI-	-69.4	539.8	27.66		-0.129	39.7
3.894	1.831	(+)	-94.9	517.8	26.53		-0.183	37.2
15.164	6.706	(-)	25.5	21.9	1.123	CEX	1.165	0.304
7.800	797.63	PI+	-121.9	507.7	25.35		-0.240	34.7
	55.89	PI-	-70.2	552.2	27.57		-0.127	39.5
3.942	1.857	(+)	-96.0	530.0	26.46		-0.181	36.9
15.539	6.894	(-)	25.9	22.2	1.110	CEX	1.163	0.296
8.000	816.89	PI+	-123.3	519.6	25.29		-0.237	34.5
	57.33	PI-	-70.9	564.7	27.49		-0.126	39.2
3.989	1.882	(+)	-97.1	542.1	26.39		-0.179	36.7
15.914	7.081	(-)	26.2	22.6	1.098	CEX	1.161	0.290
9.000	913.20	PI+	-130.1	578.5	25.03		-0.225	33.6
	64.49	PI-	-74.5	626.8	27.12		-0.119	38.1
4.218	2.002	(+)	-102.3	602.6	26.08		-0.170	35.7
17.791	8.016	(-)	27.8	24.1	1.044	CEX	1.152	0.259
10.000	1009.51	PI+	-136.3	637.2	24.81		-0.214	32.9
	71.65	PI-	-77.8	688.5	26.81		-0.113	37.2
4.435	2.116	(+)	-107.0	662.9	25.81		-0.161	34.9
19.667	8.952	(-)	29.2	25.6	0.998	CEX	1.140	0.234
11.000	1105.83	PI+	-141.9	695.8	24.63		-0.204	32.3
	78.82	PI-	-80.7	749.8	26.54		-0.108	36.4
4.641	2.224	(+)	-111.3	722.8	25.59		-0.154	34.2
21.543	9.889	(-)	30.6	27.0	0.957	CEX	1.133	0.214
12.000	1202.14	PI+	-147.1	754.2	24.47		-0.195	31.8
	85.98	PI-	-83.1	810.9	26.31		-0.102	35.7
4.839	2.327	(+)	-115.1	782.5	25.39		-0.147	33.7
23.420	10.826	(-)	32.0	28.3	0.920	CEX	1.129	0.197
13.000	1298.46	PI+	-151.9	812.5	24.34		-0.187	31.3
	93.14	PI-	-85.2	871.7	26.11		-0.098	35.2
5.030	2.425	(+)	-118.5	842.1	25.22		-0.141	33.2
25.296	11.763	(-)	33.3	29.6	0.886	CEX	1.127	0.182
14.000	1394.78	PI+	-156.3	870.8	24.22		-0.179	30.9
	100.31	PI-	-87.0	932.3	25.93		-0.093	34.7
5.213	2.520	(+)	-121.6	901.5	25.08		-0.135	32.7
27.172	12.700	(-)	34.6	30.8	0.856	CEX	1.125	0.170
15.000	1491.10	PI+	-160.3	928.9	24.12		-0.173	30.6
	107.47	PI-	-88.5	992.8	25.77		-0.089	34.2
5.390	2.611	(+)	-124.4	960.9	24.94		-0.129	32.3
29.049	13.637	(-)	35.9	31.9	0.829	CEX	1.124	0.159
16.000	1587.42	PI+	-163.9	987.1	24.02		-0.166	30.3
	114.64	PI-	-89.7	1053.2	25.63		-0.085	33.8
5.561	2.700	(+)	-126.8	1020.1	24.83		-0.124	32.0
30.925	14.575	(-)	37.1	33.1	0.804	CEX	1.122	0.149
17.000	1683.74	PI+	-167.3	1045.1	23.94		-0.160	30.0
	121.80	PI-	-90.7	1113.4	25.50		-0.081	33.5
5.727	2.785	(+)	-129.0	1079.3	24.72		-0.119	31.7
32.802	15.512	(-)	38.3	34.1	0.782	CEX	1.121	0.141

K- -W-S GEV	S-OMEGA Q-2*Q**2		RE C 1/GEV	IM C 1/GEV	S TOT MB		RHO	DS/DT MB/GEV**2
18.000	1780.06	PI+	-170.3	1103.2	23.87		-0.154	29.8
	128.97	PI-	-91.4	1173.6	25.39		-0.078	33.1
5.889	2.868	(+)	-130.8	1138.4	24.63		-0.115	31.4
34.678	16.450	(-)	39.4	35.2	0.761	CEX	1.121	0.1336
19.000	1876.38	PI+	-173.0	1161.2	23.80		-0.149	29.6
	136.13	PI-	-91.9	1233.7	25.28		-0.074	32.8
6.046	2.949	(+)	-132.5	1197.5	24.54		-0.111	31.1
36.555	17.388	(-)	40.6	36.2	0.742	CEX	1.120	0.1270
20.000	1972.70	PI+	-175.5	1219.3	23.74		-0.144	29.4
	143.29	PI-	-92.2	1293.7	25.19		-0.071	32.6
6.199	3.027	(+)	-133.9	1256.5	24.46		-0.107	30.9
38.431	18.325	(-)	41.7	37.2	0.725	CEX	1.119	0.1210
22.000	2165.34	PI+	-179.8	1335.3	23.64		-0.135	29.1
	157.62	PI-	-92.2	1413.7	25.02		-0.065	32.1
6.495	3.178	(+)	-136.0	1374.5	24.33		-0.099	30.5
42.184	20.201	(-)	43.8	39.2	0.693	CEX	1.118	0.1106
24.000	2357.98	PI+	-183.1	1451.4	23.55		-0.126	28.8
	171.95	PI-	-91.4	1533.5	24.88		-0.060	31.7
6.778	3.322	(+)	-137.3	1492.4	24.22		-0.092	30.2
45.937	22.077	(-)	45.9	41.0	0.666	CEX	1.117	0.1019
26.000	2550.62	PI+	-185.7	1567.5	23.48		-0.118	28.6
	186.28	PI-	-90.0	1653.2	24.76		-0.054	31.4
7.049	3.461	(+)	-137.8	1610.4	24.12		-0.086	29.9
49.690	23.953	(-)	47.8	42.8	0.641	CEX	1.117	0.0945
28.000	2743.27	PI+	-187.5	1683.8	23.42		-0.111	28.4
	200.61	PI-	-88.0	1772.9	24.66		-0.050	31.1
7.310	3.594	(+)	-137.7	1728.3	24.04		-0.080	29.7
53.443	25.829	(-)	49.7	44.6	0.620	CEX	1.116	0.0881
30.000	2935.91	PI+	-188.6	1800.1	23.37		-0.105	28.2
	214.94	PI-	-85.4	1892.6	24.57		-0.045	30.9
7.563	3.722	(+)	-137.0	1846.4	23.97		-0.074	29.5
57.196	27.705	(-)	51.6	46.2	0.600	CEX	1.116	0.0826
35.000	3417.52	PI+	-188.7	2091.6	23.27		-0.090	27.9
	250.76	PI-	-76.8	2192.0	24.39		-0.035	30.4
8.160	4.025	(+)	-132.7	2141.8	23.83		-0.062	29.1
66.578	32.395	(-)	56.0	50.2	0.558	CEX	1.115	0.0715
40.000	3899.13	PI+	-185.4	2384.0	23.21		-0.078	27.7
	286.58	PI-	-65.3	2491.8	24.26		-0.026	30.1
8.716	4.306	(+)	-125.4	2437.9	23.73		-0.051	28.9
75.961	37.086	(-)	60.1	53.9	0.525	CEX	1.114	0.0631
45.000	4380.75	PI+	-179.3	2677.4	23.17		-0.067	27.5
	322.41	PI-	-51.4	2792.2	24.16		-0.018	29.8
9.238	4.570	(+)	-115.4	2734.8	23.67		-0.042	28.7
85.344	41.776	(-)	63.9	57.4	0.497	CEX	1.114	0.0565
50.000	4862.36	PI+	-170.7	2972.0	23.15		-0.057	27.5
	358.23	PI-	-35.4	3093.4	24.09		-0.011	29.7
9.733	4.820	(+)	-103.0	3032.7	23.62		-0.034	28.5
94.726	46.467	(-)	67.6	60.7	0.473	CEX	1.114	0.0512

K- -W-S GEV	S-OMEGA Q-2*Q**2		RE C 1/GEV	IM C 1/GEV	S TOT MB		RHO	DS/DT MB/GEV**2
55.000	5343.97	PI+	-159.8	3268.	23.13		-0.049	27.4
	394.05	PI-	-17.5	3395.	24.04		-0.005	29.5
10.203	5.058	(+)	-88.7	3331.	23.59		-0.027	28.4
104.109	51.158	(-)	71.1	63.9	0.452	CEX	1.113	0.0468
60.000	5825.59	PI+	-146.9	3564.	23.13		-0.041	27.4
	429.87	PI-	2.1	3698.	24.00		0.001	29.4
10.653	5.284	(+)	-72.4	3631.	23.57		-0.020	28.4
113.491	55.849	(-)	74.5	66.9	0.434	CEX	1.113	0.0431
65.000	6307.20	PI+	-132.2	3862.	23.14		-0.034	27.4
	465.70	PI-	23.3	4002.	23.97		0.006	29.4
11.085	5.502	(+)	-54.4	3932.	23.56		-0.014	28.4
122.874	60.540	(-)	77.7	69.8	0.418	CEX	1.113	0.0400
70.000	6788.82	PI+	-115.8	4161.	23.15		-0.028	27.4
	501.52	PI-	45.9	4306.	23.96		0.011	29.3
11.500	5.711	(+)	-34.9	4234.	23.55		-0.008	28.3
132.256	65.231	(-)	80.9	72.7	0.404	CEX	1.113	0.0374
75.000	7270.43	PI+	-97.8	4461.	23.16		-0.022	27.4
	537.34	PI-	69.9	4612.	23.94		0.015	29.3
11.901	5.913	(+)	-14.0	4536.	23.55		-0.003	28.3
141.639	69.922	(-)	83.9	75.4	0.391	CEX	1.113	0.0350
80.000	7752.05	PI+	-78.5	4762.	23.18		-0.016	27.5
	573.17	PI-	95.1	4918.	23.94		0.019	29.3
12.289	6.108	(+)	8.3	4840.	23.56		0.002	28.4
151.021	74.613	(-)	86.8	78.0	0.380	CEX	1.113	0.0330
85.000	8233.66	PI+	-57.8	5064.	23.20		-0.011	27.5
	608.99	PI-	121.5	5225.	23.94		0.023	29.3
12.665	6.297	(+)	31.9	5145.	23.57		0.006	28.4
160.404	79.305	(-)	89.7	80.6	0.369	CEX	1.113	0.0312
90.000	8715.28	PI+	-35.9	5367.	23.22		-0.007	27.6
	644.81	PI-	149.0	5533.	23.94		0.027	29.3
13.030	6.481	(+)	56.6	5450.	23.58		0.010	28.4
169.787	83.996	(-)	92.4	83.1	0.359	CEX	1.112	0.0295
95.000	9196.89	PI+	-12.8	5671.	23.25		-0.002	27.6
	680.63	PI-	177.5	5842.	23.95		0.030	29.3
13.385	6.659	(+)	82.4	5757.	23.60		0.014	28.5
179.169	88.687	(-)	95.1	85.5	0.351	CEX	1.112	0.0281
100.000	9678.50	PI+	11.5	5976.	23.27		0.002	27.7
	716.46	PI-	207.0	6152.	23.96		0.034	29.4
13.731	6.833	(+)	109.2	6064.	23.61		0.018	28.5
188.552	93.378	(-)	97.8	87.9	0.342	CEX	1.112	0.0268
105.000	10160.12	PI+	36.7	6282.	23.30		0.006	27.7
	752.28	PI-	237.4	6463.	23.97		0.037	29.4
14.069	7.002	(+)	137.0	6373.	23.63		0.022	28.5
197.934	98.069	(-)	100.3	90.2	0.335	CEX	1.112	0.0256
110.000	10641.74	PI+	62.9	6589.	23.33		0.010	27.8
	788.10	PI-	268.7	6774.	23.98		0.040	29.4
14.399	7.168	(+)	165.8	6682.	23.65		0.025	28.6
207.317	102.760	(-)	102.9	92.5	0.327	CEX	1.112	0.0245

K- -W-S GEV	S-OMEGA Q-2*Q**2		RE C 1/GEV	IM C 1/GEV	S TOT MB		RHO	DS/DT MB/GEV**2
115.000	11123.35	PI+	90.1	6897.	23.36		0.013	27.9
	823.92	PI-	300.8	7087.	24.00		0.042	29.5
14.721	7.330	(+)	195.4	6992.	23.68		0.028	28.7
216.700	107.452	(-)	105.3	94.7	0.321	CEX	1.112	0.0235
120.000	11604.96	PI+	118.2	7206.	23.38		0.016	27.9
	859.75	PI-	333.7	7400.	24.01		0.045	29.5
15.036	7.488	(+)	225.9	7303.	23.70		0.031	28.7
226.082	112.143	(-)	107.7	96.9	0.314	CEX	1.112	0.0226
125.000	12086.58	PI+	147.1	7516.	23.41		0.020	28.0
	895.57	PI-	367.3	7714.	24.03		0.048	29.6
15.345	7.643	(+)	257.2	7615.	23.72		0.034	28.8
235.465	116.834	(-)	110.1	99.0	0.308	CEX	1.112	0.0217
130.000	12568.19	PI+	176.9	7826.	23.44		0.023	28.1
	931.39	PI-	401.7	8028.	24.05		0.050	29.6
15.648	7.795	(+)	289.3	7927.	23.75		0.036	28.8
244.847	121.525	(-)	112.4	101.1	0.303	CEX	1.112	0.0210
135.000	13049.81	PI+	207.4	8138.	23.47		0.025	28.2
	967.22	PI-	436.9	8344.	24.07		0.052	29.7
15.945	7.944	(+)	322.1	8241.	23.77		0.039	28.9
254.230	126.217	(-)	114.7	103.2	0.298	CEX	1.112	0.0202
140.000	13531.43	PI+	238.7	8450.	23.50		0.028	28.2
	1003.04	PI-	472.6	8660.	24.09		0.055	29.7
16.236	8.090	(+)	355.7	8555.	23.80		0.042	29.0
263.612	130.908	(-)	117.0	105.2	0.293	CEX	1.112	0.0196
145.000	14013.04	PI+	270.7	8763.	23.53		0.031	28.3
	1038.86	PI-	509.1	8977.	24.11		0.057	29.8
16.523	8.234	(+)	389.9	8870.	23.82		0.044	29.0
272.995	135.599	(-)	119.2	107.2	0.288	CEX	1.112	0.0189
150.000	14494.66	PI+	303.4	9077.	23.56		0.033	28.4
	1074.68	PI-	546.1	9295.	24.13		0.059	29.9
16.804	8.375	(+)	424.8	9186.	23.85		0.046	29.1
282.378	140.290	(-)	121.3	109.1	0.283	CEX	1.112	0.0183
155.000	14976.27	PI+	336.8	9392.	23.59		0.036	28.5
	1110.51	PI-	583.8	9614.	24.15		0.061	29.9
17.081	8.514	(+)	460.3	9503.	23.87		0.048	29.2
291.760	144.982	(-)	123.5	111.0	0.279	CEX	1.112	0.0178
160.000	15457.89	PI+	370.8	9707.	23.63		0.038	28.6
	1146.33	PI-	622.0	9933.	24.17		0.063	30.0
17.353	8.651	(+)	496.4	9820.	23.90		0.051	29.3
301.143	149.673	(-)	125.6	112.9	0.275	CEX	1.112	0.0173
165.000	15939.50	PI+	405.5	10023.	23.66		0.040	28.6
	1182.15	PI-	660.8	10253.	24.20		0.064	30.0
17.622	8.785	(+)	533.2	10138.	23.93		0.053	29.3
310.525	154.364	(-)	127.7	114.8	0.271	CEX	1.112	0.0168
170.000	16421.12	PI+	440.7	10340.	23.69		0.043	28.7
	1217.97	PI-	700.2	10574.	24.22		0.066	30.1
17.886	8.918	(+)	570.5	10457.	23.95		0.055	29.4
319.908	159.055	(-)	129.7	116.7	0.267	CEX	1.112	0.0163

K- -W-S GEV	S-OMEGA Q-2*Q**2		RE C 1/GEV	IM C 1/GEV	S TOT MB		RHO	DS/DT MB/GEV**2
175.000	16902.73	PI+	476.6	10658.	23.72		0.045	28.8
	1253.80	PI-	740.1	10895.	24.24		0.068	30.2
18.146	9.048	(+)	608.3	10777.	23.98		0.056	29.5
329.291	163.747	(-)	131.7	118.5	0.264	CEX	1.112	0.0159
180.000	17384.35	PI+	513.0	10977.	23.75		0.047	28.9
	1289.62	PI-	780.5	11217.	24.27		0.070	30.2
18.403	9.177	(+)	646.8	11097.	24.01		0.058	29.5
338.673	168.438	(-)	133.7	120.3	0.260	CEX	1.112	0.0155
185.000	17865.96	PI+	550.0	11296.	23.78		0.049	28.9
	1325.44	PI-	821.4	11540.	24.29		0.071	30.3
18.656	9.304	(+)	685.7	11418.	24.03		0.060	29.6
348.056	173.129	(-)	135.7	122.0	0.257	CEX	1.112	0.0151
190.000	18347.58	PI+	587.5	11616.	23.81		0.051	29.0
	1361.27	PI-	862.8	11863.	24.31		0.073	30.4
18.906	9.429	(+)	725.1	11739.	24.06		0.062	29.7
357.438	177.820	(-)	137.7	123.8	0.254	CEX	1.112	0.0147
195.000	18829.19	PI+	625.5	11936.	23.84		0.052	29.1
	1397.09	PI-	904.7	12187.	24.34		0.074	30.4
19.153	9.553	(+)	765.1	12062.	24.09		0.063	29.8
366.821	182.512	(-)	139.6	125.5	0.251	CEX	1.112	0.0144
200.000	19310.81	PI+	664.1	12258.	23.87		0.054	29.2
	1432.91	PI-	947.0	12512.	24.36		0.076	30.5
19.396	9.675	(+)	805.5	12385.	24.11		0.065	29.8
376.203	187.203	(-)	141.5	127.2	0.248	CEX	1.112	0.0140
220.000	21237.27	PI+	823.0	13549.	23.98		0.061	29.5
	1576.20	PI-	1120.7	13817.	24.46		0.081	30.8
20.340	10.148	(+)	971.9	13683.	24.22		0.071	30.1
413.734	205.968	(-)	148.8	133.9	0.237	CEX	1.112	0.0128
240.000	23163.73	PI+	989.1	14852.	24.10		0.067	29.8
	1719.49	PI-	1301.0	15132.	24.55		0.086	31.0
21.243	10.600	(+)	1145.1	14992.	24.32		0.076	30.4
451.264	224.733	(-)	155.9	140.2	0.228	CEX	1.112	0.0118
260.000	25090.19	PI+	1161.8	16164.	24.21		0.072	30.1
	1862.78	PI-	1487.2	16456.	24.65		0.090	31.3
22.109	11.034	(+)	1324.5	16310.	24.43		0.081	30.7
488.795	243.498	(-)	162.7	146.3	0.219	CEX	1.112	0.0110
280.000	27016.65	PI+	1340.4	17485.	24.32		0.077	30.4
	2006.08	PI-	1679.0	17789.	24.74		0.094	31.5
22.942	11.451	(+)	1509.7	17637.	24.53		0.086	31.0
526.325	262.263	(-)	169.3	152.2	0.212	CEX	1.112	0.0102
300.000	28943.11	PI+	1524.5	18815.	24.42		0.081	30.7
	2149.37	PI-	1875.8	19131.	24.83		0.098	31.8
23.746	11.854	(+)	1700.2	18973.	24.63		0.090	31.2
563.855	281.028	(-)	175.6	158.0	0.205	CEX	1.112	0.0096
350.000	33759.27	PI+	2006.6	22176.	24.67		0.090	31.4
	2507.59	PI-	2388.0	22519.	25.05		0.106	32.4
25.645	12.805	(+)	2197.3	22348.	24.86		0.098	31.9
657.681	327.941	(-)	190.7	171.5	0.191	CEX	1.112	0.0083

K- -W-S GEV	S-OMEGA Q-2*Q**2		RE C 1/GEV	IM C 1/GEV	S TOT MB		RHO	DS/DT MB/GEV**2
400.000	38575.42	PI+	2516.1	25586.	24.91		0.098	32.0
	2865.82	PI-	2925.6	25954.	25.27		0.113	33.0
27.414	13.690	(+)	2720.9	25770.	25.09		0.106	32.5
751.507	374.854	(-)	204.8	184.2	0.179	CEX	1.112	0.0073
450.000	43391.57	PI+	3049.3	29039.	25.13		0.105	32.6
	3224.05	PI-	3485.4	29432.	25.47		0.118	33.6
29.075	14.522	(+)	3267.4	29236.	25.30		0.112	33.1
845.333	421.767	(-)	218.0	196.1	0.170	CEX	1.112	0.0066
500.000	48207.73	PI+	3603.6	32533.	25.34		0.111	33.2
	3582.28	PI-	4064.9	32948.	25.66		0.123	34.2
30.646	15.308	(+)	3834.2	32741.	25.50		0.117	33.7
939.159	468.680	(-)	230.7	207.5	0.162	CEX	1.112	0.0060
600.000	57840.04	PI+	4766.6	39631.	25.72		0.120	34.3
	4298.73	PI-	5275.0	40088.	26.02		0.132	35.2
33.568	16.771	(+)	5020.8	39860.	25.87		0.126	34.7
1126.811	562.506	(-)	254.2	228.7	0.148	CEX	1.112	0.0050
700.000	67472.34	PI+	5991.9	46861.	26.07		0.128	35.3
	5015.19	PI-	6543.9	47358.	26.35		0.138	36.1
36.256	18.115	(+)	6267.9	47110.	26.21		0.133	35.7
1314.463	656.332	(-)	276.0	248.3	0.138	CEX	1.112	0.0044
800.000	77104.64	PI+	7270.2	54210.	26.39		0.134	36.2
	5731.64	PI-	7863.0	54743.	26.65		0.144	37.0
38.757	19.367	(+)	7566.6	54476.	26.52		0.139	36.6
1502.114	750.158	(-)	296.4	266.6	0.130	CEX	1.112	0.0038
900.000	86736.95	PI+	8594.6	61665.	26.68		0.139	37.1
	6448.10	PI-	9225.8	62233.	26.93		0.148	37.9
41.107	20.542	(+)	8910.2	61949.	26.80		0.144	37.5
1689.766	843.983	(-)	315.6	283.9	0.123	CEX	1.112	0.0034
1000.000	96369.27	PI+	9959.7	69219.	26.95		0.144	37.9
	7164.56	PI-	10627.5	69819.	27.19		0.152	38.6
43.329	21.654	(+)	10293.6	69519.	27.07		0.148	38.3
1877.418	937.809	(-)	333.9	300.3	0.117	CEX	1.112	0.0031

K		RE		S TOT			DS/DT	
GEV/C		1/GEV	%	MB	%		MB/GEV**2	%
0.020	PI+	0.17	-1.7	-0.11	-4.1		-67.07	-3.5
	PI-	0.21	2.4	0.14	2.4		70.39	5.0
	(+)	0.19	-26.3	0.02	0.3		-4.70	-41.8
	(-)	0.02	0.2	0.13	7.9	CEX	12.72	0.4
0.040	PI+	0.09	-1.1	-0.13	-4.5		-7.63	-2.2
	PI-	0.23	2.7	0.28	4.9		19.95	5.6
	(+)	0.16	242.8	0.08	1.7		0.27	27.4
	(-)	0.07	0.8	0.21	14.2	CEX	11.78	1.7
0.060	PI+	0.03	-0.5	0.18	5.8		-0.63	-0.9
	PI-	0.30	3.4	0.59	10.5		11.92	7.1
	(+)	0.16	11.2	0.39	8.8		1.28	22.7
	(-)	0.14	1.9	0.20	16.9	CEX	8.73	3.8
0.079	PI+	0.15	-6.6	0.48	11.5		-0.60	-8.2
	PI-	0.18	1.9	0.53	9.3		4.40	4.1
	(+)	0.16	4.7	0.50	10.2		1.70	10.6
	(-)	0.01	0.2	0.02	3.0	CEX	0.40	0.5
0.097	PI+	0.10	4.6	0.74	13.3		0.81	15.0
	PI-	0.21	2.1	0.79	13.6		3.92	4.7
	(+)	0.15	2.5	0.76	13.4		2.02	6.3
	(-)	0.05	1.4	0.03	19.4	CEX	0.69	2.7
0.112	PI+	-0.01	-0.2	0.82	10.5		0.59	1.8
	PI-	0.14	1.3	0.81	12.7		2.50	3.3
	(+)	0.07	0.7	0.82	11.5		1.35	2.6
	(-)	0.08	3.7	-0.00	0.5	CEX	0.40	7.5
0.130	PI+	-0.06	-0.4	0.26	2.0		-0.35	-0.4
	PI-	0.14	1.1	0.63	8.1		2.20	2.9
	(+)	0.04	0.3	0.45	4.3		1.01	1.2
	(-)	0.10	-19.0	0.19	-7.5	CEX	-0.18	-20.1
0.153	PI+	0.07	0.3	0.59	2.5		2.61	1.1
	PI-	0.17	1.1	0.82	7.4		2.71	3.1
	(+)	0.12	0.6	0.70	4.1		2.86	1.9
	(-)	0.05	-1.1	0.11	-1.8	CEX	-0.41	-2.5
0.172	PI+	0.29	0.8	0.30	0.8		6.54	1.7
	PI-	0.10	0.5	0.64	4.2		2.07	1.9
	(+)	0.20	0.7	0.47	1.8		4.10	1.8
	(-)	-0.09	1.2	0.17	-1.6	CEX	0.42	0.9
0.185	PI+	0.77	1.8	-0.82	-1.6		10.93	2.0
	PI-	0.19	0.9	0.30	1.5		2.45	1.9
	(+)	0.48	1.5	-0.26	-0.7		6.12	2.0
	(-)	-0.29	2.7	0.56	-3.7	CEX	1.14	1.5
0.200	PI+	1.39	2.6	-1.56	-2.2		17.45	2.2
	PI-	0.38	1.5	0.25	0.9		4.38	2.8
	(+)	0.89	2.3	-0.66	-1.4		10.17	2.5
	(-)	-0.50	3.6	0.90	-4.1	CEX	1.49	1.2
0.218	PI+	1.06	1.7	-1.29	-1.3		8.01	0.7
	PI-	-0.10	-0.4	-0.16	-0.4		-1.57	-0.8
	(+)	0.48	1.1	-0.73	-1.0		1.87	0.3
	(-)	-0.58	3.5	0.56	-1.7	CEX	2.71	1.4

Table 80/3 (Karlsruhe-Helsinki)

K		RE		S TOT			DS/DT	
GEV/C		1/GEV	%	MB	%		MB/GEV**2	%
0.247	PI+	-0.31	-0.6	0.02	0.0		-4.11	-0.2
	PI-	-0.06	-0.2	0.43	0.7		2.17	0.8
	(+)	-0.19	-0.4	0.22	0.2		0.64	0.1
	(-)	0.13	-0.9	0.20	-0.4	CEX	-3.21	-0.9
0.267	PI+	-0.20	-0.7	0.64	0.3		11.91	0.5
	PI-	0.25	1.3	0.69	1.0		5.98	2.1
	(+)	0.03	0.1	0.66	0.5		9.37	0.9
	(-)	0.23	-4.1	0.02	-0.0	CEX	-0.85	-0.2
0.280	PI+	1.03	17.6	-0.51	-0.2		-9.57	-0.4
	PI-	0.91	7.9	0.72	1.0		7.52	2.7
	(+)	0.97	11.2	0.11	0.1		3.30	0.3
	(-)	-0.06	-2.1	0.62	-0.9	CEX	-8.65	-1.8
0.290	PI+	0.93	-6.7	-0.28	-0.1		-8.15	-0.4
	PI-	0.48	8.5	0.99	1.4		7.71	3.0
	(+)	0.70	-17.0	0.36	0.3		4.53	0.5
	(-)	-0.23	-2.3	0.64	-0.9	CEX	-9.51	-2.0
0.295	PI+	0.79	-3.4	-0.05	-0.0		-4.33	-0.2
	PI-	0.40	14.3	1.09	1.6		7.95	3.3
	(+)	0.60	-5.8	0.52	0.4		6.09	0.7
	(-)	-0.20	-1.5	0.57	-0.9	CEX	-8.56	-1.8
0.301	PI+	0.77	-2.3	0.18	0.1		-0.84	-0.0
	PI-	0.19	-275.	1.16	1.7		7.98	3.5
	(+)	0.48	-2.8	0.67	0.5		7.60	0.9
	(-)	-0.29	-1.7	0.49	-0.8	CEX	-8.05	-1.7
0.305	PI+	0.58	-1.4	0.36	0.2		3.11	0.2
	PI-	-0.00	0.2	1.09	1.7		7.27	3.4
	(+)	0.29	-1.3	0.73	0.6		8.41	1.0
	(-)	-0.29	-1.5	0.36	-0.6	CEX	-6.43	-1.4
0.310	PI+	0.25	-0.5	0.62	0.3		9.48	0.5
	PI-	-0.21	5.3	0.93	1.5		6.08	3.0
	(+)	0.02	-0.1	0.77	0.6		9.53	1.2
	(-)	-0.23	-1.0	0.15	-0.3	CEX	-3.49	-0.8
0.320	PI+	0.11	-0.2	1.01	0.6		16.16	1.0
	PI-	-0.49	7.0	0.61	1.1		4.12	2.4
	(+)	-0.19	0.6	0.81	0.7		10.23	1.4
	(-)	-0.30	-1.1	-0.20	0.4	CEX	-0.18	-0.0
0.331	PI+	0.83	-1.2	1.90	1.3		20.78	1.4
	PI-	-0.46	5.0	0.54	1.0		3.51	2.4
	(+)	0.18	-0.5	1.22	1.2		11.56	1.8
	(-)	-0.65	-2.1	-0.68	1.4	CEX	1.18	0.3
0.351	PI+	1.31	-1.6	2.65	2.2		19.71	1.7
	PI-	-0.25	2.3	-0.08	-0.2		0.01	0.0
	(+)	0.53	-1.1	1.29	1.6		7.88	1.6
	(-)	-0.78	-2.2	-1.36	3.6	CEX	3.96	1.3
0.378	PI+	-2.38	2.7	1.39	1.5		36.16	4.3
	PI-	-0.61	5.8	-1.07	-3.0		-3.20	-4.4
	(+)	-1.49	3.0	0.16	0.2		9.13	2.7
	(-)	0.89	2.3	-1.23	4.4	CEX	14.70	6.0

K		RE		S TOT			DS/DT	
GEV/C		1/GEV	%	MB	%		MB/GEV**2	%
0.408	PI+	-1.57	1.8	1.15	1.6		21.44	3.5
	PI-	-0.43	5.7	-2.28	-7.5		-6.51	-13.0
	(+)	-1.00	2.1	-0.56	-1.1		1.68	0.7
	(-)	0.57	1.4	-1.71	8.7	CEX	11.56	5.9
0.427	PI+	0.05	-0.1	1.46	2.5		8.56	1.7
	PI-	-0.23	5.0	-0.30	-1.1		-0.76	-1.8
	(+)	-0.09	0.2	0.58	1.3		2.97	1.6
	(-)	-0.14	-0.3	-0.88	5.6	CEX	1.86	1.1
0.456	PI+	0.26	-0.3	0.69	1.4		1.68	0.4
	PI-	-0.712423.		-0.99	-3.6		-2.66	-7.1
	(+)	-0.22	0.5	-0.15	-0.4		0.15	0.1
	(-)	-0.49	-1.1	-0.84	8.2	CEX	-1.27	-0.9
0.490	PI+	-0.31	0.4	0.37	1.0		3.09	1.1
	PI-	0.56	12.3	0.50	1.8		1.59	4.1
	(+)	0.12	-0.3	0.43	1.3		1.14	1.1
	(-)	0.44	1.0	0.07	-1.3	CEX	2.40	1.9
0.532	PI+	0.71	-0.9	0.78	2.7		-0.64	-0.3
	PI-	0.92	10.2	0.52	1.8		2.01	4.6
	(+)	0.81	-2.4	0.65	2.3		0.43	0.6
	(-)	0.11	0.2	-0.13	68.8	CEX	0.52	0.5
0.573	PI+	0.33	-0.5	0.49	2.1		0.09	0.1
	PI-	0.45	3.2	1.38	4.6		4.61	9.2
	(+)	0.39	-1.4	0.93	3.5		2.07	3.7
	(-)	0.06	0.1	0.45	14.3	CEX	0.56	0.6
0.614	PI+	0.78	-1.2	0.27	1.4		-1.55	-1.4
	PI-	0.32	1.6	1.41	4.4		5.01	8.1
	(+)	0.55	-2.4	0.84	3.2		1.75	3.9
	(-)	-0.23	-0.5	0.57	9.1	CEX	-0.05	-0.1
0.658	PI+	-0.35	0.6	0.16	0.9		1.02	1.3
	PI-	-0.52	-2.0	1.89	5.0		7.10	8.2
	(+)	-0.44	2.6	1.03	3.7		3.21	7.3
	(-)	-0.09	-0.2	0.87	8.1	CEX	1.70	2.2
0.675	PI+	0.59	-1.0	0.03	0.2		-1.08	-1.6
	PI-	-3.25	-12.8	0.87	2.1		1.14	1.1
	(+)	-1.33	8.6	0.45	1.6		2.08	4.4
	(-)	-1.92	-4.7	0.42	3.3	CEX	-4.10	-5.6
0.705	PI+	-0.16	0.3	0.07	0.4		0.37	0.7
	PI-	-0.62	-3.6	0.78	1.7		3.35	3.0
	(+)	-0.39	2.3	0.42	1.4		1.54	2.9
	(-)	-0.23	-0.7	0.35	2.3	CEX	0.63	1.0
0.725	PI+	0.21	-0.4	0.21	1.4		0.03	0.1
	PI-	-0.38	-3.5	1.06	2.3		4.88	4.5
	(+)	-0.09	0.5	0.64	2.1		2.03	3.9
	(-)	-0.29	-1.0	0.43	2.8	CEX	0.84	1.7
0.750	PI+	-0.04	0.1	0.12	0.8		0.23	0.6
	PI-	-0.09	-1.7	0.91	2.1		4.06	4.2
	(+)	-0.07	0.3	0.52	1.8		1.58	3.3
	(-)	-0.03	-0.1	0.39	2.7	CEX	1.14	3.0

K GEV/C		RE 1/GEV	RE %	S TOT MB	S TOT %		DS/DT MB/GEV**2	DS/DT %
0.777	PI+	0.48	-1.2	0.34	2.3		0.05	0.2
	PI-	-0.59	-17.6	0.66	1.7		2.68	3.3
	(+)	-0.06	0.3	0.50	1.8		1.44	3.4
	(-)	-0.54	-2.6	0.16	1.3	CEX	-0.16	-0.6
0.800	PI+	-0.01	0.0	0.31	2.0		0.49	1.9
	PI-	0.20	3.3	0.87	2.3		3.40	4.7
	(+)	0.09	-0.7	0.59	2.2		1.57	4.1
	(-)	0.10	0.5	0.28	2.6	CEX	0.75	3.4
0.822	PI+	0.05	-0.2	0.29	1.8		0.45	1.9
	PI-	-0.55	-4.8	0.54	1.5		1.87	2.8
	(+)	-0.25	2.7	0.42	1.6		1.18	3.3
	(-)	-0.30	-1.4	0.13	1.3	CEX	-0.03	-0.2
0.851	PI+	0.04	-0.2	0.11	0.6		0.17	0.7
	PI-	-0.46	-2.3	0.32	0.9		0.99	1.4
	(+)	-0.21	7.1	0.21	0.8		0.60	1.6
	(-)	-0.25	-1.1	0.11	1.1	CEX	-0.04	-0.2
0.875	PI+	-0.11	0.5	0.29	1.6		0.62	2.7
	PI-	-0.02	-0.1	0.33	0.9		1.31	1.6
	(+)	-0.06	-2.5	0.31	1.1		0.92	2.2
	(-)	0.05	0.2	0.02	0.2	CEX	0.09	0.4
0.895	PI+	-0.06	0.3	0.23	1.1		0.49	2.0
	PI-	-0.33	-1.0	0.16	0.4		0.46	0.5
	(+)	-0.20	-3.1	0.19	0.6		0.58	1.2
	(-)	-0.14	-0.5	-0.03	-0.3	CEX	-0.22	-0.8
0.923	PI+	-0.19	1.0	0.01	0.0		0.08	0.3
	PI-	0.10	0.3	-0.11	-0.2		-0.50	-0.4
	(+)	-0.04	-0.5	-0.05	-0.2		-0.20	-0.3
	(-)	0.14	0.5	-0.06	-0.5	CEX	-0.02	-0.1
0.954	PI+	0.15	-0.8	0.02	0.1		-0.01	-0.0
	PI-	1.25	4.5	-0.13	-0.2		-0.11	-0.1
	(+)	0.70	14.2	-0.06	-0.1		-0.16	-0.2
	(-)	0.55	2.4	-0.07	-0.5	CEX	0.20	0.6
0.975	PI+	0.45	-2.5	0.14	0.6		0.21	0.7
	PI-	0.40	2.2	-0.02	-0.0		0.03	0.0
	(+)	0.42	359.6	0.06	0.1		0.26	0.3
	(-)	-0.03	-0.2	-0.08	-0.4	CEX	-0.29	-0.8
1.000	PI+	0.40	-2.4	1.23	5.1		3.02	9.4
	PI-	2.61	-444.	1.19	2.0		7.44	4.0
	(+)	1.51	-17.2	1.21	2.9		5.12	5.6
	(-)	1.10	13.6	-0.02	-0.1	CEX	0.21	0.6
1.030	PI+	-0.38	2.4	0.44	1.8		1.21	3.6
	PI-	4.35	-20.4	1.06	1.8		5.02	2.9
	(+)	1.98	-10.8	0.75	1.8		2.66	3.0
	(-)	2.36	-80.5	0.31	1.9	CEX	0.91	3.4
1.055	PI+	0.33	-2.3	0.13	0.5		0.27	0.8
	PI-	3.87	-11.8	1.03	1.9		3.99	2.6
	(+)	2.10	-8.9	0.58	1.5		1.69	2.1
	(-)	1.77	-18.8	0.45	3.3	CEX	0.88	4.2

K		RE		S TOT			DS/DT	
GEV/C		1/GEV	%	MB	%		MB/GEV**2	%
1.080	PI+	0.33	-2.6	0.06	0.3		0.12	0.3
	PI-	3.31	-8.5	0.84	1.7		2.53	2.0
	(+)	1.82	-7.1	0.45	1.2		1.12	1.5
	(-)	1.49	-11.2	0.39	3.5	CEX	0.41	2.7
1.113	PI+	0.40	-4.1	0.17	0.6		0.41	1.1
	PI-	1.23	-3.2	0.98	2.3		3.73	3.7
	(+)	0.82	-3.4	0.57	1.7		1.80	2.8
	(-)	0.42	-2.9	0.41	5.0	CEX	0.54	5.9
1.154	PI+	0.40	-6.3	0.24	0.9		0.67	1.7
	PI-	0.79	-2.4	0.27	0.7		0.77	0.9
	(+)	0.60	-3.0	0.26	0.8		0.75	1.2
	(-)	0.20	-1.5	0.01	0.2	CEX	-0.05	-0.9
1.174	PI+	0.22	-4.4	0.12	0.4		0.34	0.8
	PI-	0.62	-2.0	0.46	1.2		1.58	2.0
	(+)	0.42	-2.4	0.29	0.9		0.91	1.5
	(-)	0.20	-1.6	0.17	3.6	CEX	0.11	2.6
1.210	PI+	-0.53	22.1	0.02	0.1		0.07	0.1
	PI-	-0.30	1.1	0.49	1.3		1.96	2.6
	(+)	-0.41	2.9	0.25	0.8		0.95	1.6
	(-)	0.11	-1.0	0.24	7.1	CEX	0.14	5.3
1.235	PI+	-1.21	88.4	-0.13	-0.4		-0.40	-0.8
	PI-	0.08	-0.3	1.05	2.9		3.99	5.6
	(+)	-0.56	4.5	0.46	1.3		1.70	2.8
	(-)	0.65	-5.8	0.59	24.2	CEX	0.19	10.0
1.280	PI+	-0.99	108.1	0.01	0.0		0.03	0.1
	PI-	0.17	-0.8	0.77	2.1		2.88	4.1
	(+)	-0.41	3.8	0.39	1.1		1.46	2.3
	(-)	0.58	-5.9	0.38	39.2	CEX	-0.01	-1.3
1.324	PI+	-0.60	15.3	0.03	0.1		0.15	0.2
	PI-	0.64	-3.4	0.51	1.4		1.80	2.6
	(+)	0.02	-0.2	0.27	0.7		1.02	1.5
	(-)	0.62	-8.4	0.24	-64.5	CEX	-0.09	-18.0
1.360	PI+	-1.48	15.9	0.19	0.5		0.88	1.1
	PI-	0.37	-2.0	0.27	0.7		0.94	1.3
	(+)	-0.55	4.0	0.23	0.6		0.95	1.3
	(-)	0.93	-20.5	0.04	-2.9	CEX	-0.07	-21.0
1.400	PI+	-1.14	6.3	-0.06	-0.2		-0.10	-0.1
	PI-	-0.05	0.3	0.01	0.0		0.06	0.1
	(+)	-0.60	3.2	-0.03	-0.1		-0.01	-0.0
	(-)	0.54	-157.	0.04	-1.8	CEX	-0.02	-3.8
1.430	PI+	0.94	-3.6	0.11	0.3		0.27	0.3
	PI-	0.98	-5.0	0.16	0.4		0.44	0.6
	(+)	0.96	-4.2	0.13	0.3		0.36	0.5
	(-)	0.02	0.6	0.02	-1.0	CEX	-0.01	-1.6
1.473	PI+	0.80	-2.1	0.20	0.5		0.64	0.7
	PI-	1.25	-6.1	0.00	0.0		-0.18	-0.3
	(+)	1.03	-3.5	0.10	0.3		0.19	0.2
	(-)	0.23	2.7	-0.10	4.1	CEX	0.08	7.0

K		RE		S TOT			DS/DT	
GEV/C		1/GEV	%	MB	%		MB/GEV**2	%
1.505	PI+	-0.31	0.7	0.31	0.8		1.40	1.5
	PI-	0.48	-2.3	0.01	0.0		-0.02	-0.0
	(+)	0.08	-0.3	0.16	0.4		0.62	0.8
	(-)	0.39	3.2	-0.15	6.7	CEX	0.14	8.9
1.550	PI+	1.12	-2.1	-0.19	-0.5		-1.12	-1.3
	PI-	0.79	-3.8	-0.12	-0.4		-0.55	-0.8
	(+)	0.95	-2.5	-0.16	-0.4		-0.81	-1.1
	(-)	-0.16	-1.0	0.03	-2.0	CEX	-0.04	-2.2
1.590	PI+	1.75	-3.0	0.24	0.6		0.27	0.3
	PI-	0.37	-1.9	0.13	0.4		0.43	0.7
	(+)	1.06	-2.7	0.19	0.5		0.43	0.6
	(-)	-0.69	-3.5	-0.05	5.8	CEX	-0.15	-6.2
1.640	PI+	-0.03	0.1	0.05	0.1		0.19	0.3
	PI-	0.05	-0.3	0.10	0.3		0.34	0.5
	(+)	0.01	-0.0	0.07	0.2		0.26	0.4
	(-)	0.04	0.2	0.02	-22.4	CEX	0.01	0.4
1.680	PI+	1.05	-1.7	-0.13	-0.4		-0.80	-1.2
	PI-	0.14	-0.8	-0.05	-0.1		-0.18	-0.3
	(+)	0.60	-1.5	-0.09	-0.3		-0.43	-0.7
	(-)	-0.46	-2.0	0.04	8.7	CEX	-0.11	-3.7
1.720	PI+	0.13	-0.2	-0.06	-0.2		-0.23	-0.4
	PI-	0.12	-0.8	-0.05	-0.1		-0.17	-0.3
	(+)	0.13	-0.3	-0.05	-0.2		-0.20	-0.3
	(-)	-0.01	-0.0	0.00	0.5	CEX	-0.00	-0.0
1.760	PI+	0.60	-0.9	0.04	0.1		-0.05	-0.1
	PI-	-0.16	1.1	-0.07	-0.2		-0.25	-0.4
	(+)	0.22	-0.6	-0.02	-0.0		-0.10	-0.2
	(-)	-0.38	-1.6	-0.06	-3.7	CEX	-0.11	-3.4
1.800	PI+	0.83	-1.3	0.08	0.2		-0.00	-0.0
	PI-	-0.23	1.6	-0.10	-0.3		-0.35	-0.6
	(+)	0.30	-0.8	-0.01	-0.0		-0.10	-0.2
	(-)	-0.53	-2.2	-0.09	-4.3	CEX	-0.16	-4.9
1.840	PI+	0.67	-1.1	0.05	0.2		-0.03	-0.1
	PI-	0.40	-2.9	-0.00	-0.0		-0.03	-0.0
	(+)	0.54	-1.4	0.03	0.1		-0.01	-0.0
	(-)	-0.13	-0.6	-0.03	-1.0	CEX	-0.04	-1.3
1.880	PI+	2.01	-3.3	0.23	0.8		0.17	0.3
	PI-	0.65	-4.6	0.12	0.3		0.39	0.6
	(+)	1.33	-3.6	0.17	0.5		0.36	0.6
	(-)	-0.68	-3.0	-0.05	-1.9	CEX	-0.16	-5.2
1.920	PI+	0.42	-0.7	0.06	0.2		0.09	0.2
	PI-	0.08	-0.5	0.05	0.1		0.18	0.3
	(+)	0.25	-0.7	0.06	0.2		0.15	0.3
	(-)	-0.17	-0.8	-0.01	-0.2	CEX	-0.03	-1.2
1.980	PI+	2.85	-5.1	0.20	0.7		-0.02	-0.0
	PI-	-0.96	5.6	0.23	0.6		0.91	1.3
	(+)	0.94	-2.6	0.21	0.6		0.58	1.0
	(-)	-1.91	-9.7	0.01	0.4	CEX	-0.27	-9.9

K		RE		S TOT			DS/DT	
GEV/C		1/GEV	%	MB	%		MB/GEV**2	%
2.030	PI+	0.39	-0.7	-0.06	-0.2		-0.26	-0.5
	PI-	-2.20	11.3	0.01	0.0		0.22	0.3
	(+)	-0.90	2.4	-0.02	-0.1		0.05	0.1
	(-)	-1.29	-7.3	0.04	1.0	CEX	-0.14	-5.6
2.070	PI+	2.13	-4.0	0.02	0.1		-0.36	-0.7
	PI-	-2.12	9.8	-0.02	-0.0		0.11	0.2
	(+)	0.01	-0.0	0.00	0.0		0.00	0.0
	(-)	-2.12	-13.2	-0.02	-0.4	CEX	-0.24	-10.6
2.150	PI+	1.67	-3.2	-0.04	-0.2		-0.42	-0.9
	PI-	-1.22	4.7	-0.29	-0.8		-0.95	-1.4
	(+)	0.22	-0.6	-0.17	-0.5		-0.58	-1.0
	(-)	-1.45	-11.5	-0.12	-3.5	CEX	-0.20	-11.2
2.200	PI+	2.30	-4.6	-0.02	-0.1		-0.44	-0.9
	PI-	-1.49	5.1	-0.18	-0.5		-0.51	-0.8
	(+)	0.41	-1.0	-0.10	-0.3		-0.39	-0.7
	(-)	-1.89	-17.6	-0.08	-2.3	CEX	-0.17	-11.7
2.280	PI+	2.43	-4.8	-0.08	-0.3		-0.62	-1.2
	PI-	-0.07	0.2	-0.12	-0.3		-0.43	-0.6
	(+)	1.18	-2.8	-0.10	-0.3		-0.49	-0.8
	(-)	-1.25	-14.0	-0.02	-0.6	CEX	-0.07	-7.1
2.340	PI+	3.20	-6.2	-0.05	-0.2		-0.62	-1.2
	PI-	-0.78	2.2	-0.05	-0.1		-0.10	-0.2
	(+)	1.21	-2.8	-0.05	-0.2		-0.32	-0.6
	(-)	-1.99	-23.7	0.00	0.1	CEX	-0.08	-10.7
2.400	PI+	0.95	-1.8	0.09	0.3		0.16	0.3
	PI-	0.25	-0.7	0.08	0.2		0.26	0.4
	(+)	0.60	-1.3	0.09	0.3		0.22	0.4
	(-)	-0.35	-4.1	-0.01	-0.4	CEX	-0.02	-3.1
2.460	PI+	0.16	-0.3	0.01	0.0		-0.00	-0.0
	PI-	0.07	-0.2	0.03	0.1		0.09	0.2
	(+)	0.11	-0.2	0.02	0.1		0.04	0.1
	(-)	-0.04	-0.4	0.01	0.6	CEX	0.00	0.4
2.500	PI+	-0.58	1.0	0.05	0.2		0.24	0.5
	PI-	0.54	-1.4	-0.03	-0.1		-0.15	-0.2
	(+)	-0.02	0.0	0.01	0.0		0.04	0.1
	(-)	0.56	5.7	-0.04	-2.5	CEX	0.02	3.0
2.550	PI+	-1.16	2.0	-0.02	-0.1		0.09	0.2
	PI-	0.65	-1.7	-0.03	-0.1		-0.16	-0.3
	(+)	-0.25	0.5	-0.03	-0.1		-0.06	-0.1
	(-)	0.91	8.4	-0.00	-0.2	CEX	0.05	9.7
2.590	PI+	0.11	-0.2	0.00	0.0		-0.01	-0.0
	PI-	0.30	-0.8	-0.07	-0.2		-0.26	-0.4
	(+)	0.20	-0.4	-0.03	-0.1		-0.13	-0.2
	(-)	0.09	0.8	-0.04	-2.6	CEX	-0.00	-1.0
2.620	PI+	0.04	-0.1	-0.04	-0.1		-0.15	-0.3
	PI-	0.70	-1.8	-0.09	-0.3		-0.37	-0.6
	(+)	0.37	-0.7	-0.07	-0.2		-0.26	-0.5
	(-)	0.33	2.7	-0.02	-1.7	CEX	0.01	2.4

K		RE		S TOT			DS/DT	
GEV/C		1/GEV	%	MB	%		MB/GEV**2	%
2.650	PI+	0.03	-0.0	0.02	0.1		0.06	0.1
	PI-	1.03	-2.6	-0.07	-0.2		-0.34	-0.6
	(+)	0.53	-1.0	-0.03	-0.1		-0.14	-0.3
	(-)	0.50	3.9	-0.05	-3.8	CEX	0.02	3.2
2.700	PI+	0.51	-0.8	-0.10	-0.3		-0.40	-0.8
	PI-	1.11	-2.9	-0.14	-0.4		-0.57	-1.0
	(+)	0.81	-1.5	-0.12	-0.4		-0.49	-0.9
	(-)	0.30	2.2	-0.02	-1.5	CEX	0.01	2.4
2.780	PI+	0.70	-1.0	0.14	0.4		0.32	0.6
	PI-	1.58	-4.0	-0.03	-0.1		-0.23	-0.4
	(+)	1.14	-2.1	0.05	0.2		0.04	0.1
	(-)	0.44	2.8	-0.08	-6.8	CEX	0.01	1.1
2.850	PI+	0.13	-0.2	-0.06	-0.2		-0.19	-0.4
	PI-	0.48	-1.2	0.06	0.2		0.15	0.3
	(+)	0.30	-0.5	0.00	0.0		-0.03	-0.1
	(-)	0.17	1.0	0.06	4.4	CEX	0.03	3.6
2.900	PI+	0.12	-0.2	-0.08	-0.3		-0.27	-0.5
	PI-	0.37	-0.9	-0.04	-0.1		-0.15	-0.3
	(+)	0.24	-0.4	-0.06	-0.2		-0.22	-0.4
	(-)	0.13	0.7	0.02	1.7	CEX	0.02	1.9
2.950	PI+	0.58	-0.8	-0.02	-0.1		-0.14	-0.3
	PI-	-0.96	2.4	0.03	0.1		0.16	0.3
	(+)	-0.19	0.3	0.00	0.0		0.03	0.1
	(-)	-0.77	-4.2	0.02	1.6	CEX	-0.04	-5.1
3.010	PI+	0.39	-0.5	0.01	0.0		-0.03	-0.1
	PI-	-0.85	2.1	0.02	0.1		0.14	0.3
	(+)	-0.23	0.4	0.02	0.1		0.07	0.1
	(-)	-0.62	-3.4	0.01	0.5	CEX	-0.04	-4.2
3.090	PI+	0.17	-0.2	-0.01	-0.0		-0.04	-0.1
	PI-	0.03	-0.1	-0.06	-0.2		-0.21	-0.4
	(+)	0.10	-0.2	-0.03	-0.1		-0.12	-0.2
	(-)	-0.07	-0.4	-0.03	-1.6	CEX	-0.01	-1.6
3.150	PI+	0.37	-0.5	-0.02	-0.1		-0.11	-0.2
	PI-	0.47	-1.1	-0.14	-0.4		-0.49	-0.9
	(+)	0.42	-0.7	-0.08	-0.3		-0.29	-0.6
	(-)	0.05	0.3	-0.06	-3.3	CEX	-0.02	-2.2
3.200	PI+	1.21	-1.6	-0.10	-0.3		-0.43	-0.9
	PI-	1.62	-3.8	-0.32	-1.0		-1.14	-2.1
	(+)	1.42	-2.3	-0.21	-0.7		-0.77	-1.5
	(-)	0.20	1.1	-0.11	-6.2	CEX	-0.03	-3.5
3.270	PI+	0.15	-0.2	-0.13	-0.4		-0.38	-0.8
	PI-	1.02	-2.3	-0.24	-0.7		-0.84	-1.6
	(+)	0.59	-1.0	-0.18	-0.6		-0.61	-1.2
	(-)	0.44	2.5	-0.06	-3.1	CEX	0.00	0.3
3.350	PI+	-0.29	0.4	-0.00	-0.0		0.02	0.0
	PI-	0.46	-1.0	-0.10	-0.3		-0.34	-0.6
	(+)	0.08	-0.1	-0.05	-0.2		-0.16	-0.3
	(-)	0.38	2.2	-0.05	-2.6	CEX	0.00	0.2

K		RE		S TOT			DS/DT	
GEV/C		1/GEV	%	MB	%		MB/GEV**2	%
3.410	PI+	0.35	-0.4	-0.07	-0.3		-0.25	-0.6
	PI-	0.80	-1.7	-0.17	-0.5		-0.58	-1.1
	(+)	0.58	-0.9	-0.12	-0.4		-0.42	-0.9
	(-)	0.22	1.3	-0.05	-2.6	CEX	-0.01	-0.9
3.470	PI+	-0.77	1.0	0.00	0.0		0.08	0.2
	PI-	-0.02	0.0	-0.04	-0.1		-0.12	-0.2
	(+)	-0.39	0.6	-0.02	-0.1		-0.02	-0.0
	(-)	0.37	2.3	-0.02	-1.1	CEX	0.01	1.5
3.530	PI+	-0.15	0.2	-0.05	-0.2		-0.13	-0.3
	PI-	0.18	-0.4	-0.10	-0.3		-0.34	-0.6
	(+)	0.01	-0.0	-0.08	-0.3		-0.23	-0.5
	(-)	0.16	1.0	-0.03	-1.6	CEX	-0.00	-0.4
3.650	PI+	-0.89	1.1	-0.04	-0.1		-0.02	-0.0
	PI-	0.56	-1.1	0.01	0.0		0.02	0.0
	(+)	-0.17	0.3	-0.01	-0.0		-0.02	-0.0
	(-)	0.72	4.4	0.02	1.6	CEX	0.04	6.5
3.810	PI+	-0.23	0.3	-0.15	-0.5		-0.40	-0.9
	PI-	0.67	-1.3	-0.13	-0.4		-0.44	-0.9
	(+)	0.22	-0.3	-0.14	-0.5		-0.43	-0.9
	(-)	0.45	2.6	0.01	0.6	CEX	0.02	3.6
4.120	PI+	0.48	-0.5	-0.09	-0.3		-0.30	-0.7
	PI-	0.34	-0.6	-0.12	-0.4		-0.38	-0.8
	(+)	0.41	-0.6	-0.11	-0.4		-0.34	-0.7
	(-)	-0.07	-0.4	-0.01	-0.9	CEX	-0.01	-1.1
4.230	PI+	0.12	-0.1	0.02	0.1		0.03	0.1
	PI-	0.72	-1.3	-0.13	-0.4		-0.45	-0.9
	(+)	0.42	-0.6	-0.06	-0.2		-0.20	-0.4
	(-)	0.30	1.5	-0.07	-5.3	CEX	-0.01	-2.1
4.480	PI+	0.62	-0.7	0.03	0.1		0.03	0.1
	PI-	0.88	-1.6	-0.18	-0.6		-0.60	-1.3
	(+)	0.75	-1.0	-0.08	-0.3		-0.27	-0.6
	(-)	0.13	0.7	-0.11	-7.6	CEX	-0.03	-5.0
4.600	PI+	0.07	-0.1	-0.03	-0.1		-0.07	-0.2
	PI-	1.16	-2.1	-0.21	-0.7		-0.68	-1.5
	(+)	0.62	-0.8	-0.12	-0.4		-0.37	-0.9
	(-)	0.54	2.7	-0.09	-6.7	CEX	-0.01	-1.9
4.680	PI+	-1.10	1.1	0.50	1.9		1.47	3.6
	PI-	-1.79	3.2	0.72	2.4		2.29	5.0
	(+)	-1.45	1.9	0.61	2.2		1.87	4.4
	(-)	-0.34	-1.7	0.11	8.0	CEX	0.02	4.7
4.770	PI+	-0.66	0.7	-0.01	-0.0		0.02	0.1
	PI-	-0.52	0.9	0.09	0.3		0.29	0.6
	(+)	-0.59	0.8	0.04	0.1		0.15	0.3
	(-)	0.07	0.3	0.05	3.5	CEX	0.02	3.3
4.840	PI+	-0.88	0.9	-0.02	-0.1		0.00	0.0
	PI-	-0.12	0.2	0.03	0.1		0.09	0.2
	(+)	-0.50	0.6	0.00	0.0		0.04	0.1
	(-)	0.38	1.9	0.03	1.8	CEX	0.02	3.7

K GEV/C		RE 1/GEV	%	S TOT MB	%		DS/DT MB/GEV**2	%
4.970	PI+	0.27	-0.3	-0.01	-0.1		-0.05	-0.1
	PI-	0.40	-0.7	-0.01	-0.0		-0.03	-0.1
	(+)	0.34	-0.4	-0.01	-0.0		-0.04	-0.1
	(-)	0.07	0.3	0.00	0.3	CEX	0.00	0.6
5.000	PI+	1.84	-1.8	-0.06	-0.2		-0.27	-0.7
	PI-	1.49	-2.6	-0.03	-0.1		-0.13	-0.3
	(+)	1.67	-2.1	-0.04	-0.1		-0.20	-0.5
	(-)	-0.17	-0.8	0.02	1.2	CEX	-0.00	-0.0
5.060	PI+	-0.38	0.4	-0.02	-0.1		-0.03	-0.1
	PI-	0.49	-0.8	0.02	0.1		0.05	0.1
	(+)	0.06	-0.1	0.00	0.0		0.00	0.0
	(-)	0.43	2.1	0.02	1.5	CEX	0.02	3.7
5.150	PI+	-0.30	0.3	-0.04	-0.1		-0.09	-0.2
	PI-	0.27	-0.5	-0.02	-0.1		-0.07	-0.2
	(+)	-0.02	0.0	-0.03	-0.1		-0.08	-0.2
	(-)	0.28	1.3	0.01	0.7	CEX	0.01	2.1
5.230	PI+	-0.57	0.6	-0.03	-0.1		-0.05	-0.1
	PI-	0.24	-0.4	-0.04	-0.1		-0.13	-0.3
	(+)	-0.17	0.2	-0.04	-0.1		-0.10	-0.2
	(-)	0.41	1.9	-0.00	-0.3	CEX	0.01	2.0
5.360	PI+	-0.41	0.4	-0.05	-0.2		-0.10	-0.3
	PI-	0.48	-0.8	-0.09	-0.3		-0.27	-0.6
	(+)	0.03	-0.0	-0.07	-0.2		-0.19	-0.5
	(-)	0.45	2.1	-0.02	-1.5	CEX	0.01	1.2
5.560	PI+	1.43	-1.4	-0.02	-0.1		-0.13	-0.4
	PI-	-1.32	2.2	-0.12	-0.4		-0.30	-0.7
	(+)	0.06	-0.1	-0.07	-0.3		-0.20	-0.5
	(-)	-1.37	-6.3	-0.05	-3.7	CEX	-0.04	-10.1
5.800	PI+	0.43	-0.4	0.05	0.2		0.11	0.3
	PI-	-0.17	0.3	0.03	0.1		0.10	0.2
	(+)	0.13	-0.2	0.04	0.1		0.11	0.3
	(-)	-0.30	-1.3	-0.01	-0.7	CEX	-0.01	-2.1
5.910	PI+	0.44	-0.4	0.06	0.2		0.15	0.4
	PI-	-0.60	1.0	-0.04	-0.2		-0.11	-0.3
	(+)	-0.08	0.1	0.01	0.0		0.03	0.1
	(-)	-0.52	-2.3	-0.05	-4.3	CEX	-0.02	-6.2
6.000	PI+	-0.65	0.6	0.00	0.0		0.04	0.1
	PI-	0.32	-0.5	-0.03	-0.1		-0.09	-0.2
	(+)	-0.16	0.2	-0.01	-0.0		-0.03	-0.1
	(-)	0.49	2.2	-0.01	-1.2	CEX	0.01	1.6

K		RE		S TOT			DS/DT	
GEV/C		1/GEV	%	MB	%		MB/GEV**2	%
0.429	PI+	1.60	-1.8	-0.83	-1.4		-16.75	-3.3
	PI-	-1.79	41.0	0.18	0.6		1.31	3.2
	(+)	-0.09	0.2	-0.33	-0.8		-1.08	-0.6
	(-)	-1.70	-4.0	0.51	-3.3	CEX	-13.28	-7.7
0.480	PI+	3.20	-3.8	-0.28	-0.7		-18.79	-5.9
	PI-	-1.38	-41.9	-0.35	-1.3		-1.22	-3.2
	(+)	0.91	-2.3	-0.31	-0.9		-3.51	-3.1
	(-)	-2.29	-5.3	-0.04	0.6	CEX	-12.99	-9.9
0.539	PI+	3.66	-4.8	0.73	2.6		-12.41	-6.4
	PI-	1.49	15.2	0.02	0.1		0.91	2.0
	(+)	2.57	-7.8	0.37	1.3		-3.29	-4.7
	(-)	-1.08	-2.5	-0.35	-79.7	CEX	-4.92	-5.0
0.578	PI+	5.66	-8.0	0.02	0.1		-17.76	-12.4
	PI-	1.29	8.7	-0.15	-0.5		0.46	0.9
	(+)	3.48	-12.5	-0.07	-0.2		-4.39	-8.1
	(-)	-2.19	-5.1	-0.09	-2.5	CEX	-8.52	-9.9
0.617	PI+	2.56	-3.9	0.16	0.8		-6.33	-6.0
	PI-	0.72	3.5	-0.00	-0.0		0.61	1.0
	(+)	1.64	-7.3	0.08	0.3		-1.22	-2.7
	(-)	-0.92	-2.1	-0.08	-1.3	CEX	-3.28	-4.1
0.656	PI+	0.94	-1.6	0.23	1.4		-1.58	-2.0
	PI-	1.23	4.8	-0.01	-0.0		1.11	1.3
	(+)	1.08	-6.4	0.11	0.4		-0.33	-0.8
	(-)	0.15	0.3	-0.12	-1.2	CEX	0.19	0.3
0.687	PI+	4.05	-7.4	0.09	0.6		-6.85	-11.0
	PI-	1.17	5.1	0.49	1.1		3.15	2.9
	(+)	2.61	-16.6	0.29	1.0		-0.34	-0.7
	(-)	-1.44	-3.7	0.20	1.4	CEX	-3.02	-4.3
0.723	PI+	2.91	-6.0	0.09	0.6		-3.93	-8.5
	PI-	0.58	5.1	0.24	0.5		1.31	1.2
	(+)	1.75	-9.4	0.17	0.5		-0.41	-0.8
	(-)	-1.16	-3.9	0.07	0.5	CEX	-1.81	-3.6
0.770	PI+	2.83	-7.1	0.18	1.2		-2.58	-8.1
	PI-	0.83	24.7	0.33	0.8		1.45	1.7
	(+)	1.83	-10.0	0.25	0.9		-0.11	-0.2
	(-)	-1.00	-4.6	0.07	0.6	CEX	-0.91	-3.1
0.820	PI+	2.83	-9.2	0.38	2.4		-1.29	-5.4
	PI-	0.47	4.3	-0.06	-0.2		-0.09	-0.1
	(+)	1.65	-16.6	0.16	0.6		0.08	0.2
	(-)	-1.18	-5.7	-0.22	-2.2	CEX	-1.55	-7.6
0.874	PI+	1.88	-8.3	0.26	1.4		-0.33	-1.4
	PI-	0.19	0.7	0.06	0.2		0.35	0.4
	(+)	1.04	45.0	0.16	0.6		0.53	1.3
	(-)	-0.84	-3.4	-0.10	-1.0	CEX	-1.04	-4.6
0.928	PI+	1.11	-6.0	0.17	0.8		0.02	0.1
	PI-	-0.50	-1.4	-0.43	-0.9		-2.49	-1.8
	(+)	0.31	3.7	-0.13	-0.4		-0.43	-0.7
	(-)	-0.80	-3.0	-0.30	-2.2	CEX	-1.60	-5.0

Table 80/4 (CMU-LBL)

K		RE		S TOT			DS/DT	
GEV/C		1/GEV	%	MB	%		MB/GEV**2	%
0.978	PI+	2.62	-14.8	0.43	1.8		0.35	1.1
	PI-	-3.26	-20.2	-0.32	-0.5		-2.69	-1.5
	(+)	-0.32	43.6	0.05	0.1		0.23	0.3
	(-)	-2.94	-17.4	-0.37	-2.1	CEX	-2.80	-7.8
1.005	PI+	1.98	-11.9	0.18	0.7		-0.03	-0.1
	PI-	-0.11	2.5	0.12	0.2		0.74	0.4
	(+)	0.93	-8.8	0.15	0.4		0.50	0.5
	(-)	-1.05	-17.2	-0.03	-0.2	CEX	-0.29	-0.9
1.030	PI+	0.71	-4.6	0.32	1.3		0.65	2.0
	PI-	-0.21	1.0	0.28	0.5		1.72	1.0
	(+)	0.25	-1.3	0.30	0.7		1.19	1.3
	(-)	-0.46	15.6	-0.02	-0.1	CEX	-0.01	-0.0
1.060	PI+	1.20	-8.7	0.33	1.3		0.64	1.9
	PI-	1.57	-4.5	0.24	0.5		0.57	0.4
	(+)	1.38	-5.7	0.29	0.7		0.69	0.8
	(-)	0.19	-1.8	-0.04	-0.3	CEX	-0.17	-0.8
1.103	PI+	1.47	-13.7	0.20	0.8		0.35	1.0
	PI-	-0.19	0.5	0.58	1.3		2.72	2.5
	(+)	0.64	-2.6	0.39	1.1		1.21	1.8
	(-)	-0.83	5.8	0.19	2.1	CEX	0.66	6.2
1.137	PI+	1.16	-14.8	0.18	0.6		0.39	1.0
	PI-	-0.23	0.7	0.34	0.8		1.51	1.7
	(+)	0.46	-2.2	0.26	0.8		0.78	1.3
	(-)	-0.69	5.1	0.08	1.3	CEX	0.34	5.3
1.196	PI+	0.92	-28.3	-0.07	-0.2		-0.25	-0.5
	PI-	1.77	-6.4	0.43	1.1		1.13	1.5
	(+)	1.35	-8.8	0.18	0.5		0.39	0.7
	(-)	0.43	-3.5	0.25	6.5	CEX	0.09	3.0
1.247	PI+	2.11	-199.	-0.01	-0.0		-0.03	-0.1
	PI-	1.19	-5.2	0.23	0.6		0.60	0.8
	(+)	1.65	-13.8	0.11	0.3		0.21	0.3
	(-)	-0.46	4.2	0.12	5.8	CEX	0.15	9.5
1.297	PI+	1.75	-107.	0.09	0.3		0.33	0.5
	PI-	1.34	-6.8	0.27	0.7		0.78	1.1
	(+)	1.55	-14.5	0.18	0.5		0.53	0.8
	(-)	-0.21	2.3	0.09	19.8	CEX	0.04	5.7
1.347	PI+	1.66	-23.5	-0.09	-0.2		-0.45	-0.6
	PI-	0.31	-1.7	0.18	0.5		0.61	0.9
	(+)	0.99	-7.7	0.04	0.1		0.06	0.1
	(-)	-0.67	11.8	0.13	-13.3	CEX	0.04	11.5
1.395	PI+	1.08	-6.4	-0.09	-0.2		-0.53	-0.6
	PI-	0.90	-4.8	-0.00	-0.0		-0.14	-0.2
	(+)	0.99	-5.6	-0.05	-0.1		-0.33	-0.4
	(-)	-0.09	10.2	0.04	-2.2	CEX	-0.02	-4.0
1.437	PI+	2.16	-7.7	-0.09	-0.2		-0.83	-0.9
	PI-	1.47	-7.4	0.19	0.5		0.50	0.7
	(+)	1.82	-7.6	0.05	0.1		-0.12	-0.1
	(-)	-0.35	-8.4	0.14	-5.8	CEX	-0.09	-12.1

K		RE		S TOT			DS/DT	
GEV/C		1/GEV	%	MB	%		MB/GEV**2	%
1.498	PI+	2.29	-5.2	-0.17	-0.4		-1.40	-1.5
	PI-	1.47	-7.0	0.14	0.4		0.32	0.5
	(+)	1.88	-5.8	-0.02	-0.0		-0.47	-0.6
	(-)	-0.41	-3.5	0.16	-6.9	CEX	-0.14	-9.3
1.550	PI+	2.55	-4.7	-0.08	-0.2		-1.18	-1.4
	PI-	1.41	-6.8	0.18	0.5		0.47	0.7
	(+)	1.98	-5.3	0.05	0.1		-0.27	-0.4
	(-)	-0.57	-3.4	0.13	-8.0	CEX	-0.16	-7.8
1.590	PI+	2.58	-4.4	-0.07	-0.2		-1.19	-1.5
	PI-	1.78	-8.9	0.21	0.6		0.54	0.8
	(+)	2.18	-5.5	0.07	0.2		-0.27	-0.4
	(-)	-0.40	-2.1	0.14	-15.4	CEX	-0.12	-4.9
1.627	PI+	0.99	-1.6	0.19	0.5		0.32	0.4
	PI-	1.57	-8.4	0.31	0.9		0.94	1.5
	(+)	1.28	-3.2	0.25	0.7		0.59	0.9
	(-)	0.29	1.4	0.06	-21.1	CEX	0.07	2.6
1.671	PI+	0.91	-1.4	-0.06	-0.2		-0.53	-0.8
	PI-	2.04	-11.9	0.20	0.6		0.51	0.8
	(+)	1.47	-3.7	0.07	0.2		-0.09	-0.1
	(-)	0.57	2.5	0.13	37.7	CEX	0.16	5.4
1.715	PI+	2.85	-4.5	-0.49	-1.5		-2.56	-3.9
	PI-	1.71	-10.8	0.33	0.9		1.04	1.7
	(+)	2.28	-5.7	-0.08	-0.2		-0.74	-1.2
	(-)	-0.57	-2.4	0.41	41.8	CEX	-0.04	-1.4
1.790	PI+	3.34	-5.3	-0.23	-0.7		-1.71	-2.9
	PI-	0.71	-5.0	0.42	1.2		1.47	2.3
	(+)	2.02	-5.2	0.10	0.3		-0.04	-0.1
	(-)	-1.31	-5.4	0.32	16.6	CEX	-0.16	-4.9
1.840	PI+	2.78	-4.5	0.07	0.2		-0.54	-1.0
	PI-	0.86	-6.1	0.52	1.5		1.82	2.8
	(+)	1.82	-4.8	0.29	0.9		0.68	1.2
	(-)	-0.96	-4.0	0.22	8.8	CEX	-0.09	-2.6
1.895	PI+	3.43	-5.8	0.15	0.5		-0.38	-0.7
	PI-	-0.46	3.2	0.48	1.3		1.80	2.7
	(+)	1.48	-4.0	0.32	1.0		0.84	1.5
	(-)	-1.95	-8.7	0.16	5.4	CEX	-0.26	-8.3
1.940	PI+	1.90	-3.3	0.44	1.5		0.87	1.7
	PI-	-0.16	1.0	0.68	1.9		2.52	3.8
	(+)	0.87	-2.4	0.56	1.7		1.74	3.0
	(-)	-1.03	-4.9	0.12	3.7	CEX	-0.09	-3.1
1.995	PI+	5.39	-9.6	0.43	1.5		0.17	0.3
	PI-	-2.66	15.0	0.39	1.1		1.65	2.4
	(+)	1.36	-3.7	0.41	1.2		1.19	2.1
	(-)	-4.03	-21.1	-0.02	-0.5	CEX	-0.55	-20.5

AMPLITUDES IN THE UNPHYSICAL REGION BELOW THRESHOLD

OMEGA**2 / μ^2	$\tilde{\tilde{C}}/\mu^{-2}$	$\tilde{C}^{+}-g^2/m\,\mu^{-1}$
0.00	-0.463	-1.468
0.10	-0.480	-1.353
0.20	-0.498	-1.234
0.30	-0.517	-1.110
0.40	-0.536	-0.980
0.50	-0.557	-0.844
0.60	-0.579	-0.702
0.70	-0.602	-0.551
0.80	-0.626	-0.389
0.81	-0.629	-0.373
0.82	-0.631	-0.356
0.83	-0.634	-0.339
0.84	-0.636	-0.321
0.85	-0.639	-0.304
0.86	-0.641	-0.286
0.87	-0.644	-0.269
0.88	-0.646	-0.251
0.89	-0.649	-0.232
0.90	-0.651	-0.214
0.91	-0.654	-0.195
0.92	-0.656	-0.176
0.93	-0.658	-0.157
0.94	-0.660	-0.137
0.95	-0.663	-0.117
0.96	-0.665	-0.097
0.97	-0.667	-0.075
0.98	-0.668	-0.052
0.99	-0.669	-0.027
1.00	-0.665	0.010

Table 80/5